

Regulation and role of Siah proteins in *Helicobacter pylori*-mediated gastric cancer

By

LOPAMUDRA DAS

LIFE11201004002

**National Institute of Science Education and Research (NISER)
Bhubaneswar**

*A thesis submitted to the
Board of Studies in Life Sciences*

*In partial fulfilment of requirements
for the Degree of*

DOCTOR OF PHILOSOPHY

Of

HOMI BHABHA NATIONAL INSTITUTE

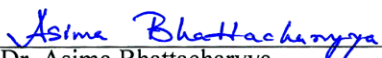


February, 2017

Homi Bhabha National Institute

Recommendations of the Viva Voce Committee

As members of the Viva Voce Committee, we certify that we have read the dissertation prepared by Lopamudra Das entitled “**Regulation and role of Siah proteins in *Helicobacter pylori*-mediated gastric cancer**” and recommend that it may be accepted as fulfilling the thesis requirement for the award of Degree of Doctor of Philosophy.

 Chairman: Prof. Snehasikta Swarnakar, IICB	Date: 27/2/17
 Guide / Convener: Dr. Asima Bhattacharyya	Date:
 External Examiner: Prof. Snehasikta Swarnakar, IICB	Date: 27/2/17
External member (Doctoral Committee): Prof. Jagneshwar Dandapat (ABSENT. Letter attached)	Date:
 Member 1: Dr. Harapriya Mohapatra	Date: 27/2/17
 Member 2: Dr. Chandan Goswami	Date: 27/2/17
 Member 3: Dr. Subhasis Chattopadhyay	Date: 27/2/17

Final approval and acceptance of this thesis is contingent upon the candidate's submission of the final copies of the thesis to HBNI.

I/We hereby certify that I/we have read this thesis prepared under my/our direction and recommend that it may be accepted as fulfilling the thesis requirement.

Date: 27/02/2017

Place: NISER BHUBANESWAR


Dr. Asima Bhattacharyya
PhD Thesis Supervisor

STATEMENT BY AUTHOR

This dissertation has been submitted in partial fulfilment of requirements for an advanced degree at Homi Bhabha National Institute (HBNI) and is deposited in the Library to be made available to borrowers under rules of the HBNI.

Brief quotations from this dissertation are allowable without special permission, provided that accurate acknowledgement of source is made. Requests for permission for extended quotation from or reproduction of this manuscript in whole or in part may be granted by the Competent Authority of HBNI when in his or her judgment the proposed use of the material is in the interests of scholarship. In all other instances, however, permission must be obtained from the author.



Signature
Lopamudra Das
Dt-27/02/2017

DECLARATION

I, hereby declare that the investigation presented in the thesis has been carried out by me. The work is original and has not been submitted earlier as a whole or in part for a degree/ diploma at this or any other Institution/ University.

A handwritten signature in black ink on a light gray rectangular background. The signature reads "Lopamudra Das" in a cursive script.

Signature
Lopamudra Das
Dt-27/02/2017

CERTIFICATE

This is to certify that the thesis entitled “**Regulation and role of Siah proteins in *Helicobacter pylori*-mediated gastric cancer**”, which is being submitted by Mrs. Lopamudra Das in partial fulfilment of the degree of Doctor of Philosophy in Life Sciences of Homi Bhabha National Institute is a record of her own research work carried by her. She has carried out her investigations for the last five years on the subject matter of the thesis under my supervision at National Institute of Science Education and Research, Bhubaneswar. To the best of our knowledge, the matter embodied in this thesis has not been submitted for the award of any other degree.



Signature of the Candidate

Dt-27/02/2017

Lopamudra Das
National Institute of Science
Education and Research (NISER)
Bhubaneswar



Signature of the Supervisor

Dt-27/02/2017

Dr. Asima Bhattacharyya
Reader F
National Institute of Science
Education and Research (NISER)
Bhubaneswar

List of Publications

a. Published

1. Regulation of Noxa-mediated apoptosis in *Helicobacter pylori*-infected gastric epithelial cells. Suvasmita Rath, **Lopamudra Das**, Shrikant Babanrao Kokate, B M Pratheek, Subhasis Chattopadhyay, Chandan Goswami, Ranajoy Chattopadhyay, Sheila Eileen Crowe, Asima Bhattacharyya. *FASEB J.* 2015 Mar; 29(3): 796-8
2. Cobalt chloride-mediated protein kinase C α (PKC α) phosphorylation induces hypoxia-inducible factor 1 α (HIF1 α) in the nucleus of gastric cancer cell. Suvasmita Rath, Aditya Anand, Nilabh Ghosh, **Lopamudra Das**, Shrikant Babanrao Kokate, Pragyesh Dixit, Swetapadma Majhi, Niranjana Rout, Shivaram Prasad Singh, Asima Bhattacharyya. *Biochem Biophys Res Commun.* 2016 Feb 26; 471(1): 205-12
3. *ETS2 and Twist1 promote invasiveness of *Helicobacter pylori*-infected gastric cancer cells by inducing Siah2. **Lopamudra Das**, Shrikant Babanrao Kokate, Suvasmita Rath, Niranjana Rout, Shivaram Prasad Singh, Sheila Eileen Crowe, Asish K Mukhopadhyay, Asima Bhattacharyya. *Biochem. J.* (2016) **473**, 1629–1640
4. Inhibition of Histone/Lysine Acetyltransferase Activity by CTK7A Selectively Kills Hypoxic Gastric Cancer Cells. Suvasmita Rath, **Lopamudra Das**, Shrikant Babanrao Kokate, Nilabh Ghosh, Pragyesh Dixit, Niranjana Rout, Shivaram P Singh, Subhasis Chattopadhyay, Hassan Ashktorab, Duane T Smoot, Mahadeva M Swamy, Tapas K Kundu, Sheila E Crowe, Asima Bhattacharyya. *Int J Biochem Cell Biol.* 2017 Jan;82:28-40

b. Under Review:

1. **Helicobacter pylori* enhances membrane-bound β -Catenin degradation in the gastric epithelial cancer cell via ETS2- mediated Siah1 induction. #**Lopamudra Das**, #Shrikant Babanrao Kokate, Pragyesh Dixit, Suvasmita Rath, Niranjana Rout, Shivaram Prasad Singh, Asima Bhattacharyya.

c. Other Publications:

1. *Role of Siah1 in *Helicobacter pylori*-infected gastric epithelial cancer cells. **Lopamudra Das**, Shrikant Babanrao Kokate, Suvasmita Rath, Shivaram P. Singh, Asima Bhattacharyya. *International Journal of Molecular Medicine* 01/2014; 34:S46-S46.

*pertaining to this thesis; #contributed equally



Signature of the student

Dt-27/02/2017

Conference Presentations

ORAL PRESENTATIONS

“Role of Siah1 in *Helicobacter pylori*-infected gastric epithelial cancer cells”, **Lopamudra Das**, Shrikant Babanrao Kokate, Suvasmita Rath, Shivaram P. Singh, Asima Bhattacharyya. 19th World Congress on Advances in Oncology and 17th International Symposium on Molecular Medicine, October 9-11, 2014, Athens, Greece

“Selective killing of hypoxic gastric epithelial cancer cells showing metastatic properties”. Suvasmita Rath, **Lopamudra Das**, Shrikant Babanrao Kokate, Tapas K Kundu, Shivaram P. Singh, Asima Bhattacharyya. 2nd International Meet on Advanced Studies in Cell Signaling Network, IICB, Kolkata, Dec 13-15, 2014

“Regulation of *Helicobacter pylori*-mediated gastric cancer: a perspective on Siah2”, **Lopamudra Das**, Shrikant Babanrao Kokate, Suvasmita Rath, Shivaram P. Singh, Asima Bhattacharyya. 2nd International Meet on Advanced Studies in Cell Signaling Network, IICB, Kolkata, Dec 13-15, 2014

POSTER PRESENTATIONS:

“Regulation of hypoxia-Inducible factor 1 α in gastric cancer metastasis”. Suvasmita Rath, **Lopamudra Das**, Tapas K Kundu, Asima Bhattacharyya. 81st Annual Meeting of Society of Biological Chemists (India), Science City, Kolkata, Nov 2012

“Regulation and role of the E3 ubiquitin ligase SIAH1 in *Helicobacter pylori*-mediated gastric cancer”. **Lopamudra Das**, Shrikant Babanrao Kokate, Suvasmita Rath, Shivaram P Singh, Asima Bhattacharyya. 2nd International Meet on Advanced Studies in Cell Signaling Network, IICB, Kolkata, Dec 13-15, 2014

“Regulation of apoptosis induction in hypoxic gastric epithelial cancer cells with metastatic properties”. Suvasmita Rath, **Lopamudra Das**, Shrikant Babanrao Kokate, Tapas K Kundu, Shivaram P Singh, Asima Bhattacharyya. 2nd International Conference on Frontiers in Biological Sciences, NIT, Rourkela, 22-24 Jan, 2015

“Regulation of Mitochondria-Mediated Apoptosis Induction in Hypoxic Gastric Epithelial Cancer Cells. Suvasmita Rath, Shrikant Babanrao Kokate, **Lopamudra Das**, Tapas K Kundu, Shivaram P Singh, Asima Bhattacharyya. Cell Symposia: Multifaceted Mitochondria, P 1.088, 2015 – Chicago, IL, USA”.

Dedicated to my family.....

ACKNOWLEDGEMENT

I am expressing my deepest gratefulness to my project supervisor Dr. Asima Bhattacharyya for her valuable guidance and constructive criticism that endured the enthusiasm to completion this project. Her advice and valuable suggestions throughout these years have made me believe in myself and encouraged me to accomplish this work.

I would also avail this opportunity to express my sincere thanks to the director of NISER, Prof. V. Chandrasekhar, for allowing me to work in this institute. I am very much gratified to my doctoral committee members Prof. Jagdishwar Dandapat, Dr. Subhasis Chattopadhyaya, Dr. Chandan Goswami, Dr. Harapriya Mohapatra for their critical evaluation and valuable suggestions during my work. I would like to thank Prof. Shivaram Prasad Singh of SCB Med College, Cuttack and Prof Niranjana Rout, AHRCC, Cuttack for providing tissue samples used in this study

I am thankful to my lab members Mrs. Suvasmita Rath, Mr. Shrikant B Kolate, Mr. Pragyesh Dixit, Mr. Nilabhi Ghosh, Mr. Aditya Anand and Mr. Indrajit Poirah for their help and inspiration in completing this thesis. I appreciate all my batchmates (especially Dr. Sanjima Pal and Ashutosh Jha) along with juniors for their constant support and motivation throughout the work which kept me going.

I am grateful to all the faculty members and staff of SBS for their blessings and encouragement. I sincerely appreciate the help received from all the scientists who gifted plasmids constructs used in this study. I acknowledge the central instrumentation facilities, computer centre, library staff and timely help received from the academic, non-academic staff at NISER.

My parents are the greatest motivational force behind me in completing my work and perhaps no word of acknowledgment is sufficient for them. I am highly indebted to my husband Dr. Debasis Bisoi for his constant support, encouragement and inspiration at every phase of my life. A special thanks to my elder sister, brother-in law, and brother for encouragement and support. With lots of Love I would like to appreciate my daughter Jagrutee for her unconditional love.

CONTENTS

	Page No.
SYNOPSIS	i-x
ABBREVIATIONS	xi-xv
LIST OF FIGURES	xvi-xviii
LIST OF TABLES	xviii
Chapter 1. INTRODUCTION	
1.1. Ubiquitination and Ubiquitin-Mediated Proteasomal Degradation	1-5
1.2. RING Type E3 ubiquitin Ligases and their Involvement in Human Cancers	5-7
1.3. Siah Proteins and their Roles in Cancer Progression	7-8
1.4. Gastric Cancer	9-10
1.5. Gastric Carcinogenesis by <i>H. pylori</i>	10-15
<i>1.5.1. Overview</i>	10-12
<i>1.5.2. Epidemiology and routes of transmission</i>	12
<i>1.5.3. Pathogenesis</i>	12-15
1.6. Intercellular Junctions and their Roles in Cancer Invasion and Metastasis	15-21
<i>1.6.1. Intercellular junctions</i>	15-17
<i>1.6.2. Role of cadherins and β-catenin during cancer invasion</i>	17-20
<i>1.6.3. RING finger E3 ubiquitin ligases regulate E-cadherin-catenin complex during cancer metastasis</i>	20-21
1.7. Objectives	21
Chapter 2. MATERIALS AND METHODS	
2.1. Materials Used	23-27

2.1.1. Cell lines	23
2.1.2. <i>H. pylori</i> strains	23
2.1.3. Competent cells	23
2.1.4. Human gastric cancer biopsy specimen	23
2.1.5. Plasmid constructs, siRNAs and antibodies	24
2.1.6. Reagents, kits, and instruments	24-27
<i>For cell culture</i>	24
<i>For <i>H. pylori</i> culture</i>	24
<i>For bacterial culture</i>	24
<i>For polymerase chain reaction (PCR) RNA/DNA</i>	24-25
<i>For cloning</i>	25
<i>For transfection and stable cells</i>	25
<i>For immunoblotting</i>	25
<i>For chromatin immunoprecipitation assay and immunoprecipitation assay</i>	25
<i>For DNA binding assay</i>	26
<i>For tissue sectioning</i>	26
<i>For soft agar assay</i>	26
<i>For transwell migration and invasion assay</i>	26
<i>Kits</i>	26
<i>Instruments</i>	26-27
2.2. Methodology	27-54
2.2.1. Culture of human gastric cancer cells (GCCs) MKN45, AGS, Kato III and immortalized normal gastric epithelial cells HFE145	27
2.2.2. Cell freezing and revival	27-28
2.2.3. <i>H. pylori</i> culture and infection of cells	28

2.2.4. Cloning, expression and site-directed mutagenesis	28-36
2.2.4.1. Cloning of human <i>siah1</i> gene	28-32
2.2.4.2. Cloning and mutation of human <i>siah1</i> and <i>siah2</i> promoters	32-35
2.2.4.3. Transient transfection	36
2.2.5. Infection of GCCs with <i>H. pylori</i>	37
2.2.6. Whole cell lysate preparation from GCCs after <i>H. pylori</i> infection	37
2.2.7. Isolation of membrane, cytosol and nuclear fractions from MKN45 cells after <i>H. pylori</i> infection	37-39
2.2.8. Sodium dodecyl sulfate polyacrylamide gel electrophoresis (SDS)	39-41
2.2.9. Immunoblotting	41-43
2.2.10. Total RNA isolation and real time RT-PCR in MKN45 cells to study expression of <i>Siah1</i> and <i>Siah2</i> after <i>H. pylori</i> infection	43-45
2.2.11. In vitro binding assay	45-46
2.2.12. In vivo binding assay	46-48
2.2.13. Dual luciferase reporter assay	49
2.2.14. Immunoprecipitation (IP) assay	49-50
2.2.15. Generations of stable cell lines overexpressing <i>ETS2</i>, <i>Twist1</i>, <i>Siah1</i> and <i>Siah2</i>	50
2.2.16. Embedding and sectioning of gastric biopsy samples	50-51
2.2.17. Immunofluorescence and confocal microscopy	51-52
2.2.18. Wound-healing assay or scratch assay	52
2.2.19. Anchorage-independent growth assay	52-53
2.2.20. Transwell migration and invasion assay	53-54
2.2.21. Statistical analysis	54

Chapter 3. RESULTS

3.1. *H. pylori* Induced Expression of Siah Proteins in Cultured

Human GCCs	56-60
3.2. Identification of Transcription Factors Regulating Expression of Siah1 and Siah2	60-63
3.3. Induced Expression of ETS2, Twist1, Siah1 and Siah2 in <i>H. pylori</i> -Infected Human GCCs	63-68
3.4. ETS2 Binds with the 5' UTR of <i>siah1</i> in <i>H. pylori</i> -Infected GCCs	68-69
3.5. ETS2 and Twist1 Bind with <i>siah2</i> Promoter in <i>H. pylori</i> -Infected GCCs	70-71
3.6. Cloning of <i>siah1</i> 5' UTR and <i>siah2</i> Promoter to Prepare Luciferase Constructs and Generation of Respective Mutants	72-73
3.7. ETS2 Augments <i>siah1</i> Transcription in <i>H. pylori</i> -Infected GCCs	73-75
3.8. ETS2 and Twist1 Enhance <i>siah2</i> Transcription in <i>H. pylori</i> -Infected GCCs	75-78
3.9. Discussion	78-79
Chapter 4. RESULTS	
4.1. Cloning of Human <i>siah1</i> Gene	81
4.2. Siah1 Mediates Degradation of Membrane-Bound β -catenin in <i>H. pylori</i> -Infected GCCs	82-88
4.3. Siah Induces Cell Migration and Invasion in <i>H. pylori</i> -Infected GCCs	88-93
4.4. ETS2 and Twist1 Induce Migration and Invasion of <i>H. pylori</i> -Infected GCCs	93-95
4.5. Discussion	95-97
Chapter 5. SUMMARRY AND CONCLUSION	99-100
BIBLIOGRAPHY	102-118
APPENDIX	119-131
PUBLICATIONS	



Homi Bhabha National Institute

Ph. D. PROGRAMME

- | | | |
|---|---|---|
| 1. Name of the Student | : | Lopamudra Das |
| 2. Name of the Constituent Institution | : | National Institute of Science Education and
Research (NISER) |
| 3. Enrolment no | : | LIFE11201004002 |
| 4. Title of the thesis | : | Regulation and Role of Siah Proteins in
<i>Helicobacter pylori</i> -Mediated Gastric
Cancer |
| 5. Board of studies | : | Life Sciences |

SYNOPSIS

Understanding the role of Siah Proteins and its regulation during *Helicobacter pylori*-mediated gastric cancer is the primary objective of this thesis.

Ubiquitin-mediated proteasomal degradation pathways control protein structure, function, assembly, localization as well as denaturation [1]. This pathway involves a series of enzymatic reactions catalyzed by a cascade of enzymes, *i.e.* E1 ubiquitin-activating enzymes, E2 ubiquitin-conjugating enzymes and E3 ubiquitin-ligase enzyme that causes transfer of E2-linked ubiquitin to a Lys residue of a targeted protein. The tagged proteins get degraded either by the 26S proteasome or by the lysosome [2]. The importance of E3 ligase lies in that it confers specificity to ubiquitination by identifying the target proteins and thus acts as a mediator for transfer of ubiquitin from an E2 ubiquitin-conjugating enzyme to the target protein [1]. The really interesting new gene (RING) family of E3 ubiquitin ligases play crucial role in regulating cancer progression and metastasis for adenocarcinoma [3] and have drawn attention as potential drug targets [4]. The evolutionarily conserved seven in absentia homolog (Siah) proteins belong to the RING family of E3 ubiquitin ligases. So far three *siah* genes have been identified in human *i.e.* *siah-1*, *siah-2* and *siah-3* [5, 6]. There are no reports on the role of Siah3 in cancer progression whereas the other two Siah proteins were shown to interact with and regulate the stability of multiple factors involved in oncogenesis including prolyl hydroxylases, β -catenin, NUMB, tumour necrosis factor receptor 2-associated factor and Sprouty [7-11]. Induced expression of Siah proteins in various cancers supports their tumour-promoting role [12-16]. Moreover, elevated level of Siah2 expression in breast, prostate and liver cancer cells has been linked with malignancy and cancer invasiveness [12, 13]. But limited number of studies are available that explored role of Siah proteins in gastric cancer progression. Gastric cancer is the most common malignant cancer and is a leading cause of cancer-related mortality. Due to its complex initiation and progression mechanism it

is generally diagnosed at later stages when the cancer has already started metastasizing [17, 18]. Infection with *H. pylori* is the prime factor responsible for gastric cancer. *H. pylori* colonizes nearly half of the world population and has been recognized as a type I carcinogen for gastric cancer [19]. Therefore, understanding the role of Siah proteins in the complex process of gastric cancer progression and metastasis is imperative in the *H. pylori*-infected gastric epithelium. It is interesting to identify transcription factors regulating expression of Siah proteins as there are very few reports. So far, Siah1 has been mainly reported as a tumour-suppressor but Siah2 has been portrayed as a tumour-promoting agent. This discrepancy in function suggests that a Siah1 and Siah2 might have different set of downstream target proteins modulating various signalling network [20]. Hence, identifying the regulation of Siah protein expression and in-depth understanding of their functions during gastric cancer progression are important. This thesis work focuses to understand the role of Siah proteins and their regulation during *H. pylori*-mediated gastric cancer progression. This thesis has been structured into five chapters and contents of each chapter have been discussed briefly as follows.

Chapter 1: Introduction:

This is the introductory section of the thesis that includes a review of literature on role of *H. pylori* in gastric cancer. A discussion on the cell-cell attachment complex on the cell membrane, followed by literature studies on the degradation of membrane-bound β -catenin during *H. pylori* infection and its role in cell migration is explained in this chapter. Focus is given on elaborating E3 ubiquitin ligases and Siah proteins belonging to the RING finger family of ubiquitin ligases. This chapter collates the current understanding on Siah proteins during cancer progression and its potential as a potential target for therapy.

Chapter 2: Experimental procedures

Chapter 2 includes description of various strains of *H. pylori*, gastric cancer cell lines, reagents, chemicals, tissue samples used for completion of the thesis work. It also includes the details of experimental procedures/methodologies employed to complete the objectives of this thesis. This chapter illustrates the culture techniques used for various gastric epithelial cell lines and *H. pylori* as well as method of infecting cell lines with *H. pylori*.

This chapter also includes description of several molecular biology techniques used for the study. Cloning of human *siah1* gene into the mammalian expression vector pcDNA3.1⁺, cloning of human *siah1* and *siah2* promoters in the pGL3 basic (luciferase reporter vector) and mutation at the ETS2-binding site for human *siah1* promoter and mutation at the ETS2 and Twist1-binding sites for the human *siah2* promoter using site-directed mutagenesis are explained. The procedure for examining the mRNA status is also incorporated in this chapter. The detailed methodology to examine protein expressions using techniques such as immunoblotting, immunoprecipitation, fluorescence microscopy and confocal microscopy are elucidated. Methods for *in vitro* DNA-protein binding assay, chromatin immunoprecipitation assay and dual luciferase assay are also included in this chapter.

Detailed procedures for generation of stable cell lines expressing Siah1, Siah2, ETS2 and Twist1 are explained in this chapter. Cell migration and invasiveness, as assessed by wound healing assay, soft agar assay, transwell migration and invasion assays are illustrated in this chapter. Methods employed to study human gastric biopsy samples using fluorescence microscopy are included in this chapter.

Chapter 3: Transcriptional regulation of Siah proteins in *H. pylori*-infected human gastric cancer cells (GCCs)

This chapter describes the status of Siah1 and 2 proteins in *H. pylori*-infected GCCs. Transcription factors regulating Siah expression has also not been studied in *H. pylori*-

infected GCCs. Analysis has been performed with Siah1 5' UTR and Siah2 promoter using bioinformatics tool such as MatInspector (professional version 6.2.2). ETS2 is implicated in having very high probability of binding to Siah1 5' UTR whereas ETS2 and Twist1 both are shown to have very high probability of binding to Siah2 promoter. The metastasis promoting role of Twist1 has been reported in various cancers [21, 22] including gastric cancer [23] while enhancement of lymph node and distant metastases are reported in Twist1-expressing gastric cancer cells [24]. So far, ETS2 has been linked with increased apoptosis or tumour suppression in gastric cancer [25]. This chapter experimentally proves that ETS2 and Twist1 mediate *H. pylori*-induced Siah2 expression and ETS2 is the transcriptional regulator of Siah1.

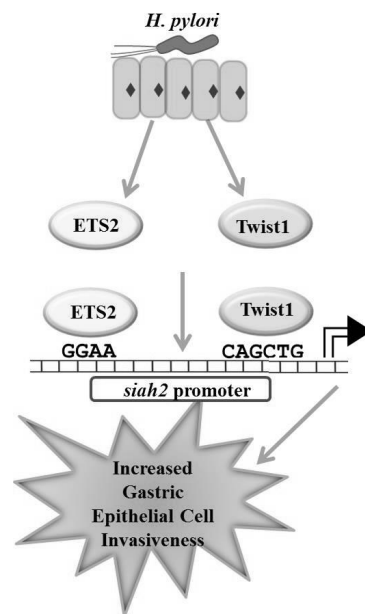
Chapter 4: Role of Siah proteins in inducing gastric cancer metastasis

H. pylori induce inflammatory responses and neoplastic changes owing to the loss of the epithelial barrier function of the gastric epithelium accompanied by loss of epithelial cell morphology and cell to cell adhesions [26]. The membrane-bound cadherin-catenin complex is responsible for cell-cell adhesion. The other pool of β -catenin is in the cytosolic compartment. The membrane-bound β -catenin is an integral component of the adherens junctions linking cadherin receptors with the actin cytoskeleton while the nonmembranous cytoplasmic-nuclear pool play a role in Wnt signalling [27]. Chapter 4 describes studies related to ETS2-mediated Siah1 induction resulting in degradation of membrane-bound β -catenin in *H. pylori*-infected gastric cancer cells. Induced expression of Siah1 protein is observed after infection in gastric cancer cell lines. Here we report for the first time that the membrane-bound β -catenin is a target of proteasomal degradation mediated by Siah1. We show that following *H. pylori* infection, Siah1 is upregulated in the cytosolic fraction but it does not degrade the cytosolic β -catenin. Surprisingly, a decrease in membrane-bound β -catenin is noticed in the infected gastric cancer cells. *H. pylori*-mediated degradation of β -

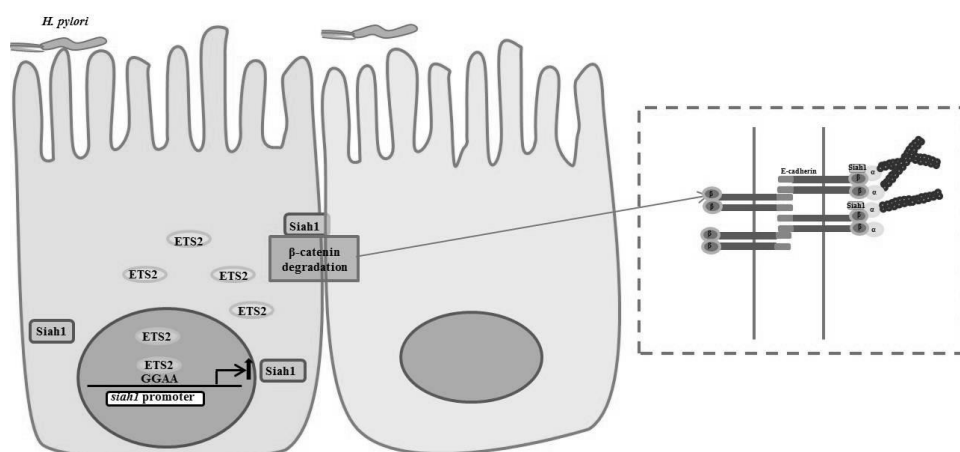
catenin is further enhanced in gastric cancer cells with ectopic expression of Siah1. Furthermore, we notice that Siah1 overexpression significantly enhance the ability of cell migration and invasiveness. ETS2-mediated Siah2 induction also shows an increase in cell invasiveness and migration with *H. pylori* infection in GCCs.

Chapter 5: Summary and conclusion

Chapter 5 presents concluding remarks on our findings which demonstrate crucial roles of Siah proteins during *H. pylori* infection in gastric cancer cells promoting invasion and migration. Our studies also indicate ETS2-mediated induction of Siah1 and ETS2 and Twist1-mediated induction of Siah2 in *H. pylori*-infected gastric epithelial cancer cells. Furthermore, our findings provide an important insight towards the fact that although Siah1 and Siah2 are induced by ETS2 and have roles in gastric cancer metastasis, their cellular targets are not the same. Thus, Siah1 and Siah2 are not showing functional redundancy at least in promoting gastric cancer.



Summary Figure: Mechanism of Siah2 induction and degradation of membrane bound β -catenin during *H. pylori* infection. *H. pylori* infection induces ETS2 and Twist1 expression in gastric epithelial cells. ETS2 and Twist1 bind to the *siah2* promoter and mediate Siah2 expression in *H. pylori*-infected in gastric cancer cells. Induced expression of Siah2 enhances metastatic properties of gastric cancer cells.



Summary Figure: Siah1 induced in *H. pylori*-infected gastric cancer cell degrades membrane bound β-catenin. *H. pylori* infection induces ETS2 expression. ETS2 binds to the siah1 promoter and promotes Siah1 transcription in *H. pylori*-infected gastric cancer cells. Induced expression of Siah1 results in the degradation of membrane bound β-catenin. As a result, infected cells become more migratory and invasive.

References:

- [1] A. Ciechanover, The ubiquitin-proteasome pathway: on protein death and cell life, The EMBO journal, 17 (1998) 7151-7160.
- [2] D. Rotin, S. Kumar, Physiological functions of the HECT family of ubiquitin ligases, Nature reviews. Molecular cell biology, 10 (2009) 398-409.
- [3] S.C. Pavlides, K.T. Huang, D.A. Reid, L. Wu, S.V. Blank, K. Mittal, L. Guo, E. Rothenberg, B. Rueda, T. Cardozo, L.I. Gold, Inhibitors of SCF-Skp2/Cks1 E3 ligase block estrogen-induced growth stimulation and degradation of nuclear p27kip1: therapeutic potential for endometrial cancer, Endocrinology, 154 (2013) 4030-4045.
- [4] M. Shen, S. Schmitt, D. Buac, Q.P. Dou, Targeting the ubiquitin-proteasome system for cancer therapy, Expert Opin Ther Targets, 17 (2013) 1091-1108.
- [5] S.A. Hasson, L.A. Kane, K. Yamano, C.H. Huang, D.A. Sliter, E. Buehler, C. Wang, S.M. Heman-Ackah, T. Hessa, R. Guha, S.E. Martin, R.J. Youle, High-content genome-wide

RNAi screens identify regulators of parkin upstream of mitophagy, *Nature*, 504 (2013) 291-295.

[6] J. Qi, H. Kim, M. Scortegagna, Z.A. Ronai, Regulators and effectors of Siah ubiquitin ligases, *Cell biochemistry and biophysics*, 67 (2013) 15-24.

[7] H. Habelhah, I.J. Frew, A. Laine, P.W. Janes, F. Relaix, D. Sassoon, D.D. Bowtell, Z. Ronai, Stress-induced decrease in TRAF2 stability is mediated by Siah2, *The EMBO journal*, 21 (2002) 5756-5765.

[8] S.I. Matsuzawa, J.C. Reed, Siah-1, SIP, and Ebi collaborate in a novel pathway for beta-catenin degradation linked to p53 responses, *Molecular cell*, 7 (2001) 915-926.

[9] R.J. Nadeau, J.L. Toher, X. Yang, D. Kovalenko, R. Friesel, Regulation of Sprouty2 stability by mammalian Seven-in-Absentia homolog 2, *J Cell Biochem*, 100 (2007) 151-160.

[10] K. Nakayama, I.J. Frew, M. Hagensen, M. Skals, H. Habelhah, A. Bhoumik, T. Kadoya, H. Erdjument-Bromage, P. Tempst, P.B. Frappell, D.D. Bowtell, Z. Ronai, Siah2 regulates stability of prolyl-hydroxylases, controls HIF1alpha abundance, and modulates physiological responses to hypoxia, *Cell*, 117 (2004) 941-952.

[11] L. Susini, B.J. Passer, N. Amzallag-Elbaz, T. Juven-Gershon, S. Prieur, N. Privat, M. Tuynnder, M.C. Gendron, A. Israel, R. Amson, M. Oren, A. Telerman, Siah-1 binds and regulates the function of Numb, *Proc Natl Acad Sci U S A*, 98 (2001) 15067-15072.

[12] M. Malz, A. Aulmann, J. Samarin, M. Bissinger, T. Longerich, S. Schmitt, P. Schirmacher, K. Breuhahn, Nuclear accumulation of seven in absentia homologue-2 supports motility and proliferation of liver cancer cells, *International journal of cancer*, 131 (2012) 2016-2026.

[13] J. Qi, K. Nakayama, R.D. Cardiff, A.D. Borowsky, K. Kaul, R. Williams, S. Krajewski, D. Mercola, P.M. Carpenter, D. Bowtell, Z.A. Ronai, Siah2-dependent concerted activity of

HIF and FoxA2 regulates formation of neuroendocrine phenotype and neuroendocrine prostate tumors, *Cancer Cell*, 18 (2010) 23-38.

[14] J. Qi, K. Nakayama, S. Gaitonde, J.S. Goydos, S. Krajewski, A. Eroshkin, D. Bar-Sagi, D. Bowtell, Z. Ronai, The ubiquitin ligase Siah2 regulates tumorigenesis and metastasis by HIF-dependent and -independent pathways, *Proc Natl Acad Sci U S A*, 105 (2008) 16713-16718.

[15] A.U. Ahmed, R.L. Schmidt, C.H. Park, N.R. Reed, S.E. Hesse, C.F. Thomas, J.R. Molina, C. Deschamps, P. Yang, M.C. Aubry, A.H. Tang, Effect of disrupting seven-in-absentia homolog 2 function on lung cancer cell growth, *J Natl Cancer Inst*, 100 (2008) 1606-1629.

[16] P. Chan, A. Moller, M.C. Liu, J.E. Sceneay, C.S. Wong, N. Waddell, K.T. Huang, A. Dobrovic, E.K. Millar, S.A. O'Toole, C.M. McNeil, R.L. Sutherland, D.D. Bowtell, S.B. Fox, The expression of the ubiquitin ligase SIAH2 (seven in absentia homolog 2) is mediated through gene copy number in breast cancer and is associated with a basal-like phenotype and p53 expression, *Breast Cancer Res*, 13 (2011) R19.

[17] A. Jemal, R. Siegel, E. Ward, Y. Hao, J. Xu, T. Murray, M.J. Thun, Cancer statistics, 2008, *CA Cancer J Clin*, 58 (2008) 71-96.

[18] S. Tsugane, S. Sasazuki, Diet and the risk of gastric cancer: review of epidemiological evidence, *Gastric Cancer*, 10 (2007) 75-83.

[19] C. de Martel, J. Ferlay, S. Franceschi, J. Vignat, F. Bray, D. Forman, M. Plummer, Global burden of cancers attributable to infections in 2008: a review and synthetic analysis, *The Lancet. Oncology*, 13 (2012) 607-615.

[20] C.S. Wong, A. Moller, Siah: a promising anticancer target, *Cancer research*, 73 (2013) 2400-2406.

- [21] M. Shiota, A. Zardan, A. Takeuchi, M. Kumano, E. Beraldi, S. Naito, A. Zoubeidi, M.E. Gleave, Clusterin mediates TGF-beta-induced epithelial-mesenchymal transition and metastasis via Twist1 in prostate cancer cells, *Cancer research*, 72 (2012) 5261-5272.
- [22] M. Croset, D. Goehrig, A. Frackowiak, E. Bonnelye, S. Ansieau, A. Puisieux, P. Clezardin, TWIST1 expression in breast cancer cells facilitates bone metastasis formation, *J Bone Miner Res*, 29 (2014) 1886-1899.
- [23] Z. Yang, X. Zhang, H. Gang, X. Li, Z. Li, T. Wang, J. Han, T. Luo, F. Wen, X. Wu, Up-regulation of gastric cancer cell invasion by Twist is accompanied by N-cadherin and fibronectin expression, *Biochemical and biophysical research communications*, 358 (2007) 925-930.
- [24] G.Q. Ru, H.J. Wang, W.J. Xu, Z.S. Zhao, Upregulation of Twist in gastric carcinoma associated with tumor invasion and poor prognosis, *Pathology oncology research : POR*, 17 (2011) 341-347.
- [25] Y.L. Liao, L.Y. Hu, K.W. Tsai, C.W. Wu, W.C. Chan, S.C. Li, C.H. Lai, M.R. Ho, W.L. Fang, K.H. Huang, W.C. Lin, Transcriptional regulation of miR-196b by ETS2 in gastric cancer cells, *Carcinogenesis*, 33 (2012) 760-769.
- [26] P. Correa, M.B. Piazuelo, *Helicobacter pylori* Infection and Gastric Adenocarcinoma, *US gastroenterology & hepatology review*, 7 (2011) 59-64.
- [27] B. Baum, M. Georgiou, Dynamics of adherens junctions in epithelial establishment, maintenance, and remodeling, *The Journal of cell biology*, 192 (2011) 907-917.

ABBREVIATIONS

AJs	Adherens junction
AlpA/B	Adherence-associated lipoprotein A and B
APS	Ammonium persulfate
ATP	Adenosine tri phosphate
BabA	Blood group antigen-binding adhesin
BARD1	Breast cancer1-associated RING domain 1
bp	Base pair
BMI1	B-cell-specific moloney murine leukaemia virus integration site 1
BIRC2	Baculoviral IAP repeat-containing protein2
BRCA1	Breast cancer1
BSA	Bovine serum albumin
C-terminal	Carboxyl terminal
C/EBP δ	CCAAT/enhancer-binding protein delta
<i>cag</i>	Cytotoxin-associated gene
Cbl	Casitas B-lineage lymphoma
ccRCC	Clear-cell renal cell carcinoma
CER	Cytoplasmic extraction reagent
ChIP	Chromatin immunoprecipitation
CNRs	Cadherin-related neuronal receptor
CO ₂	Carbon dioxide
CP	Core particle
CRL	Cullin RING ligases
Cys	Cysteine
DUB	Deubiquitinating enzymes

DMSO	Dimethyl sulfoxide
Dvl	Dishevelled
EBS	ETS2 binding site
E-cadherin	Epithelial cadherin
EDTA	Ethylene-diamine-tetra-acetic acid
EMT	Epithelial-mesenchymal transition
FBS	Fetal bovine serum
FZD	Cell surface receptor Frizzled
GCCs	Gastric cancer cells
Gly	Glycine
<i>H. pylori</i>	<i>Helicobacter pylori</i>
HCC	Hepato cellular carcinoma
HDAC	Histone deacetylase
HECT	Homology to E6-associated protein carboxyl terminus
HIF1 α	Hypoxia-inducible factor1 α
His	Histidine
HopO	<i>Helicobacter</i> -specific outer membrane proteins O
HopQ	<i>Helicobacter</i> -specific outer membrane proteins Q
HopZ	<i>Helicobacter</i> -specific outer membrane proteins Z
HpaA	<i>H. pylori</i> adhesion A
HRP	Horse radish peroxidase
Hsp60	Heat shock protein 60
HtrA	High temperature requirement A
IceA	Induced by contact with epithelium A
IHC	Immunohistochemistry

IL	Interleukin
IP	Immunoprecipitation
IRAC	The international agency for research on cancer
kb	Kilo base
kDa	Kilo Dalton
LAR	Luciferase assay reagent
LEF	Lymphoid Enhancer Factor
Lys	Lysine
LRP5/6	Low Density Lipoprotein Receptor-Related Protein 5/6
MALT	Mucosa-associated lymphoid tissue
MAPK	Mitogen-activated protein kinases
MDCK	Madin Darby canine kidney
MDM2	Murine double minute2
MMPs	Matrix metalloprotease
MOI	Multiplicity of infection
Mut	Mutant
N-terminal	Amino terminal
Nap	Neutrophil activating protein
NER	Nuclear extraction reagent
NFDM	Non-fat dry milk
OipA	Outer inflammatory protein A
PAGE	Polyacrlamide gel electrophoresis
PAI	Pathogenicity island
PBS	Phosphate-buffered saline
PFA	Paraformaldehyde

PHD	Plant homeo-domain
PVDF	Polyvinylidene fluoride
pVHL	von Hippel-Lindau tumor-suppressor protein
RING	Really interesting new gene
RNF4	RING finger protein4
RP	Regulatory particle
RT	Room temperature
RT-PCR	Reverse transcription polymerase chain reaction
SabA	Sialic acid-binding adhesion
SIAH	Seven in absentia homolog
SIP	Siah-interactin protein
siRNA	Short interfering RNA
SDS	Sodium dodecyl sulfate
β -TrCP	β -Transducin repeat-Containing Protein
TAE	Tris-acetate buffer
TBS	Tris-buffered saline
TBS	Twist1 binding site
TCF4	T cell factor4
TE	Tris-EDTA
T4SS	Type IV secretion system
TJs	Tight junctions
TLR	Toll-like receptor
TNF	Tumor necrosis factor
TRAF	TNF receptor associated factor
TRIM	Tripartite motiff

TSA	Tripticase soy agar
Tyr	Tyrosine
VacA	Vacuolating cytotoxin geneA
VHL	von Hippel-Lindau
WT	Wild type
ZO-1	Zona occludens 1

LIST OF FIGURES

	Description	Page No.
Chapter 1		
Figure 1.1.1	The ubiquitin-proteasome pathway	4
Figure 1.1.2	Types of E3 ubiquitin ligases	5
Figure 1.3.1	The RING domain structure of Siah proteins	7
Figure 1.4.1	The mechanism of metastasis progression	10
Figure 1.5.1.1	Disease <i>pathogenesis</i> by <i>H. pylori</i>	12
Figure 1.5.3.1	<i>Major virulence factors of H. pylori</i>	15
Figure 1.6.1.1	Adherens junction of epithelial cell	17
Figure 1.6.2.1	Cadherin bound β -catenin in cell-cell adhesion and cytoplasmic β -catenin in Wnt signalling	19
Figure 1.6.2.2	Disruption of epithelial junction by <i>H. pylori</i>	20
Chapter 3		
Figure 3.1.1	<i>H. pylori</i> induce Siah1 and Siah2 protein expression in MKN45 cells	57-58
Figure 3.1.2	<i>H. pylori</i> enhances Siah1 and Siah2 mRNA and proteins expression in GCCs	59-60
Figure 3.2.1	Analysis of human <i>siah1</i> promoter and 5'UTR	61
Figure 3.2.2	Sequence analysis of human <i>siah2</i> promoter	62
Figure 3.3.1	<i>H. pylori</i> infection induces parallel expression of ETS2, Twist1, Siah1 and Siah2 proteins in MKN45 cells	63-64
Figure 3.3.2	<i>H. pylori</i> infection induces ETS2, Twist1, Siah1 and Siah2 proteins in MKN45 cells	65
Figure 3.3.3	<i>H. pylori</i> infection induces ETS2 and Twist1 expression in GCCs	66-67

Figure 3.3.4	Coexistence of ETS2, Twist1, Siah1 and Siah2 proteins in human gastric adenocarcinoma biopsy sample	67-68
Figure 3.4.1	Binding of ETS2 with the EBS of <i>siah1</i> 5' UTR after <i>H. pylori</i> -infection	69
Figure 3.5.1	ETS2 binds with the EBS and Twist1 binds with the TBS of <i>siah2</i> promoter after <i>H. pylori</i> -infection	71
Figure 3.6.1	Cloning of human <i>siah1</i> 5'UTR and <i>siah2</i> promoter	72-73
Figure 3.7.1	ETS2 enhances <i>siah1</i> transcription in <i>H. pylori</i> -infected GCCs	74
Figure 3.7.2	ETS2 enhances Siah1 protein expression in <i>H. pylori</i> -infected GCCs	75
Figure 3.8.1	ETS2 and Twist1 augment <i>siah2</i> transcription in <i>H. pylori</i> -infected GCCs	76
Figure 3.8.2	ETS2 and Twist1 augment <i>siah2</i> transcription and expression in <i>H. pylori</i> -infected GCCs	77-78
Chapter 4		
Figure 4.1.1	Cloning of human <i>siah1</i> gene	81
Figure 4.2.1	Degradation of membrane-bound β -catenin in <i>H. pylori</i> -infected GCCs	83-84
Figure 4.2.2	Siah-mediated degradation of membrane-bound β -catenin in <i>H. pylori</i> -infected GCCs	85-86
Figure 4.2.3	Siah1 binds to membrane-bound β -catenin in <i>H. pylori</i> -infected GCCs and status of membrane bound E-cadherin in <i>H. pylori</i> -infected GCCs	87-88
Figure 4.3.1	Elevated Siah expression enhances cell motility and wound-healing property in <i>H. pylori</i> -infected GCCs	89
Figure 4.3.2	Elevated Siah expression enhances cell migration and	

	Invasiveness of <i>H. pylori</i> -infected GCCs	90-91
Figure 4.3.3	Siah suppression reduces cell migration and invasiveness of <i>H. pylori</i> -infected GCCs	91-93
Figure 4.4.1	ETS2 and Twist 1 enhances cell motility, wound-healing and invasive property of <i>H. pylori</i> -infected GCCs	93-95

LIST OF TABLES

	Description	Page No.
Table 1.	Parameters for transient transfection	36
Table 2.	Reagents used for cell fractionation using NE-PER kit	38

INTRODUCTION

Chapter 1

INTRODUCTION

1.1. Ubiquitination and Ubiquitin-Mediated Proteasomal Degradation

Protein ubiquitination involves attachment of ubiquitin to targeted proteins which subsequently leads to regulation of many cellular processes. Ubiquitinated proteins can be targeted for degradation or they can regulate cell cycle and growth, or take part in intracellular trafficking, as well as localization [1]. Ubiquitin is a small protein (seventy six amino acid) modifier which is highly conserved and found only in eukaryotic system.

Ubiquitin has seven Lys residues (Lys⁶, Lys¹¹, Lys²⁷, Lys²⁹, Lys³³, Lys⁴⁸ and Lys⁶³). Homotypic or heterotypic linkages of proteins with Lys residues of ubiquitin determine the fate of proteins. Polyubiquitination leads to proteasomal degradation of target proteins [2]. Polyubiquitinated proteins are targeted for degradation by the 26S proteasome pathway. The 26S proteasome complex is highly conserved in eukaryotes in terms of its structure and function. This complex consists of a barrel-shaped 20S protease core particle (CP) in the middle part [3]. The CP consists of two identical inner β and outer α units stacked on one another forming an axial heptameric ring. The central β -ring is formed of seven different β -subunits β 1–7, and the peripheral α -ring is also formed of seven different α -subunits, α 1–7 [3]. The 19S regulatory particle (RP) forms a cap at each end of the 20S CP. The 19S RP can be further divided into the base and lid (sub complexes). The 19S RP regulates the proteolytic function of the core protease [3]. Attachment of ubiquitin to the target protein is a reversible process mediated by specific ubiquitin ligases and proteases {known as deubiquitinating enzymes (DUBs)}. DUBs counteract activity of specific ubiquitin ligases by removing ubiquitin and editing ubiquitin chains. DUBs also maintain free ubiquitin monomers in the cellular pool [4].

Ubiquitination of targeted proteins involves a series of enzymatic reactions catalyzed by a cascade of enzymes. Ubiquitin molecules get covalently attached to the target protein

and tagged proteins get degraded either by the 26S proteasome or by the lysosome [5]. Ubiquitin conjugation to the target proteins involves E1 ubiquitin-activating enzymes that activate ubiquitin at its C-terminal Gly through a thio-ester bond in an ATP-dependent manner. At first, transfer of activated ubiquitin to Cys residues of E2 ubiquitin-conjugating enzymes takes place. E3 ubiquitin-ligase enzyme causes transfer of E2-linked ubiquitin to a Lys residue of a targeted protein. As illustrated in fig. 1.1.1. The importance of E3 ligase is that it confers specificity to ubiquitination by identifying target proteins and thus acts as a mediator for transfer of ubiquitin from an E2 ubiquitin-conjugating enzyme to the target protein [1]. E3 ubiquitin-ligases either exist as single polypeptides or in multimeric complexes [1]. They are classified into three distinct types based on recognition of substrate specificity and structure of the domains: N-end rule E3s specifically targeting protein substrates bearing destabilizing N-terminal residues; E3s containing the homology to E6-associated protein (E6AP) carboxyl terminus (HECT) domain and E3s with the really interesting new gene (RING) finger, including its derivatives, the U-box and the plant homeo-domain (PHD) [6]. Over six hundred E3s are encoded by the human genome [6]

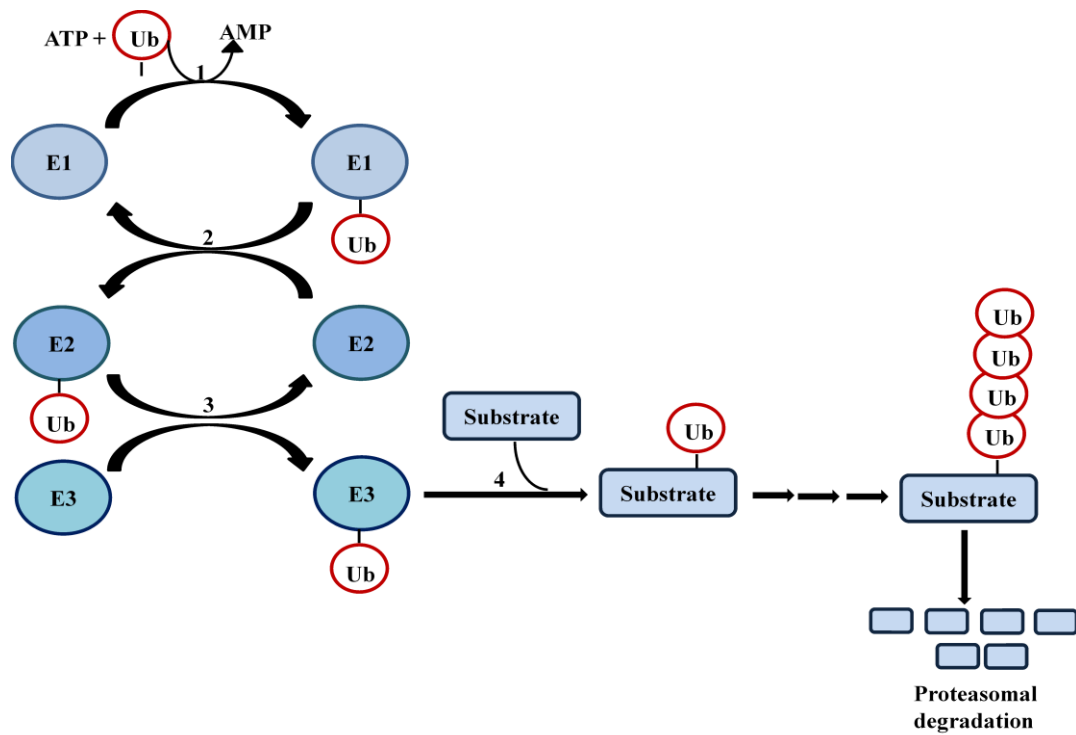


Figure 1.1.1 The ubiquitin-proteasome pathway

The RING type and the HECT type are the two most commonly found E3s. Human E3s are dominated by the RING family members (nearly ninety five percent) and only twenty eight enzymes belong to the HECT family. The basic difference between these two families lies in the way of substrate presentation. The HECT type E3 forms an intermediate thioester bond with the C terminus of ubiquitin of an E2 through a conserved Cys residue and then transfers that to the substrate. Whereas, the RING E3s are scaffold proteins that bring the E2s in close proximity to their substrates to aid in ubiquitin transfer [5]. As demonstrated in figure 1.1.2. RING E3s are elaborately discussed in the next section.

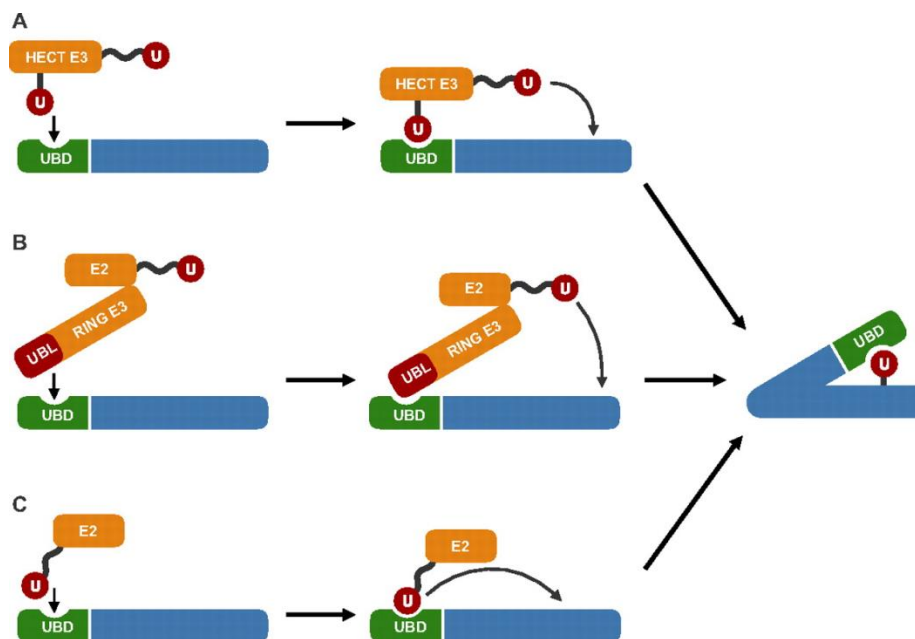


Figure 1.1.2 Types of E3 ubiquitin ligases (Courtesy Ref: [7])

1.2. RING Type E3 Ubiquitin Ligases and their Involvement in Human Cancers

RING domain E3 ubiquitin ligases form the largest family of human E3 ubiquitin ligases. Members of this family contain a classic $C_3H_2C_3$ or C_3HC_4 RING (that is, three conserved Cys residues followed by two conserved His and then three additional conserved Cys or three conserved Cys residues followed by a conserved His and then four additional conserved Cys) finger domain with a characteristic linear sequence of Cys- X_2 -Cys- X_{9-39} -Cys- X_{1-3} -His- X_{2-3} -Cys/His- X_2 -Cys- X_{4-48} -Cys- X_2 -Cys, where X stands for any amino acid [8]. A typical RING finger consists of Zn^{2+} -coordinating domain with Cys and His residues spaced sequentially, and aids in E2-dependent ubiquitination of targeted substrate [9].

Monomers, dimers or multi-subunit complex family members exist within the RING finger family. Homodimers and heterodimers are formed due to dimerization of the RING finger domains or neighbouring regions. Homodimer RING finger E3s include cellular inhibitor of apoptosis or BIRC2 (cIAP), RNF4, seven in absentia homologue (Siah), and TNF receptor associated factor 2 (TRAF2) [10-12]. Heterodimeric family members include murine double minute 2 (MDM2), also known as HDM2 in human and MDMX or MDM4 (HDMX

or HDM4 in human), breast cancer 1 (BRCA1) and BRCA1-associated RING domain 1 (BARD1), RING1b (known as RNF2) and B-cell-specific moloney murine leukaemia virus integration site 1 (BMI1) [13, 14]. For heterodimers, one RING domain is used to stabilize the active E2-binding RING domain and generally lacks ligase activity. The cullin RING ligase (CRL) superfamily belongs to multi-subunit RING E3s [15].

Members of the RING family E3 ubiquitin ligases play important roles in many biological processes including DNA repair, cell cycle, apoptosis pathway, lysosome degradation, and angiogenesis [9]. Several members of these subfamilies have been associated with various disease pathogenesis including cancer. RING finger E3 ubiquitin ligases have been implicated either as oncogenes or as tumor suppressors. Many members of CRL superfamily have been linked to tumor progression including breast cancer, skin cancer, colorectal cancer and gastric cancer [16]. Likewise various members of the tripartite motif (TRIM) superfamily are also known for regulating cancer progression. The tumor suppressor BRCA1 is often mutated in breast and ovarian cancer [17]. Cbl, Cbl-b, and Cbl-c are members of casitas B-lineage lymphoma (Cbl) RING ubiquitin ligase family that have been implicated in myeloid lymphoma, breast cancer, gastric cancer, and lung cancer [18-22]. The oncoprotein MDM2 is upregulated in many cancers targeting ubiquitin-mediated degradation of tumor-suppressor protein p53 [23].

Metastasis is a critical event during cancer progression and is the foremost causes of cancer-related mortality. Tumor microenvironment plays a crucial role in metastasis progression and one such key factor is hypoxia or low oxygen tension [24]. During hypoxia, the RING finger E3 ubiquitin ligase von Hippel-Lindau (VHL) tumor suppressor protein (pVHL) is found to be inactivated in clear-cell renal cell carcinoma (ccRCC), thus activating the hypoxia pathway via hypoxia inducible factor1 α (HIF1 α) [25]. Another class of RING

finger E3 ubiquitin ligases regulating HIF1 α stability are the Siah proteins. The role of Siah proteins in cancer progression and metastasis are elaborated here.

1.3. Siah Proteins and their Roles in Cancer Progression

Human homolog of the *Drosophila* seven in absentia (*sina*) protein Siah superfamily of RING finger E3 ubiquitin ligases has three members- Siah1, Siah2 and Siah3. Structural analysis of highly conserved Siah proteins reveals that these are dimeric proteins with two novel zinc fingers. A Siah protein has a divergent N-terminal with a highly conserved catalytic RING domain and a substrate-binding domain at the C-terminal. As shown in figure 1.3.1. The substrate-binding domain show structural homology with tumor necrosis factor (TNF) receptor associated factor (TRAF) proteins [12]. More than 30 diverse substrates have been identified that interact with Siah proteins. Siah proteins can either directly interact with their substrates or require adaptor proteins such as siah-interacting protein (SIP) for interaction [26, 27]. Thus, Siah proteins regulate a number of fundamental cellular processes including protein degradation, angiogenesis, inflammation, cell proliferation, cell migration and apoptosis [28-32] and therefore, play critical roles in maintaining cellular homeostasis.

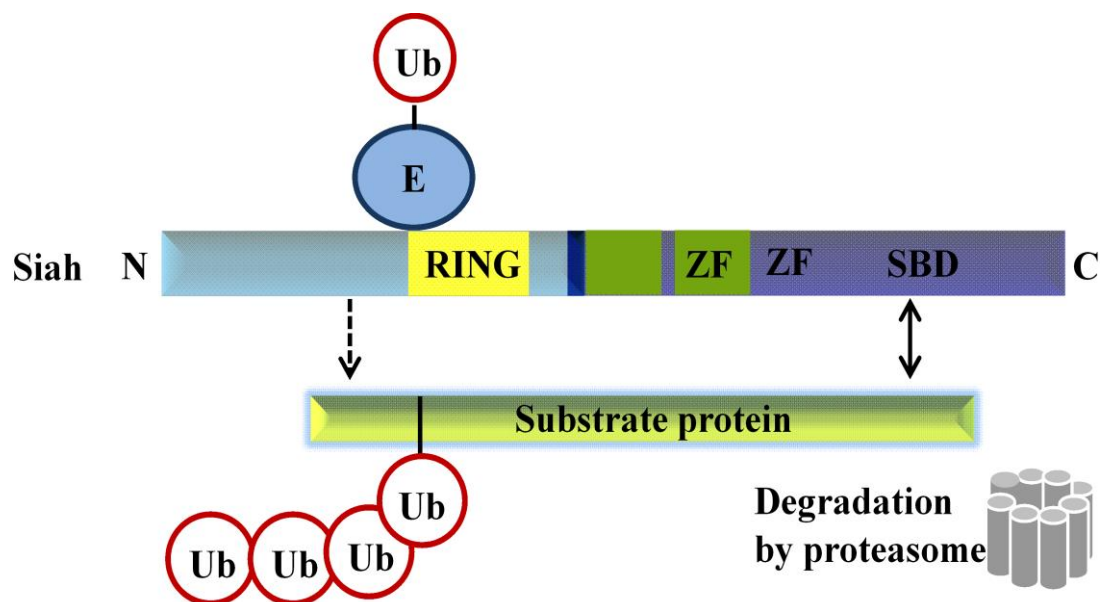


Figure 1.3.1 The RING domain structure of Siah proteins

Siah1 and Siah2 proteins regulate the stability of several oncogenic factors such as prolyl hydroxylases, β -catenin, NUMB, TRAF2, Sprouty2, and CCAAT/enhancer-binding protein delta (C/EBP δ) [26, 27, 33-35]. Specifically in hypoxic microenvironment, Siah2 regulates the hippo signalling pathway that plays a critical role in tissue growth and results in survival and growth of hypoxic tumor cells [36]. Siah3, the newest member in the Siah family, however, has not been functionally characterized yet. Siah1 and Siah2 have oncogenic functions in animal models, while *in vitro* cell-based assays suggest tumor-promoting roles for Siah2 and apoptosis-inducing role for Siah1 [37]. As both proteins have structural similarity, they often show functional redundancy. As a result, some substrates are targeted by both Siah proteins while some are targeted by one and not by the other. This redundancy can be attributed to either post-translational modification of these proteins or their subcellular localization. [37].

In spite of the increasing research interest on Siah proteins, there are very few reports on their transcriptional regulation during disease processes including cancer. Siah2 is transcriptionally upregulated by estrogen in estrogen-responsive breast cancer [38]. Wnt5 α induces Siah2 expression in colon cancer cells [39]. Hypoxia, which is known to induce Siah2, [34] does so by inducing the p38 MAPK and Akt pathways [40, 41]. Siah1 is transcriptionally induced by E2F1, p53 and Sp1 and causes apoptosis [42, 43]. Surprisingly, there has not been any study to understand the mechanism of expression of Siah2 proteins in gastric cancer cells (GCCs), while only one study has shown that Siah1 has a rare inactivating mutation in gastric cancer tissue [44]. Thus, the role of Siah1 in regulating gastric cancer is not possibly limited to its tumor-suppressive role. This notion is further potentiated by studies on animal models which portray Siah1 as a tumor-promoter [37].

1.4. Gastric Cancer

Stomach cancer is the fifth lethal malignancy in the world and its poor prognosis makes it the third leading cause of cancer-related mortality [45]. Developing countries such as Asia, Latin America, central and eastern Europe have very high burden of gastric cancer as compared to the developed countries like North America and western Europe where it is no longer a common cancer [46]. It is twice more prevalent in males in the developing countries as compared to females [47]. *Helicobacter pylori* (*H. pylori*) infection is considered as the greatest risk factor for causing gastric carcinogenesis along with environmental factors, host and bacterial genetic polymorphisms. Diet and smoking habit also play roles in causing this disease [48]. Adenocarcinoma is the most common type of stomach cancer originating from the glandular cells of the stomach lining. Lauren has classified adenocarcinoma into two types i.e. intestinal and diffuse according to the histological features [49].

More than 90% of gastric cancer-associated deaths can be attributed to metastasis [50]. This metastatic state is achieved by activation of epithelial to mesenchymal transition (EMT) programs in epithelial cells. At first, morphology of epithelial cells is changed, followed by loss of cell–cell adhesion along with remodelling of cell–matrix adhesion which results in dissemination of primary tumors to cause metastasis [51]. This mechanism is depicted in figure 1.4.1. The role of EMT in cancer cells are much more than invasion. These include increased cancer cell motility and enhanced resistance to senescence, chemotherapy and immunotherapy. It also allows cancer cells to avoid anoikis, oncogene-induced cell death, and overall immune defence. The next section would elaborately describe the role of *H. pylori* in gastric cancer progression and metastasis.

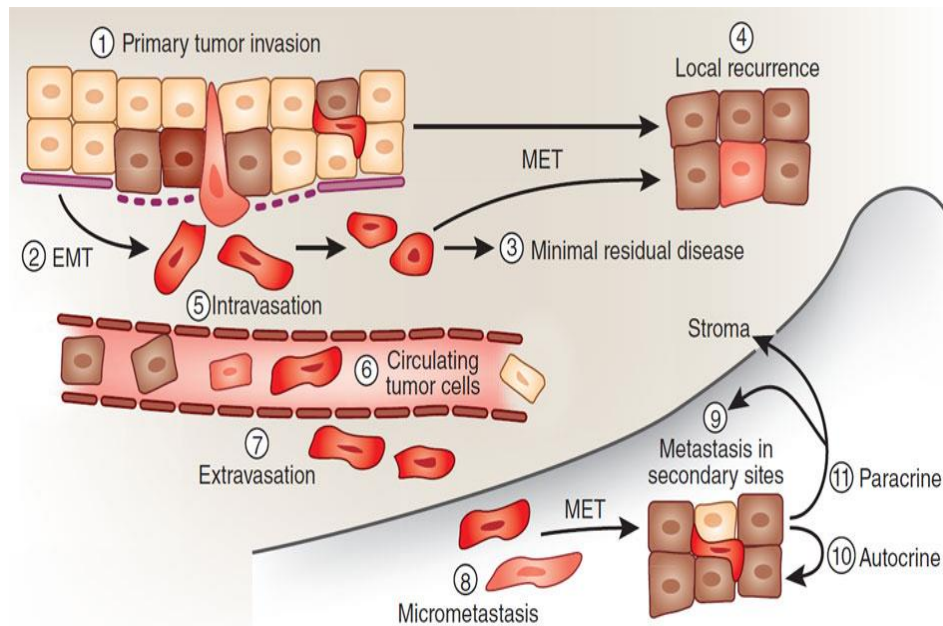


Figure 1.4.1 The mechanism of metastasis progression (Courtesy Ref: [52])

1.5. Gastric Carcinogenesis by *H. pylori*

1.5.1. Overview

In 1989 the first member under the newly formed genus *Helicobacter* was named *H. pylori* [53]. It is a spiral-shaped bacterium (0.5 x 5 µm in length) with a tuft of 5-7 polar sheathed flagella and is a non-spore forming, micro-aerophilic and Gram-negative human pathogen [54, 55]. It has colonized human stomach and has coexisted with humans for nearly thousand years [56] and its infection induce gastric inflammation, chronic gastritis and causes various diseases including peptic ulceration, mucosa-associated lymphoid tissue (MALT) lymphoma and gastric adenocarcinoma [57]. In 1994, the international agency for research on cancer (IARC) has recognized *H. pylori* as a type I carcinogenic pathogen for humans [57].

In 1984, Barry J Marshall and Robin Warren first cultured this bacterium from human gastric biopsies [58]. They found *H. pylori* infection to be the etiological agent for upper gastrointestinal diseases. Initially this organism was named *Campylobacter pyloridis* by Marshall *et al.* in 1984 and was subsequently renamed to *Campylobacter pylori* by Marshall *et al.* In 1987, owing to its dissemblance with the genus *Campylobacter*, it was finally

assigned to a new genus *Helicobacter* and was renamed as *Helicobacter pylori* in 1989 by Goodwin *et al* [53]. Half of the world's population are infected with *H. pylori* but only 3% of the infected individuals develop gastric cancer. In the majority of cases with *H. pylori* colonization there is an increase in inflammatory and immune responses against the bacteria and if untreated, the infection persists for decades. Infection with *H. pylori* can predispose to two equally exclusive conditions. In some cases, infection becomes chronic and leads to corpus-predominant gastritis, which includes stimulation of gastric inflammation resulting in the degradation of normal gastric glands and replacement with intestinal-type epithelium resulting in atrophic gastritis followed by intestinal metaplasia, hypochlorhydria and finally gastric cancer [59]. As illustrated in figure 1.5.1.1. In some cases, it can also lead to pangastritis or duodenal ulcer where an antrum-predominant gastritis leads to hyperchlorhydria. This difference in outcome depends on differences among individual host response to *H. pylori* infection or host genetic polymorphisms, genotypes of *H. pylori* strains, environmental factors like high salt diet, smoking habit and certain gastric commensal organisms [60].

Polymorphisms within the host innate immune factor encoding genes are crucial in pathogenesis. Polymorphism in the cytokine genes results in inter-individual disparity towards cytokine responses that contributes to an array of clinical outcome in *H. pylori*-infected individuals [61]. Studies so far have reported about polymorphism of the genes encoding IL-1 β , TNF α , IL-8, IL-17 and IL-10 or their receptors to modulate the risk of gastric cancer [62]. Similar risk for gastric cancer is also involved in hosts with polymorphism of genes involved in TLR signalling pathway [63]. Genes of several virulence factors of *H. pylori* such as cytotoxin-associated gene A (CagA), vacuolating cytotoxin A (VacA), outer inflammatory protein A (OipA), *Helicobacter*-specific outer membrane

proteins O and Q (HopO and HopQ) and the induced by contact with epithelium A (IceA) show genetic variability and play critical roles in disease pathogenesis.

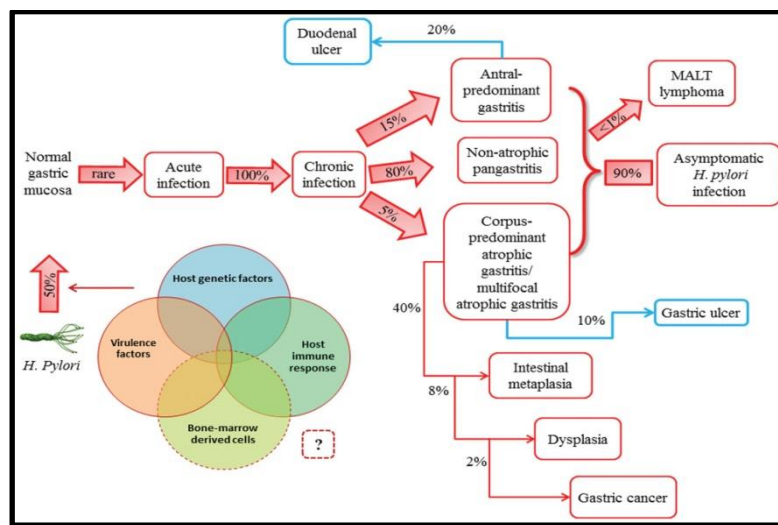


Figure 1.5.1.1 Disease pathogenesis by *H. pylori* (Courtesy: Ref [64])

1.5.2. Epidemiology and routes of transmission

H. pylori infection is global. While one-third of adults are infected in the north European and north American population, its prevalence is more than 50% in the south and eastern Europe, south America and Asia. Infection is mostly acquired during childhood where lower socioeconomic status has a higher risk of carrying the infection (Helicobacter ISSN 1523-5378). Direct transmission may occur via oral-oral, gastro-oral or faecal-oral route, whereas indirect transmission may occur through contaminated food, water and raw milk of animals (such as sheep and cow) [65].

1.5.3. Pathogenesis

The bacterium mostly adheres to the gastric epithelial lining of the antral region of the stomach. Following transmission, bacteria have to avoid host defence mechanism and therefore, follow a complex adaptation process to successfully colonize inside the human stomach. Urease enzyme produced by *H. pylori* and polar sheathed flagella helps initially in the colonization process. H⁺-gated urea channel UreI controls the urease release [66].The enzyme hydrolyzes urea into carbon dioxide and ammonia, resulting in an increase in the pH

of gastric mucosa and in the immediate vicinity of the bacterium. This allows the bacteria to neutralize gastric acidity and to persist in the highly acidic gastric lumen [66]. The spiral structure and flagella help *H. pylori* to swim through and penetrate the surface epithelium of the stomach where the more neutral pH favours for its successful colonization and growth.

H. pylori adhere to the microvilli-containing regions of mucus-secreting gastric epithelial cells via bacterial adhesins that interact with the host cell receptors. *H. pylori* adhesin-mediated colonization depends on multiple factors. Initial adherence of *H. pylori* to the gastric epithelium occurs through glycolipids or through the Lewis b antigen. This increases expression of sialic acid glycoproteins, which allow tighter binding of *H. pylori* to the epithelial cell surface. A few well-described adhesins are blood group antigen-binding adhesin (BabA), sialic acid-binding adhesin (SabA), adherence-associated lipoprotein A and B (AlpA/B), *H. pylori* adhesion A (HpaA), heat shock protein 60 (Hsp60), neutrophil activating protein (Nap), Catalase, OipA and HopZ. While the outer membrane protein of *H. pylori* BabA binds to Lewis b antigen of the host receptor, SabA is a sialic acid-binding adhesin and functions as a hemagglutinin whereas laminin is a target of both AlpA/B. The binding receptor for other adhesins still remains to be identified [67]. After the bacteria gets tightly adhered to the gastric epithelial cell, actin filament polymerization and cytoskeletal rearrangements take place followed by formation of pedestal and cup-like projections.

Some strains of *H. pylori* are more virulent than others and develop more clinical complications post infection. Although *H. pylori* possess a number of virulence factors, two classical virulence determinants expressed by *H. pylori* are the CagA protein encoded by the *cag* pathogenicity island (*cag* PAI) and the VacA. Based on whether the *H. pylori* strains express CagA or not, they are broadly classified into two families i.e. CagA-positive and CagA-negative strains. CagA is the strongest virulence factor within the *cag* PAI. The CagA-negative strain is less virulent.

The *cag* PAI is nearly 40 kb DNA insertion element inserted in the chromosomal glutamate racemase gene flanked by 31 bp direct repeats and encodes between 27-31 proteins [68]. The 140 kDa CagA protein is a terminal gene product of the *cag* PAI. After *H. pylori* adheres to the epithelial surface of the host cells, the *cag* PAI encodes a type IV secretion system (T4SS) that forms a syringe-like structure and penetrates the gastric epithelial cells facilitating the translocation of CagA and other bacterial virulence proteins into the eukaryotic cells. After translocation into the host cells, the CagA is tyrosine (tyr) phosphorylated at the glutamate-proline-isoleucine-tyrosine-alanine (EPIYA) motif gets converted into Cag A^{P-Tyr}[60]. Phosphorylation of the EPIYA motif of CagA triggers numerous cellular signaling pathways in the infected gastric epithelial cells leading to the expression of proinflammatory cytokines and chemokines along with deregulation of signalling pathways that control cell morphology, adhesion and transformation resulting in “the hummingbird phenotype” [69]. This morphological feature makes *H. pylori*-infected cells more motile. Even if CagA is nonphosphorylated, it may lead to aberrant catenin activation, disruption of intercellular junctions and loss of epithelial cellular polarity [70]. The other important virulent factor VacA also contributes towards change of epithelial cell structure and function. It triggers a series of events leading to the modification of endolysosomal trafficking followed by cellular vacuolation, immune cell inhibition, mitochondrial damage and apoptosis [62, 71, 72]. One of the important events during persistent *H. pylori* colonization and gastric cancer progression is the disruption of tight junctions and cellular transformation. The next section describes intracellular adhesion, its significance in cancer invasion and metastasis followed by the role of *H. pylori* on these junctions.

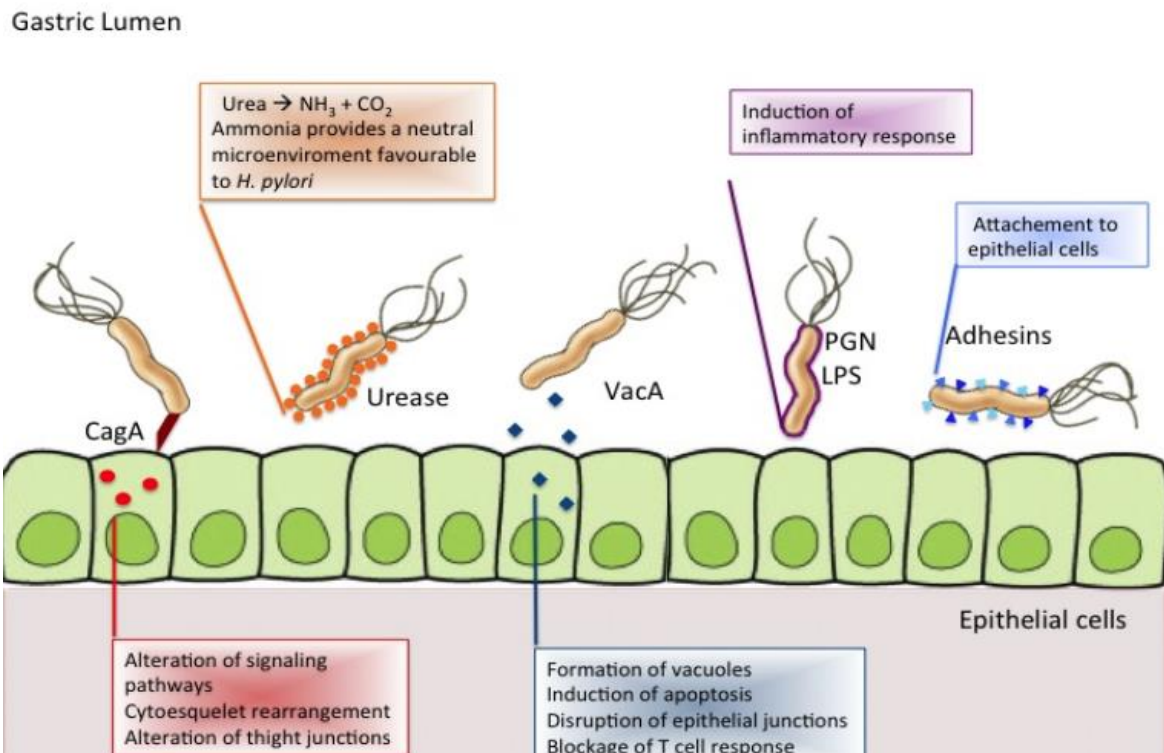


Figure 1.5.3.1 Major virulence factors of *H. pylori* (Courtesy: Ref [64])

1.6. Intercellular Junctions and their Roles in Cancer Invasion and Metastasis

1.6.1. Intercellular junctions

A number of intercellular junctions are present in vertebrates that help in adhesion between epithelial cells. These are tight junctions (TJs), cadherin-based adherens junction (AJs) (attached to the actin cytoskeleton), gap junctions (which allow chemical interactions between neighbouring cells), desmosomes (help in connecting to the intermediate filament of cytoskeleton), cell-extracellular matrix interactions mediated by integrins and other molecules [73]. As illustrated in figure 1.6.1.1. These are together known as the intercellular junctional complexes and play important roles in integrating a number of cellular processes that include maintenance of cytoskeletal dynamics to cellular proliferation, transcription, and differentiation [73, 74]. AJs also called zonula adherens are an important component of cell-cell junctions and are key features of all epithelial sheets. They also transfer signal from the environment to the inside of cells. Cadherins are the most important components present in the transmembrane core of AJs. In most solid tissues, they cluster at sites of cell-cell contact

[73]. There are nearly 80 members of cadherin super-family which includes classic cadherins, desmogleins, desmocollins, protocadherins, cadherin-related neuronal receptor (CNRs), fat-related cadherins, seven-pass transmembrane cadherins, and receptor tyrosine kinase (RET). These classical cadherins are the main intermediaries of calcium-dependent cell–cell adhesion [75]. Classical cadherins have five ectodomains which are responsible for binding with calcium ion and these domains are also responsible for homophilic interactions between epithelial cadherins (E-cadherins) of adjacent cells. Thus cadherins provide a strong adhesive link between cells [73, 76, 77]. The inner cytoplasmic tail of the cadherin is responsible for forming the nexus with the cytoskeleton β -catenin and p120 catenin. α -catenin acts as a bridge for binding β -catenin to actin and several actin-associated proteins that help E-cadherin to modulate actin filament organization. Binding of microtubules to cadherin occurs through p120 catenin. It also prevents cadherin endocytosis and degradation. Intra or inter cellular signals generated can also be transduced to the nucleus to alter gene expression Through the cytoplasmic tails of E-cadherin [78]. Adenocarcinoma is of epithelial origin and loss of epithelial characteristics from the original tissue along with appearance of mesenchymal cells is an important hallmark of advanced cancers. During invasion phase, cancerous cells must lose their structural integrity to attain a mesenchymal phenotype [79]. Hence, irrespective of signalling pathways that may get activated in one or the other tumor types, these events must ultimately result in loosening of intercellular junctions.

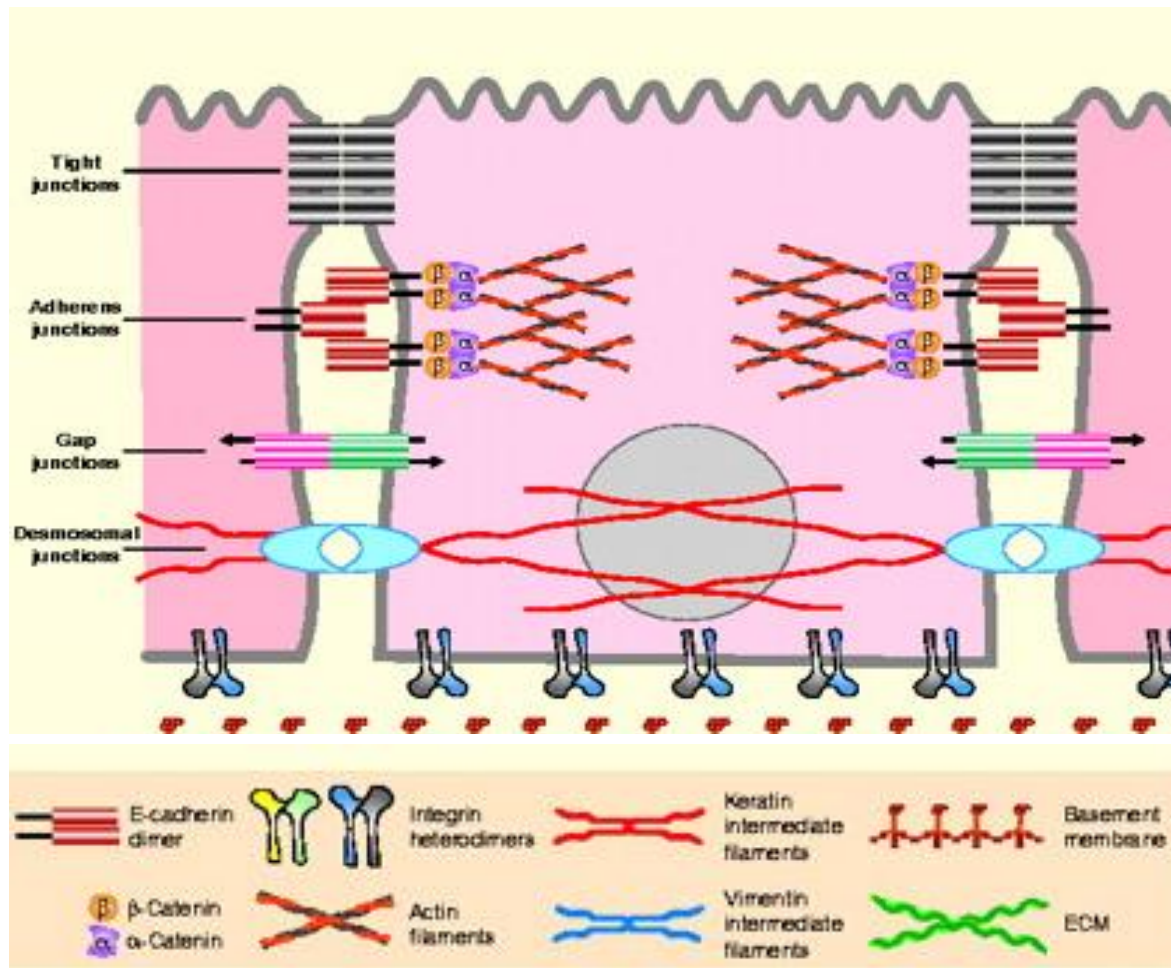


Figure 1.6.1.1 Adherens junction of epithelial cell (Courtesy: Ref [80])

1.6.2. Role of cadherins and β -catenin during cancer invasion

Cell-cell adhesions are degraded in epithelial cells during EMT. As reported in several tumors, reduced expression of E-cadherin along with an increased N-cadherin expression lead to cell detachment from epithelial clusters during EMT [81-83]. Several groups have demonstrated that overexpression of E-cadherin in epithelial tumor cells result in the reversal from an invasive, mesenchymal phenotype to a benign, epithelial phenotype [84, 85]. Active turnover of E-cadherin can occur through clathrin-mediated endocytosis that is critical for rapid transition between epithelial and mesenchymal states [78].

In 1989, β -catenin was identified as a binding partner of E-cadherin by Nagafuchi and Takeichi [86]. In vertebrates, two separate pools of β -catenin with two different cellular

functions have been reported- one is the membrane-bound pool and the other one is the cytoplasmic pool [87, 88]. Membrane β -catenin is involved in cell-cell adhesion. Cadherin mutants lacking the β -catenin-binding domain are often poorly adhesive suggesting their importance in cadherin function. Similarly, mutations in β -catenin results in loss of E-cadherin function with reduced cell-cell adhesion [89]. Loss of E-cadherin-catenin complex also promotes cancer progression in humans [90].

The non-membranous cytoplasmic-nuclear pool of β -catenin function is cadherin-independent and functions as transcriptional activator in Wnt/ β -catenin signalling pathway [91]. The Wnt/ β -catenin signaling pathway activates transcription factors or cellular activities such as cell proliferation and differentiation or maintenance of stemness [92]. The canonical Wnt/ β -catenin signaling pathway is activated through the binding of insoluble Wnt protein to its cell surface receptor frizzled (FZD) and co-receptor low density lipoprotein receptor-related protein 5/6 (LRP5/6) complexes. This complex deactivates GSK-3 β via intracellular protein dishevelled (Dvl). Inactivated GSK-3 β results in stabilization of transcription cofactor β -catenin making it free from the destruction complex to enter inside the nucleus and interact with transcription factors of the T cell factor 4 (TCF 4) /lymphoid enhancer factor (LEF) family to initiate transcription of Wnt target genes [93]. In the absence of Wnt signaling cascade, the destruction complex formed with the participation of proteins Axin-APC-GSK3 β ubiquitinates β -catenin via the ubiquitin ligase β -transducin repeat-containing protein (β -TrCP) and leads to proteasome mediated degradation of β -catenin [92]. So far, various studies have reported the role of Wnt/ β -catenin signalling pathway in gastric cancer progression [94, 95]. This is shown in figure 1.6.2.1.

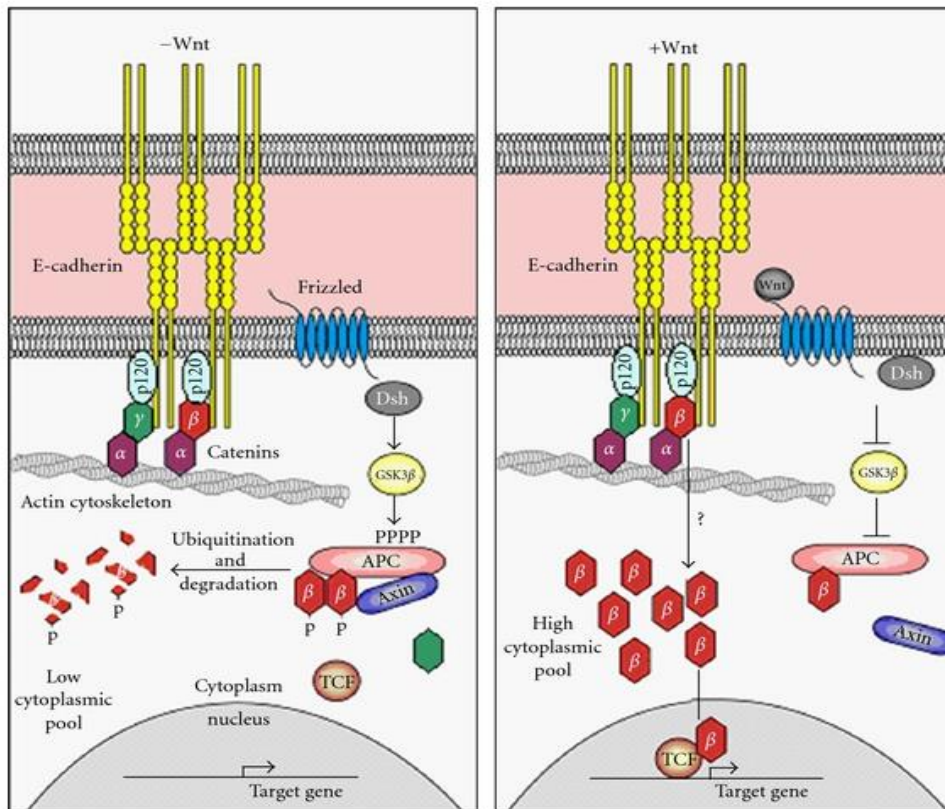


Figure 1.6.2.1 Cadherin-bound β -catenin in cell-cell adhesion and cytoplasmic β -catenin in Wnt signalling (Courtesy: Ref [90])

The critical role *H. pylori* play in regulating tight junctions, and E-cadherin-catenin complex during gastric cancer progression is now illustrated. *H. pylori* disrupt the intercellular apical junctions of epithelial cells by targeting the epithelial adhesion receptors, E-cadherin and specific cellular receptors and stimulate various signalling pathways to degrade the tight junctions [62]. The virulent factor CagA interacts with junction proteins like E-cadherin and zona occludens 1 (ZO-1), and alters the TJs or AJs in a phosphorylation-independent manner. The unphosphorylated form of CagA disrupts the cell-cell junction and results in loss of cell polarity whereas the phosphorylated form of CagA deregulates multiple signalling pathway cell shape and adhesion. The high temperature requirement A (HtrA) proteases secreted by *H. pylori* cleave E-cadherin [96]. Thus the displaced E-

cadherin, via Akt-dependent inactivation of the β -catenin inhibitor, GSK3 β releases the oncogenic protein β -catenin [97]. The released oncogenic protein β -catenin gets accumulated in the perinuclear endocytic recycling compartment and upon Wnt activation is translocated to the nucleus and activates the β -catenin-mediated signalling pathways that alter the gastric epithelial cells [98].

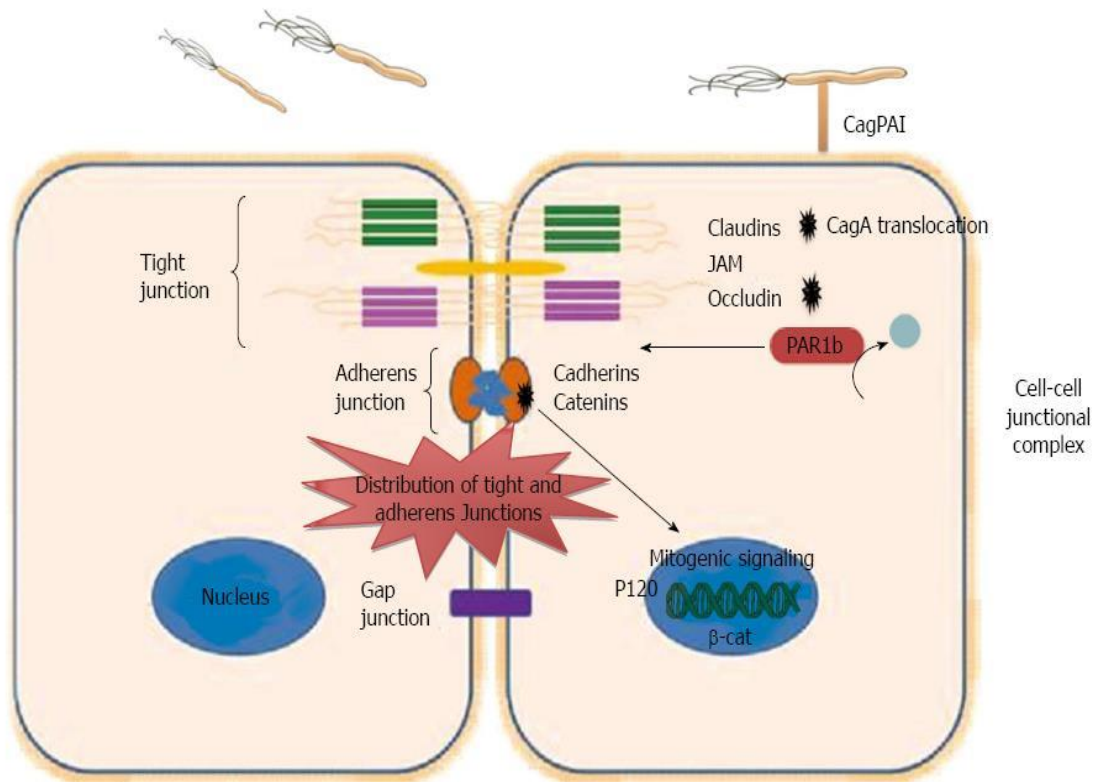


Figure 1.6.2.2 Disruption of epithelial junction by *H. pylori* (Courtesy: Ref [98])

1.6.3. RING finger E3 ubiquitin ligases regulate E-cadherin-catenin complex during cancer metastasis

The RING finger ubiquitin ligase Hakai was the first E3 ubiquitin identified that target cell membrane-bound E-cadherin as well as β -catenin [99]. It ubiquitinates E-cadherin leading to the internalization of the E-cadherin complex and enhances migration of the Madin Darby canine kidney (MDCK) epithelial cells [99, 100]. The fate of cadherin-bound β -catenin after the complex is dissociated from the AJ is still not clear but is considered to be either

degraded or recycled [101]. Another E3 ubiquitin ligase, Ozz-E3, ubiquitinates only the membrane-bound, but not cytosolic β -catenin at the sarcolemma and causes its proteasomal degradation [102]. However, the effect of Siah proteins on AJs and therefore, on metastasis is not known.

1.7. Objectives

In light of the above-mentioned information, the following objectives were set-

1. To study expression of Siah proteins in the *H. pylori*-infected gastric epithelium
2. To decipher factors regulating expression of Siah proteins during *H. pylori* infection
3. To identify target molecules regulated by Siah proteins and their roles in gastric cancer

MATERIALS AND METHODS

Chapter 2

2. MATERIALS AND METHODS

2.1. Materials Used

2.1.1. Cell lines

The human gastric cancer cells (GCCs) MKN45, AGS, Kato III and NCI-N87 were procured from the University of Virginia, USA. The immortalized non-neoplastic human gastric epithelial cell HFE145 was received as a gift from Dr. Hassan Ashktorab, Department of Medicine, Howard University, USA. Details of several stable cell lines generated in our lab are mentioned later.

2.1.2. H. pylori strains

Three strains of *H. pylori* were used in this study: *H. pylori* 26695, a *cag* PAI (+) strain; strain 8-1, a *cag* PAI (-) strain (both strains were obtained from the University of Virginia, USA) and strain D154, a *cag* PAI (-) strain (received from the archived collection of *H. pylori* strains at National Institute of Cholera and Enteric Diseases, Kolkata, India).

2.1.3. Competent cells

For cloning of plasmids, Subcloning Efficiency DH5 α Competent Cells (#18265017, Invitrogen, USA) were used. For cloning after site-directed mutagenesis, XL10-Gold Ultracompetent cells (#200314, Agilent, USA) were used.

2.1.4. Human gastric cancer biopsy specimen

Gastric biopsy samples (from the antral gastric mucosa) were collected from gastric cancer patients undergoing diagnostic esophagogastroduodenoscopy following a National Institute of Science Education and Research (NISER) Review Board-approved protocol (under the supervision of Prof. S.P Singh, SCB Medical College and pathologically certified by Prof. Niranjan Rout, AHRCC) and investigation were carried out in accordance with the Declaration of Helsinki (2013) of the World Medical Association. Written informed consent was obtained from all patients prior to the study.

2.1.5. Plasmid constructs, siRNAs and antibodies

A list of all plasmid constructs, siRNAs and antibodies used in this research are mentioned in appendix I, II and III respectively.

2.1.6. Reagents, kits, and instruments

For cell culture: Roswell park memorial institute (RPMI)-1640 media containing L-Glutamine and Sodium bicarbonate (#AL028A, HiMedia, INDIA), Fetal bovine serum (FBS) (#RM9970, HiMedia), 0.25% Trypsin, 0.02% EDTA in Ca⁺⁺-Mg⁺⁺-free Dulbecco's phosphate buffered saline (DPBS) solution (#TCL007, HiMedia), Dimethyl sulfoxide (DMSO) (#TC185, HiMedia), MG132 (#M7449-200UL, Sigma-Aldrich, USA), Penicillin-Streptomycin solution (#P0781, Sigma-Aldrich), 1X PBS buffer (#SH30256.02, HyClone, USA), Difco Bacto agar (#214010, BD, USA).

For *H. pylori* culture: Trypticase soy agar w/5% sheep blood (TSA) plates (#221239, BD BBL, USA), Brucella broth (#211088, BD BBL).

For bacterial culture: Ampicillin sodium salt (#194526, MP Biomedicals, USA), Glycerol (#RM1027-1LTR, HiMedia), SOC media (#15544034, Invitrogen), Luria Bertani Agar, Miller (#M1151-500G, HiMedia), Luria Bertani Broth, Miller (#M1245-500G, HiMedia).

For polymerase chain reaction (PCR) RNA/DNA: TaqMan universal PCR master mix (#4304437, Applied Biosystems, USA), human Siah1 TaqMan gene expression assay reagent (#Hs00361785_m1, Applied Biosystems), human Siah2 TaqMan gene expression assay reagent (#Hs00192581_m1, Applied Biosystems), Eukaryotic 18S rRNA (#Hs03003631_g1, Applied Biosystems), Platinum Taq DNA polymerase High Fidelity (#11304011, Invitrogen), Amplitaq Gold 360 DNA polymerase (#4398823, Invitrogen), Taq DNA polymerase (#M0273S, New England Biolabs, USA), 10mM DNTP mix (#18427088, Invitrogen), Betaine solution (#B0300-1VL, Sigma-Aldrich), 10X TE buffer pH8.0 (#ML012-500ML, HiMedia), 50X TAE (#ML012-500ML, HiMedia), Ethidium bromide solution (#MB074-

10ML, HiMedia), Agarose (#0219398425-25 g, MP Biomedicals), Gel loading dye, blue (6X) (B7021S, New England Biolabs), 1 kb DNA Ladder (#N3232S, New England Biolabs), 50 bp DNA Ladder (#N3236S, New England Biolabs).

For cloning: HindIII (#R0104S, New England Biolabs), XhoI (#R0146S, New England Biolabs), KpnI (#R0142S, New England Biolabs), Quick ligation kit (#M2200S, New England Biolabs), T4 DNA ligase (#M0202S, New England Biolabs).

For transfection and stable cells: Lipofectamine2000 (#11668019, Invitrogen), Lipofectamine 3000 (#L3000015, Invitrogen), G418 (#G8168-10ML, Sigma-Aldrich), Cloning Disc (#Z374458-100EA, Sigma-Aldrich).

For immunoblotting: 100X protease inhibitor (ML051-1ML, HiMedia), 2X Laemmli buffer (#ML021, HiMedia), β -Mercaptoethanol (#MB041-500ML, HiMedia), 10X Tris/Glycine/SDS buffer (#1610732, BIO- RAD), 10X Tris/Glycine buffer (#1610771, BIO- RAD), SDS (#MB010-500G, HiMedia), 30% Acrylamide/Bis solution (#1610156, BIO- RAD, USA), Resolving gel buffer (#1610798, BIO- RAD), Stacking gel buffer (#1610799, BIO- RAD), Glycerol (#MB 060-500ML, HiMedia), TEMED (#1610800, BIO- RAD), Ammonium persulfate (#1610700, BIO- RAD), BLUelf prestained protein ladder (#BM008-500, BR Biochem, India), 10X TBS (ML029-5X100ML, HiMedia), 10X PBS (ML023-2X500ML, HiMedia), Polyvinylidenedifluoride membrane (PVDF)(#IPVH00010, Millipore, India), Tween 20 (RM156-500G, HiMedia), BSA Cohn fraction V (#RM3151, HiMedia), Skim milk powder (#RM1254-500G, HiMedia), Restore plus western blot stripping buffer (#46430, ThermoFischer scientific, USA), SuperSignal west femto maximum sensitivity substrate (#34095, ThermoFischer scientific).

For chromatin immunoprecipitation assay and immunoprecipitation assay: 37% formaldehyde (#MB059-500ML, HiMedia), Protein A/G PLUS-Agarose (#sc-2003, Santa Cruz Biotechnology).

For DNA binding assay: Dynabeads M-280 Streptavidin (#11205D, Invitrogen), DynaMag-2 Magnet (#12321D, Invitrogen).

For tissue sectioning: Poly-L-lysine solution (#P8920-100ML, Sigma Aldrich), Tissue Freezing Medium (#3808609E, Leica, Germany). Fluoromount G (#0100-01, Southern Biotech, USA).

For soft agar assay: Bacto agar (#199835, MP Biomedicals), Dulbecco's Modified Eagle Medium/ Nutrient Mixture F-12 Ham (DMEM/ F12, 1:1 mixture) media (#AT140A, HiMedia).

For transwell migration and invasion assay: Growth Factor Reduced BD Matrigel, 8 µm inserts (# 354483, BD Biocoat), Tissue Culture-treated, 8 µm inserts for 24-well plates (# 353097, BD Biocoat).

Kits: Genomic DNA isolation kit- FlexiGene DNA Kit (#51204, Qiagen,USA), Gel extraction kit- QIAquick gel extraction kit (#28706, Qiagen), PCR purification kit- (#28104, Qiagen). Miniprep Kit- QIAprep Spin Miniprep Kit (#27106, Qiagen), Maxiprep kit- (#43776, Qiagen), Site-directed mutagenesis- Quick change multi Site-directed mutagenesis kit (#200517, Agilent technology), Nuclear and cytoplasmic extraction reagents- NE-PER (#78833, ThermoFischer Scientific), Qiagen RNeasy mini kit- (#74106, Qiagen), SuperScript First-Strand c-DNA Synthesis kit- (#11904-018, Invitrogen), QuikChIP chromatin immunoprecipitation kit- (#30101K, Imgenex, India), QuikChIP DNA purification kit- (#30401K, Imgenex), Dual-Luciferase Reporter Assay- (#E1910, Promega)

Instruments: Cell culture Hood (Model No. Cell Gard ES NU-480-400E Class II, Nuair, USA), Cell culture incubator (New Brunswick Galaxy 170R, Eppendorf, Germany), Centrifuge (Sorvall Biofuge Stratos, Model No. D35720, Thermo Scientific), UV/Vis spectrophotometer (Model No-DU 720 General purpose UV/Vis spectrophotometer, Beckman Coulter),Centrifuge (Model No. 5415-R, Eppendorf), PCR (PCR Mastercycler pro

vapo. protect, Eppendorf), Mini-protean tetra system gel apparatus (Model No. 165-8003, Bio-Rad), mini transblot cell wet transfer apparatus (Model No. 170-3940, Bio-Rad), transblot sd semidry blot apparatus (Model No.170-3940, Bio-Rad), ChemiDoc XRS (Model No. 1708265, Bio-Rad Laboratories, USA), Real Time-RT PCR (Model No7500, Applied Biosystem), Cryostat (Model No. LEICA CM3050 S, Leica Biosystems), Fluorescence microscope (Model No.BX51, Olympus Co., Japan), Laser scanning confocal microscope (Model No.LSM 780, Carl Zeiss, Germany), Bright field inverted microscope (Primo vert, Carl Zeiss).

2.2. Methodology

2.2.1. Culture of human gastric cancer cells (GCCs) MKN45, AGS, KatoIII and immortalized normal gastric epithelial cells HFE145

MKN45, AGS, KatoIII and HFE145 were maintained in RPMI-1640 media supplemented with 10 % FBS (heat-inactivated). All cells were cultured in T-75 flasks and incubated inside a 37°C incubator maintaining 5% CO₂ and 95% humidity.

For passaging, the old media was decanted off from the T-75 flask and adherent gastric cancer cells were treated with 3 ml of prewarmed trypsin-EDTA solution. The trypsin-EDTA-treated flask was placed inside the incubator with 5% CO₂ at 37°C for 5 minutes to detach cells from the flask. Sterile serological pipettes were used to gently dislodge cells from the flask and to add in a centrifuge tube containing fresh complete media. Cells were counted using a Neubauer improved haemocytometer under an inverted microscope followed by its centrifugation at 300xg for 8 minutes at room temperature (RT). Resuspension of the cell pellet was done in a small volume of medium followed by seeding in fresh T-75 flasks.

2.2.2. Cell freezing and revival

Cell freezing was performed usually at a lower passage number when cells became confluent (70-80%) from the previous passage. A confluent T-75 flask was trypsinized with 3 ml of

prewarmed trypsin-EDTA solution and trypsinized cells were added in a centrifuge tube to fresh complete media. Cells were pelleted at 300xg for 8 minutes at 4°C. Supernatant was discarded and cell pellet was resuspended in freezing mix (20% DMSO in FBS). Cells were aliquoted into freezing vials and kept overnight at -80 °C followed by storage at liquid nitrogen for long term preservation.

2.2.3. *H. pylori* culture and infection of cells

H. pylori were grown on TSA plates and were incubated at 37°C in a microaerophilic environment of 90 % N₂, 1% O₂, 10 % CO₂. After 48-72 h of incubation, colonies grown on plates were inoculated in brucella broth supplemented with 10 % heat-inactivated FBS. After 18 h of incubation, an aliquot of bacteria in broth was taken for OD in a spectrophotometer. OD₆₀₀ → 0.3 was equivalent to 2x10⁸ CFU/ml. Culture that reached OD between 0.5 to 1 was pelleted at 300xg for 10 min at 4°C and used to infect GCCs after resuspending bacteria in complete RPMI-1640 media to reach desirable multiplicity of infection (MOI).

2.2.4. Cloning, expression and site-directed mutagenesis

2.2.4.1. Cloning of human *siah1* gene

Primer design: Primers were designed for cloning of human *siah1* gene (GenBank: BC044920.1) by using Integrated DNA Technology (IDT) software. A Detailed list of primers is given in Appendix IV)

Human genomic DNA isolation: Human genomic DNA was isolated from AGS cells using Qiagen flexi gene DNA kit as instructed by the manufacturer. Amplification of *siah1* gene (848 bp) from genomic DNA was performed as follows.

Polymerase chain reaction (PCR): *siah1* gene was amplified from human genomic DNA isolated from AGS cells using Platinum Taq DNA polymerase High Fidelity (HIF). PCR was set up using the following reaction mixture: 5 µl 10X HIF buffer (1X), 1 µl 10 mM dNTP (0.2mM), 2 µl 50 mM MgSO₄ (2.0 mM), 1 µl forward primer (10 pmole) 1 µl reverse primer

(10 pmole), 1 μ l genomic DNA (250 ng), 0.5 μ l HIF Taq polymerase, 38.5 μ l H₂O. The reaction condition for PCR is mentioned in Appendix V. The amplified PCR product (848 bp) was run on 1.2% agarose gel to qualitatively examine the desired PCR product.

Agarose gel electrophoresis and gel extraction of the PCR product: To isolate and purify the desired DNA of *siah1*, agarose gel electrophoresis was performed with the amplified PCR product. 0.8% agarose gels were prepared in 1X TAE buffer and 0.5 μ g/ml ethidium bromide was added. The gel was run at 90 V for 30 min in a horizontal electrophoresis unit and band position of DNA along with its corresponding molecular weight markers in the gel was visualized using an ultraviolet (UV) transilluminator. The amplified *siah1* PCR product in the agarose gel was excised by using a scalpel. The gel was weighed and to one gel volume three volumes of QG buffer was added. The mixture was incubated at 50°C for 10 min and vortexed at every 2-3 min for a complete dissolution of the gel. To the mixture, one gel volume of isopropanol was added and mixed. The sample was loaded to the spin column and incubated for 2 min. The column was subsequently centrifuged for 1 min at 16,100xg and the flow through was discarded. 0.5 ml of QG buffer was added to the column and was centrifuged for 1 min at 16,100xg and the flow through was discarded. The column was then incubated with 0.75 ml of buffer PE for 2 min and was centrifuged at top speed for 1 min. Finally, 30 μ l EB buffer was added to the column and DNA was eluted into a fresh microcentrifuge tube by centrifuging at top speed for 1min. The purified PCR product was subjected to restriction digestion.

Restriction digestion of purified PCR product: HindIII (on the F primer) and XhoI (on the R primer) were used to clone *siah1* in pcDNA3.1⁺ vector. Restriction digestion of the PCR product and vector was performed using 1 μ g of template DNA in a 37°C water bath for 3 h. For restriction digestion, the following reaction mixture was used: 5 μ l 10X buffer 2 (1X), 0.5 μ l XhoI (20,000 U/ml NEB), 0.5 μ l HindIII (20,000 U/ml NEB), 15 μ l PCR product (1

µg), 29 µl H₂O. The following reaction mixture was used for restriction digestion of the empty vector: 5 µl 10X buffer 2 (1X), 0.5 µl XhoI (20,000 U/ml NEB), 0.5 µl HindIII (20,000 U/ml NEB), 1 µl pcDNA3.1⁺ (1 µg), 43 µl H₂O. The digested PCR product and vector was then purified using PCR purification kit.

Purification of restriction digested product: The restriction digested products were subjected to purification using PCR purification kit. Five volumes of buffer PB1 was added to one volume of restriction digested products, mixed and was applied to QIAquick column. The column was centrifuged at 16,100xg for 1 min and the flow through was discarded. 0.75 ml PE buffer was added to the column and centrifuged for 1 min at 16,100xg. At the final step, DNA was eluted with 20 µl of EB buffer after centrifugation at top speed.

DNA Ligation: The empty vector and *siah1* gene were ligated using the Quick ligation kit. DNA ligation was performed at 16°C for 30 min. The ligation calculator software was used to calculate the amount of vector and insert for the reaction. Vector to insert ratio was 1:6. Calculation for ligation mix (20 µl): 10 µl 2X Quick ligation reaction buffer (1X), 1.46 µl vector (75 ng), 2.18 µl insert (70.66 ng), 1 µl ligase, 5.36 µl H₂O.

Transformation: 3 µl of ligation mix and 50 µl *Escherichia coli* DH5α competent cells were mixed by swirling and incubated on ice for 30 min. Heat shock was given by incubating tubes in 42°C water bath for 45 sec. 450 µl SOC media was added to the cell within 2 min of the heat shock, mixed and incubated for 1 h at 37°C in a shaker. L-shaped spreader was used to spread the bacterial suspension uniformly on LB agar plates containing 75 µg/ml ampicillin and the plate was incubated for overnight at 37°C.

Selection of positive clones: One colony was picked up from the plate with the help of autoclaved toothpick. The toothpick was used to inoculate a gridded master plate and also to inoculate 5 ml LB broth with 100 µg/ml of ampicillin and incubated at 37°C for 16 h with shaking. Plasmid DNA was isolated from bacterial culture using miniprep kit.

Miniprep plasmid isolation: Overnight bacterial culture was centrifuged at 6800xg for 3 min at RT. The bacterial pellet was resuspended in 250 µl buffer P1 followed by addition of 250 µl buffer P2, inverted 10-12 times till the solution turned evenly blue and was kept for 5 min at RT to lyse bacteria. 350 µl buffer N3 was added and was mixed thoroughly by inverting the tubes 10-12 times till the solution became colourless. It was centrifuged for 10 min and the supernatant was applied to spin column. After a 60 sec of centrifugation, the column was washed with 500 µl of buffer PB followed by 750 µl of buffer PE. 30 µl of EB buffer was added to the column, incubated for 1 min followed by centrifugation for 1 min at top speed to elute DNA. To select the correct recombinant, restriction digestion was performed once more with Hind III/Xho I enzyme. The restriction digested products along with their corresponding undigested plasmids were run on 1.2% agarose gel. 848 bp release was obtained from only one clone and were checked by sequencing (outsourced). As the result of sequencing was positive for *siah1* gene, the plasmid was amplified by maxiprep.

Maxiprep of plasmid: To get higher yield of the selected positive clone Maxiprep was done. The positive clone was picked up from the master plate and inoculated into 100 ml LB broth with 100 µg/ml of ampicillin and incubated for 16 h at 37°C. The culture was centrifuged at 6000xg for 15 min at 4°C. The bacterial pellet was resuspended in 10 ml of buffer P1 followed by addition of 10 ml of buffer P2, mixed thoroughly by vigorously inverting 4-6 times till the blue color appears and incubated for 5 min at RT. 10 ml of prechilled buffer P3 was added to the mixture and mixed by vigorously inverting 4-6 times. The lysate was transferred into the barrel of the Qiafilter cartridge. The mix was then incubated for 10 min at RT. During the incubation period, hispeed maxi tip was equilibrated by adding 10 ml Buffer QBT. Bacterial lysates were filtered into the previously equilibrated hispeed tip. The clear lysate was allowed to enter the resin through gravity flow. 60 ml Buffer QC was added to the Qiagen tip. DNA was eluted into a 50 ml of centrifuge tube by adding 15 ml Buffer QF to the

Qiagen tip. 10.5 ml of isopropanol was added to precipitate DNA. After 5 min of incubation, the mixture was transferred to a 30 ml syringe, the plunger was inserted and by using constant pressure, the mixture was filtered through Qiaprecipitator. 2 ml 70% ethanol was added to the syringe and was filtered through Qiaprecipitator. The outlet nozzle of Qiaprecipitator was air-dried to prevent ethanol carryover. The Qiaprecipitator was attached to a 5 ml syringe and 500 µl of prewarmed TE buffer was added to the syringe. The plunger was inserted to collect DNA from the other side in a DNase/RNase free microfuge tube.

2.2.4.2. Cloning and mutation of human *siah1* and *siah2* promoters

Primer design: Primers were designed for cloning of human *siah1* 5' UTR (GenBank: AJ400626.1) and human *siah2* promoter (NM_005067.5). The human *siah1* 5' UTR and *siah2* promoter are highly GC rich regions. For successful cloning, two different primer sets were designed. One set of primers were having no restriction enzymes site while the second set of primer was designed with restriction site inserted (vide Appendix VI). Integrated DNA Technology (IDT) software was used to design primers for the target sequences.

Human genomic DNA isolation: Human genomic DNA was isolated from MKN45 cells using Qiagen flexi gene DNA kit as instructed by manufacturer. Amplification of *siah1* 5' UTR and *siah2* promoter from genomic DNA was performed as follows.

PCR: *siah1* 5' UTR and *siah2* promoter were amplified from human genomic DNA isolated from MKN45 cell lines using AmpliTaq Gold360 DNA polymerase. For both *siah* promoters the first set of PCR was set up with primers that had no restriction site. For *siah1* 5' UTR PCR: 50 µl reaction volume was set up as follows- 5 µl 10X AmpliTaq Gold 360 Buffer (1X), 4 µl 10 mM dNTP mix (0.2 mM each), 6 µl 25 mM MgCl₂ (3.0 mM), 2 µl forward primer (20 pmole), 2 µl reverse primer (20 pmole), 10 µl 360 GC Enhancer, 3 µl genomic DNA (250 ng), 2 µl AmpliTaq Gold 360 DNA polymerase (10 U), 16 µl H₂O. The reaction

condition for PCR is mentioned in Appendix VII. The amplified PCR product (656 bp) was run on 1.2% agarose gel to qualitatively examine the desired PCR product.

For *siah2* promoter PCR: 50 µl reaction volume was set up as follows- 5 µl 10X AmpliTaq Gold 360 Buffer (1X), 4 µl 10 mM dNTP mix (0.2 mM each), 4 µl 25 mM MgCl₂ (2.0 mM), 2 µl forward primer (20 pmole), 2 µl Reverse Primer (20 pmole), 10 µl 360 GC Enhancer, 3 µl genomic DNA (250 ng), 1 µl AmpliTaq Gold 360 DNA polymerase (5 U), 19 µl H₂O. The reaction condition for PCR is mentioned in Appendix VII. The amplified PCR product (545 bp) was run on 1.2% agarose gel to qualitatively examine the desired PCR product.

PCR purification: The amplified PCR products were PCR purified using Qiagen PCR purification kit as described earlier.

PCR on PCR: PCR was performed on the purified PCR product with the second set of primers i.e. primers with restriction site. Forward primer had KpnI and the reverse primer had HindIII site. For *siah1* 5' UTR PCR on PCR: 50 µl reaction volume was set up as follows- 5 µl 10X AmpliTaq Gold 360 Buffer (1X), 4 µl 10 mM dNTP mix (0.2 mM each), 6 µl 25 mM MgCl₂ (3.0 mM), 2 µl Forward Primer (20 pmole), 2 µl Reverse Primer (20 pmole), 10 µl 360 GC Enhancer, 1 µl PCR product (10 ng), 1 µl Ampli Taq Gold 360 DNA polymerase (5 U), 15 µl H₂O. The reaction condition for PCR is mentioned in Appendix VII. The amplified PCR product (454 bp) was run on 1.2% agarose gel to qualitatively examine the desired PCR product.

For *siah2* promoter PCR on PCR: 50 µl reaction volume was set up as follows: 5 µl 10X AmpliTaq Gold 360 Buffer (1X), 4 µl 10 mM dNTP mix (0.2 mM each), 4 µl 25 mM MgCl₂ (2.0 mM), 2 µl Forward Primer (20 pmole), 2 µl Reverse Primer (20 pmole), 10 µl 360 GC Enhancer, 1 µl PCR product (13.3 ng), 1 µl AmpliTaq Gold 360 DNA polymerase (5 U), 21 µl H₂O. The reaction condition for PCR is mentioned in Appendix VII. The amplified

PCR product (543 bp) was run on 1.2% agarose gel to qualitatively examine the desired PCR product.

PCR purification: The amplified PCR products were purified using Qiagen PCR purification kit as described earlier.

Restriction digestion of purified PCR product: Kpn I and Hind III restriction sites were used (Kpn I on the forward primer and Hind III on the reverse primer) to clone *siah1* 5' UTR and *siah2* promoter in pGL3 basic vector. Restriction digestion of the PCR product and the vector was performed using 1 µg of template DNA in a 37°C water bath for 3 h.

For restriction digestion of *siah1* 5' UTR, the following reaction mixture was prepared: 5 µl 10X buffer 2 (1X), 5 µl of 10X BSA (1X), 2.5 µl KpnI (20,000 U/ml NEB), 1 µl HindIII (20,000 U/ml NEB), 14.7 µl PCR product (1 µg), 21.8 µl H₂O. For restriction digestion of *siah2* promoter, the following reaction mixture was used: 5 µl 10X buffer 2 (1X), 5 µl 10X BSA (1X), 2.5 µl KpnI (20,000 U/ml NEB), 1 µl HindIII (20,000 U/ml NEB), 10 µl PCR product (1 µg), 26.5µl H₂O.

For restriction digestion of empty vector the following set of reaction mixture was prepared: 5 µl 10X buffer 2 (1X), 5 µl 10X BSA (1X), 2.5 µl KpnI (20,000 U/ml NEB), 1 µl HindIII (20,000 U/ml NEB), 1 µl PCR product (1 µg), 35.5 µl H₂O. The digested PCR products and vector were then purified using PCR purification kit.

Purification of restriction digested product: The restriction digested products were subjected to purification using PCR purification kit as described earlier.

DNA Ligation: To ligate purified digested products of empty vector, *siah1* 5' UTR and *siah2* promoter, T4 DNA ligase was used. DNA ligation was performed at 16°C for 12 h. The ligase calculator software did the calculation for the amount of vector and insert to be used in the reaction for ligation. Vector to insert ratio was 1:6.

Calculation for ligation mix for *siah1* 5' UTR (10 μ l): 1 μ l 10X T4 ligase buffer (1X), 2.07 μ l vector (75 ng), 1.27 μ l insert (40 ng), 1 μ l ligase, 4.66 μ l H₂O.

Calculation for ligation mix for *siah2* promoter (10 μ l): 1 μ l 10X T4 ligase buffer (1X), 2.07 μ l vector (75 ng), 1.64 μ l insert (49.96 ng), 1 μ l ligase, 4.28 μ l H₂O.

Transformation of ligated product was done as described earlier, followed by plasmid isolation using miniprep plasmid kit. Restriction digestion of the isolated plasmid was performed to select the positive clone which was confirmed by sequencing. To further amplify the plasmid, maxiprep was done using maxiprep plasmid isolation kit.

Mutation at ETS2 binding site (EBS) of *siah1* 5' UTR and EBS and Twist1 binding site (TBS) of *siah2* promoter: Site-directed mutagenesis was done at EBS for *siah1* 5' UTR and EBS and TBS for *siah2* promoter using Quick change multi site-directed mutagenesis kit. Primer sequence is mentioned in Appendix VIII.

The mutagenesis reaction mix (25 μ l) had the following components: 2.5 μ l 10X Quikchange multi reaction buffer (1X), 0.75 μ l Quik solution, 1 μ l dsDNA template (100 ng), 1 μ l primer (100 ng), 1 μ l dNTP, 1 μ l Quik change multi enzyme, 17.75 μ l H₂O. The PCR reaction conditions for site-directed mutagenesis are mentioned in Appendix VIII.

Amplified PCR products were treated with 1 μ L (10 U/ μ L) Dpn I restriction enzyme (an endonuclease; targeted sequence: 5'-Gm6ATC-3' and is specific for methylated and hemimethylated DNAs) and incubated at 37°C for 2 h. Parental strands of DNA were digested at specific sites by this enzyme leaving the new strand intact. After digestion, Dpn I-treated DNAs from mutagenesis reaction were transformed into XL10-Gold ultracompetent cells as discussed previously. The mutant closed-circle ssDNA was converted into a duplex form *in vivo*. Mutants were confirmed by restriction digestion and sequencing; positive clones were further amplified by maxi prep method.

2.2.4.3. Transient transfection

Lipofectamine2000 reagent was used for transient transfection of various plasmid constructs and Lipofectamine3000 was used for transient transfection of siRNA. The cell:DNA:Lipofectamine ratio for different cell-culture plate sizes is mentioned in Table 1. MKN45 cells were plated in cell-culture plate with an appropriate volume of complete growth media and placed inside an incubator at 37°C and 5 % CO₂ 24 h prior to transfection. Growth media was gently aspirated from the wells and fresh complete growth media was added to cells 1 h before transfection. Two reaction mixtures were prepared in DNase, RNase and pyrogen-free 1.5 ml microfuge tube. Mix A contained required amount of DNA in serum free media (SFM) and mix B contained required amount of Lipofectamine2000/3000 reagent in serum free media. Tubes were incubated for 5 minutes at RT. Mix A and B were mixed together by gently pipetting up and down 5 times and the reaction tube was incubated for 25 minutes at 25°C to allow complex formation. Reaction mixture containing transfection complexes was added drop-wise to cells in plate and the plate was swirled gently to ensure uniform distribution of the complex. Cells with the complex mix were incubated in the incubator for 24 h at 37°C and 5% CO₂. Cells were then treated as per experimental protocol.

Table 1. Parameters for transient transfection (Adapted from Invitrogen)

Culture plate	Volume of plating media in (µl)	Cell No. per plate	DNA (µg) in and dilution volume SFM (µl)	DNA-Lipid complex added to cells (µl)
96-well	100	4x10 ⁴	0.1(µg) in 10 (µl)	20
24-well	500	2x10 ⁵	0.8 (µg) in 50 (µl)	100
12-well	1000	4x10 ⁵	1.6 (µg) in 100 (µl)	200
6-well	2000	1x10 ⁶	4 (µg) in 250 (µl)	500

2.2.5. Infection of GCCs with H. pylori

24 h prior to infection, 1×10^6 MKN45 cells were seeded in 6-well cell culture plate with 1.5 ml of complete media in each well. Plates were placed inside a 37°C incubator maintaining 5% CO₂. As described earlier, *H. pylori* was inoculated in Brucella broth supplemented with 10% heat-inactivated fetal bovine serum and were agitated for 18 h inside an incubator at 37°C and 10% CO₂. 1 ml of the broth with bacteria was taken in cuvette and its OD was measured in a spectrophotometer. The rest amount of broth was centrifuged down at 300xg for 10 min. The supernatant was discarded and the pellet was resuspended in desired volume of RPMI-1640 complete media. Cells were infected with *H. pylori* at 100, 200 and 300 MOI for 3 h and 6 h time point.

2.2.6. Whole cell lysate preparation from GCCs after H. pylori infection

After infection, plates were placed inside the incubator at 37°C and 5% CO₂ for the required time. Plates were taken out from the incubator and placed on ice bath. Cells were scraped gently, centrifuged at 250xg for 5 min at 4°C and the supernatant was thrown away. 40 µl of 2X protease inhibitor cocktail was added to the pellet and vortexed. 40 µl of 2X sample buffer with β-mercaptoethanol was added to the mix, vortexed and boiled at 100°C for 8 min to prepare the whole cell lysate.

2.2.7. Isolation of membrane, cytosol and nuclear fractions from MKN45 cells after H. pylori infection

For membrane, cytosolic and nuclear fraction isolation, NE-PER nuclear and cytoplasmic extraction reagents was used. The cytoplasmic and nuclear fractions were isolated as per the instruction of manufacturer whereas the membrane fraction was isolated from the cytoplasmic fraction as described below. 2×10^6 MKN45 cells were plated in 60 mm cell culture dish 24 h prior to infection, and were incubated at 5% CO₂ and 37°C. Cells were left uninfected or were infected with *H. pylori* for various time points and were centrifuged down

at 500xg for 5 min. The supernatant was discarded and other reagents were added based on packed cell volume as mentioned below.

Table 2. Reagents used for cell fractionation using NE-PER kit (Adapted from NE-PER manual)

Packed Cell Volume (μl)	CER I (μl)	CER II (μl)	NER (μl)
10	100	5.5	50
20	200	11	100
50	500	27.5	250
100	1000	55	500

2×10^6 cells is equivalent to 20μl packed cell volume.

A premix of protease inhibitor cocktail and ice-cold CER I buffer was added to the pellet and vortexed vigorously for 15 sec. The pellet was incubated on ice for 10 min. After incubation, CER II was added and vortexed vigorously for 5 sec and followed by 1 min incubation on ice. Tubes were again vortexed for 5 sec followed by centrifugation at 16000xg for 5 min at 4°C. The insoluble pellet containing nuclei was resuspended in ice-cold NER supplemented with protease inhibitor and vortexed for 15 sec. The suspension was incubated on ice and vortexed for 15 sec with 10 min interval for a total of 40 min. Finally, tubes were centrifuged at 16000xg for 10 min and the supernatant (nuclear extract) was collected in prechilled microcentrifuge tubes and stored at -80°C till further processing.

To isolate the membrane fraction, the supernatant (cytoplasmic extract) was immediately transferred to prechilled microcentrifuge tubes and was again subjected to centrifugation at 16000xg for 40 min at 4°C. The pellet obtained after centrifugation was the

membrane fraction and the supernatant was the cytoplasmic fraction. Both were stored at -80 °C until used.

2.2.8. Sodium dodecyl sulfate polyacrylamide gel electrophoresis (SDS)

Based on molecular mass, protein samples were separated by SDS-PAGE following Laemmli method (1970).

Stock solutions:

Acrylamide solution or solution A: 30 % acrylamide and bis-acrylamide solution, 29:1.

Resolving gel buffer or solution B: Resolving gel buffer, 1.5M Tris-HCl buffer pH 8.8.

Stacking gel buffer or solution C: Stacking gel buffer, 0.5M Tris-HCl buffer pH 6.8.

Glycerol: A 50 % glycerol solution was prepared by adding 50 ml glycerol with 50 ml double distilled water.

TEMED: N, N, N', N',-Tetramethylethylenediamine was used as an essential catalyst for polymerization of SDS PAGE.

Ammonium persulfate (APS): A 10% solution was made by dissolving 20 mg of APS in 200 µl double distilled water. APS is an oxidizing agent used with TEMED for catalyzation of SDS PAGE.

Working solutions:

Resolving gel solution: The stock solutions were mixed in the following proportions to obtain a 7.5% resolving gel solution, calculation for 2 gels: 2.25 ml of Solution A, 2.25 ml of Solution B, 2 ml of Double distilled water, 2.5 ml of 50% glycerol, 5 µl of TEMED, 70 µl of 10% APS. To prepare other percentages of gel, the volume of solution A and double distilled water were changed appropriately while volume of other components remained the same.

Stacking gel solutions: The stock solutions were mixed in the following proportions (for 2 gels): 900 µl of Solution A, 1.5 ml of Solution C, 3.6 ml of double distilled water, 6 µl of

TEMED, 36 μ l of 10% APS. APS and TEMED were added to the solution just prior to polymerization.

Electrophoresis buffer: Gel running 1X TGS buffer containing 25 mM Tris-HCl, 190 mM glycine and 0.1% SDS was prepared from 10X TGS buffer by adding 100 ml of 10X TGS and 900 ml of double distilled water.

Sample denaturing (Laemmli) buffer: Laemmli buffer was prepared by adding ready to use 2X Laemmli buffer and 5% (v/v) β -mercaptoethanol (to 750 μ l 2X Laemmli buffer 37.5 μ l β -mercaptoethanol was added). This denaturing buffer was stored at -20 °C for upto one month.

Protease inhibitor cocktail: 2X protease inhibitor cocktail mix was prepared from 100X protease inhibitor cocktail by adding 3.6 μ l 100X protease inhibitor cocktail and 176.4 μ l molecular biology grade water.

Polymerization:

Mini-PROTEAN tetra system (Bio-Rad) was used to carry out gel electrophoresis. The short glass plates and 1 mm thick spacer glass plates were assembled inside the casting frame as per instructions provided by manufacturer. Initially, the resolving gel solution was prepared, swirled gently and poured in between the two glass plates up to a height of three-fourth of the total height. Stacking gel solution was very slowly layered upon the resolving gel so that the level of the separating gel was not disturbed. A 1 mm thick 10-well comb was inserted into the stacking gel solution and the solutions were allowed to solidify at RT for 20-30 minutes. The comb was gently removed after complete polymerization of both solutions. Glass plates were removed from the casting frame and placed within the buffer dam. Electrophoresis buffer was added to the inner chambers of the apparatus till it overflowed to remove unpolymerized acrylamide and air bubbles. The outer chamber was also filled with electrophoresis buffer upto the required level.

Sample preparation:

Sample preparation methodology has already been explained above. Samples stored at -80°C were taken out, thawed and ran on gel.

Sample loading and electrophoresis:

Preheated samples were loaded in wells of the polyacrylamide gel. To know the molecular masses of sample proteins, one of the empty wells was loaded with marker proteins of known molecular mass. The inner chamber was then gently filled up with electrophoresis buffer.

The electrophoresis chamber was connected to a power pack and electrophoresis was carried out initially for 15 min at a constant voltage of 130 volts. Then it was changed to a constant voltage of 180 volts for 75 min i.e. till the bromophenol blue dye front was just out from the base of the gel.

2.2.9. Immunoblotting

The Towbin *et al.* (1979) method was used to perform immunoblotting. The details are given below.

Immunoblotting solutions:

Tris-buffered saline (TBS): 1X TBS was prepared from 10X TBS by adding 100 ml of 10X TBS to 900 ml of double distilled water.

Phosphate-buffered saline (PBS): 1X PBS was prepared from 10X PBS by adding 100 ml of 10X PBS to 900 ml of double distilled water.

Tween-20 wash solution (TBST): 0.1% (v/v) Tween-20 was dissolved in TBS.

Primary antibody dilution buffer: 3% (w/v) bovine serum albumin (BSA) dissolved in TBST.

Blocking buffer or secondary antibody dilution buffer: 5% non-fat-dry-milk (NFDM) dissolved in TBST.

Transfer buffer for PVDF membrane: 100 ml of 10X TG buffer was dissolved in 700 ml of double distilled water and 200 ml of methanol. 0.0375 gm of SDS was added to 1X TG buffer.

Procedure for transfer of protein onto PVDF membrane: Wet transfer: To transfer higher molecular weight protein, wet transfer methodology was followed. The transfer of protein onto PVDF membrane was performed in Mini trans-blot cell. Initially protein samples were separated based on their molecular mass in SDS polyacrylamide gel. The gel was immediately transferred to pre-chilled transfer buffer and was kept for 5 min. To reduce hydrophobicity of PVDF membrane, it was soaked in pre-chilled methanol for 1 min followed by a washing in water. The membrane was then placed in pre-chilled transfer buffer. A glass casserole was filled with pre-chilled transfer buffer. Mini gel holder cassette was placed inside the casserole with its gray side down. Pre-wetted foam pad was placed on the gray side of the cassette. A sheet of Mini trans-blot filter paper soaked in transfer buffer was placed on the foam pad. The equilibrated gel was then placed over the filter paper. The pre-wetted membrane was placed over the gel. A glass tube was gently rolled over the membrane to remove air bubbles trapped in between. The sandwich was completed by placing filter paper on the membrane and another foam pad on the top. The cassette was firmly closed and placed inside the module. The module was placed inside the tank along with a cooling unit and a stir bar. The tank was filled with chilled transfer buffer till the blotting mark on the tank. The lid was placed and the cables were plugged into the power supply. Transfer was carried out at a “constant voltage” of 40 volt for 4 h.

Semi-dry Transfer: To transfer of low molecular weight proteins, the semi-dry transfer technique was used. After SDS gel electrophoresis was over the processing of PVDF and gel was similar to that of wet transfer. A thick filter paper was soaked in transfer buffer and was placed over the transfer assembly on the anode followed by placement of a PVDF membrane,

the electrophoresed gel and another thick paper (towards the cathode). After rolling out air bubbles from the assembly, transfer was carried out at 25 volt for 35 min.

After transfer, the blotting sandwich was dismantled for both wet and semi-dry transfers and the PVDF membrane was transferred to TBS for 5 min. The membrane was then placed in blocking solution for 1 h in a shaker, to prevent non-specific binding of IgG. The membrane was transferred to the primary antibody solution and kept at RT for 1 h with constant shaking. The membrane was then kept at 4°C for overnight incubation with constant shaking. The membrane was washed thrice for 10 min each with TBST, and then transferred into the secondary antibody solution containing horse-radish peroxidase (HRP)-conjugated IgG. It was incubated in the secondary antibody solution at RT for 1 h with constant shaking. The membrane was washed thrice with TBST for 5 min each. For detecting HRP on immunoblots, supersignal west femto maximum sensitivity substrate kit was used. This kit contained two solutions: luminol and stable peroxide solution. Both solutions were mixed at equal volume just before detection and were applied uniformly over the blot. The blot was covered with clear plastic wrap and imaging was done with Chemidoc XRS equipped with Quantity 1-D analysis software version 4.6.9 (Bio-rad Laboratories).

Reprobing of the PVDF membrane: Reprobing of the PVDF membrane was done with restore plus western blot stripping buffer. After the blot was developed, it was washed thrice with TBST 5 min each followed by an incubation in stripping buffer for 30 min with constant shaking at 37°C. The blot was washed thrice with TBST for 15 min each at RT followed by blocking, incubation with antibodies and detection as described above.

2.2.10. Total RNA isolation and real time RT-PCR in MKN45 cells to study expression of Siah1 and Siah2 after H. pylori infection

1x10⁶ MKN45 cells were seeded in 6-well cell culture plate 24 h prior to infection and were placed inside an incubator at 37°C and 5 % CO₂. On the next day, cells were infected with *H.*

pylori. Total RNA was isolated using Qiagen RNeasy mini kit. Uninfected and *H. pylori*-infected cells were harvested with a new cell scraper. Harvested cells were placed inside microcentrifuge tubes and centrifuged down at 500xg for 5 min. Supernatant was gently aspirated and the cell pellet was loosened by flicking the tubes. 350 µl of buffer RLT (with 1% β-mercaptoethanol) was added and cells were homogenized with a 20-gauge needle fitted to an RNase-free syringe. 350 µl of 70% ethanol was added to the homogenized lysate and was mixed thoroughly by pipetting. 700 µl of the sample was added to an RNeasy-mini column placed in a 2 ml collection tube and was centrifuged down at 8000xg for 15 s. The flow through in collection tube was discarded and 350 µl buffer RW1 was added to the column and was centrifuged at 8000xg for 15 s. The flow through in the collection tube was discarded. On-column DNase digestion was performed to prevent contamination from genomic DNA. For this, 80 µl DNase mix (10 µl of DNase 1 stock solution + 70 µl of Buffer RDD) was added to the mini column and was incubated for 15 min at RT. 350 µl of buffer RW1 was added and was centrifuged at 8000xg for 15 s. The flow through in the collection tube was discarded. 500 µl of buffer RPE was next added and centrifuged at 8000xg for 15 s and the flow through was discarded. 500 µl of buffer RPE was added, centrifuged at 8000xg for 2 min and the flow through was discarded from the collection tube and was again centrifuged down at top speed for 1 min. The mini column was transferred to a 1.5 ml centrifuge tube, 30 µl of RNase-free water was added to the column, incubated for 1 min and was centrifuged at 8000xg for 1 min. The RNA yield was estimated spectrophotometrically.

First strand cDNA was synthesized from total RNA using SuperScript First Strand Synthesis System for RT-PCR. Initially, RNA/Primer mix was prepared in a DNase/RNase free 0.2 ml microfuge tube. The RNA/Primer mix consisted of 0.5 µg total RNA, 1 µl random hexamers, 1 µl 10 mM dNTP mix and the volume was made upto 10 µl by adding DEPC-treated H₂O. Tubes were incubated at 65°C for 5 min and then on ice for 1 min. Then, 2 µl

10X RT buffer (1X), 4 μ l 25 mM MgCl₂, 2 μ l 0.1 M DTT, 1 μ l RNaseOUT were added to the RNA/Primer mix and was incubated at 65°C for 5 min. 9 μ l reaction mixture was added to the RNA/Primer mix, mixed gently and given a brief centrifugation. The mix was then incubated at 25°C for 2 min. 1 μ l (50 units) of SuperScriptII RT was added to each tube and incubated at 25°C for 10 min. Next, reaction tubes were incubated at 42°C for 50 min. The reaction was terminated by incubating at 70°C for 15 min and was chilled on ice. The reactions were collected by brief centrifugation. To degrade RNA, 1 μ l RNase H was added to each tube and was incubated for 20 min at 37°C. The synthesized cDNA was used to perform Real time RT-PCR in the 7500 Real-time PCR system (Applied Biosystems). The reaction mixture consisted of 12.5 μ l Taqman universal mix, 1.25 μ l 20X primer/probe, 1.5 μ l cDNA, 9.75 μ l DEPC-treated H₂O. The PCR conditions are mentioned in Appendix IX.

2.2.11. In vitro binding assay

Annealing of single stranded (ss) complementary oligonucleotides (oligos) in STE buffer:

The 5' biotinylated complementary oligos of human *siah1* 5' UTR at EBS and *siah2* promoter at EBS and TBS were annealed. The list of 5' biotinylated wild type (WT) and mutant (Mut) oligos are mentioned in Appendix X. These oligos were reconstituted in DNase, RNase-free DEPC-treated H₂O at 100 pmol/ μ l concentration. Complimentary DNA strands were annealed in STE buffer (1X TE, 100 mM NaCl). 40 μ l (4000 pmol) of each strand of complimentary oligos were added in 500 μ l reaction volume. The reaction mixture with oligonucleotide was incubated at 80°C for 15 min followed by slow cooling to room temperature and was stored at -20°C.

Nuclear lysate preparation: 5x10⁶ MKN45 cells were seeded in 100 mm cell culture dish 24 h prior to infection and were placed inside an incubator maintaining 37°C and 5 % CO₂. On the next day, cells were infected with *H. pylori* or were left untreated. Nuclear isolation was done

for treated and untreated cells using NE-PER nuclear and cytoplasmic extraction kits as described earlier.

Processing of dynabeads M-280 streptavidin and gel running: Dynabeads were resuspended in the supplied vial by rotating to get a homogeneous suspension and 20 μ l of it was taken in a microfuge tube. The microfuge tube was placed on a magnet for 1 min and the supernatant was discarded. The tube was removed from the magnet and beads were resuspended in equal volume of 2X binding and washing buffer (B&W buffer, 10 mM Tris HCl pH 7.5, 1 mM EDTA, 2 M NaCl), next, beads and were washed again as per the instruction mentioned above. After washing, the buffer was removed and was resuspended in binding buffer (1X binding buffer EMSA kit pierce, 2.5% glycerol, 5 mM MgCl₂, 10 mM EDTA) twice of the original volume. Biotinylated oligo was next added and beads were incubated for 10 min with gentle rotation/short tapping. Microfuge tubes were placed on the magnet and beads were separated using magnet. Beads were washed three times with 1X B&W buffer and were then incubated with infected or uninfected nuclear lysates for 30 min at room temperature. Beads were washed twice with 1X B&W buffer followed by resuspension in 25 μ l of sample buffer with β -mercaptoethanol and was boiled at 100°C for 10 min. Proteins were resolved in a polyacrylamide gel and electrotransferred to a PVDF membrane for detection.

2.2.12. *In vivo binding assay*

5x10⁶ MKN45 cells were seeded in 100 mm cell culture dish 24 h prior to transfection and the next day cells were either left uninfected or were infected with *H. pylori*. ChIP assay was performed with nuclear lysates using QuikChIP kit. To cross-link protein/DNA complex in the nucleus, 3 h post-infection cells were centrifuged at 3000xg for 5 min and 10 ml of 1% formaldehyde solution (270 μ l of 37% formaldehyde added to 10 ml of cell culture media) was added to cells after gently aspirating out old media. Cells were incubated at 37°C for 10 min. To stop cells getting over-fixed, 1 ml of 10X glycine was added to the tube, gently

swirled to mix and incubated at room temperature for 5 min. Cells were centrifuged at 3000xg for 5 min and media was removed as much as possible without disturbing the cell pellet. Cells were washed two times with 10 ml of ice cold PBS. Then, 1 ml of ice cold PBS (supplemented with PMSF and PIC) was added and centrifuged at 7000xg at 4°C for 5 min. The supernatant was discarded. The pellet was resuspended in 1 ml of SDS lysis buffer (supplemented with PMSF and PIC) and was incubated on ice for 10 min. The lysate was sonicated on ice at 40% of the max speed with 25 pulses for 30 sec on and 30 sec rest on ice. The sonicated lysate was centrifuged at 7000xg at 4°C for 10 min to pellet the insoluble material. The supernatant was transferred to fresh microfuge tubes and stored at -80°C. The next day, 200 µl of supernatant and 800 µl of ChIP dilution buffer containing PIC were taken in microfuge tubes. To remove molecules that can non-specifically bind to the protein A/G agarose, 75 µl of salmon sperm DNA/protein A/G agarose was added to the tubes and rotated for 30 min at 4°C. Samples were centrifuged at 3000xg for 1 min. Supernatant was taken in a fresh microfuge tube. 10 µl sample of the supernatant was aliquoted into a fresh microfuge tube and stored at 4°C to be used as input. 5 µg of immunoprecipitating antibody was added to the supernatant of both control and infected sample and 5 µg of IgG was added to the control lysate. Tubes were rotated overnight at 4°C. To collect the antibody/antigen/DNA complex, 60 µl of salmon sperm DNA/protein A/G agarose was added to the tubes and rotated for 1 h at 4°C. The protein/A/G agarose/antibody/chromatin complex was collected after centrifugation at 3000xg for 1 min. The supernatant was discarded and the complex was washed on a rotating platform with wash buffers A, B, C and D. 500 µl of elution buffer was added to the input tube and set aside. 250 µl of elution buffer was added to the protein A/G agarose/antibody/chromatin complex. Tubes were incubated at RT for 15 min followed by centrifugation at 3000xg for 1 min and the supernatant was collected. The elution step was again repeated for the second time and the eluates were combined (total volume ~500 µl). To

reverse cross-link of DNA and protein complex, 20 μ l of 5M NaCl was added to the eluates and incubated at 65°C for overnight. Next day, 1 μ l of RNase A was added and incubated at 37°C for 30 min. 10 μ l of 0.5 M EDTA, 20 μ l of 1 M Tris HCl pH 6.5, and 2 μ l 10 mg/ml proteinase K was added and incubated at 45°C, for 1 h. The DNA was purified using QuikChIP DNA purification kit. 750 μ l of binding buffer was added to 500 μ l of the reversed cross-link eluates and was loaded on spin column fitted with collection tube. Columns were incubated for 1 min at RT followed by centrifugation at 8000xg for 1 min at RT. The flow through was discarded and 700 μ l of column wash solution was added, centrifuged at 8000xg for 30 sec at RT. The column was removed from the collection tube and the flowthrough was discarded and again centrifuged at 8000xg for 30 sec at RT. The column was fitted on a microfuge tube and 15 μ l of elution buffer was added, incubated for 1 min at RT followed by centrifugation at 8000xg for 1 min at RT. The DNA concentration was measured using a spectrophotometer as well as by gel running. The eluted DNA was used to perform PCR using primer from ETS2/Twist1 binding regions of *siah1* 5' UTR and *siah2* promoter. Primer pairs used for performing PCR is mentioned in Appendix XI.

PCR for Siah1 was set up using the following reaction mixture: 5 μ l 10X buffer (1X), 1 μ l 10 mM dNTP (0.2 mM), 1 μ l primer F (10 pmole), 1 μ l primer R (10 pmole), 1 μ l DNA (20 ng), 5 μ l mix (2.7 M betaine, 6.7 mM DTT, 6.7% DMSO, 55 μ g/ml BSA), 2 μ l NEB Taq polymerase, 34 μ l H₂O. The reaction condition for PCR is mentioned in Appendix XI. The amplified PCR product was run on 1.2% agarose gel.

PCR for Siah2 was set up using the following reaction mixture: 5 μ l 10X HIF buffer (1X), 1 μ l 10 mM dNTP (0.2 mM), 2 μ l 50 mM MgSO₄ (2.0 mM), 1 μ l Primer F (10 pmole), 1 μ l Primer R (10 pmole), 1 μ l DNA (20 ng), 1 μ l HIF Taq polymerase, 38 μ l H₂O. The reaction condition for PCR is mentioned in Appendix XI. The amplified PCR product was run on 1.2% agarose gel.

2.2.13. Dual luciferase reporter assay

Cell lysate preparation: 24 h prior to transfection, MKN45 cells were plated in 24-well culture plates with cell density of 2×10^5 cells per well. Plates were placed inside an incubator at 37°C with 95% humidity and 5% CO_2 . Cells were transfected with Lipofectamine2000 reagent. Transfected cells were infected with *H. pylori* or were left untreated. Cells were scraped in media and harvested at 500xg for 5 min. The pellet was resuspended in 83.33 μl passive lysis buffer (PLB). Cells were vortexed and kept at room temperature for 5 min followed by two freeze and thaw cycles (at -70°C and 37°C for 20 min each).

Dual luciferase assay protocol: 15 μl cell lysates were added to wells of a 96-well plate. The luminometer was programmed to perform a 2 sec pre-measurement delay followed by a 10-sec measurement read for luciferase activity. 75 μl of the luciferase assay reagent II (LARII) equilibrated to RT was added to each well using a multi-channel pipette and mixed by pipetting 2-3 times. The plate was placed immediately inside the luminometer and readings were recorded. The plate was taken out, 75 μl of stop and glo buffer was added and placed inside the luminometer for readings.

2.2.14. Immunoprecipitation (IP) assay

To study interaction of membrane-bound β -catenin with Siah1 protein, immunoprecipitation assay (IP) was performed. 5×10^6 cells were seeded in 100 mm cell culture dish 1 day prior to infection. Membrane fraction was isolated from uninfected and *H. pylori*-infected cells as mentioned earlier. To the membrane fraction, 200 μl of TEN buffer (150 mM NaCl, 50 mM Tris pH 7.5, 1 mM EDTA) supplemented with 1% Triton X-100 and protease inhibitor cocktail (10 $\mu\text{l}/\text{ml}$) was added. Tubes were kept on ice for 30 min with vortexing at every 10 min interval for complete lysis. 800 μl TEN buffer supplemented with protease inhibitor cocktail (10 $\mu\text{l}/\text{ml}$) but without Triton X-100 was added to each tube. Siah1 antibody was added to cell lysate at 1:50 dilution, whereas equal amount of IgG B was added to uninfected

cell lysates and was incubated overnight at 4°C with shaking. After overnight incubation, 15 µl of 50% protein A/G plus-agarose was added to each tube and was again incubated for 3 h with shaking at 4°C. The agarose-bound immunocomplex was centrifuged down and the pellet was washed twice with ice cold 1X PBS (230 g for 5 min). 25 µl of sample buffer supplemented with 5% β-mercaptoethanol was added to the pellet and cooked. Lysates were then loaded onto SDS gel, Proteins were separated based on their molecular weight followed by immunoblotting. Detection was performed as described previously.

2.2.15. Generations of stable cell lines overexpressing ETS2, Twist1, Siah1 and Siah2

Both MKN45 and AGS cells were used to stably express ETS2, Twist1, Siah1, Siah2 and the empty vector pcDNA3.1⁺. 24 h prior to transfection, cells were seeded in a 96-well plate. Cells were transfected as described previously and 36 h post transfection, cells were trypsinized and re-plated in a 6-well plate. 300 µg/ml of G418 was added to select cells expressing the desired protein. After each 3 days, old media was discarded and fresh media with 300 µg/ml of G418 was added. This pressure was maintained till colonies were obtained from single cells and positive colonies were selected using cloning disc. Colonies were placed in a 12-well plate and were kept under the selection pressure by adding 300 µg/ml of G418. After the colonies were confluent, they were transferred to T-75 flask and were allowed to grow till 70-80% confluency is reached. Flasks were trypsinized and cells were frozen using freezing mix as described earlier. To confirm the expression of desired protein, 0.5×10^6 cells were taken out from the trypsinized flasks and boiled in sample buffer with 5% β-mercaptoethanol. Immunoblotting was performed as described previously.

2.2.16. Embedding and sectioning of gastric biopsy samples

Gastric biopsies were stored overnight in 4% PFA followed by storage in 25% sucrose solution. 24 h prior to sectioning, the cryostat instrument was brought to -20°C. Just prior to sectioning, poly-L-lysine coating was given over glass slides where tissue sections would be

mounted and incubated at 37°C for 30 min. Tissue sample was placed over specimen holder and was embedded in OCT media followed by immediate freezing by placing it inside the cryostat. 10 µm thick sections were prepared from adenocarcinoma and control samples. Tissue section was processed for immunofluorescence staining as described in the next section.

2.2.17. Immunofluorescence and confocal microscopy

To study ETS2, Twist1, Siah1 and Siah2 expression in adenocarcinoma gastric biopsies, tissue sections were immunostained with their respective antibodies. The tissue section was washed with 1X PBS followed by treatment with 0.5% Triton-X-100 in PBS for 20 min. Tissue section was blocked with 3% FBS in PBST for 1 h. The section was then incubated with primary antibody diluted in blocking buffer for 1 h at RT followed by overnight incubation at 4°C. The section was washed with PBST three times of 5 min each followed by incubation with fluorescently conjugated secondary antibodies diluted in blocking buffer for 1 h at RT. The section was washed two times with PBST for 5 min each and then incubated for 20 min with DAPI diluted in PBS. Final washing was with 1X PBS, and the section was mounted with fluoromount G. Digital images were captured for the immunofluorescence stained sections in a fluorescence microscope. (Refer to appendix III for dilutions of antibodies used).

For immunofluorescence staining of AGS and MKN45 cells, 0.2×10^6 cells were grown on coverslips. Uninfected or *H. pylori*-infected cells were fixed with 4% PFA in PBS and permeabilized with 0.1% Triton-X-100 as described earlier. Cells were incubated with blocking buffer (3% BSA in PBST) for 1 h, followed by overnight incubation with respective primary antibodies diluted in blocking buffers. After overnight incubation, cells were washed twice in PBST followed by treatment with secondary antibody for 1 h at RT. Cells were stained with DAPI and mounted in fluoromount G as described earlier. Cells were scanned

for imaging either by a fluorescence microscope or confocal microscope. For confocal microscopy, images were captured using a LSM-TPMT camera system (Carl Zeiss) and Zen 2010 software (Carl Zeiss). Images were analysed using LSM software (Carl Zeiss) and were processed using Adobe Photoshop CS4.

2.2.18. Wound-healing assay or scratch assay

Wound-healing properties of Siah1, Siah2, ETS2 and Twist1 expressing cells in the presence of *H. pylori* was studied by performing scratch assay using AGS cells stably expressing these proteins. One day prior to infection, 1×10^6 AGS cells stably expressing Siah1, Siah2, ETS2, Twist1 or pcDNA3.1⁺ were seeded in 6-well cell culture plate. After a monolayer was formed on the next day of plating, a wound was marked over the monolayer with a 200 μ l pipette tip. To remove dislodged cells, old media was discarded and fresh media was added to wells. Cells were either infected with *H. pylori* or left uninfected for 24 h. Cell migration in the wound was studied for a span of 24 h and images were taken at 6 h, 12 h and 24 h time points using a bright-field microscope. The number of cells migrated was counted using ImageJ 1.43 software (NIH).

2.2.19. Anchorage-independent growth assay

Soft agar assay was performed with uninfected or *H. pylori*-infected MKN45 cells stably expressing Siah1, Siah2, ETS2, Twist1 or pcDNA3.1⁺ to study anchorage-independent growth of cells. Cells were seeded in between two different layers of agar and anchorage-independent growth of cells was studied after colony was formed. MKN45 cells stably expressing Siah1, Siah2, ETS2, Twist1 or pcDNA3.1⁺ were seeded in 24-well cell culture plate at a density of 0.1×10^6 . Next day, cells were either infected with *H. pylori* for 6 h or left uninfected and treated with gentamicin for 2 h to kill extracellular bacteria. Cells were harvested and mixed with top agar.

First a layer of 0.6% bottom agar was prepared in 6-well cell culture plate from a mixture of 1.2% Bacto agar (1.2 gm of Bacto agar dissolved in 100 ml of distilled H₂O, autoclaved and maintained at 50°C to prevent solidification) added to equal volume of Dulbecco's Modified Eagle Medium/ Nutrient Mixture F-12 Ham (DMEM/ F12, 1:1 mixture) media. After adding the bottom layer, the plate was kept inside incubator at 37°C for 30 min. Then 0.3% top agar was prepared by adding 1.2% agar suspension, 2X media (DMEM/F12, 1:1 mixture), gentamicin treated cells (0.1×10^4) and distilled H₂O. The plate with bottom agar was taken out from the incubator and the top agar with cells was plated over the bottom agar. Plates were placed inside humidified incubators containing 5% CO₂ and maintained at 37°C for 3 weeks. Cells were fed twice weekly with fresh media. Visible colonies started appearing on the top agar. The number of colonies appeared were directly counted and the colony size was compared between various treatment groups.

2.2.20. Transwell migration and invasion assay

Transwell migration and invasion assay was performed to study invasive properties of GCCs overexpressing Siah1 or Siah2. Transwell migration assay was performed using 8- μ m pore size Transwell Biocoat control inserts whereas Transwell invasion assay was performed with 8- μ m pore size Transwell Biocoat matrigel-coated inserts. AGS cells were seeded in a 24-well cell culture plate 24 h prior to transfection. AGS cells were either transfected with overexpression plasmid Siah1, Siah2, pcDNA3.1⁺ or with siRNA of Siah1, Siah2 and control duplex using a methodology described earlier. 36 h post transfection, cells were harvested and 0.5×10^4 cells were seeded on Transwell control inserts or coated matrigel inserts placed inside a 24-well plate. The upper chamber was filled with serum free RPMI media whereas the lower chamber was filled with complete media. Cells were infected with *H. pylori* or left uninfected and was kept inside a 37°C humidified incubator at with 5% CO₂. Inserts were taken out after 24 h of incubation and cells on the top surface of Transwell were scraped off

with a cotton swab. Inserts were washed in 1X PBS. Cells in the lower side of inserts were fixed with 4% paraformaldehyde for 30 min, washed with 1X PBS followed by permeabilization with 0.5% Triton-X-100 in PBS. Cells were then incubated for 30 min in haematoxylin and washed with 1X PBS. Inserts were air dried for 1 h, and then membrane was cut from the insert and mounted over glass slides keeping the lower side down. The number of cells migrated and invaded was counted using a bright field microscope.

2.2.21. Statistical analysis

Densitometric analyses of western blot images were done by Quantity 1-D Analysis software version 4.6.9 (Bio-rad Laboratories). Statistical analysis of quantitative data was performed by Student's *t* tests. Values were given as mean±SEM. Statistical significance was determined at * $P < 0.05$.

RESULTS

Chapter 3

3. RESULTS

3.1. *H. pylori* Induced Expression of Siah Proteins in Cultured Human GCCs:

The status of Siah expression in gastric cancer was not known. To study the expression of Siah proteins after *H. pylori* infection on human GCCs, MKN45 cells were infected with *cag* PAI(+) *H. pylori* strain 26695 at MOI 100 and 200 for 3 h and 6 h. Western blots performed with whole cell lysates showed induced expression of both Siah1 and 2 proteins post infection (p.i) (Fig. 3.1.1A and Fig. 3.1.1B). Although representative western blot analysis (n=3) revealed Siah1 and 2 induction with 200 MOI at 3 h and 6 h time points, 200 MOI at 6 h was optimal for induction of both Siah1 and 2 proteins. All cells were infected by *H. pylori* at MOI 200. To assess the optimum time for Siah1 and 2 expression, a time-kinetic study was performed with uninfected and 1 h, 3 h, and 6 h *H. pylori*-infected whole cell lysates, Western blot analysis revealed that 6 h was the optimum time required for expression of both Siah1 and 2 proteins after infection with *H. pylori* (Fig.3.1.1C and Fig. 3.1.1D). Hence, all future experiments were performed with strain 26695 at 200 MOI for 6 h time point unless mentioned otherwise. Immunofluorescence microscopy of MKN45 cells also showed induced expression of Siah1 and 2 proteins further confirming role of *H. pylori* as a potent inducer of Siah (Fig. 3.1E and Fig. 3.1F).

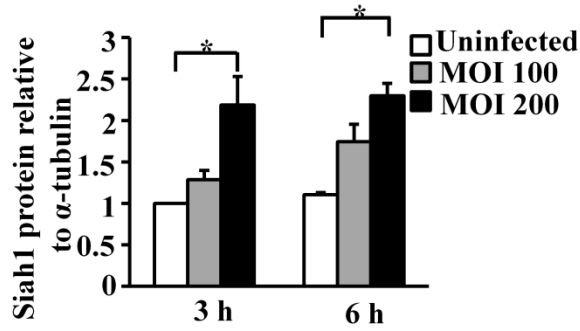
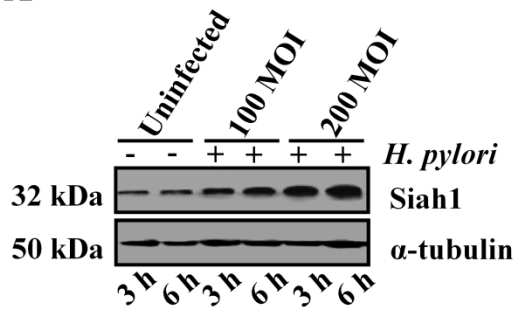
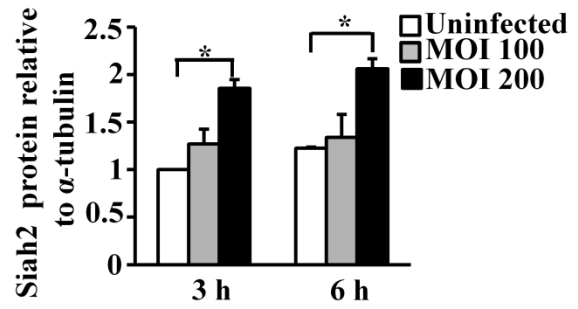
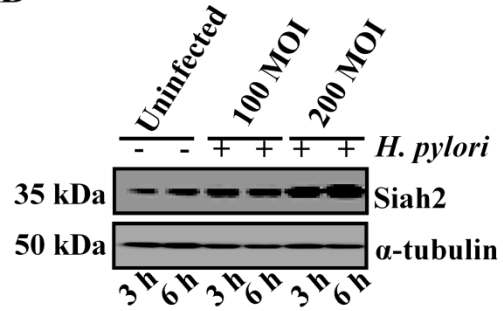
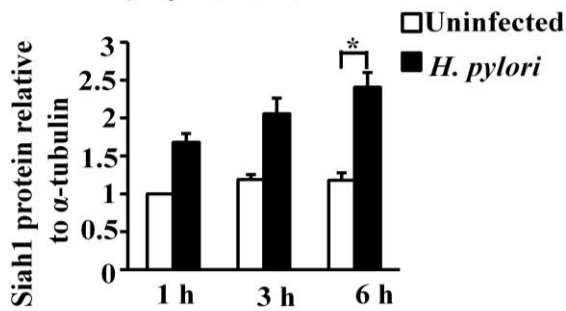
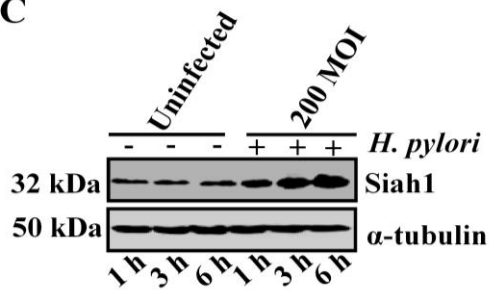
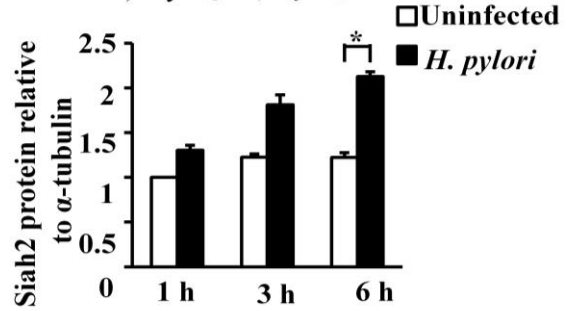
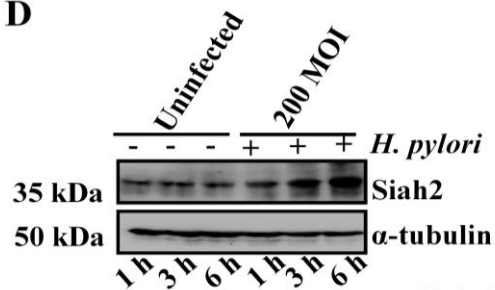
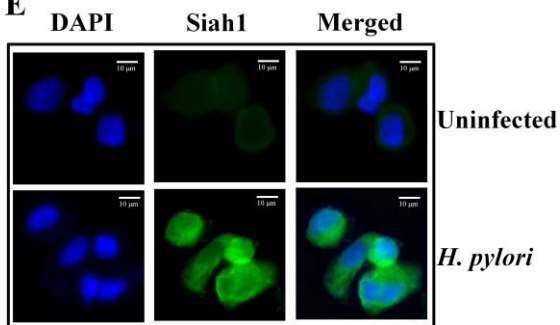
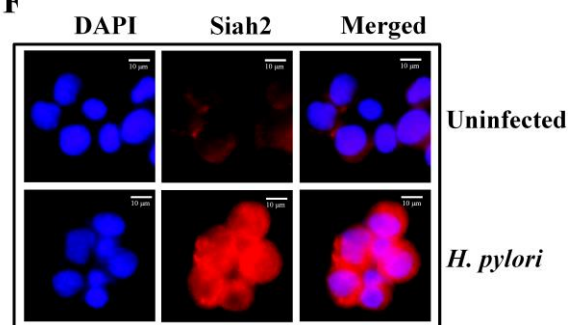
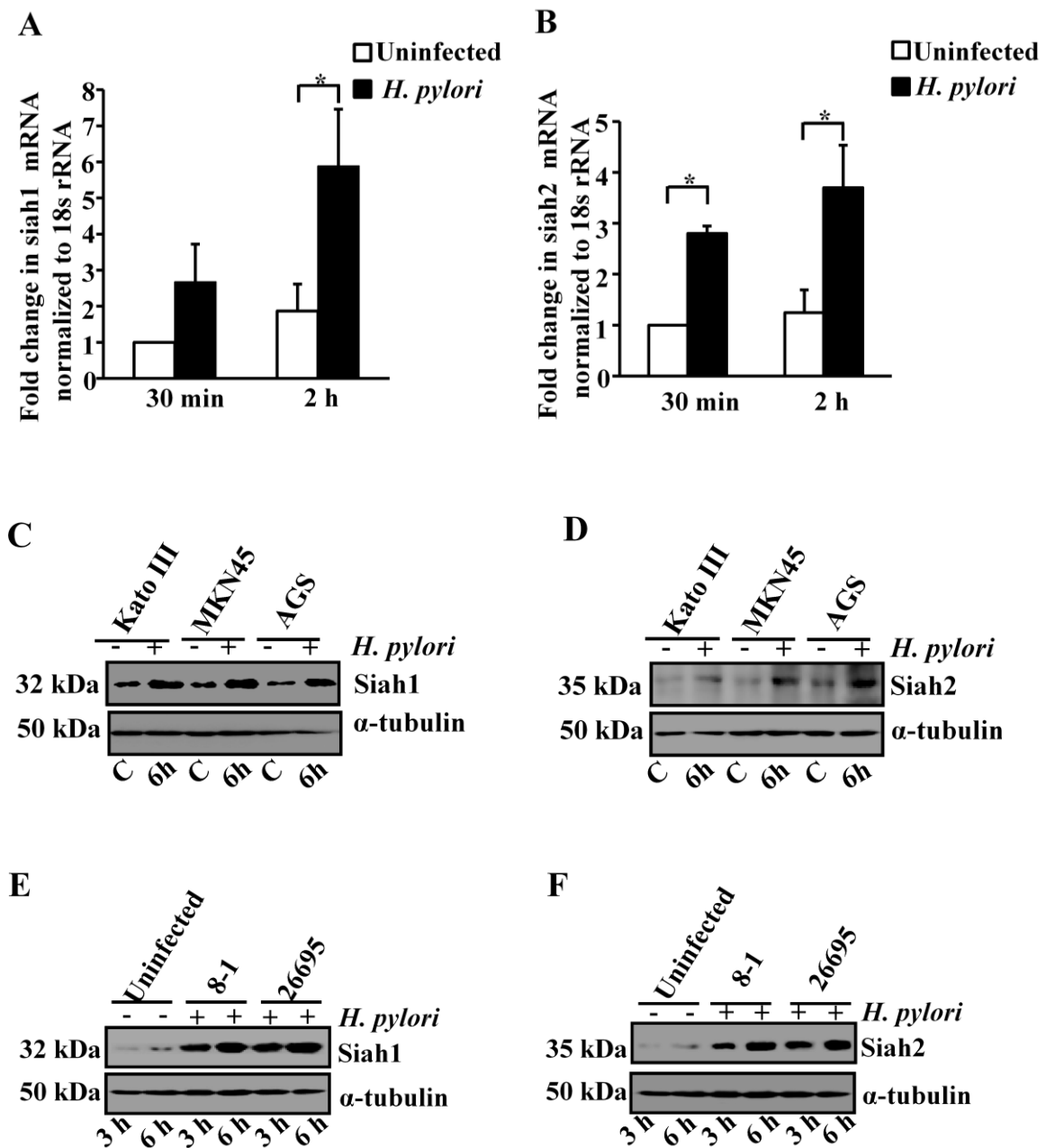
A**B****C****D****E****F**

Figure 3.1.1 *H. pylori* induce Siah1 and Siah2 protein expression in MKN45 cells. (A) Western blot of total cell lysates from uninfected and *H. pylori*-infected (3 h and 6 h with MOI 100 and 200) MKN45 cells shows induced level of Siah1 protein expression in infected GCCs. α -tubulin is the loading control. A graphical representation of the western blot data reveal that MOI 200 at 6 h is optimal for Siah1 induction. Bar represents normalized data (mean \pm SEM, n=3), *P<0.05. (B) A representative western blot (n=3) shows optimal induction of Siah2 protein at MOI 200 and 6 h time point from uninfected and infected whole cell lysates of MKN45 cells. Bar depicts normalized data (mean \pm SEM, n=3), *P<0.05. (C) Time kinetics of Siah1 protein expression in the infected MKN45 cells. Western blot analysis reveal 6 h is optimum for Siah1 induction. Bar represents normalized data (mean \pm SEM, n=3), *P<0.05. (D) A representative time course study of Siah2 protein expression in uninfected and *H. pylori*-infected MKN45 cells shows 6 h as optimal time for Siah2 expression. A graphical representation of the data reveals that 6 h is optimal for Siah2 induction. Bar represents normalized data (mean \pm SEM, n=3), *P<0.05. (E-F) A representative fluorescence microscopy (n=3) showing Siah1 expression in panel E and Siah2 induction in panel F of *H. pylori*-infected MKN45 cells.

The status of Siah1 and 2 expression at transcriptional level was also studied. Real-time RT-PCR performed with uninfected and infected cells showed significant increase in Siah1 and 2 messenger RNA level 2 h p.i. as compared to uninfected cells (Fig. 3.1.2A and Fig. 3.1.2B). As the expression of proteins often alters with cell lines, two other human GCCs Kato III and AGS were examined for their expression of Siah proteins. Western blot results showed significant induction of Siah1 and 2 proteins p.i. in Kato III and AGS cells (Fig. 3.1.2C and 3.1.2D). Earlier studies indicated p53 as a transcriptional regulator of Siah1 protein [103]. Western blotting of cell lysates prepared from p53-null KatoIII cells confirmed that the expression of Siah1 in *H. pylori*-infected GCCs was p53-independent. To identify the

effect of *cag* PAI on the expression of Siah proteins, we infected MKN45 cells with an isogenic *cag* PAI(-) mutant strain 8-1 and compared with the effect of strain 26695. Western blot results revealed no difference in the efficacy of *cag*(-) strains in inducing Siah proteins suggesting that induction of Siah proteins was *cag* PAI-independent (Fig. 3.1.2E and Fig. 3.1.2F). Further, the expression of Siah1 and Siah2 proteins in non-neoplastic, immortalized HFE145 cells was studied in the presence or absence of *H. pylori*. A similar effect of ETS2 and Twist1 expression was observed as in MKN45 cells (Fig. 3.1.2 G and Fig. 3.1.2 H)



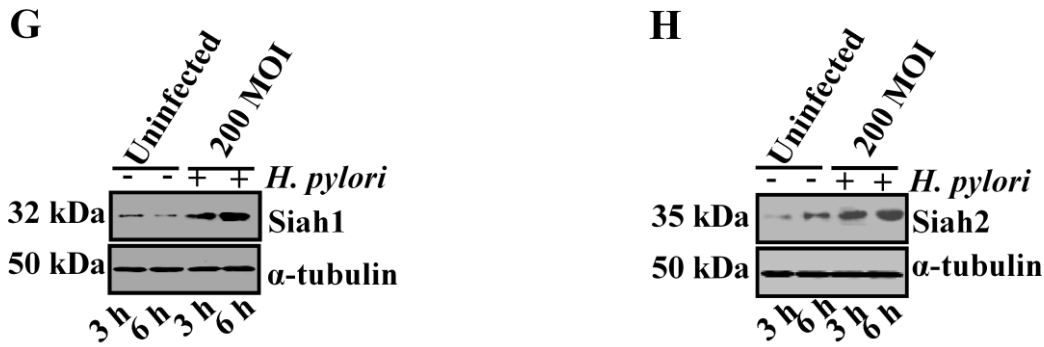


Figure 3.1.2 *H. pylori* enhances *Siah1* and *Siah2* mRNA and protein expression in GCCs. (A-B) Graphical analysis of real time RT-PCR data of uninfected and *H. pylori*-infected MKN45 cells reveal induced expression of *Siah1* and *Siah2* at transcriptional level. Bar represents normalized data (mean \pm SEM, n=3), *P<0.05. (C-D) Representative western blot results (n=3) showing expression of *Siah1* and *Siah2* from whole cell lysates isolated from uninfected and *H. pylori*-infected (MOI 200 and 6 h) KatoIII, MKN45 and AGS cells. (E-F) Western blot results (n=3) showing *Siah1* and *Siah2* expression from whole cell lysates isolated from uninfected and 26695 or 8-1 *H. pylori*-infected MKN45 cells, respectively. (G-H) Representative western blot (n=3) results showing expression of *Siah1* (G) and (H) *Siah2* in non-neoplastic immortalized HFE145 cells.

3.2. Identification of Transcription Factors Regulating Expression of *Siah1* and *Siah2*

Very few reports exist that describe the transcriptional regulation of Siah proteins. In order to understand the transcriptional regulation of Siah proteins, we analyzed both *siah1* and *siah2* promoters using the Genomatix Suite of sequence analysis tool MatInspector (professional version 6.2.2). A number of transcription factor binding sites were implicated in *siah1* and *siah2* promoters {as 5' untranslated region (UTR) might be involved in gene regulation, we also analyzed UTR regions}. Oncogenic transcription factor E26 transformation-specific 2 (ETS2) was showing very high probability of binding to the *siah1* 5' UTR at the putative ETS2 binding site (EBS). The core element GGAA/T [42, 104] was found to be located

between +92 to +95, GenBank: AJ400626.1. (Fig. 3.2.1). For *siah2* promoter, ETS2 and Twist-related protein1 (Twist1) showed very high probability of binding to the putative EBS {(GGAA/T) between -465 bp to -462 bp} and Twist1 binding site (TBS) {(CANNTG), [105] 431 to 426 bp upstream of the *siah2* transcription initiation site} (Fig. 3.2.2).

```

- 239  CGGGCGCAGC AACGGTAGCC GAGTAGCCCC CGCACCTACT GCCGCCTTT
- 189  GAGACCCGCA CAGCTACGCC CGCGGAGGCC GCCGCCGGCC GCGCCAACG
- 139  CTGTGCGCCT GCGCGCCCGC GAAAGCCCCG CCCCCCAGG CTCCAGCG
- 89   GCGGGACCGC GCCTCCTCAT GGCCGCCGCC GCAGTGTGTG GTATTTAGC
- 39   GGGGCGCGCG GCGGGCTCGA GGACGCGCGA AACGGCGGCG GCGGCGGCC
      11  GGGGGGAGCC GGGGCGGCCG TTGCGGGGCG CGCTCTCGAG AGGCGGCGG
      61  GGCCAGGGT  GTCCCGTCGG TCTCGGCGCC GGGAAGAGGC GGTGGCGCT
                               EBS
     111  CCCGCGGTGG CGGGGGTTGG CGACGGAGCG CGTTGGTGCC AGGACCGGG
     161  TCCGAGGCGC GCTCTCCGCC CACAG

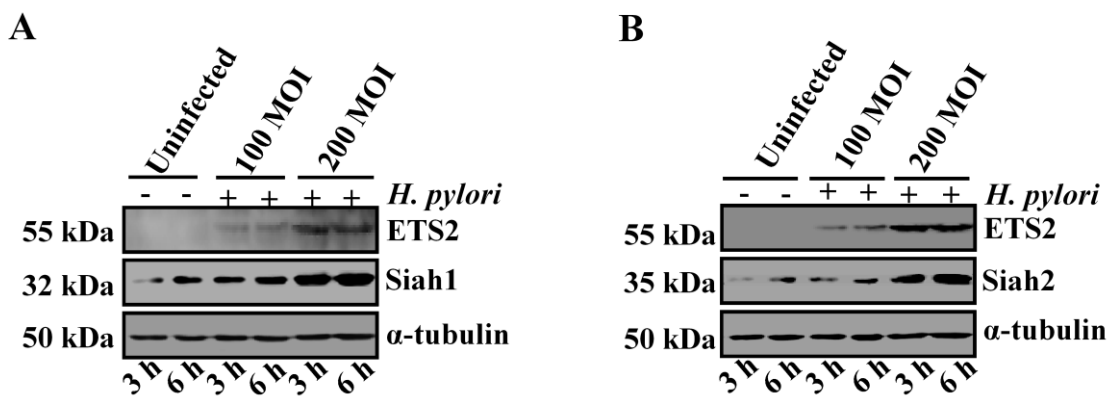
```

Figure 3.2.1 Analysis of human *siah1* promoter and 5'UTR. The EBS of human *siah1* promoter is depicted inside the box and is located between +92 to +95. The first exon of *siah1* cDNA is assumed to be at position +1 [42]

The oncogenic transcription factor Twist1 belongs to the basic-helix-loop-helix proteins (bHLH) family and its metastasis promoting role has been implicated in various cancers [106] including gastric cancer [107]. Several members from the evolutionarily conserved ETS family have been implicated in cancer progression along with ETS2 [108]. While Twist1 expression in GCCs were linked to the enhancement of lymph node and distant metastasis [109], ETS2 expression was linked with increased apoptosis or tumor suppression [110]. Therefore, it was imperative to study expression of ETS2 in relation to the Siah1 expression and Twist1 and ETS2 in relation to the expression of Siah2.

3.3. Induced Expression of ETS2, Twist1, Siah1 and Siah2 in *H. pylori*-Infected Human GCCs

In order to study the expression of ETS2 and Twist1 proteins in *H. pylori*-infected human GCCs, western blotting was performed with uninfected and *H. pylori*-infected whole cell lysates. Dose-kinetics performed at 3 h and 6 h p.i. with MOI 100 and 200 showed that MOI 200 was more effective in inducing ETS2, Siah1 or Siah2 expression than MOI 100 (Fig. 3.3.1 A and Fig. 3.3.1 B). Similarly, 200 MOI was more effective in inducing Twist1 and Siah2 expression than 100 MOI (Fig. 3.3.1 C).



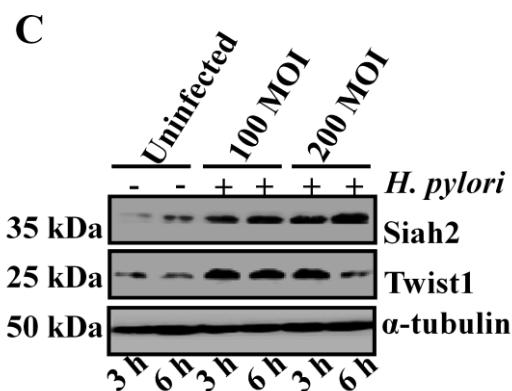


Figure 3.3.1 *H. pylori* infection induces parallel expression of ETS2, Twist1, Siah1 and Siah2 proteins in MKN45 cells. (A) A representative western blot (n=3) shows MOI 200 of *H. pylori* as the optimal dose for induction of ETS2 and Siah1 at 3 h and 6 h p.i.. (B) A representative western blot (n=3) of whole cell lysates from uninfected and *H. pylori*-infected MKN45 cells reveal MOI 200 as optimum for induction of ETS2 and Siah2 at 3 h and 6 h p.i. (C) A representative western blot (n=3) shows parallel expression of Twist1 and Siah2.

Next, a time-dependent study was performed at 200 MOI to study expression of ETS2 and Siah1 (Fig. 3.3.2 A) or ETS2, Twist1 and Siah2 (Fig. 3.3.2 B). While ETS2 expression was not observed at any time point in uninfected cell lysates, expression of ETS2 was observed starting from 1 h p.i. and that continued at similar level even at 6 h p.i. Induced ETS2 and Siah2 expression was also observed starting from 1 h p.i. which was maintained till 6 h p.i., but Twist1 protein expression was optimal at 3 h p.i. and decreased at 6 h. As pretreatment of cells with the proteasomal inhibitor MG132 (50 μ M dose for 6 h) rescued Twist1 from being degraded (Fig. 3.3.2C), definitely decreased expression of Twist1 at 6 h p.i. was related to its proteasomal degradation.

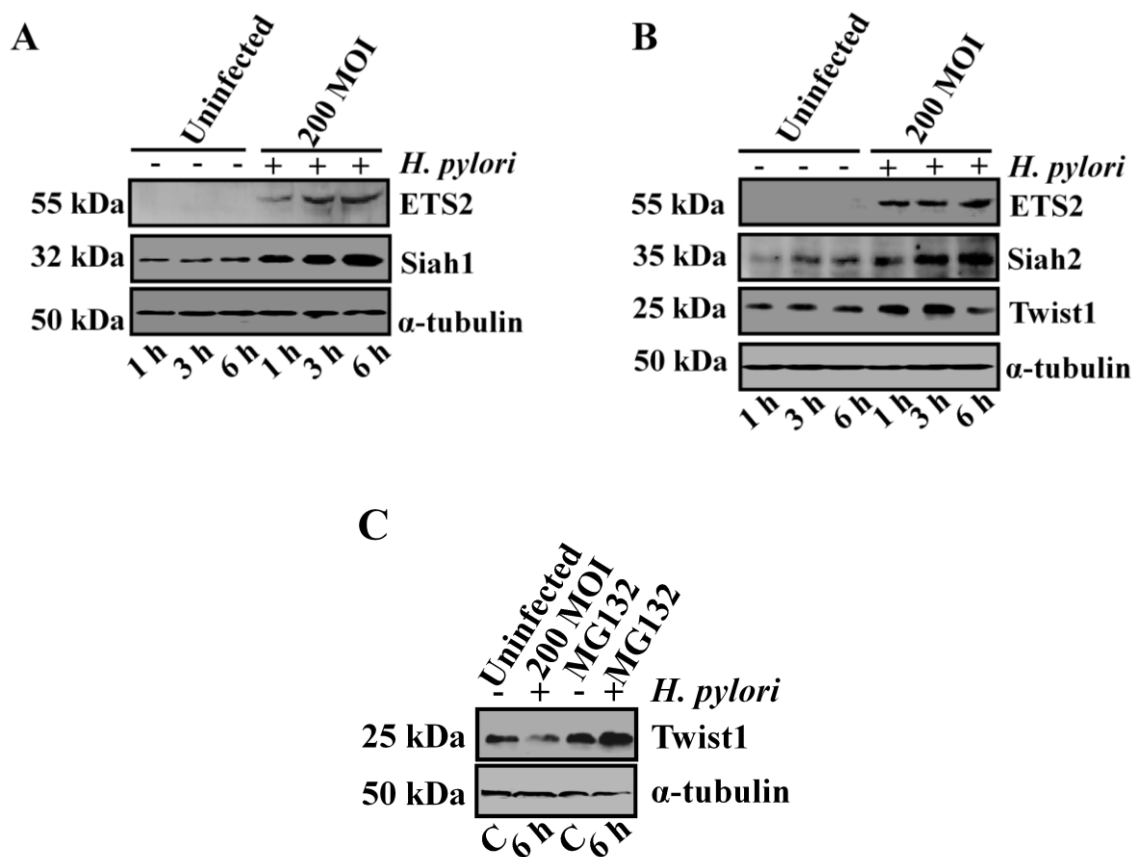


Figure 3.3.2 *H. pylori* infection induces ETS2, Twist1, Siah1 and Siah2 proteins in MKN45 cells. (A) Time kinetics (1 h, 3 h and 6 h) of ETS2 and Siah1 protein expression in total cell lysates of uninfected or *H. pylori*-infected MKN45 cells at MOI 200 (n=3). (B) A representative western blot of time kinetics (1 h, 3 h and 6 h) for ETS2, Twist1 and Siah2 protein expression in cell lysates of uninfected or *H. pylori*-infected MKN45 cells at MOI 200 (n=3). (C) Western blot (n=4) depicting Twist1 protein expression in whole cell lysates from uninfected or infected MKN45 cells that are either pretreated with 50 μ M of MG132 for 6 h prior to infection or are left untreated.

To further study the status of ETS2 and Twist1 proteins in other human GCCs, western blotting was performed with whole cell lysates of Kato III, AGS (MKN45 cells were kept as positive control) at 3 h p.i. (MOI 200). Western blot analysis from three independent experiments (n=3) revealed noticeable enhancement in ETS2 (Fig. 3.3.3 A) and Twist1

proteins (Fig. 3.3.3 B) in all cell lines. Furthermore, two other *cag*(-) strains of *H. pylori* 8-1 and D154 were also equally effective as the *cag*(+) strain 26695 in inducing ETS2 and Twist1 expression (Fig. 3.3.3 C and Fig. 3.3.3 D). Further, expression of ETS2 and Twist1 proteins in non-neoplastic, immortalized HFE145 cells was studied in the presence or absence of *H. pylori*. A similar effect of ETS2 and Twist1 expression was observed as in MKN45 cells (Fig. 3.3.3 E and Fig. 3.3.3 F).

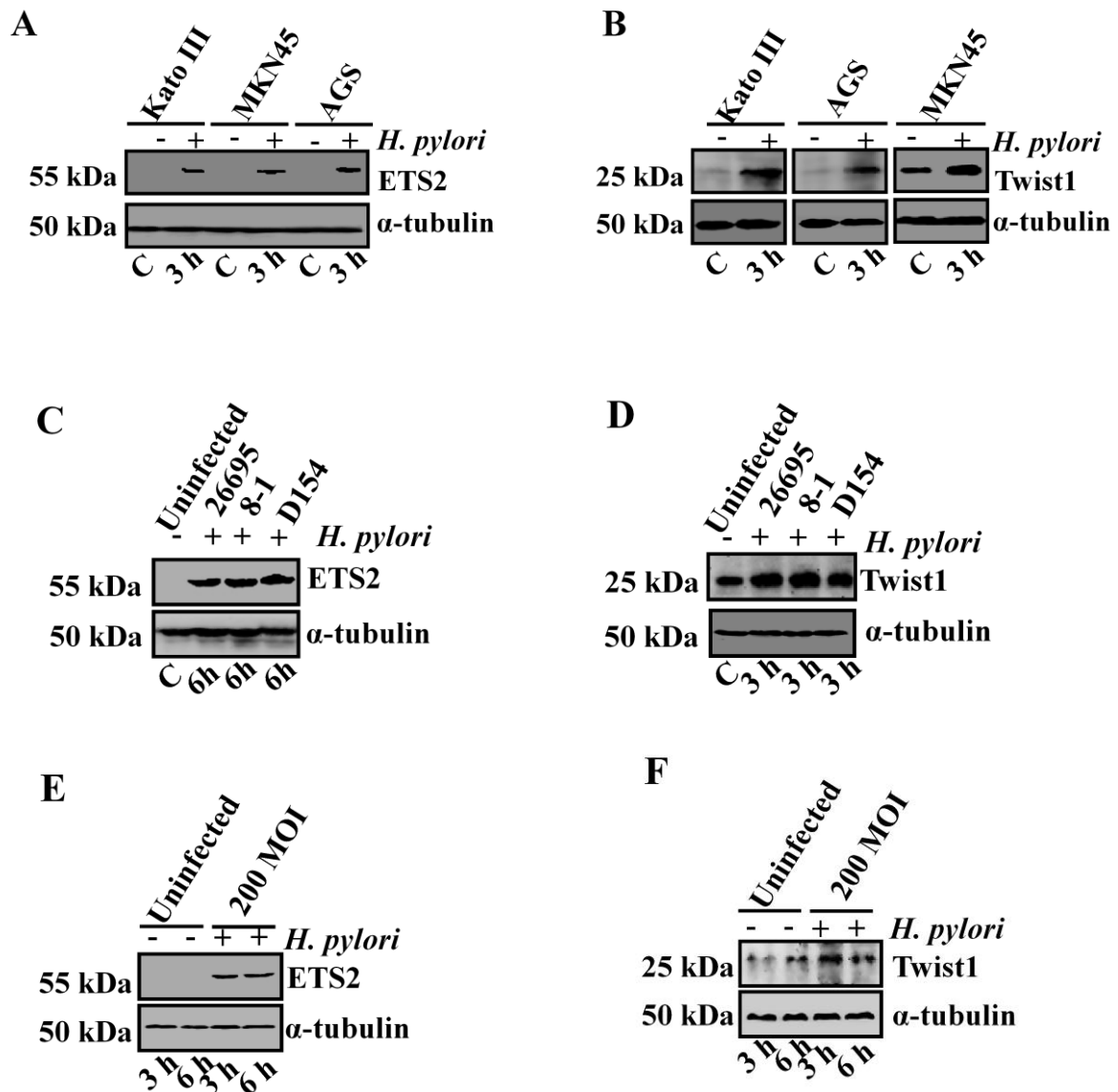
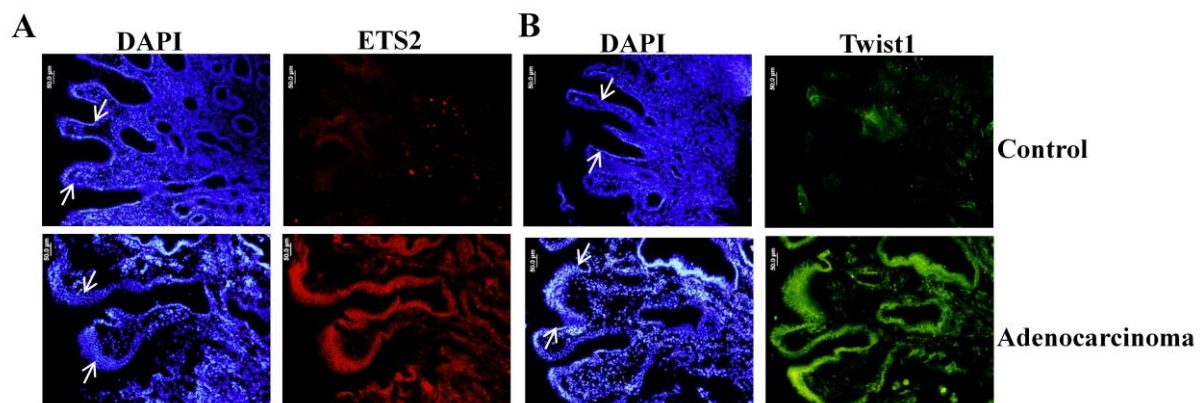


Figure 3.3.3 *H. pylori* infection induces *ETS2* and *Twist1* expression in GCCs (A) Western blot (n=3) for *ETS2* expression in whole cell lysates prepared from uninfected or infected (MOI 200 of *H. pylori* for 3 h) Kato III, MKN45 and AGS cells. (B) A representative western blot (n=3) showing *Twist1* expression in uninfected and *H. pylori*-infected Kato III, MKN45 and AGS cells. (C) A representative western blot (n=3) showing equal effectiveness of strain 8-1, D154 and 26695 in inducing *ETS2* (D) and *Twist1* protein expression. (E) A representative western blot (n=3) result showing expression of *ETS2* and (F) *Twist1* in non-neoplastic immortalized HFE145 cells.

To further study the expression of *ETS2*, *Twist1*, *Siah1* and *Siah2* proteins in gastric adenocarcinoma, antral biopsy samples (stage III) were collected from consenting patients undergoing gastric endoscopy. Fluorescence microscopy of gastric cancer biopsy samples and adjacent non-cancer gastric tissue samples showed a marked increase in *ETS2*, *Twist1*, *Siah1* and *Siah2* expression in adenocarcinoma biopsy samples compared to non-cancer tissues (Fig. 3.3.4 A, Fig. 3.3.4 B, Fig. 3.3.4 C and Fig. 3.3.4 D). Nevertheless, the status of *H. pylori* infection in studied adenocarcinoma samples could not be directly confirmed as previous case histories were absent, urea-breath test and urease-test negativity of patients at the time of sample collection. However, this data confirmed of coexistence of *ETS2*, *Twist1*, *Siah1* and *Siah2* in gastric adenocarcinoma.



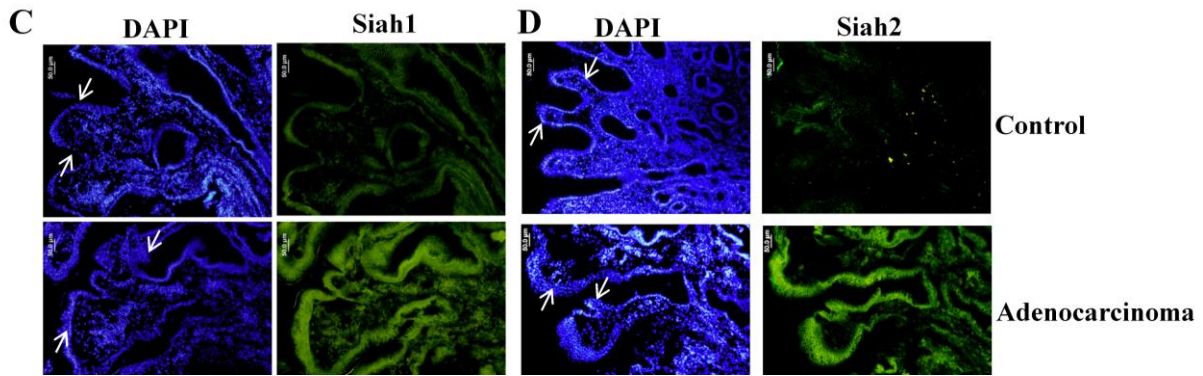


Figure 3.3.4 Coexistence of ETS2, Twist1, Siah1 and Siah2 proteins in human gastric adenocarcinoma biopsy samples. Fluorescence microscopy of gastric cancer biopsy samples and adjacent non-cancer gastric tissue samples ($n=4$ for each group) reveal induced expression of (A) ETS2, (B) Twist1, (C) Siah1 and (D) Siah2 in cancer biopsy samples as compared to non-cancer tissues. Arrows point to the epithelial lining of the gastric mucosa.

3.4. ETS2 Binds with the 5' UTR of *siah1* in *H. pylori*-Infected GCCs

To determine if indeed ETS2 binds with the EBS in the 5' UTR of *siah1* in uninfected and *H. pylori*-infected MKN45 cells, initially a DNA pull-down assay using streptavidin-coated magnetic beads was performed. 5' biotinylated oligonucleotides of Siah1 promoter WT or EBS-Mut (Appendix X) were coated on magnetic beads just prior to incubation with nuclear lysates prepared from *H. pylori*-infected (MOI 200, 3 h) or uninfected MKN45 cells. Western blotting of bead-bound proteins showed ETS2 binding with the WT EBS in the *siah1* 5'UTR only in the infected cells (Fig. 3.4.1A). Western blots of input nuclear lysates revealed expression of ETS2 in the nuclear fraction (as was found in whole cell lysates). HDAC1 was used as a nuclear loading control.

To further validate ETS2 binding with *siah1* EBS, ChIP assay was performed. Nuclear lysates of uninfected and *H. pylori*-infected (MOI 200, 3 h) MKN45 cells were immunoprecipitated using ETS2-specific antibody. PCR products was obtained only from the *H. pylori*-infected immunocomplex representing the *siah1* promoter and 5' UTR flanking the

EBS (S= specific PCR product). No PCR product was obtained from the 5' far upstream sequence (NS= non-specific PCR product) (Fig. 3.4.1 B).

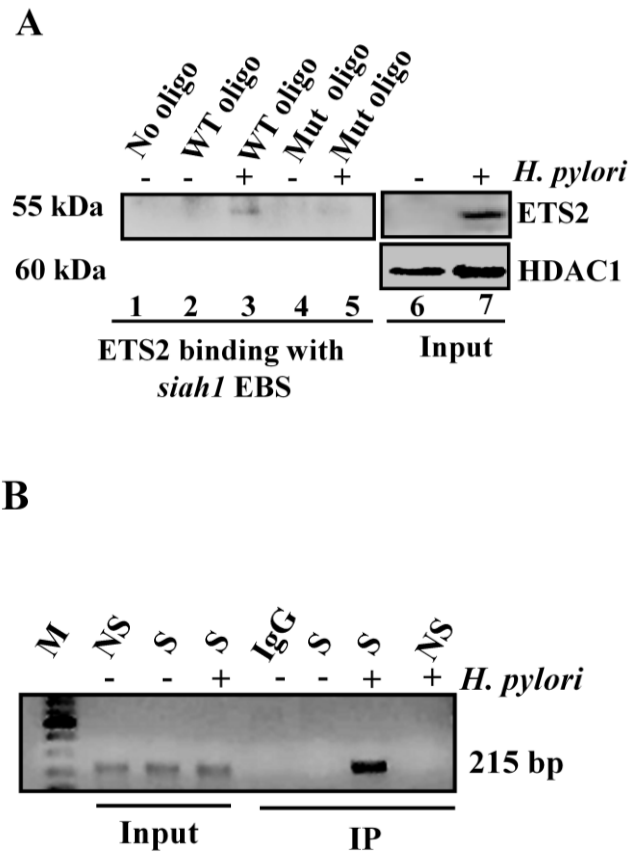


Figure 3.4.1 Binding of ETS2 with the EBS of *siah1* 5' UTR after *H. pylori*-infection. (A) Western blot ($n=3$) showing binding of bead-bound proteins to the WT EBS biotinylated oligo of the *siah1* 5'UTR only in the infected cells but not to the Mut EBS biotinylated oligo. Western blot results of input nuclear lysates shows ETS2 protein expression in the infected lanes. HDAC1 is the loading control. (B) ChIP analysis of uninfected and *H. pylori*-infected ETS2 immunocomplex for *siah1* EBS. IgG= immunoglobulin G; M= MW marker; NS= non-specific primer, S= specific primer.

3.5. ETS2 and Twist1 Bind with *siah2* Promoter in *H. pylori*-Infected GCCs

In vitro DNA binding assay was performed to study ETS2 binding with the *siah2* EBS and Twist1 binding with *siah2*TBS in uninfected and infected MKN45 cells. After 3 h of *H. pylori* infection in MKN45 cells, nuclear extracts were prepared. 5' biotinylated WT and Mut EBS and TBS *siah2* promoter oligonucleotides were synthesized (Appendix X). Magnetic beads were coated with oligonucleotides as described before. Western blots performed with bead-bound proteins revealed ETS2 binding with the *siah2* EBS (Fig. 3.5.1 A) and Twist1 with *siah2* TBS only after *H. pylori* infection (Fig 3.5.1 B). Input nuclear lysates were also run simultaneously to study the expression of ETS2 (Fig. 3.5.1 A) and Twist1 (Fig. 3.5.1 B). HDAC1 was used as a nuclear loading control. Western blot data of input lysates showed both ETS2 and Twist1 increment in the nuclear fractions after *H. pylori* infection. While no ETS2 expression was detected in the uninfected cells, low level of Twist1 expression was observed in the nucleus of uninfected cells.

ChIP assay was also performed to detect binding of ETS2 and Twist1 to the *siah2* promoter *in vivo*. Nuclear lysates of uninfected or 3 h of *H. pylori*- infected MKN45 cells were assessed by using ETS2 (Fig. 3.5.1 C) and Twist1 (Fig. 3.5.1 D) antibodies. No PCR product was obtained from the immunocomplex corresponding to the 5' far upstream sequence (NS= non-specific PCR product) while PCR products of DNA in these immunocomplexes corresponding to the *siah2* promoter flanking the EBS and TBS (S= specific PCR product) further confirmed ETS2 and Twist1 binding with the *siah2* promoter.

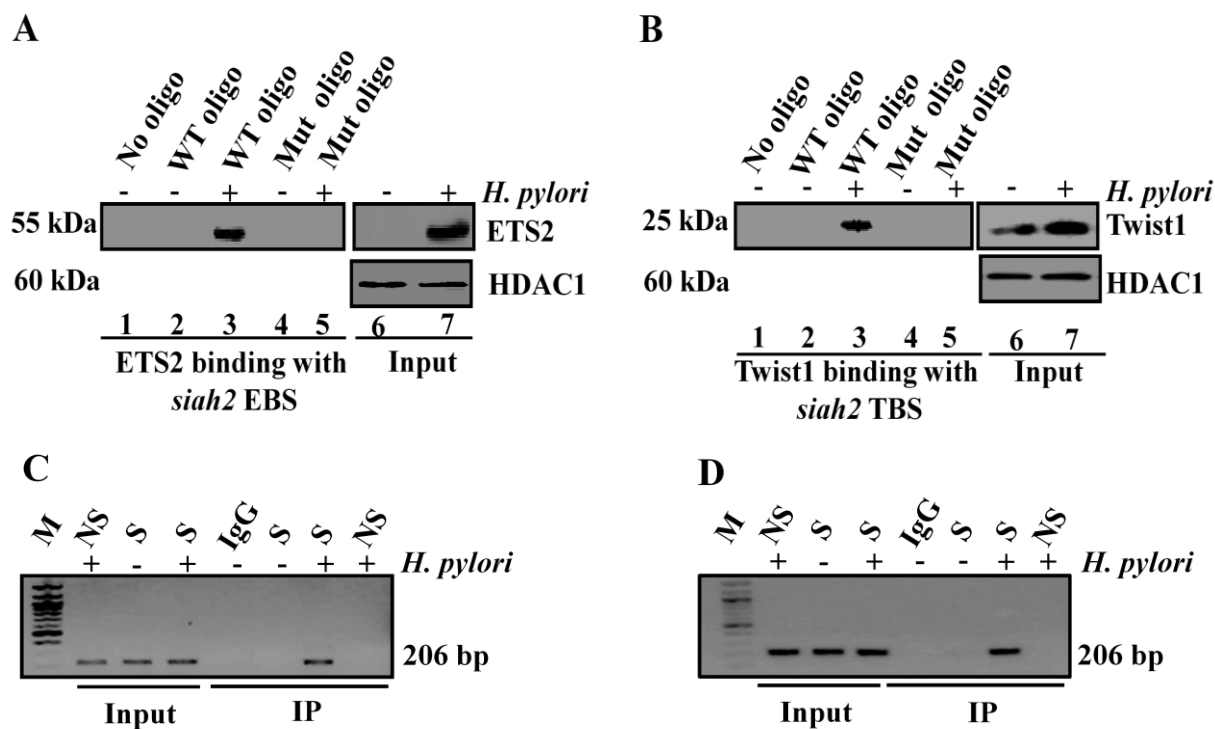
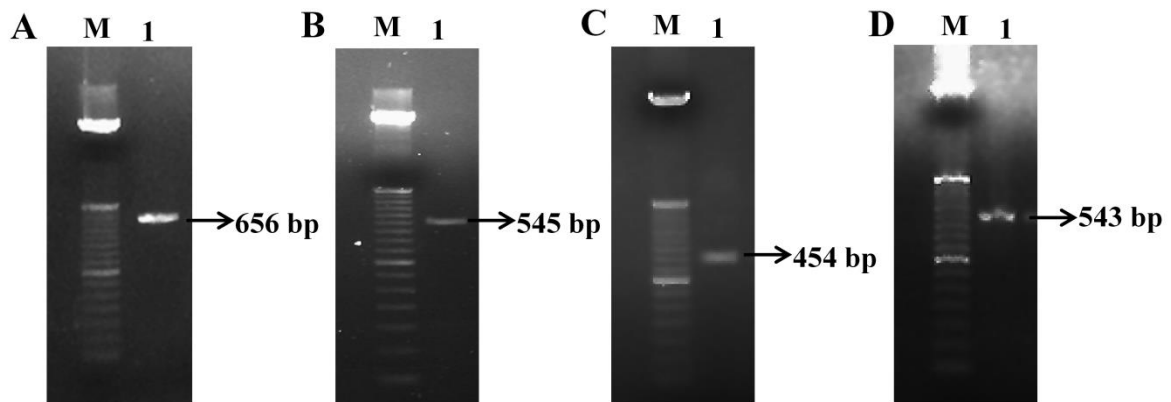


Figure 3.5.1 ETS2 binds with the EBS and Twist1 binds with the TBS of *siah2* promoter after *H. pylori*-infection. (A) A representative western blot ($n=3$) results depicting *H. pylori*-induced binding of ETS2 with the *siah2* promoter ($n=3$). ETS2 binds specifically to the WT EBS only but not with the EBS-Mut oligo. Western blot of input nuclear lysates shows ETS2 expression only in the infected lysates. HDAC1 is the loading control for nuclear lysates. (B) Western blot results ($n=3$) depicting *H. pylori*-induced binding of Twist1 with the *siah2* promoter ($n=3$). Twist1 binds to the WT TBS only but not with the TBS-Mut oligo. Western blot of input nuclear lysates shows Twist1 expression only in the infected lysates. HDAC1 is the loading control for nuclear lysates. (C) ChIP assay result of uninfected and *H. pylori*-infected ETS2 immunocomplex for *siah2* EBS. (D) ChIP assay result of uninfected and *H. pylori*-infected Twist1 immunocomplex for *siah2* TBS. IgG= immunoglobulin G; M= MW marker; NS= non-specific primer, S= specific primer.

3.6. Cloning of *siah1* 5' UTR and *siah2* Promoter to Prepare Luciferase Constructs and Generation of Respective Mutants

Initially, human *siah1* 5' UTR and *siah2* promoter were amplified from genomic the DNA with designed primer pairs (Further details of primer pair used is mentioned in Appendix VI) (Fig 3.6.1 A and Fig. 3.6.1 B). Then, a second PCR was performed with purified PCR products of the previous PCR and the second set of primers with restriction site inserted and was then cloned in pGL3 basic luciferase vector Further details of primer pair used is mentioned in Appendix VI) (Fig. 3.6.1 C and Fig. 3.6.1 D) (Details of cloning and mutagenesis of *siah1* 5' UTR and *siah2* promoter is already mentioned in section 2.2.4.2). To further amplify, the construct was transformed into DH5 α competent cells. Amplified plasmids were isolated and purified. Restriction digestion was performed to initially screen the correct clone (Fig. 3.6.1 E). The correct clone was sent for sequencing. Mutations were generated from the WT plasmid using site-directed mutagenesis kit. The correct construct containing the mutation was confirmed by sequencing.



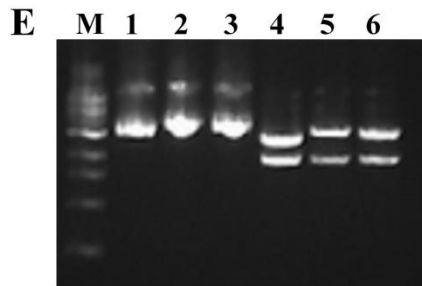


Figure 3.6.1 Cloning of human *siah1* 5'UTR and *siah2* promoter. (A) Amplification of human *siah1* 5'UTR using primers without any restriction enzyme site. M=Marker lane (50 bp of DNA ladder was used) and Lane1=Desired PCR product. (B) Amplification of human *siah2* promoter using primers without any restriction enzyme site. M=Marker lane (50 bp of DNA ladder was used) and Lane1=Desired PCR product. (C) Amplification of human *siah1* 5'UTR using the PCR product obtained from lane A as template and primers with restriction enzyme site inserted. M=Marker lane (50 bp of DNA ladder was used) and Lane1=Desired PCR product.(D) Amplification of human *siah2* promoter using template of PCR product obtained from lane B and primers with restriction enzyme site inserted. M=Marker lane (50 bp of DNA ladder was used) and Lane1=Desired PCR product. (E)Restriction digestion of pGL3 basic, *siah1* 5'UTR cloned into pGL3 basic and *siah2* promoter cloned into pGL3 basic using *Bam*H1 and *Hind* III. M=Marker (1kbp DNA ladder), 1=undigested pGL3 basic, 2=Undigested *siah2* promoter plasmid, 3= Undigested *siah1* 5' UTR plasmid, 4=Restriction digested pGL3 basic, 5=Restriction digested *siah2* promoter plasmid, 6=Restriction digested *siah1* 5'UTR plasmid.

3.7. ETS2 Augments *siah1* Transcription in *H. pylori*-Infected GCCs

In order to study the role of ETS2 in *siah1* transactivation, dual luciferase assay was performed. For this, MKN45 cells were co-transfected with the WT or EBS-Mut *siah1* reporter construct along with *Renilla* luciferase construct pRLTK followed by infection with *H. pylori* for 1 h. Data revealed a significant enhancement in *siah1* transactivation in *H. pylori*-infected *siah1* EBS-WT expressing cells, while reduced *siah1* transactivation was

observed in EBS-mut expressing cells, thus confirming ETS2-mediated *siah1* transcription in *H. pylori*-infected GCCs (Fig.3.7.1 A). To further validate the role of ETS2 in *siah1* transcription, ETS2 was ectopically expressed along with the WT *siah1* 5'UTR construct and the *Renilla* luciferase construct pRLTK. Dual luciferase assay was performed with uninfected or 1 h *H. pylori*-infected cell lysates. Dual luciferase assay data revealed that ectopic ETS2 expression could significantly augment *H. pylori*-mediated *siah1* transcription (Fig.3.7.1 B).

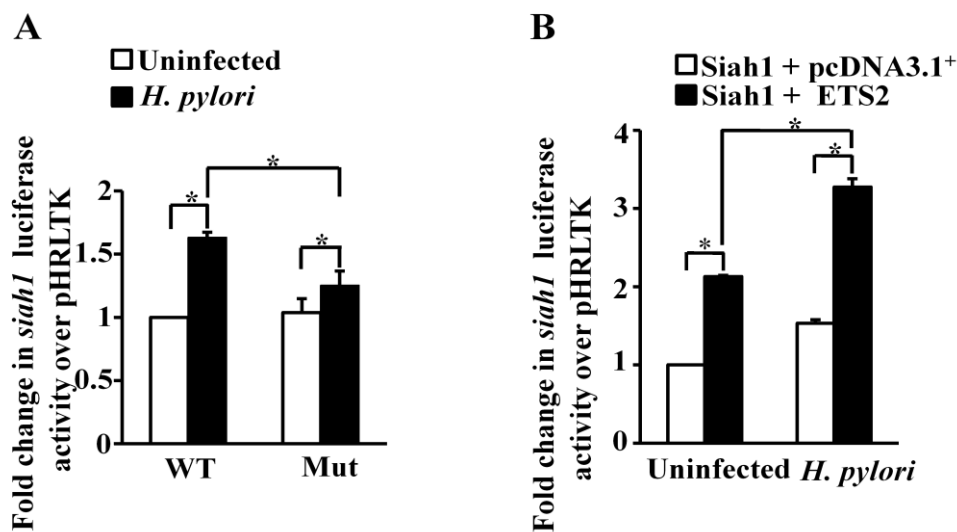


Figure 3.7.1 ETS2 enhances *siah1* transcription in *H. pylori*-infected GCCs. (A) Graphical analysis of luciferase activities (mean±SEM, n=3) of WT and ETS2-Mut *siah1* 5' UTR-transfected MKN45 cells. Bar graphs depict normalized data (mean±SEM, n=3), *P<0.05. (D) Dual luciferase assay data showing the effect of ectopic ETS2 expression and *H. pylori* infection and transcriptional activation of WT *siah1* 5' UTR (mean±SEM, n=3) *P<0.05.

To know whether ETS2 regulates Siah1 expression at protein level, western blotting was performed with whole cell lysates of MKN45 cells transfected with ETS2 siRNA or control duplex and infected with *H. pylori* or left uninfected. A substantial reduction in Siah1 expression was observed in ETS2-suppressed cells as compared to the control duplex-

transfected cells after *H. pylori* infection, thus further confirming that ETS2 could mediate Siah1 expression during *H. pylori* infection (Fig.3.7.2).

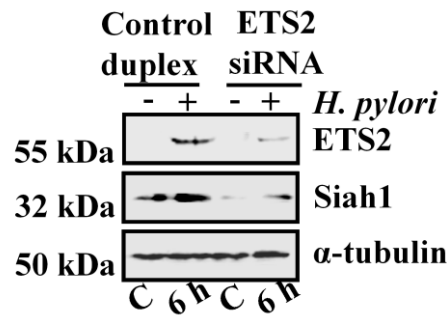


Figure 3.7.2 ETS2 enhances Siah1 protein expression in *H. pylori*-infected GCCs. Western blot ($n=3$) result showing the effect of ETS2 suppression with Siah1 protein expression in ETS2 siRNA transiently transfected MKN45 cells that were either left uninfected or infected with *H. pylori*.

3.8. ETS2 and Twist1 Enhance *siah2* Transcription in *H. pylori*-Infected GCCs

To study the role of ETS2 and Twist1 in *siah2* transcription following *H. pylori* infection, dual luciferase assays were performed. Simultaneous transfection of the *Renilla* luciferase construct phRLTK and the WT or EBS or TBS-Mut *siah2*-reporter constructs in MKN45 cells showed a significant enhancement of *siah2* transactivation in 2 h *H. pylori*-infected and WT *siah2* luciferase construct-transfected cells. Considerable reduction of *siah2* transactivation in the EBS Mut (Fig.3.8.1 A) or TBS Mut-expressing infected cells (Fig.3.8.1 B) confirmed that ETS2 and Twist1 mediated *siah2* transcription in *H. pylori*-infected GCCs.

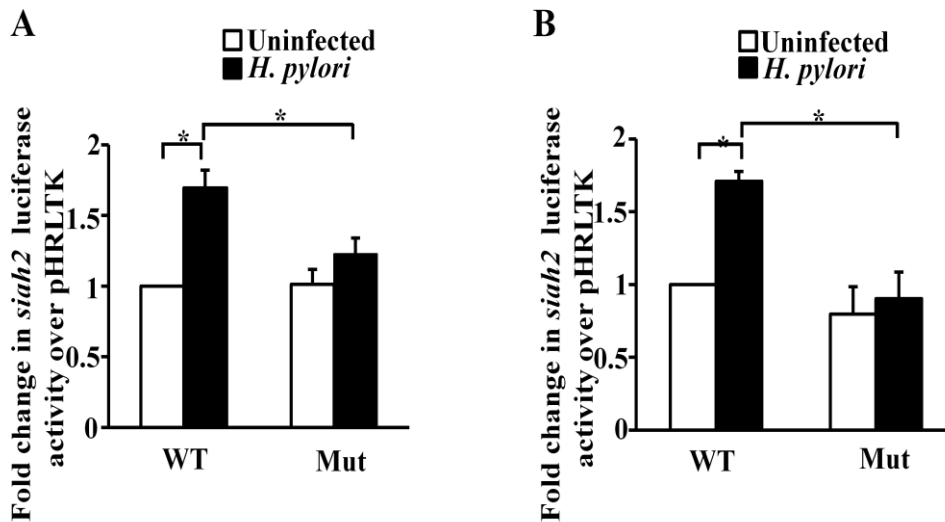


Figure 3.8.1 ETS2 and Twist1 augment siah2 transcription in *H. pylori*-infected GCCs. (A) Bar graphs depict dual luciferase assay results (mean±SEM, n=3) of WT and ETS2-Mut *siah2* promoter-transfected MKN45 cells in the presence or absence of *H. pylori*. Bar graphs depict normalized data (mean±SEM, n=3), *P<0.05. (B) Graphical analysis of dual luciferase activities (mean±SEM, n=3) driven by the WT and Twist1-Mut *siah2* promoter-transfected in MKN45 cells in the presence or absence of *H. pylori*. Bar graphs depict normalized data (mean±SEM, n=3) *P<0.05.

Overexpression of ETS2 plasmid construct along with WT *siah2* promoter construct and the pRLTK construct followed by infection with *H. pylori* for 2 h revealed that ETS2 overexpression significantly enhanced *siah2* transcription (Fig.3.8.2 A). Twist1 overexpression also showed a similar inducing effect on *siah2* luciferase activity (Fig 3.8.2 B). ETS2 and Twist1 overexpression followed by western blotting further established the importance of these proteins in inducing Siah2 expression following *H. pylori* infection (Fig. 3.8.2 C and Fig. 3.8.2 D, respectively). Although Twist1 expression was high in uninfected Twist1-expressing cells as compared to the infected pcDNA3.1⁺-expressing cells, Siah2 expression was less in uninfected Twist1-expressing cells which indicated towards the

likelihood of post-translational modification(s) of Twist1 followed by *H. pylori* that might have played a role in its activation.

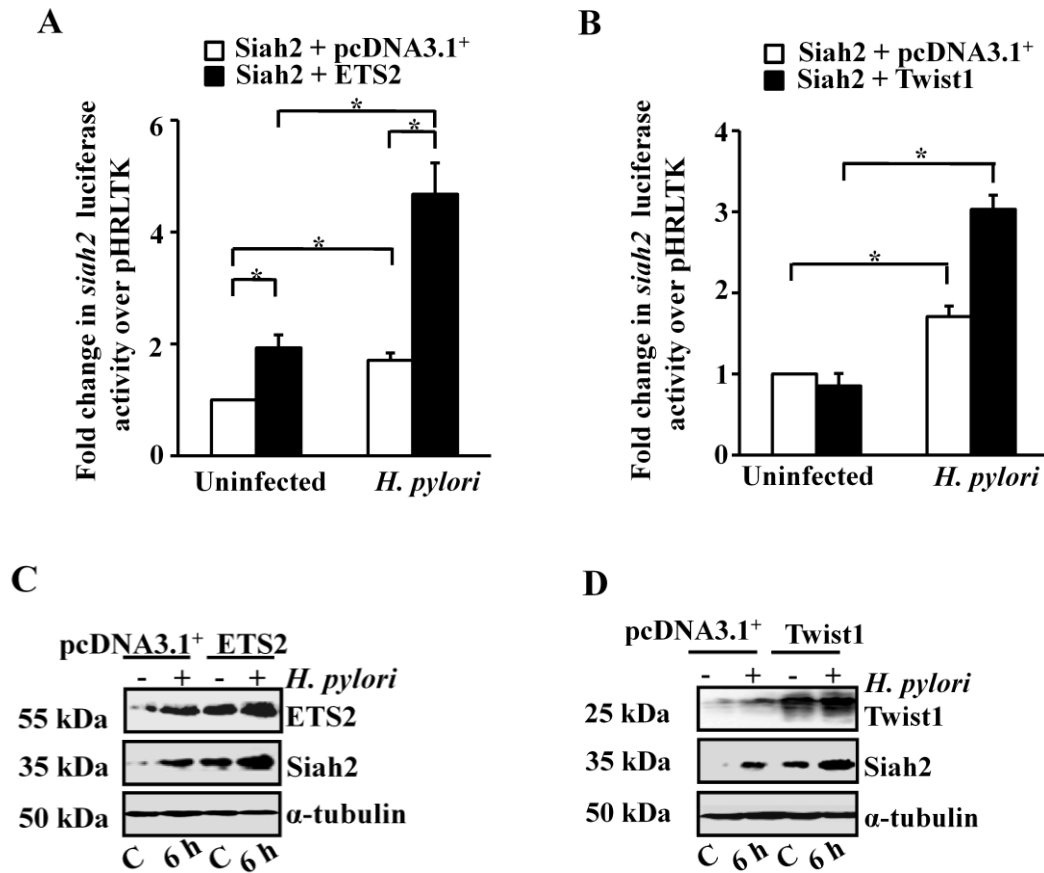


Figure 3.8.2 ETS2 and Twist1 augment siah2 transcription and expression in *H. pylori*-infected GCCs. (A) Bar graph of dual luciferase assay results (mean \pm SEM, n=3) showing the efficacy of ectopically expressing ETS2 on transcriptional activation of WT *siah2* promoter in the presence of *H. pylori*. Bar graphs depict normalized data (mean \pm SEM, n=3), *P<0.05. (B) Bar graph of dual luciferase assay results (mean \pm SEM, n=3) showing the efficacy of ectopically expressing Twist1 on transcriptional activation of WT *siah2* promoter in the presence of *H. pylori*. Bar graphs depict normalized data (mean \pm SEM, n=3), *P<0.05. (C) Western blot result (n=3) showing the effect of ETS2 overexpression in Siah2 protein in uninfected and *H. pylori*-infected MKN45 cells. (D) Western blot results (n=3) showing the

effect of Twist1 ectopic expression on Siah2 protein expression in uninfected and H. pylori-infected MKN45 cells.

3.9. Discussion

Despite a decline in gastric cancer incidence, it still remains a threat to patients with high rate of mortality associated with it [111]. As it remains asymptomatic at its early stage, and its detection usually occurs at late stage, mortality from this disease is associated with metastasis which presents either with peritoneal dissemination or hematogenous spread to the liver and lungs [112]. Infection with *H. pylori* is considered as the most potent risk factor for development of gastric cancer. Understanding the mechanism contributing to gastric cancer initiation and progression could provide a better therapeutic strategy. We observed induction of both Siah1 and Siah2 proteins in *H. pylori*-infected GCCs and identified ETS2 and Twist1 as two novel inducers of Siah proteins. While ETS2 enhanced Siah1 transcription in *H. pylori*-infected GCCs, Siah2 expression was induced by both ETS2 and Twist1. Gastric cancer biopsy samples collected from metastatic gastric tumors also exhibited noticeable induction of ETS2, Twist1, Siah1 and Siah2 expression that is in sync with our *in vitro* data. Thus, we concluded that both Siah1 and Siah2 might play significant roles in *H. pylori*-mediated gastric cancer metastasis and also predict that Siah1 and Siah2 along with ETS2 and Twist1, could be promising therapeutic targets for gastric cancer.

ETS2 can concurrently induce both Siah proteins in *H. pylori*-infected GCCs. As Twist1-binding site is absent in Siah1, we speculate that these isotypes can still be differentially regulated since ETS2 and Twist1 expression might vary depending on the staging of gastric cancer. Upregulation of Siah1 protein in p53-dependent manner has been widely accepted to be associated with apoptosis [44, 103, 113]. Remarkably, we found that Siah1 induction in *H. pylori*-infected GCCs was not dependent on p53 as it was also induced after infection in p53-null Kato III cells. Our data corroborated earlier findings that showed

that cells expressing gain-of-function mutant of p53 were able to promote growth and tumorigenesis by interacting with ETS2 and enhancing its expression whereas, in cells lacking p53 or with Mut p53, ETS2 knockdown resulted in tumor suppression [114, 115]). Mut p53/ETS2 complex could prevent ubiquitin-mediated degradation of ETS2, thus activating several processes that promote cancer progression [116]. As basal expression of Siah1 was also noticed in uninfected GCCs when ETS2 protein was not expressed, it is clear that p53 and ETS2-independent mechanisms of Siah1 expression might exist.

Findings of Bebb *et al.* suggested of *H. pylori*-mediated disruption of the adherens junction [117]. They showed that acute *H. pylori* infection-mediated disruption of β -catenin was independent of the *cag* PAI status. We also established that *siah1* and *siah2* induction by ETS2 and Twist1 in infected GCCs was independent of the *cag* PAI. Our assumption is that other *cag*-independent virulence factors might regulate ETS2 and Twist1. Two other virulent factors BabA and VacA are also highly associated with the risk of gastric cancer [60]. Strains 26695 and 8-1 have *vacA* s1/m1 genotype, while D154 has *vacA* s2/m2 genotype. Further investigation is required on the role of *babA* and *vacA* on the epithelial expression of ETS2, Twist1, Siah1 and Siah2.

This work uncovered a new mechanism of *H. pylori*-mediated Siah1 and Siah2 induction mediated via ETS2 and Twist1 expression. As both ETS2 and Twist1 can promote tumor growth and metastasis, the next part of this thesis investigated the metastasis-promoting role of Siah1 and Siah2 in *H. pylori*-infected GCCs.

Chapter 4

4. RESULTS

4.1. Cloning and expression of Human *siah1* Gene

Human *siah1* gene was amplified and cloned into an empty expression vector pcDNA3.1⁺ (Further details for cloning of *siah1* is mentioned in section 2.2.4.1) (Fig. 4.1.1A). The *siah1* expressing plasmid was transformed into DH5 α competent cells as already described before to further amplify the plasmid. Amplified plasmids were isolated from bacteria and purified followed by its transient transfection in GCCs to study its expression. 24 h post transfection, AGS cells grown in coverslips were processed for immunofluorescence microscopy. Confocal microscopic studies revealed Siah1 overexpression in *siah1* construct-transfected cells as compared to the empty vector-expressing cells (Fig. 4.1.1B).

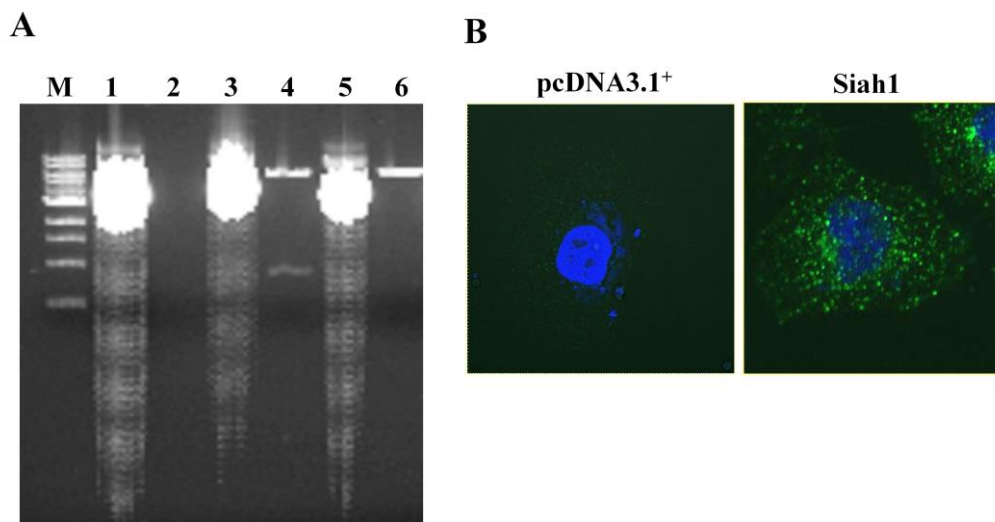
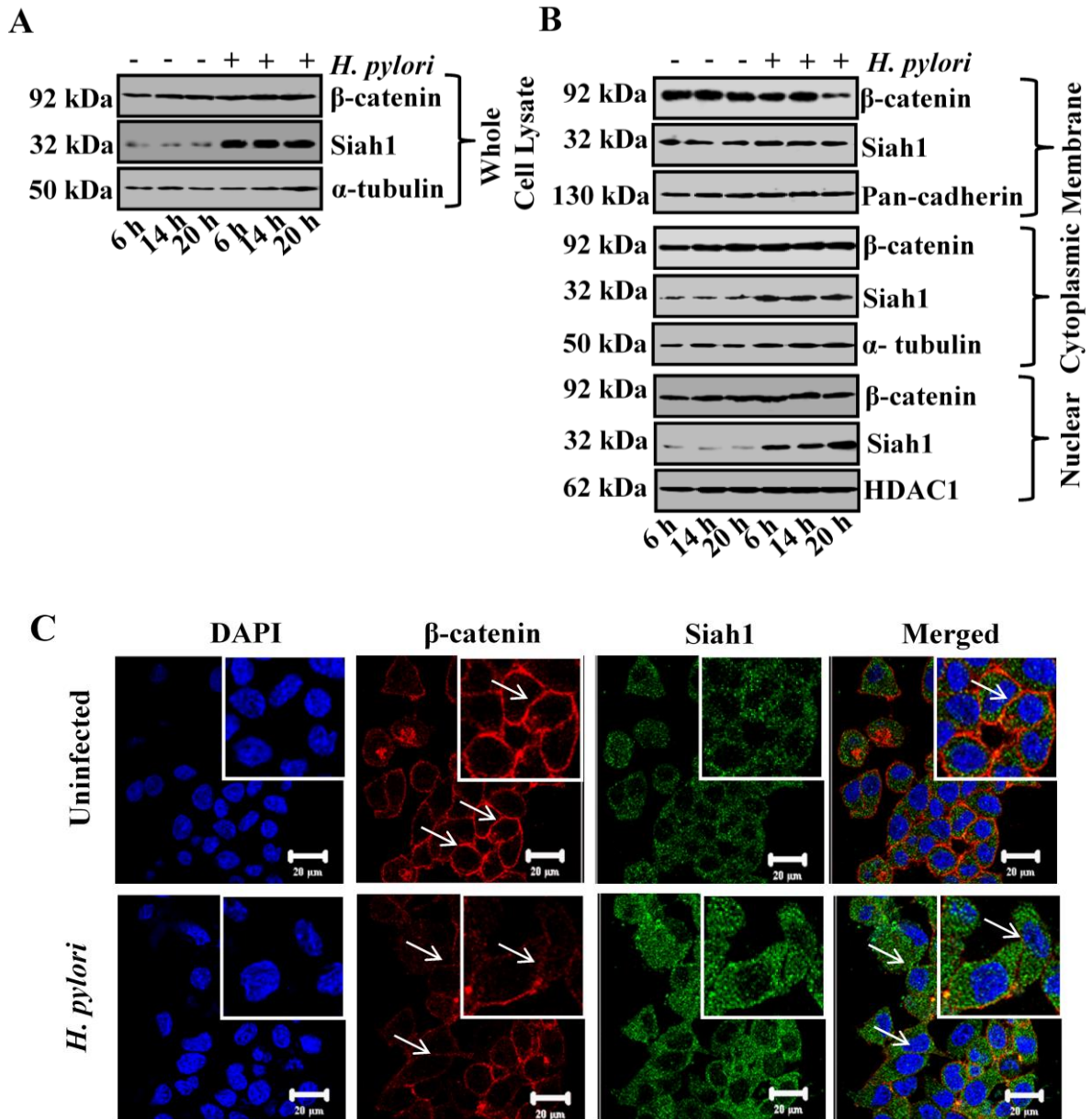


Figure 4.1.1 Cloning and expression of human *siah1* gene. (A) Cloning of *siah1* gene. Lane M= 1 kb DNA marker, Lane1= pcDNA3.1⁺ (undigested), Lane2=Gap, Lane3= *siah1* plasmid (undigested), Lane4: Restriction digested *siah1* plasmid showing *siah1* product of 848 bp. Lane4= pcDNA3.1⁺ (undigested), Lane5= pcDNA3.1⁺ (restriction digested). (B) Confocal microscopic images of AGS cells transfected with pcDNA3.1⁺ or *siah1* plasmid.

4.2. Siah1 Mediates Degradation of Membrane-Bound β -catenin in *H. pylori*-Infected GCCs

Siah1 was found to induce apoptosis and cell-cycle arrest by reducing cytosolic β -catenin [27, 118]. Siah1-mediated phosphorylation-independent degradation of β -catenin was noticed in the cytosolic compartment of hepatocytes which resulted in growth arrests and apoptosis in hepatocytes [119]. This study also revealed that, Siah1 had no effect on the membrane-bound β -catenin. Siah1-mediated degradation of cytosolic β -catenin was also reported in cervical epithelial cancer cells [120]. Elevated expression of Siah1 protein was observed at 6 h time point. So, time kinetics (6 h, 14 h and 20 h) were performed to study the expression of Siah1 protein and total β -catenin in *H. pylori*-infected cells. Western blotting was performed with whole cell lysates prepared from *H. pylori*-infected or uninfected MKN45 cells. Data revealed that although β -catenin expression level remained unchanged in the whole cell lysate before or after *H. pylori* infection (Fig. 4.2.1 A). To study the status of β -catenin in subcellular compartments, membrane-enriched fraction, cytosolic and nuclear fractions of *H. pylori*-infected and uninfected cells were western blotted. Pan-cadherin, α -tubulin, and histone-deacetylase 1 (HDAC1) served as loading controls for the membrane fraction, cytoplasmic fraction and nuclear fractions, respectively. Data revealed that β -catenin was only decreased in the membrane fraction only after 20 h of *H. pylori* infection and not in the cytosolic or nuclear compartments (Fig. 4.2.1 B). However, no change in membrane-bound Siah1 was noted following *H. pylori* infection. Siah2 was altogether absent in the membrane fraction. However, in spite of elevated cytosolic Siah1 expression in *H. pylori*-infected cells, there was no additional loss of β -catenin in the cytosol. On the contrary, nuclear fractions exhibited a time-dependent upsurge in Siah1 expression but unchanged β -catenin expression after *H. pylori* infection. Confocal microscopy of MKN45 cells further showed a reduction in membrane-bound β -catenin after 20 h of *H. pylori* infection (Fig. 4.2.1 C). E-cadherin-null

AGS cells, on the contrary, showed induced Siah1 expression in both nuclear and cytosolic fractions after *H. pylori* infection and cytosolic or nuclear β -catenin in AGS cells did not decrease p.i. (Fig. 4.2.1 D).



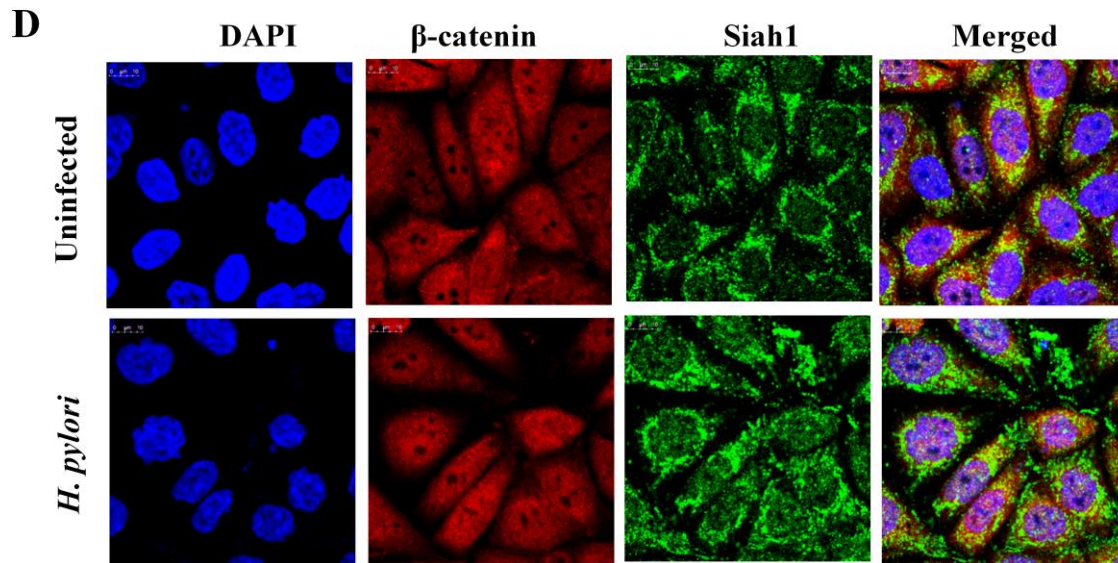


Figure 4.2.1 Degradation of membrane-bound β -catenin in *H. pylori*-infected GCCs. (A) A representative western blot ($n=3$) showing Siah1 and β -catenin protein expression in uninfected and *H. pylori*-infected (6 h, 14 h and 20 h) MKN45 whole cell lysates. (B) Western blot ($n=3$) results depicting Siah1 and β -catenin protein expression in the membrane, cytoplasmic and nuclear fractions of uninfected or *H. pylori*-infected lysates. Pan-cadherin, α -tubulin and HDAC1 are used as respective loading controls. (C) Confocal microscopy results showing reduction in membrane-bound β -catenin expression after 20 h of *H. pylori* infection in MKN45 cells ($n=3$). Arrow indicates membrane-bound β -catenin. (D) Confocal microscopy ($n=3$) showing expression of Siah1 and β -catenin in *E*-cadherin-null AGS cell line.

To study whether the loss of membrane bound β -catenin was a result of proteasome-dependent degradation or not, western blotting was performed with membrane fraction lysates of uninfected or *H. pylori*-infected MKN45 cells in the presence or absence of 50 μ M MG132. MG132 treatment rescued membrane-bound β -catenin in infected GCCs demonstrating that *H. pylori*-induced membrane-bound β -catenin loss was due to proteasomal degradation (Fig. 4.2.2 A). Ectopic Siah1 expression in MKN45 cells revealed unchanged β -

catenin expression in whole cell lysate even after 20 h of *H. pylori* infection (Fig. 4.2.2 B) while western blot with membrane fractions prepared from cells overexpressing Siah1 showed loss of β -catenin in the membrane which was markedly enhanced after *H. pylori* infection (Fig. 4.2.2 C). Transient transfection of MKN45 cells with Siah1 siRNA revealed unchanged β -catenin expression in whole cell lysates even after 20 h of *H. pylori* infection (Fig. 4.2.2 D), but this rescued the degradation of membrane-bound β -catenin after 20 h of *H. pylori* infection (Fig. 4.2.2 E),

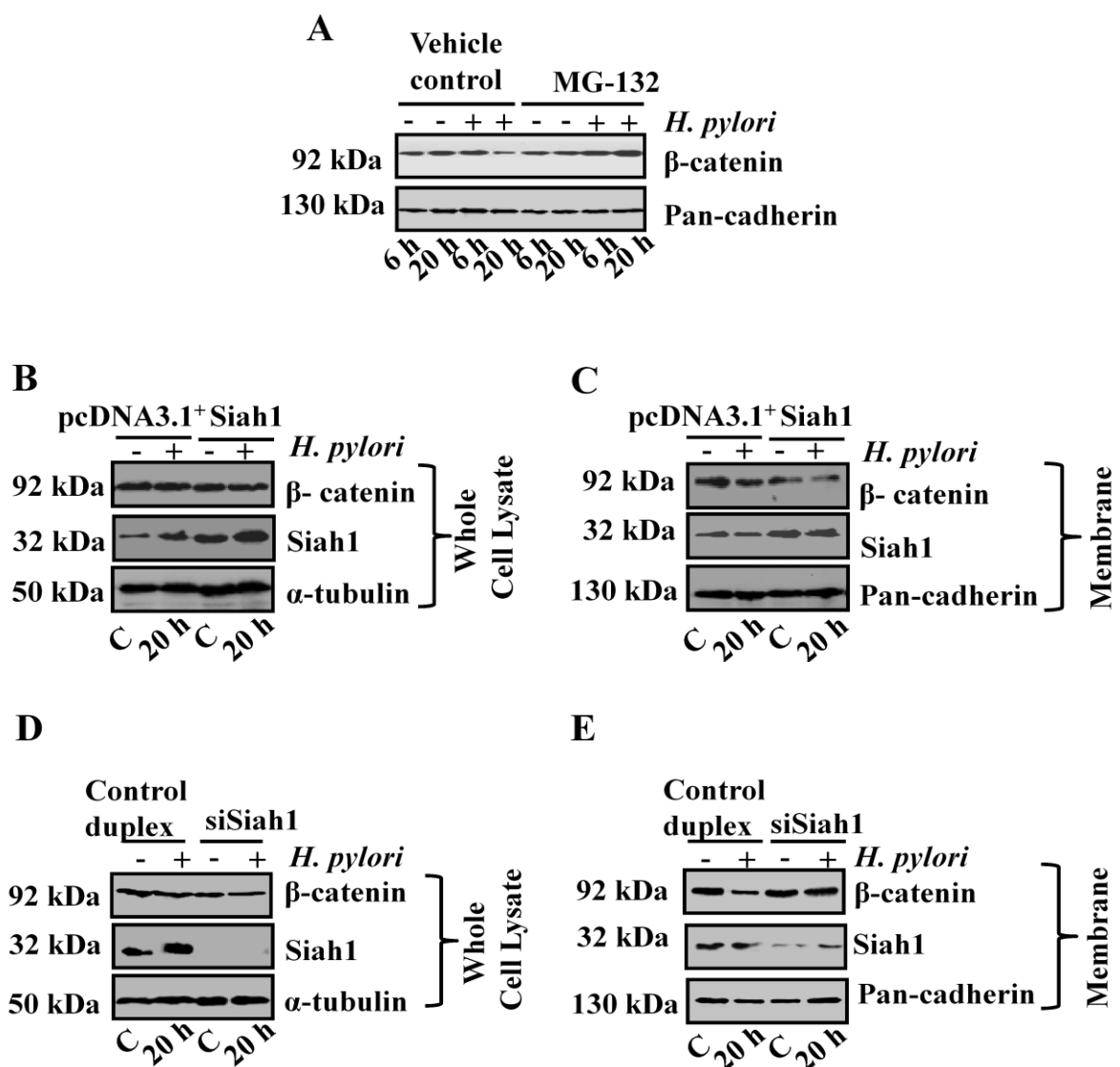


Figure 4.2.2 Siah1-mediated degradation of membrane-bound β -catenin in *H. pylori*-infected GCCs. (A) A representative western blot (n=3) showing the rescue of membrane-bound β -catenin from degradation in 20 h of *H. pylori*-infected membrane lysates by treatment with a proteasome inhibitor, MG132. (B) A representative western blot (n=3) of whole cell lysates prepared from *Siah1* or empty vector (pcDNA3.1⁺) transfected and *H. pylori*-infected or uninfected MKN45 cells. α -tubulin is the loading control. (C) Further reduction in membrane-bound β -catenin expression is seen in *Siah1*-overexpressed and *H. pylori*-infected cells. (D) A representative western blot (n=3) of whole cell lysates prepared from MKN45 cells transfected with siRNA of *Siah1* or control duplex and infected (or uninfected) with *H. pylori*. α -tubulin is the loading control. (E) Rescue of membrane-bound β -catenin expression is seen in *Siah1*-suppressed and *H. pylori*-infected cells.

Immunoprecipitation assay was performed on the membrane-rich lysates to study the interaction of membrane-bound β -catenin with *Siah1*. Result (Fig. 4.2.3 A) revealed that *Siah1* and β -catenin interacted in uninfected or infected cells at 14 h and in uninfected cells at 20 h, β -catenin was completely absent in the immunoprecipitate after 20 h of infection. Cadherin-catenin complex are known to be degraded by E3 ubiquitin ligases [99] and earlier studies reported about loss of E-cadherin from the membrane in *H. pylori*-infected GCCs [121, 122]. To study the status of E-cadherin in the membrane of *Siah1*-overexpressed cells after *H. pylori* infection, confocal microscopy was performed. For this, MKN45 cells transfected with the empty vector (pcDNA3.1⁺) or *Siah1* construct were infected with *H. pylori* for 20 h in the presence or absence of either vehicle control or 50 μ M MG132. Data revealed that neither *Siah1* overexpression nor *H. pylori* could induce E-cadherin loss in the membrane fraction of GCCs (Fig. 4.2.3 B).

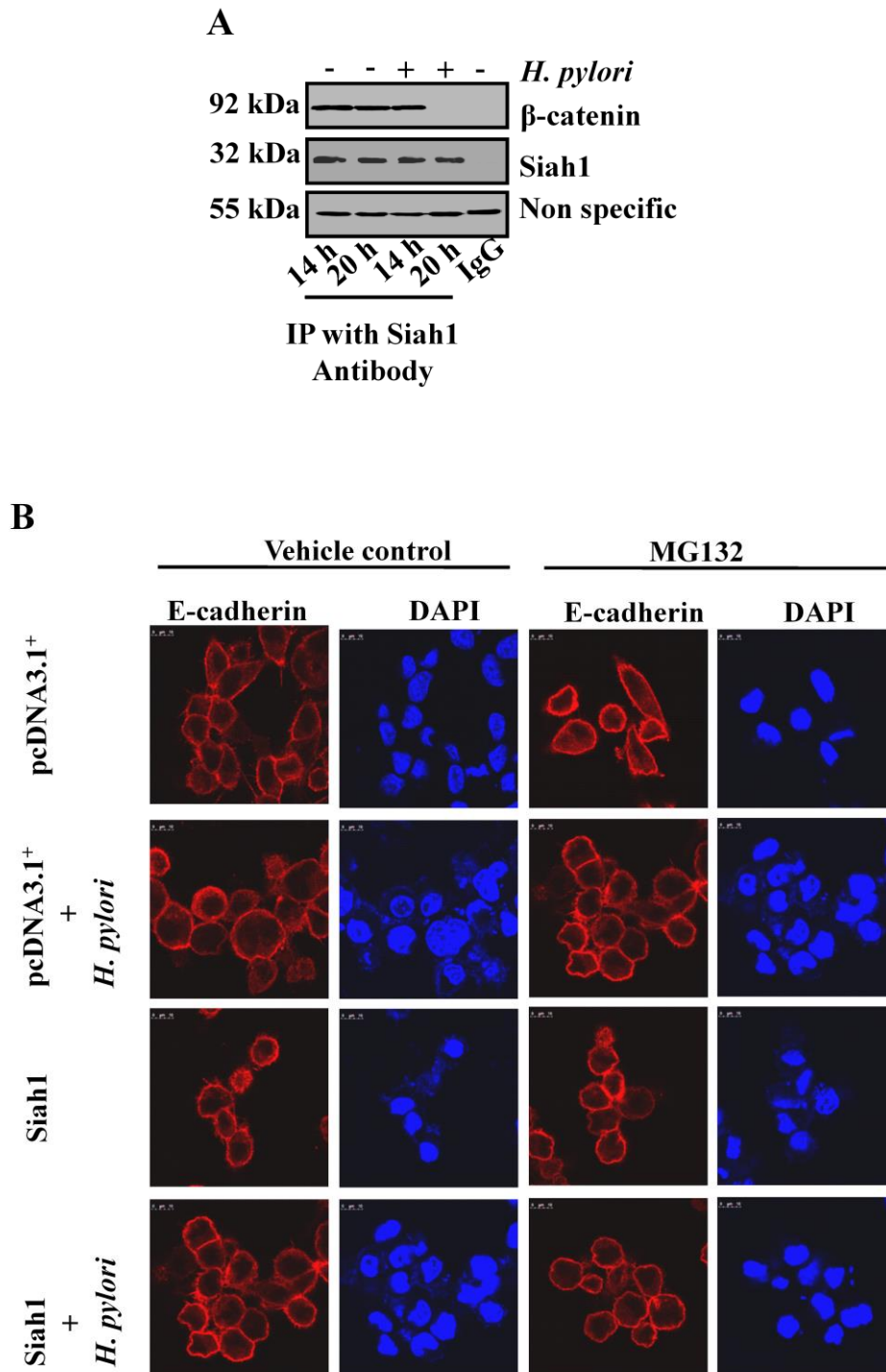


Figure 4.2.3 *H. pylori* infection induces Siah1 binding to the membrane-bound β -catenin in infected GCCs but does not change membrane bound E-cadherin expression. (A) Immunoprecipitation assay showing the interaction of membrane-bound β -catenin and Siah1. Anti-Siah1 antibody is the immunoprecipitating antibody. Nonspecific band/ loading

control= immunoglobulin heavy chain band. (B) Confocal microscopy (n=3) depicting E-cadherin expression in MKN45 cells that are transfected with empty vector (pcDNA3.1⁺) or Siah1 construct and treated with MG132 following *H. pylori*-infection (or no infection).

4.3. Siah Induces Cell Migration and Invasion in *H. pylori*-Infected GCCs

Loss of β -catenin from the adherens junction induces cancer invasiveness [123-125]. A case study has reported frequent loss of membrane-bound β -catenin in metastatic gastric cancer [126]. Our findings have also shown Siah1-mediated loss of membrane-bound β -catenin during *H. pylori* infection. As *H. pylori* infection in GCCs induces EMT and Siah2 expression also plays a critical role in metastasis [127], we were interested in studying the effect of Siah1 and Siah2 expression on cell migration and invasion of *H. pylori*-infected GCCs. Wound-healing assay was performed to study cell migration. For this study, preference was given to the highly adherent AGS cells over the partially adherent MKN45 cells as the latter grow in clumps and hence it is difficult to get a uniform monolayer using MKN45 cells. AGS cells stably expressing Siah1, Siah2 or empty vector were grown in monolayer on 35 mm cell culture plates and a wound was marked with the help of a pipette tip. Cells were incubated for 24 h in the presence or absence of *H. pylori* and cell migration was monitored through imaging. Siah1 or Siah2-expressing *H. pylori*-infected AGS cells showed significant time-dependent increase in cell migration as compared to the empty-vector-expressing *H. pylori*-infected cells (Fig. 4.3.1 A and Fig. 4.3.1 B).

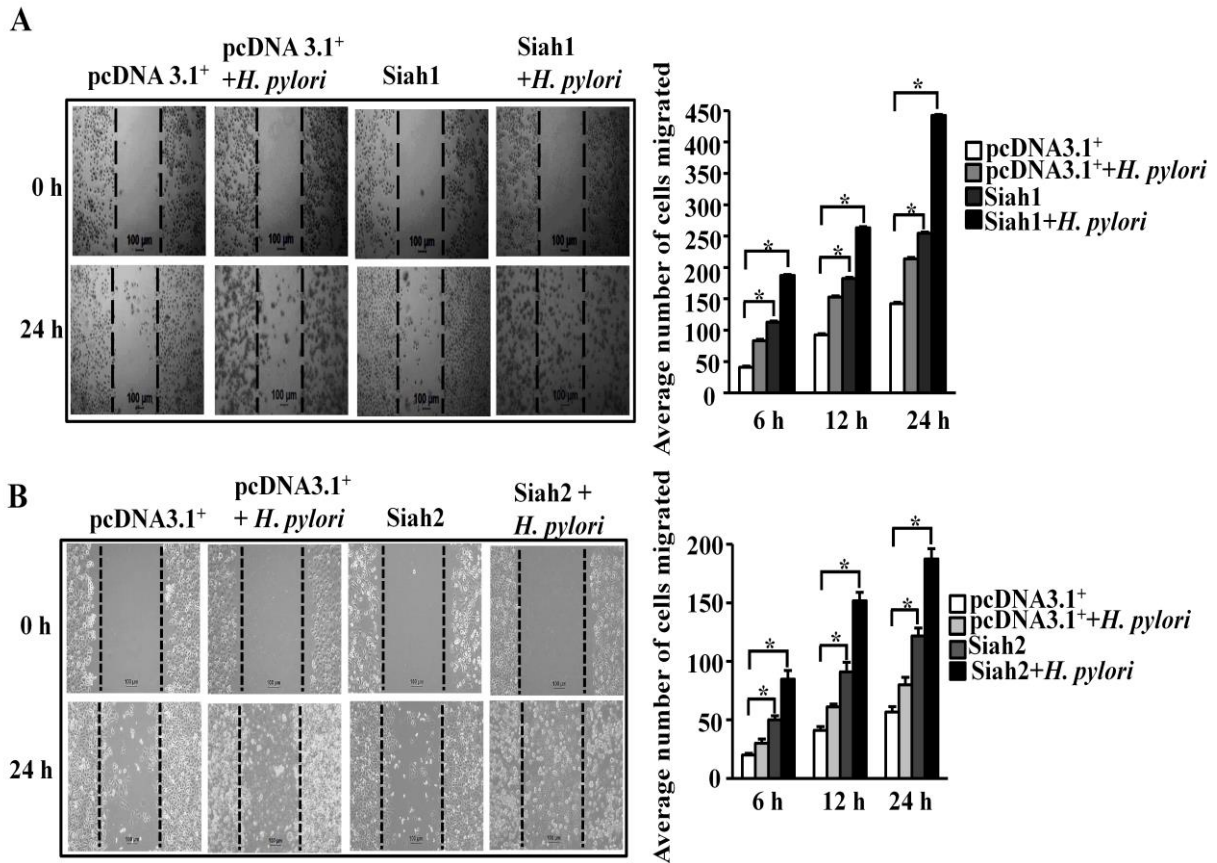


Figure 4.3.1 Elevated Siah expression enhances cell motility and wound-healing property in *H. pylori*-infected GCCs. (A) A representative scratch assay result showing enhanced migration potential of AGS cells stably expressing Siah1 and infected with *H. pylori*. Bar graphs depicts the average number of migrated cells from three independent experiment (mean±SEM, n=3), *P<0.05. Scale shown: 100 μm. (B) Scratch assay of AGS cells stably expressing Siah2 or empty vector reveals enhanced migration potential of Siah2 expressing cells infected with *H. pylori*. Bar graphs depict normalized data (mean±SEM, n=3), *P<0.05. Scale shown: 100 μm.

To further validate our results, transwell migration and matrigel invasion assay were also performed with Siah1 and Siah2-overexpressing AGS cells, or Siah1 and Siah2-suppressed AGS cells. Significant induction in cell migration and invasion was observed with exogenous Siah1 and Siah2-expressing infected cells (Fig. 4.3.2 A-D).

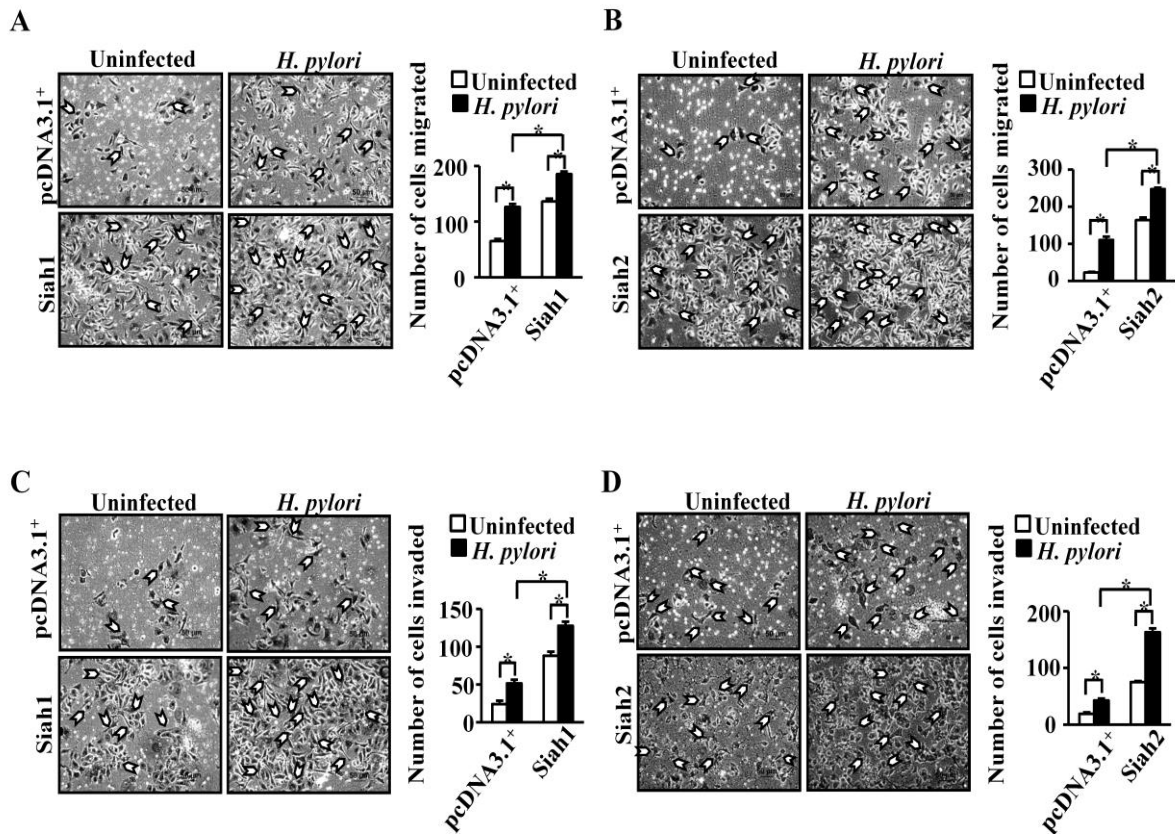
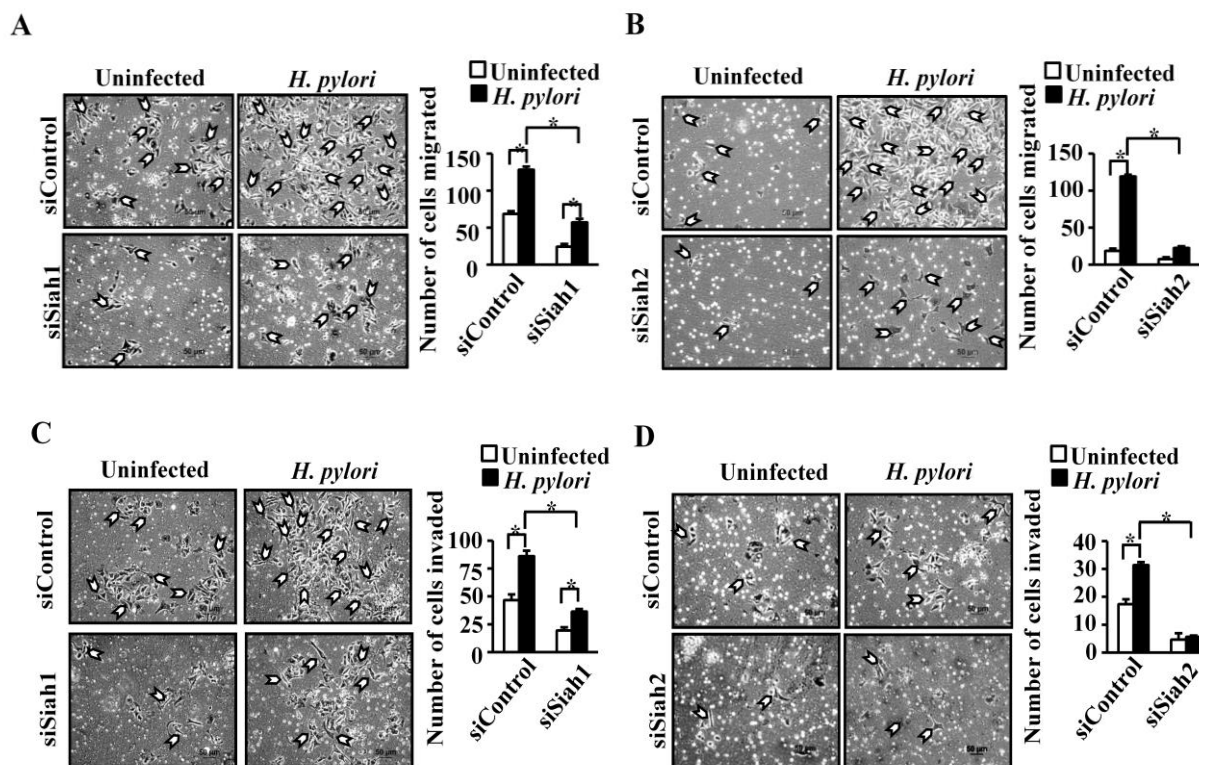


Figure 4.3.2 Elevated *Siah* expression enhances cell migration and invasiveness of *H. pylori*-infected GCCs. (A) Results of transwell migration assay with AGS cells transiently expressing *Siah1* or empty vector and infected with *H. pylori* (or uninfected). Bar graphs depicts the average number of migrated cells from three independent experiments (mean±SEM, n=3), *P<0.05. Scale shown: 100 μm (B) Results of transwell migration assay with uninfected or infected AGS cells transiently expressing *Siah2* or empty vector. Bar graph depicts the average number of migrated cells from three independent experiments (mean±SEM, n=3), *P<0.05. Scale shown: 100 μm. (C) Results of transwell invasion assay with AGS cells transiently transfected with *Siah1* construct or pcDNA3.1⁺ show an increase in invasiveness of *H. pylori*-infected GCCs. Bar graph depicts the average number of invaded cells from three independent experiments (mean±SEM, n=3), *P<0.05 (D) Results of transwell invasion assay with AGS cells transiently transfected with *Siah2* construct or

pcDNA3.1⁺ shows an increase in invasiveness of *H. pylori*-infected GCCs. Bar graph depicts the average number of invade cells from three independent experiments (mean±SEM, n=3), **P*<0.05.

Significant inhibition in cell migration and invasion was observed in siSiah1- and siSiah2-expressing infected cells as compared to control siRNA-transfected and *H. pylori*-infected cells (Fig. 4.3.3 A-D). These results were suggestive of positive effects of both Siah1 and Siah2 on *H. pylori*-induced cell migration and invasion. Anchorage independent growth was also studied in MKN45 cells stably expressing Siah1 and Siah2. A substantial increase in colony forming ability was observed in *H. pylori*-infected Siah1 and Siah2-expressing cells as compared to cells expressing the empty vector (Fig. 4.3.3 E and Fig. 4.3.3 F). Protein level of Siah1 and Siah2 in stable cells are shown underneath of Figures 4.3.3 E and 4.3.3 F, respectively.



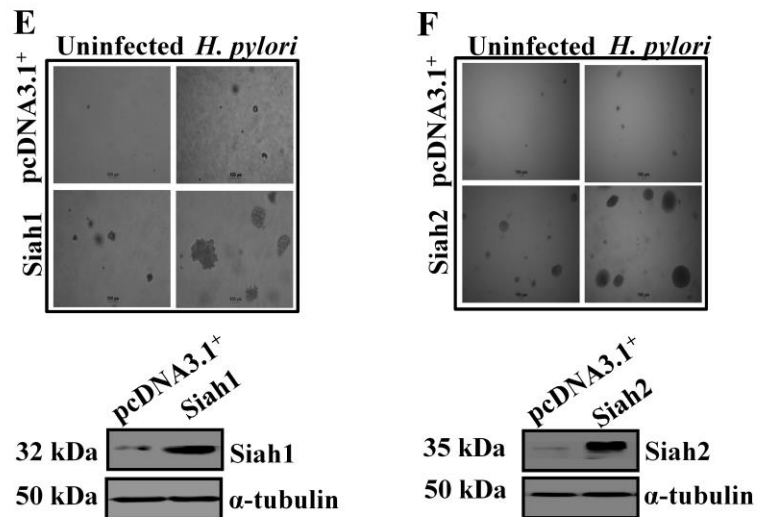
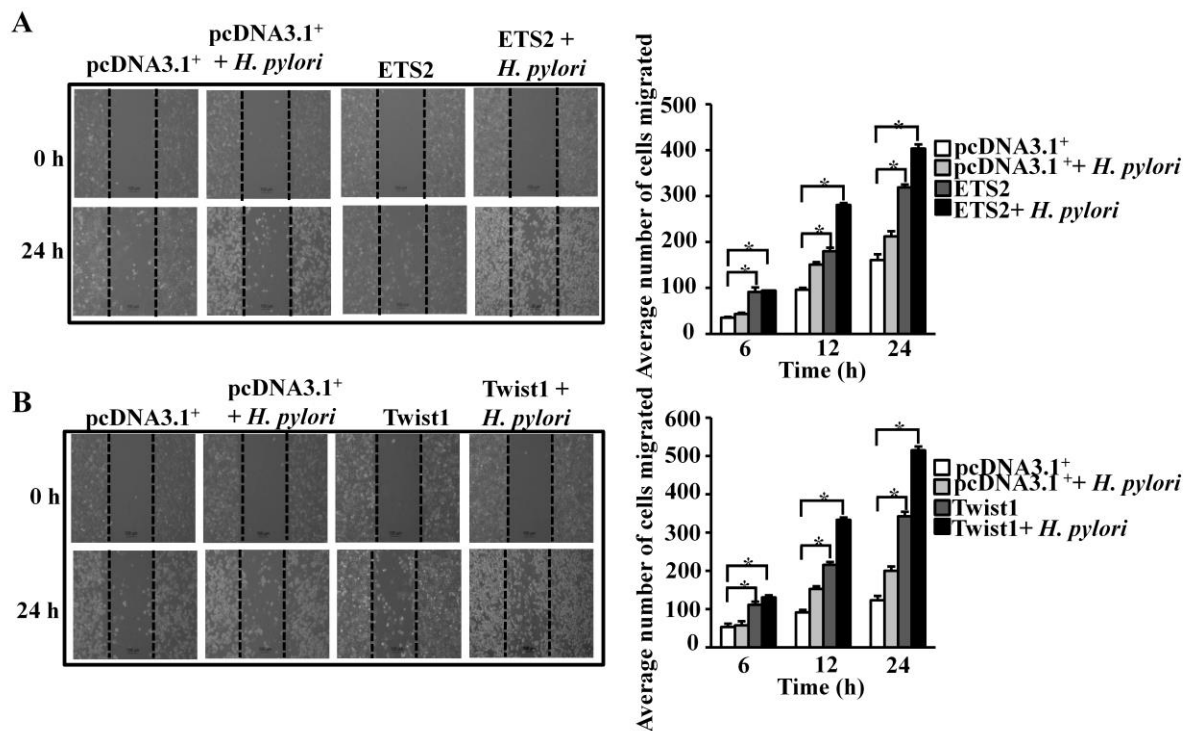


Figure 4.3.3 Siah suppression reduces cell migration and invasiveness of *H. pylori*-infected GCCs. (A) Transwell migration assay with AGS cells transiently transfected with Siah1 siRNA or control duplex siRNA shows reduction of cell migration in infected cells. Bar graph depicts the average number of migrated cells from three independent experiments (mean±SEM, n=3), *P<0.05. Scale shown: 100 μm (B) Siah1-suppressed AGS cells show reduction of cell migration in infected chambers as compared to control siRNA. Bar graphs depicts the average number of migrated cells from three independent experiments (mean±SEM, n=3), *P<0.05. Scale shown: 100 μm. (C) Results of transwell invasion assay with AGS cells transiently transfected with Siah1 siRNA or si Control RNA shows a decrease in invasiveness of *H. pylori*-infected GCCs. Bar graph depicts the average number of invaded cells from three independent experiments (mean±SEM, n=3), *P<0.05 (D) Transwell invasion assay of AGS cells transiently transfected with siSiah2 or siControl show a decrease in invasiveness of *H. pylori*-infected GCCs. Bar graphs depicts the average number of invade cells from three independent experiments (mean±SEM, n=3), *P<0.05. (E-F) Soft agar colony formation assay result performed with empty vector, Siah1 or Siah2 stably-transfected MKN45 cells. Siah1 or Siah2 overexpression show a substantial increase in colony forming

ability post *H. pylori* infection compared to cells expressing the empty vector. Accompanying western blot result depicts *Siah1* and *Siah2* protein level in the used stable cells.

4.4. ETS2 and Twist1 Induce Migration and Invasion of *H. pylori*-Infected GCCs

Wound-healing assay was performed to study the role of ETS2 and Twist in inducing migration of *H. pylori*-infected cells. Both ETS2 and Twist1-overexpressing AGS cells showed significantly increased cell migration as compared to the empty vector-expressing *H. pylori*-infected cells (Fig. 4.4.1 A and Fig. 4.4.1 B). Soft agar assay performed with ETS2 and Twist1 stably-expressing MKN45 cells showed dose-dependent increase in colony formation after *H. pylori* infection (Fig. 4.4.1 C and Fig. 4.4.1 D). Western blot results shown underneath the soft agar assay data of Fig 4.4.1 C and Fig 4.4.1 D indicated expression status of ETS2 and Twist1 in the respective stable cells used for the assay.



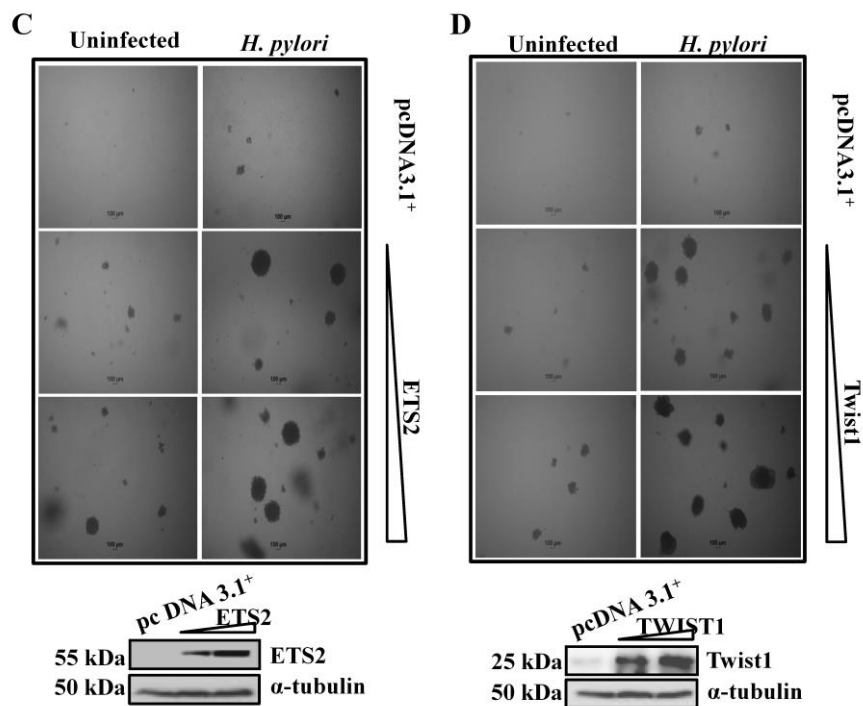


Figure 4.4.1 ETS2 and Twist 1 enhances cell motility, wound-healing and invasive property of *H. pylori*-infected GCCs. (A) A representative wound healing assay image showing enhanced cell migration in AGS cells stably expressing ETS2 and infected with *H. pylori*. Bar graph depicts the average number of migrated cells from three independent experiments (mean±SEM, n=3), *P<0.05. Scale shown: 100 μm (B) Scratch assay of AGS cells stably expressing Twist1 or empty vector reveals enhanced migration potential of Twist1 expressing stable cells infected with *H. pylori*. Bar graph depicts normalized data (mean±SEM, n=3), *P<0.05. Scale shown: 100 μm. (C) A representative soft agar assay study showing cells stably expressing ETS2 and infected with *H. pylori* have higher number of colonies as compared to empty vector (D) A representative soft agar assay study showing cells stably expressing Twist1 and infected with *H. pylori* have higher number of colonies as compared to empty vector. Western blot results show ETS2 and Twist1 protein status in stable cells.

4.5. Discussion

H. pylori colonization lasts for decades, induces inflammatory responses and histological changes that disrupt epithelial tight junctions followed by loss of epithelial barrier function of the gastric epithelium complemented by loss of epithelial cell morphology [98]. The loss of epithelial cell-to-cell adhesions take place as disruption of the junctional cadherin-catenin complex occurs via *cagA* and other virulence factors [98]. The present study reports for the first time that the oncogenic protein ETS2 enhances both *siah1* and *siah2* transcription while Twist1 enhances *siah2* transcription in the *H. pylori*-infected GCCs. Further, up-regulation of Siah1 and Siah2 in *H. pylori*-infected GCCs induces cell motility and invasiveness. Siah1 up-regulation in *H. pylori*-infected GCCs promotes loss of the membrane-bound β -catenin without affecting the cytoplasmic and nuclear pools. Moreover, we also show that *H. pylori*-mediated Siah2 induction in GCCs does not cause degradation of E-cadherin from the cell membrane.

The cadherin-catenin complex is an essential component of the adherens junctions and act as bridge between cadherin receptors and the actin cytoskeleton [98]. E-cadherin binding protein Hakai ubiquitinates and internalizes E-cadherin complex by endocytosis resulting in disruption of cell-cell adhesion [99]. Internalization of E-cadherin complex via endocytosis possibly plays a role in releasing β -catenin from the cadherin-catenin complex [128]. Else, β -catenin phosphorylation at Tyr¹⁴² can also disrupt its interaction with α -catenin and E-cadherin [129]. Another study has shown the E-cadherin-bound β -catenin accumulates at the perinuclear endocytic recycling compartment and Wnt signalling activation translocates the complex to the nucleus [130]. During EMT, Hakai-mediated ubiquitination of E-cadherin results in sorting of cadherin to lysosomes, that redirect the latter from a recycling pathway to a lysosome-mediated degradation process. Thus, the cell loses its ability to form cell-cell

contacts and remain motile [131]. E3 ubiquitin ligases Hakai and Ozz also target degradation of membrane-bound β -catenin via the ubiquitin-mediated degradation pathway [99, 102]. Src-mediated phosphorylation of the cadherin-catenin complex results in ubiquitination by Hakai. Other ubiquitin ligases such as MDM2 and K5, can also ubiquitinate and degrade E-cadherin [132, 133]. However, this study is the first one to report that the E3 ubiquitin ligase Siah1 enhances degradation of the cell membrane-bound β -catenin in the *H. pylori*-infected GCCs and inhibition of proteasomal degradation rescues membrane-bound β -catenin from being degraded by Siah1.

This work also shows that loss of membrane-bound β -catenin mediated by *H. pylori*-infection is independent of membrane E-cadherin as there is no change in membrane-localized E-cadherin following *H. pylori* infection as well as Siah1 up-regulation. *H. pylori* virulence factor CagA destabilizes the cadherin-catenin complex, thereby inducing degradation of cytoplasmic β -catenin and accumulation of nuclear β -catenin [97]. However, this study confirms that β -catenin is not lost from the cytosol and no increment in nuclear β -catenin occurs in MKN45 cells infected with *H. pylori*. Our findings matches with the report by Bebb *et al.* which shows that *H. pylori*-infection decreases membrane β -catenin without accompanying increased cytosolic and nuclear pool [117]. As only nonphosphorylated CagA interacts with E-cadherin [42, 44] and CagA always gets phosphorylated in the *H. pylori*-infected host cell [45, 46], disruption of E-cadherin- β -catenin complex is not CagA-mediated. This study reveals that loss of membrane-bound β -catenin occurs only in *H. pylori*-infected GCCs but not in uninfected GCCs. This could be due to the induced activity of Siah1 in *H. pylori*-infected GCCs. Further research is required to identify the possible role of posttranslational modification(s) in regulating Siah1 activity.

Like Siah1, Siah2 also induces migration ability and invasiveness of *H. pylori*-infected cells. As Siah2 is absent in the membrane fraction, the metastasis inducing role for

Siah2 is possibly linked to some other mechanism other than membrane-bound β -catenin degradation in *H. pylori*-infected cells. Recently, Siah2 is reported to disrupt of the tight junction integrity and cell polarity in hypoxic bone-osteosarcoma cells by degrading the tumor-suppressor protein apoptosis-stimulating proteins of p532 (ASPP2) [134]. In the majority of hepatic cell carcinomas (HCCs), nuclear accumulation of Siah2 is correlated with induced hepatic cell proliferation, tumor progression and distant metastasis [135]. The role of nuclear Siah2 in *H. pylori*-infected GCCs needs to be studied in future.

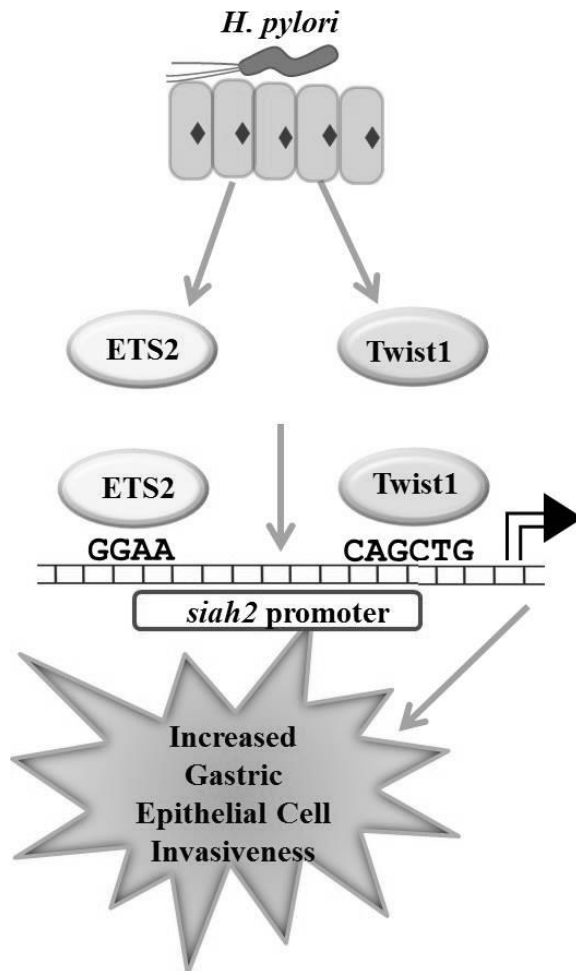
H. pylori are known to enhance cell migration [136, 137]. However, identification of the role of Siah1 and Siah2 in inducing cell motility in *H. pylori*-infected GCCs has made this study very important to understand *H. pylori*-mediated gastric carcinogenesis and metastatic progression. This study also gives clue that although ETS2 is the inducer of both Siah1 and Siah2, their effect on β -catenin are not the same. It is therefore imperative to study stage-specific expression of Siah proteins in gastric cancer which will definitely enrich us to better understand the molecular mechanism of gastric cancer.

SUMMARY AND CONCLUSION

Chapter 5

5. SUMMARY AND CONCLUSION

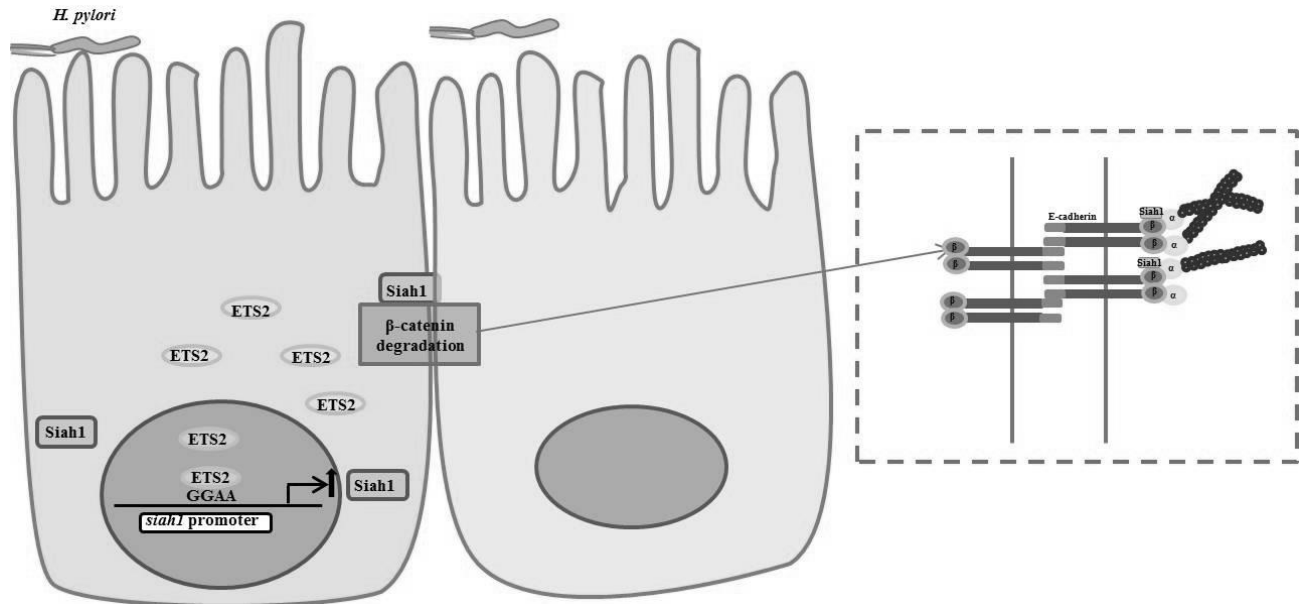
5.1. Pictorial Representation of ETS2 and Twist1-Mediated Transactivation of Siah2 Enhances Motility and Invasiveness of *H. pylori*-Infected GCCs



Summarization of the above figure:

- ❖ *H. pylori* infection induces ETS2 and Twist1 expression in gastric epithelial cells. ETS2 and Twist1 bind to the *siah2* promoter and mediate Siah2 expression in *H. pylori*-infected GCCs.
- ❖ Elevated expression of oncogenic protein Siah2 enhances motility and invasiveness of infected gastric epithelial cells.

5.2. ETS2-Mediated Siah1 Induction Enhances Membrane-Bound β -catenin Degradation in the *H. pylori*-Infected GCCs



Summary of the above figure

- ❖ *H. pylori* infection induces ETS2 expression. ETS2 binds to the *siah1* promoter and promotes *siah1* transcription in *H. pylori*-infected gastric cancer cells.
- ❖ Induced expression of Siah1 results in the degradation of membrane bound β -catenin. As a result, infected cells become more migratory and invasive.

In conclusion, this thesis work reveals crucial roles of Siah proteins during *H. pylori* infection in gastric cancer cells promoting invasion and migration. Our work shows a novel mechanism of ETS2-mediated induction of Siah1 and ETS2 and Twist1-mediated induction of Siah2 in *H. pylori*-infected gastric epithelial cancer cells. Furthermore, our findings provide an important insight towards the fact that although Siah1 and Siah2 are induced by ETS2 and have roles in gastric cancer metastasis, their cellular targets are not the same. Thus, Siah1 and Siah2 are not showing functional redundancy at least in promoting gastric cancer.

BIBLIOGRAPHY

1. Ciechanover, A. (1998) The ubiquitin-proteasome pathway: on protein death and cell life, *The EMBO journal*. 17, 7151-60.
2. Dikic, I., Wakatsuki, S. & Walters, K. J. (2009) Ubiquitin-binding domains - from structures to functions, *Nature reviews Molecular cell biology*. 10, 659-71.
3. Kim, H. M., Yu, Y. & Cheng, Y. (2011) Structure characterization of the 26S proteasome, *Biochimica et biophysica acta*. 1809, 67-79.
4. Kowalski, J. R. & Juo, P. (2012) The role of deubiquitinating enzymes in synaptic function and nervous system diseases, *Neural plasticity*. 2012, 892749.
5. Rotin, D. & Kumar, S. (2009) Physiological functions of the HECT family of ubiquitin ligases, *Nature reviews Molecular cell biology*. 10, 398-409.
6. Li, W., Bengtson, M. H., Ulbrich, A., Matsuda, A., Reddy, V. A., Orth, A., Chanda, S. K., Batalov, S. & Joazeiro, C. A. (2008) Genome-wide and functional annotation of human E3 ubiquitin ligases identifies MULAN, a mitochondrial E3 that regulates the organelle's dynamics and signaling, *PloS one*. 3, e1487.
7. Haglund, K. & Dikic, I. (2012) The role of ubiquitylation in receptor endocytosis and endosomal sorting, *Journal of cell science*. 125, 265-75.
8. Freemont, P. S. (2000) RING for destruction?, *Current biology : CB*. 10, R84-7.
9. Metzger, M. B., Hristova, V. A. & Weissman, A. M. (2012) HECT and RING finger families of E3 ubiquitin ligases at a glance, *Journal of cell science*. 125, 531-7.
10. Liew, C. W., Sun, H., Hunter, T. & Day, C. L. (2010) RING domain dimerization is essential for RNF4 function, *The Biochemical journal*. 431, 23-9.
11. Mace, P. D., Linke, K., Feltham, R., Schumacher, F. R., Smith, C. A., Vaux, D. L., Silke, J. & Day, C. L. (2008) Structures of the cIAP2 RING domain reveal conformational changes associated with ubiquitin-conjugating enzyme (E2) recruitment, *The Journal of biological chemistry*. 283, 31633-40.

12. Polekhina, G., House, C. M., Traficante, N., Mackay, J. P., Relaix, F., Sassoon, D. A., Parker, M. W. & Bowtell, D. D. (2002) Siah ubiquitin ligase is structurally related to TRAF and modulates TNF-alpha signaling, *Nature structural biology*. 9, 68-75.
13. Brzovic, P. S., Rajagopal, P., Hoyt, D. W., King, M. C. & Klevit, R. E. (2001) Structure of a BRCA1-BARD1 heterodimeric RING-RING complex, *Nature structural biology*. 8, 833-7.
14. Buchwald, G., van der Stoop, P., Weichenrieder, O., Perrakis, A., van Lohuizen, M. & Sixma, T. K. (2006) Structure and E3-ligase activity of the Ring-Ring complex of polycomb proteins Bmi1 and Ring1b, *The EMBO journal*. 25, 2465-74.
15. Hua, Z. & Vierstra, R. D. (2011) The cullin-RING ubiquitin-protein ligases, *Annual review of plant biology*. 62, 299-334.
16. Chen, P. & Yao, G. D. (2016) The role of cullin proteins in gastric cancer, *Tumour biology : the journal of the International Society for Oncodevelopmental Biology and Medicine*. 37, 29-37.
17. Welch, P. L. & King, M. C. (2001) BRCA1 and BRCA2 and the genetics of breast and ovarian cancer, *Human molecular genetics*. 10, 705-13.
18. Liyasova, M. S., Ma, K. & Lipkowitz, S. (2015) Molecular pathways: cbl proteins in tumorigenesis and antitumor immunity-opportunities for cancer treatment, *Clinical cancer research : an official journal of the American Association for Cancer Research*. 21, 1789-94.
19. Kang, J. M., Park, S., Kim, S. J., Hong, H. Y., Jeong, J. & Kim, H. S. (2012) CBL enhances breast tumor formation by inhibiting tumor suppressive activity of TGF-beta signaling, *Oncogene*. 31, 5123-31.
20. Dong, Q., Liu, Y. P., Qu, X. J., Hou, K. Z. & Li, L. L. (2010) [Expression of c-Cbl, Cbl-b, and epidermal growth factor receptor in gastric carcinoma and their clinical significance], *Chinese journal of cancer*. 29, 59-64.

21. Lo, F. Y., Tan, Y. H., Cheng, H. C., Salgia, R. & Wang, Y. C. (2011) An E3 ubiquitin ligase: c-Cbl: a new therapeutic target of lung cancer, *Cancer*. 117, 5344-50.
22. Jiao, X., Jin, B., Qu, X., Yan, S., Hou, K., Liu, Y. & Hu, X. (2011) [Expressions of c-Cbl, Cbl-b and EGFR and its role of prognosis in NSCLC], *Zhongguo fei ai za zhi = Chinese journal of lung cancer*. 14, 512-7.
23. Haupt, Y., Maya, R., Kazaz, A. & Oren, M. (1997) Mdm2 promotes the rapid degradation of p53, *Nature*. 387, 296-9.
24. Rankin, E. B. & Giaccia, A. J. (2016) Hypoxic control of metastasis, *Science*. 352, 175-80.
25. Gossage, L., Eisen, T. & Maher, E. R. (2015) VHL, the story of a tumour suppressor gene, *Nature reviews Cancer*. 15, 55-64.
26. Habelhah, H., Frew, I. J., Laine, A., Janes, P. W., Relaix, F., Sassoon, D., Bowtell, D. D. & Ronai, Z. (2002) Stress-induced decrease in TRAF2 stability is mediated by Siah2, *The EMBO journal*. 21, 5756-65.
27. Matsuzawa, S. I. & Reed, J. C. (2001) Siah-1, SIP, and Ebi collaborate in a novel pathway for beta-catenin degradation linked to p53 responses, *Molecular cell*. 7, 915-26.
28. Wong, C. S., Sceneay, J., House, C. M., Halse, H. M., Liu, M. C., George, J., Hunnam, T. C., Parker, B. S., Haviv, I., Ronai, Z., Cullinane, C., Bowtell, D. D. & Moller, A. (2012) Vascular normalization by loss of Siah2 results in increased chemotherapeutic efficacy, *Cancer research*. 72, 1694-704.
29. House, C. M., Moller, A. & Bowtell, D. D. (2009) Siah proteins: novel drug targets in the Ras and hypoxia pathways, *Cancer research*. 69, 8835-8.
30. Brauckhoff, A., Malz, M., Tschaharganeh, D., Malek, N., Weber, A., Riener, M. O., Soll, C., Samarin, J., Bissinger, M., Schmidt, J., Longerich, T., Ehemann, V., Schirmacher, P. &

- Breuhahn, K. (2011) Nuclear expression of the ubiquitin ligase seven in absentia homolog (SIAH)-1 induces proliferation and migration of liver cancer cells, *J Hepatol.* 55, 1049-57.
31. Nagano, Y., Fukushima, T., Okemoto, K., Tanaka, K., Bowtell, D. D., Ronai, Z., Reed, J. C. & Matsuzawa, S. (2011) Siah1/SIP regulates p27(kip1) stability and cell migration under metabolic stress, *Cell Cycle.* 10, 2592-602.
32. Hara, M. R., Agrawal, N., Kim, S. F., Cascio, M. B., Fujimuro, M., Ozeki, Y., Takahashi, M., Cheah, J. H., Tankou, S. K., Hester, L. D., Ferris, C. D., Hayward, S. D., Snyder, S. H. & Sawa, A. (2005) S-nitrosylated GAPDH initiates apoptotic cell death by nuclear translocation following Siah1 binding, *Nature cell biology.* 7, 665-74.
33. Nadeau, R. J., Toher, J. L., Yang, X., Kovalenko, D. & Friesel, R. (2007) Regulation of Sprouty2 stability by mammalian Seven-in-Absentia homolog 2, *J Cell Biochem.* 100, 151-60.
34. Nakayama, K., Frew, I. J., Hagensen, M., Skals, M., Habelhah, H., Bhoumik, A., Kadoya, T., Erdjument-Bromage, H., Tempst, P., Frappell, P. B., Bowtell, D. D. & Ronai, Z. (2004) Siah2 regulates stability of prolyl-hydroxylases, controls HIF1alpha abundance, and modulates physiological responses to hypoxia, *Cell.* 117, 941-52.
35. Susini, L., Passer, B. J., Amzallag-Elbaz, N., Juven-Gershon, T., Prieur, S., Privat, N., Tuynder, M., Gendron, M. C., Israel, A., Amson, R., Oren, M. & Telerman, A. (2001) Siah-1 binds and regulates the function of Numb, *Proceedings of the National Academy of Sciences of the United States of America.* 98, 15067-72.
36. Ma, B., Chen, Y., Chen, L., Cheng, H., Mu, C., Li, J., Gao, R., Zhou, C., Cao, L., Liu, J., Zhu, Y., Chen, Q. & Wu, S. (2015) Hypoxia regulates Hippo signalling through the SIAH2 ubiquitin E3 ligase, *Nature cell biology.* 17, 95-103.
37. Wong, C. S. & Moller, A. (2013) Siah: a promising anticancer target, *Cancer research.* 73, 2400-6.

38. Frasor, J., Danes, J. M., Funk, C. C. & Katzenellenbogen, B. S. (2005) Estrogen down-regulation of the corepressor N-CoR: mechanism and implications for estrogen derepression of N-CoR-regulated genes, *Proceedings of the National Academy of Sciences of the United States of America*. 102, 13153-7.
39. MacLeod, R. J., Hayes, M. & Pacheco, I. (2007) Wnt5a secretion stimulated by the extracellular calcium-sensing receptor inhibits defective Wnt signaling in colon cancer cells, *Am J Physiol Gastrointest Liver Physiol*. 293, G403-11.
40. Jing, Y., Liu, L. Z., Jiang, Y., Zhu, Y., Guo, N. L., Barnett, J., Rojanasakul, Y., Agani, F. & Jiang, B. H. (2012) Cadmium increases HIF-1 and VEGF expression through ROS, ERK, and AKT signaling pathways and induces malignant transformation of human bronchial epithelial cells, *Toxicol Sci*. 125, 10-9.
41. Mo, C., Dai, Y., Kang, N., Cui, L. & He, W. (2012) Ectopic expression of human MutS homologue 2 on renal carcinoma cells is induced by oxidative stress with interleukin-18 promotion via p38 mitogen-activated protein kinase (MAPK) and c-Jun N-terminal kinase (JNK) signaling pathways, *The Journal of biological chemistry*. 287, 19242-54.
42. Maeda, A., Yoshida, T., Kusuzaki, K. & Sakai, T. (2002) The characterization of the human Siah-1 promoter(1), *FEBS letters*. 512, 223-6.
43. Xie, W., Jin, L., Mei, Y. & Wu, M. (2009) E2F1 represses beta-catenin/TCF activity by direct up-regulation of Siah1, *Journal of cellular and molecular medicine*. 13, 1719-27.
44. Kim, C. J., Cho, Y. G., Park, C. H., Jeong, S. W., Nam, S. W., Kim, S. Y., Lee, S. H., Yoo, N. J., Lee, J. Y. & Park, W. S. (2004) Inactivating mutations of the Siah-1 gene in gastric cancer, *Oncogene*. 23, 8591-6.
45. Ferro, A., Peleteiro, B., Malvezzi, M., Bosetti, C., Bertuccio, P., Levi, F., Negri, E., La Vecchia, C. & Lunet, N. (2014) Worldwide trends in gastric cancer mortality (1980-2011), with predictions to 2015, and incidence by subtype, *Eur J Cancer*. 50, 1330-44.

46. Ferlay, J., Shin, H. R., Bray, F., Forman, D., Mathers, C. & Parkin, D. M. (2010) Estimates of worldwide burden of cancer in 2008: GLOBOCAN 2008, *International journal of cancer*. 127, 2893-917.
47. Parkin, D. M., Bray, F., Ferlay, J. & Pisani, P. (2001) Estimating the world cancer burden: Globocan 2000, *International journal of cancer*. 94, 153-6.
48. Goh, L. Y., Leow, A. H. & Goh, K. L. (2014) Observations on the epidemiology of gastrointestinal and liver cancers in the Asia-Pacific region, *Journal of digestive diseases*. 15, 463-8.
49. Lauren, P. (1965) The Two Histological Main Types of Gastric Carcinoma: Diffuse and So-Called Intestinal-Type Carcinoma. An Attempt at a Histo-Clinical Classification, *Acta pathologica et microbiologica Scandinavica*. 64, 31-49.
50. An, J. Y., Pak, K. H., Inaba, K., Cheong, J. H., Hyung, W. J. & Noh, S. H. (2011) Relevance of lymph node metastasis along the superior mesenteric vein in gastric cancer, *The British journal of surgery*. 98, 667-72.
51. Tiwari, N., Gheldof, A., Tatari, M. & Christofori, G. (2012) EMT as the ultimate survival mechanism of cancer cells, *Seminars in cancer biology*. 22, 194-207.
52. Thompson, E. W. & Haviv, I. (2011) The social aspects of EMT-MET plasticity, *Nature medicine*. 17, 1048-9.
53. GOODWIN, C. S., ARMSTRONG, J. A., CHILVERS, T., PETERS, M., COLLINS, M. D., SLY, L., McCONNELL, W. & HARPER, W. E. S. (1989) Transfer of *Campylobacter pylori* and *Campylobacter mustelae* to *Helicobacter* gen. nov. as *Helicobacter pylori* comb. nov. and *Helicobacter mustelae* comb. nov., Respectively, *International Journal of Systematic and Evolutionary Microbiology*. 39, 397-405.

54. Goodwin, C. S., McCulloch, R. K., Armstrong, J. A. & Wee, S. H. (1985) Unusual cellular fatty acids and distinctive ultrastructure in a new spiral bacterium (*Campylobacter pyloridis*) from the human gastric mucosa, *Journal of medical microbiology*. 19, 257-67.
55. Jones, D. M., Curry, A. & Fox, A. J. (1985) An ultrastructural study of the gastric campylobacter-like organism '*Campylobacter pyloridis*', *Journal of general microbiology*. 131, 2335-41.
56. Linz, B., Balloux, F., Moodley, Y., Manica, A., Liu, H., Roumagnac, P., Falush, D., Stamer, C., Prugnolle, F., van der Merwe, S. W., Yamaoka, Y., Graham, D. Y., Perez-Trallero, E., Wadstrom, T., Suerbaum, S. & Achtman, M. (2007) An African origin for the intimate association between humans and *Helicobacter pylori*, *Nature*. 445, 915-8.
57. Mishra, S. (2013) Is *Helicobacter pylori* good or bad?, *European journal of clinical microbiology & infectious diseases : official publication of the European Society of Clinical Microbiology*. 32, 301-4.
58. Marshall, B. J. & Warren, J. R. (1984) Unidentified curved bacilli in the stomach of patients with gastritis and peptic ulceration, *Lancet*. 1, 1311-5.
59. El-Omar, E. M., Oien, K., Murray, L. S., El-Nujumi, A., Wirz, A., Gillen, D., Williams, C., Fullarton, G. & McColl, K. E. (2000) Increased prevalence of precancerous changes in relatives of gastric cancer patients: critical role of *H. pylori*, *Gastroenterology*. 118, 22-30.
60. Khatoon, J., Rai, R. P. & Prasad, K. N. (2016) Role of *Helicobacter pylori* in gastric cancer: Updates, *World journal of gastrointestinal oncology*. 8, 147-58.
61. Oluwasola, A. O. (2014) Genetic determinants and clinico-pathological outcomes of *helicobacter pylori* infection, *Annals of Ibadan postgraduate medicine*. 12, 22-30.
62. Amieva, M. R. & El-Omar, E. M. (2008) Host-bacterial interactions in *Helicobacter pylori* infection, *Gastroenterology*. 134, 306-23.

63. Castano-Rodriguez, N., Kaakoush, N. O. & Mitchell, H. M. (2014) Pattern-recognition receptors and gastric cancer, *Frontiers in immunology*. 5, 336.
64. Conteduca, V., Sansonno, D., Lauletta, G., Russi, S., Ingravallo, G. & Dammacco, F. (2013) *H. pylori* infection and gastric cancer: state of the art (review), *International journal of oncology*. 42, 5-18.
65. Khalifa, M. M., Sharaf, R. R. & Aziz, R. K. (2010) *Helicobacter pylori*: a poor man's gut pathogen?, *Gut Pathogens*. 2, 1-12.
66. Kusters, J. G., van Vliet, A. H. & Kuipers, E. J. (2006) Pathogenesis of *Helicobacter pylori* infection, *Clinical microbiology reviews*. 19, 449-90.
67. Backert, S., Clyne, M. & Tegtmeyer, N. (2011) Molecular mechanisms of gastric epithelial cell adhesion and injection of CagA by *Helicobacter pylori*, *Cell communication and signaling : CCS*. 9, 28.
68. Censini, S., Lange, C., Xiang, Z., Crabtree, J. E., Ghiara, P., Borodovsky, M., Rappuoli, R. & Covacci, A. (1996) *cag*, a pathogenicity island of *Helicobacter pylori*, encodes type I-specific and disease-associated virulence factors, *Proceedings of the National Academy of Sciences of the United States of America*. 93, 14648-53.
69. Segal, E. D., Cha, J., Lo, J., Falkow, S. & Tompkins, L. S. (1999) Altered states: involvement of phosphorylated CagA in the induction of host cellular growth changes by *Helicobacter pylori*, *Proceedings of the National Academy of Sciences of the United States of America*. 96, 14559-64.
70. Bagnoli, F., Buti, L., Tompkins, L., Covacci, A. & Amieva, M. R. (2005) *Helicobacter pylori* CagA induces a transition from polarized to invasive phenotypes in MDCK cells, *Proceedings of the National Academy of Sciences of the United States of America*. 102, 16339-44.

71. Allen, L. A., Schlesinger, L. S. & Kang, B. (2000) Virulent strains of *Helicobacter pylori* demonstrate delayed phagocytosis and stimulate homotypic phagosome fusion in macrophages, *The Journal of experimental medicine*. 191, 115-28.
72. Torres, V. J., VanCompernelle, S. E., Sundrud, M. S., Unutmaz, D. & Cover, T. L. (2007) *Helicobacter pylori* vacuolating cytotoxin inhibits activation-induced proliferation of human T and B lymphocyte subsets, *J Immunol*. 179, 5433-40.
73. Perez-Moreno, M., Jamora, C. & Fuchs, E. (2003) Sticky business: orchestrating cellular signals at adherens junctions, *Cell*. 112, 535-48.
74. Franke, W. W. (2009) Discovering the molecular components of intercellular junctions--a historical view, *Cold Spring Harbor perspectives in biology*. 1, a003061.
75. Yagi, T. & Takeichi, M. (2000) Cadherin superfamily genes: functions, genomic organization, and neurologic diversity, *Genes & development*. 14, 1169-80.
76. Yonemura, S., Itoh, M., Nagafuchi, A. & Tsukita, S. (1995) Cell-to-cell adherens junction formation and actin filament organization: similarities and differences between non-polarized fibroblasts and polarized epithelial cells, *Journal of cell science*. 108 (Pt 1), 127-42.
77. Adams, C. L. & Nelson, W. J. (1998) Cytomechanics of cadherin-mediated cell-cell adhesion, *Current opinion in cell biology*. 10, 572-7.
78. Baum, B. & Georgiou, M. (2011) Dynamics of adherens junctions in epithelial establishment, maintenance, and remodeling, *The Journal of cell biology*. 192, 907-17.
79. Wu, Y. & Zhou, B. P. (2008) New insights of epithelial-mesenchymal transition in cancer metastasis, *Acta biochimica et biophysica Sinica*. 40, 643-50.
80. Radisky, D. C. (2005) Epithelial-mesenchymal transition, *Journal of cell science*. 118, 4325-6.

81. Christiansen, J. J. & Rajasekaran, A. K. (2006) Reassessing epithelial to mesenchymal transition as a prerequisite for carcinoma invasion and metastasis, *Cancer research*. 66, 8319-26.
82. Tran, N. L., Nagle, R. B., Cress, A. E. & Heimark, R. L. (1999) N-Cadherin expression in human prostate carcinoma cell lines. An epithelial-mesenchymal transformation mediating adhesion with Stromal cells, *The American journal of pathology*. 155, 787-98.
83. Kang, Y. & Massague, J. (2004) Epithelial-mesenchymal transitions: twist in development and metastasis, *Cell*. 118, 277-9.
84. Vleminckx, K., Vakaet, L., Jr., Mareel, M., Fiers, W. & van Roy, F. (1991) Genetic manipulation of E-cadherin expression by epithelial tumor cells reveals an invasion suppressor role, *Cell*. 66, 107-19.
85. Perl, A. K., Wilgenbus, P., Dahl, U., Semb, H. & Christofori, G. (1998) A causal role for E-cadherin in the transition from adenoma to carcinoma, *Nature*. 392, 190-3.
86. Nagafuchi, A. & Takeichi, M. (1989) Transmembrane control of cadherin-mediated cell adhesion: a 94 kDa protein functionally associated with a specific region of the cytoplasmic domain of E-cadherin, *Cell regulation*. 1, 37-44.
87. Maelandsmo, G. M., Holm, R., Nesland, J. M., Fodstad, O. & Florenes, V. A. (2003) Reduced beta-catenin expression in the cytoplasm of advanced-stage superficial spreading malignant melanoma, *Clinical cancer research : an official journal of the American Association for Cancer Research*. 9, 3383-8.
88. Gottardi, C. J. & Gumbiner, B. M. (2004) Distinct molecular forms of beta-catenin are targeted to adhesive or transcriptional complexes, *The Journal of cell biology*. 167, 339-49.
89. Kawanishi, J., Kato, J., Sasaki, K., Fujii, S., Watanabe, N. & Niitsu, Y. (1995) Loss of E-cadherin-dependent cell-cell adhesion due to mutation of the beta-catenin gene in a human cancer cell line, HSC-39, *Molecular and cellular biology*. 15, 1175-81.

90. Tian, X., Liu, Z., Niu, B., Zhang, J., Tan, T. K., Lee, S. R., Zhao, Y., Harris, D. C. & Zheng, G. (2011) E-cadherin/beta-catenin complex and the epithelial barrier, *Journal of biomedicine & biotechnology*. 2011, 567305.
91. Daugherty, R. L. & Gottardi, C. J. (2007) Phospho-regulation of Beta-catenin adhesion and signaling functions, *Physiology (Bethesda)*. 22, 303-9.
92. Sarkar, F. H., Li, Y., Wang, Z. & Kong, D. (2010) The role of nutraceuticals in the regulation of Wnt and Hedgehog signaling in cancer, *Cancer metastasis reviews*. 29, 383-94.
93. Kim, W., Kim, M. & Jho, E. H. (2013) Wnt/beta-catenin signalling: from plasma membrane to nucleus, *The Biochemical journal*. 450, 9-21.
94. Song, X., Xin, N., Wang, W. & Zhao, C. (2015) Wnt/beta-catenin, an oncogenic pathway targeted by *H. pylori* in gastric carcinogenesis, *Oncotarget*. 6, 35579-88.
95. Chiurillo, M. A. (2015) Role of the Wnt/beta-catenin pathway in gastric cancer: An in-depth literature review, *World journal of experimental medicine*. 5, 84-102.
96. Hoy, B., Lower, M., Weydig, C., Carra, G., Tegtmeyer, N., Geppert, T., Schroder, P., Sewald, N., Backert, S., Schneider, G. & Wessler, S. (2010) *Helicobacter pylori* HtrA is a new secreted virulence factor that cleaves E-cadherin to disrupt intercellular adhesion, *EMBO reports*. 11, 798-804.
97. Murata-Kamiya, N., Kurashima, Y., Teishikata, Y., Yamahashi, Y., Saito, Y., Higashi, H., Aburatani, H., Akiyama, T., Peek, R. M., Jr., Azuma, T. & Hatakeyama, M. (2007) *Helicobacter pylori* CagA interacts with E-cadherin and deregulates the beta-catenin signal that promotes intestinal transdifferentiation in gastric epithelial cells, *Oncogene*. 26, 4617-26.
98. Alzahrani, S., Lina, T. T., Gonzalez, J., Pinchuk, I. V., Beswick, E. J. & Reyes, V. E. (2014) Effect of *Helicobacter pylori* on gastric epithelial cells, *World journal of gastroenterology*. 20, 12767-80.

99. Fujita, Y., Krause, G., Scheffner, M., Zechner, D., Leddy, H. E., Behrens, J., Sommer, T. & Birchmeier, W. (2002) Hakai, a c-Cbl-like protein, ubiquitinates and induces endocytosis of the E-cadherin complex, *Nature cell biology*. 4, 222-31.
100. Tauriello, D. V. & Maurice, M. M. (2010) The various roles of ubiquitin in Wnt pathway regulation, *Cell Cycle*. 9, 3700-9.
101. Bryant, D. M. & Stow, J. L. (2004) The ins and outs of E-cadherin trafficking, *Trends in cell biology*. 14, 427-34.
102. Nastasi, T., Bongiovanni, A., Campos, Y., Mann, L., Toy, J. N., Bostrom, J., Rottier, R., Hahn, C., Conaway, J. W., Harris, A. J. & D'Azzo, A. (2004) Ozz-E3, a muscle-specific ubiquitin ligase, regulates beta-catenin degradation during myogenesis, *Developmental cell*. 6, 269-82.
103. Iwai, A., Marusawa, H., Matsuzawa, S., Fukushima, T., Hijikata, M., Reed, J. C., Shimotohno, K. & Chiba, T. (2004) Siah-1L, a novel transcript variant belonging to the human Siah family of proteins, regulates beta-catenin activity in a p53-dependent manner, *Oncogene*. 23, 7593-600.
104. Sementchenko, V. I. & Watson, D. K. (2000) Ets target genes: past, present and future, *Oncogene*. 19, 6533-48.
105. Chang, A. T., Liu, Y., Ayyanathan, K., Benner, C., Jiang, Y., Prokop, J. W., Paz, H., Wang, D., Li, H. R., Fu, X. D., Rauscher, F. J., 3rd & Yang, J. (2015) An evolutionarily conserved DNA architecture determines target specificity of the TWIST family bHLH transcription factors, *Genes & development*. 29, 603-16.
106. Tania, M., Khan, M. A. & Fu, J. (2014) Epithelial to mesenchymal transition inducing transcription factors and metastatic cancer, *Tumour biology : the journal of the International Society for Oncodevelopmental Biology and Medicine*. 35, 7335-42.

107. Yang, Z., Zhang, X., Gang, H., Li, X., Li, Z., Wang, T., Han, J., Luo, T., Wen, F. & Wu, X. (2007) Up-regulation of gastric cancer cell invasion by Twist is accompanied by N-cadherin and fibronectin expression, *Biochemical and biophysical research communications*. 358, 925-30.
108. Seth, A. & Watson, D. K. (2005) ETS transcription factors and their emerging roles in human cancer, *Eur J Cancer*. 41, 2462-78.
109. Ru, G. Q., Wang, H. J., Xu, W. J. & Zhao, Z. S. (2011) Upregulation of Twist in gastric carcinoma associated with tumor invasion and poor prognosis, *Pathology oncology research : POR*. 17, 341-7.
110. Liao, Y. L., Hu, L. Y., Tsai, K. W., Wu, C. W., Chan, W. C., Li, S. C., Lai, C. H., Ho, M. R., Fang, W. L., Huang, K. H. & Lin, W. C. (2012) Transcriptional regulation of miR-196b by ETS2 in gastric cancer cells, *Carcinogenesis*. 33, 760-9.
111. Tsugane, S. & Sasazuki, S. (2007) Diet and the risk of gastric cancer: review of epidemiological evidence, *Gastric Cancer*. 10, 75-83.
112. Griffin, N., Burke, C. & Grant, L. A. (2011) Common primary tumours of the abdomen and pelvis and their patterns of tumour spread as seen on multi-detector computed tomography, *Insights into imaging*. 2, 205-214.
113. Matsuzawa, S., Takayama, S., Froesch, B. A., Zapata, J. M. & Reed, J. C. (1998) p53-inducible human homologue of Drosophila seven in absentia (Siah) inhibits cell growth: suppression by BAG-1, *The EMBO journal*. 17, 2736-47.
114. Kollareddy, M., Dimitrova, E., Vallabhaneni, K. C., Chan, A., Le, T., Chauhan, K. M., Carrero, Z. I., Ramakrishnan, G., Watabe, K., Haupt, Y., Haupt, S., Pochampally, R., Boss, G. R., Romero, D. G., Radu, C. G. & Martinez, L. A. (2015) Regulation of nucleotide metabolism by mutant p53 contributes to its gain-of-function activities, *Nature communications*. 6, 7389.

115. Xiong, S., Tu, H., Kollareddy, M., Pant, V., Li, Q., Zhang, Y., Jackson, J. G., Suh, Y. A., Elizondo-Fraire, A. C., Yang, P., Chau, G., Tashakori, M., Wasylshen, A. R., Ju, Z., Solomon, H., Rotter, V., Liu, B., El-Naggar, A. K., Donehower, L. A., Martinez, L. A. & Lozano, G. (2014) Pla2g16 phospholipase mediates gain-of-function activities of mutant p53, *Proceedings of the National Academy of Sciences of the United States of America*. 111, 11145-50.
116. Do, P. M., Varanasi, L., Fan, S., Li, C., Kubacka, I., Newman, V., Chauhan, K., Daniels, S. R., Bocchetta, M., Garrett, M. R., Li, R. & Martinez, L. A. (2012) Mutant p53 cooperates with ETS2 to promote etoposide resistance, *Genes & development*. 26, 830-45.
117. Bebb, J. R., Leach, L., Zaitoun, A., Hand, N., Letley, D. P., Thomas, R. & Atherton, J. C. (2006) Effects of *Helicobacter pylori* on the cadherin-catenin complex, *J Clin Pathol*. 59, 1261-6.
118. Liu, J., Stevens, J., Rote, C. A., Yost, H. J., Hu, Y., Neufeld, K. L., White, R. L. & Matsunami, N. (2001) Siah-1 mediates a novel beta-catenin degradation pathway linking p53 to the adenomatous polyposis coli protein, *Molecular cell*. 7, 927-36.
119. Yoshibayashi, H., Okabe, H., Satoh, S., Hida, K., Kawashima, K., Hamasu, S., Nomura, A., Hasegawa, S., Ikai, I. & Sakai, Y. (2007) SIAH1 causes growth arrest and apoptosis in hepatoma cells through beta-catenin degradation-dependent and -independent mechanisms, *Oncology reports*. 17, 549-56.
120. Leung, C. O., Deng, W., Ye, T. M., Ngan, H. Y., Tsao, S. W., Cheung, A. N., Pang, R. T. & Yeung, W. S. (2014) miR-135a leads to cervical cancer cell transformation through regulation of beta-catenin via a SIAH1-dependent ubiquitin proteosomal pathway, *Carcinogenesis*. 35, 1931-40.
121. Weydig, C., Starzinski-Powitz, A., Carra, G., Lower, J. & Wessler, S. (2007) CagA-independent disruption of adherence junction complexes involves E-cadherin shedding and

implies multiple steps in *Helicobacter pylori* pathogenicity, *Experimental cell research*. 313, 3459-71.

122. Costa, A. M., Leite, M., Seruca, R. & Figueiredo, C. (2013) Adherens junctions as targets of microorganisms: a focus on *Helicobacter pylori*, *FEBS letters*. 587, 259-65.

123. Takayama, T., Shiozaki, H., Shibamoto, S., Oka, H., Kimura, Y., Tamura, S., Inoue, M., Monden, T., Ito, F. & Monden, M. (1996) Beta-catenin expression in human cancers, *The American journal of pathology*. 148, 39-46.

124. Chen, K. H., Tung, P. Y., Wu, J. C., Chen, Y., Chen, P. C., Huang, S. H. & Wang, S. M. (2008) An acidic extracellular pH induces Src kinase-dependent loss of beta-catenin from the adherens junction, *Cancer letters*. 267, 37-48.

125. Stanczak, A., Stec, R., Bodnar, L., Olszewski, W., Cichowicz, M., Kozłowski, W., Szczylik, C., Pietrucha, T., Wieczorek, M. & Lamparska-Przybysz, M. (2011) Prognostic significance of Wnt-1, beta-catenin and E-cadherin expression in advanced colorectal carcinoma, *Pathology oncology research : POR*. 17, 955-63.

126. Ebert, M. P., Yu, J., Hoffmann, J., Rocco, A., Rocken, C., Kahmann, S., Muller, O., Korc, M., Sung, J. J. & Malfertheiner, P. (2003) Loss of beta-catenin expression in metastatic gastric cancer, *Journal of clinical oncology : official journal of the American Society of Clinical Oncology*. 21, 1708-14.

127. Qi, J., Nakayama, K., Gaitonde, S., Goydos, J. S., Krajewski, S., Eroshkin, A., Barsagi, D., Bowtell, D. & Ronai, Z. (2008) The ubiquitin ligase Siah2 regulates tumorigenesis and metastasis by HIF-dependent and -independent pathways, *Proceedings of the National Academy of Sciences of the United States of America*. 105, 16713-8.

128. Howard, S., Deroo, T., Fujita, Y. & Itasaki, N. (2011) A positive role of cadherin in Wnt/beta-catenin signalling during epithelial-mesenchymal transition, *PloS one*. 6, e23899.

129. Brembeck, F. H., Schwarz-Romond, T., Bakkers, J., Wilhelm, S., Hammerschmidt, M. & Birchmeier, W. (2004) Essential role of BCL9-2 in the switch between beta-catenin's adhesive and transcriptional functions, *Genes & development*. 18, 2225-30.
130. Kam, Y. & Quaranta, V. (2009) Cadherin-bound beta-catenin feeds into the Wnt pathway upon adherens junctions dissociation: evidence for an intersection between beta-catenin pools, *PLoS one*. 4, e4580.
131. Palacios, F., Tushir, J. S., Fujita, Y. & D'Souza-Schorey, C. (2005) Lysosomal targeting of E-cadherin: a unique mechanism for the down-regulation of cell-cell adhesion during epithelial to mesenchymal transitions, *Molecular and cellular biology*. 25, 389-402.
132. Yang, J. Y., Zong, C. S., Xia, W., Wei, Y., Ali-Seyed, M., Li, Z., Broglio, K., Berry, D. A. & Hung, M. C. (2006) MDM2 promotes cell motility and invasiveness by regulating E-cadherin degradation, *Molecular and cellular biology*. 26, 7269-82.
133. Mansouri, M., Rose, P. P., Moses, A. V. & Fruh, K. (2008) Remodeling of endothelial adherens junctions by Kaposi's sarcoma-associated herpesvirus, *Journal of virology*. 82, 9615-28.
134. Kim, H., Claps, G., Moller, A., Bowtell, D., Lu, X. & Ronai, Z. A. (2014) Siah2 regulates tight junction integrity and cell polarity through control of ASPP2 stability, *Oncogene*. 33, 2004-10.
135. Malz, M., Aulmann, A., Samarin, J., Bissinger, M., Longerich, T., Schmitt, S., Schirmacher, P. & Breuhahn, K. (2012) Nuclear accumulation of septin 2 in absentia homologue-2 supports motility and proliferation of liver cancer cells, *International journal of cancer*. 131, 2016-26.
136. Krueger, S., Hundertmark, T., Kuester, D., Kalinski, T., Peitz, U. & Roessner, A. (2007) *Helicobacter pylori* alters the distribution of ZO-1 and p120ctn in primary human gastric epithelial cells, *Pathol Res Pract*. 203, 433-44.

137. Moese, S., Selbach, M., Kwok, T., Brinkmann, V., Konig, W., Meyer, T. F. & Backert, S. (2004) *Helicobacter pylori* induces AGS cell motility and elongation via independent signaling pathways, *Infect Immun.* 72, 3646-9.

APPENDIX I

PLASMID CONSTRUCTS USED

Constructs	Description	Source
pcDNA3.1 ⁺ -Siah1	WT construct	Generated
pCMV6-AC-GFP-Siah2	WT construct	Origene
pcDNA3-FLAG-ETS2	WT construct	Addgene plasmid 28128
pcDNA3-Flag-Twist	WT construct	Gifted by Dr. Kimitoshi Kohno, University of Occupational and Environmental Health, Japan
pGL3-Siah1	Luciferase construct	Generated
pGL3-Siah1-EBS mut	EBS mutation	Generated from WT Siah1 promoter
pGL3-Siah2	Luciferase construct	Generated
pGL3-Siah2-EBS mut	EBS mutation	Generated from WT Siah2 promoter
pGL3-Siah2-TBS mut	TBS mutation	Generated from WT Siah2 promoter

Constructs	Description	Source
pcDNA3.1 ⁺	Empty vector	Invitrogen
pHRLTK	Luciferase construct	Promega

APPENDIX II

siRNAs USED

siRNA	Cat No.	Company
Siah1	sc-37495	Santa Cruz Biotechnology
Control siRNA	sc-37007	Santa Cruz Biotechnology
Siah2	SR304370	Origene
ETS2	SR301471	Origene
Twist1	SR304977	Origene
Trilencer-27 universal scrambled negative control	SR30004	Origene

APPENDIX III

PRIMARY ANTIBODIES USED

Antibodies	Clone	Dilution	Company	Catalogue
Siah1	Goat Polyclonal	1:250 (WB)	Novus Biologicals	NB300-974
Siah1	Goat Polyclonal	1:100 (IF)	Santa Cruz Biotechnology	sc-5505
Siah2	Goat Polyclonal	1:250 (WB) 1:100 (IF)	Santa Cruz Biotechnology	sc-5505
Siah2	Rabbit Polyclonal	1:500 (WB) 1:100 (IF)	Abcam	ab72064
ETS2	Rabbit Polyclonal	1:1000 (WB) 1:100 (IF)	Santa Cruz Biotechnology	sc-22803
Anti-Twist1	Mouse Polyclonal	1:250 (WB) 1:50 (IF)	Abcam	ab50887
β -catenin	Rabbit Monoclonal	1:5000 (WB) 1:250 (IF)	Abcam	ab32572
E-Cadherin	Rabbit Polyclonal	1:1000 (WB) 1:100 (IF)	Cell Signalling Technology	3195
α -tubulin	Rabbit Monoclonal	1:10000 (WB)	Abcam	ab52866

Antibodies	Clone	Dilution	Company	Catalogue
PAN-Cadherin	Rabbit Polyclonal	1:1000 (WB)	Cell Signalling Technology	4068
HDAC1	Rabbit Polyclonal	1:1000 (WB)	Cell Signalling Technology	2062

SECONDARY ANTIBODIES USED

Antibodies	Conjugate	Dilution	Company	Catalogue
Anti-mouse IgG	HRP	1:3000 (WB)	Cell Signalling Technology	7076
Anti-rabbit IgG	HRP	1:3000 (WB)	Cell Signalling Technology	7074
Anti-goat IgG	HRP	1:5000 (WB)	Abcam	ab6741
Alexa Fluor 488 chicken anti-mouse IgG	Fluorescence	1:500 (IF)	Invitrogen	A21200
Alexa Fluor 488 goat anti-rabbit IgG	Fluorescence	1:500 (IF)	Invitrogen	A11070
Alexa Fluor 594 chicken anti-mouse IgG	Fluorescence	1:500 (IF)	Invitrogen	A21201
Alexa Fluor 594 chicken anti-rabbit IgG	Fluorescence	1:500 (IF)	Invitrogen	A21442

Antibodies	Conjugate	Dilution	Company	Catalogue
Alexa Fluor 488 donkey anti-goat IgG	Fluorescence	1:500 (IF)	Invitrogen	A11055
DAPI	Dye	1:2000	Invitrogen	D3571

WB=Western blot; IF=Immunofluorescence

APPENDIX IV

*PRIMER SEQUENCES FOR *siah1* CLONING*

Primer	Sequence
Forward	5' AAAAGCTTCAAATGAGCCGTCAGACTGCTACAGCATT 3'
Reverse	5' CCTCGAGTCAACACATGGAAATAGTTACATTGATG 3'

APPENDIX V

*REACTION CONDITION FOR PCR OF *siah1* GENE*

	Temperature (°C)	Time (min)	No. of cycles
Initial Denaturation	94	2	1
Denaturation	94	1	35
Annealing	58.8	1	
Extension	68	1	
Final extension	68	10	1

APPENDIX VI

*PRIMER SEQUENCES USED FOR *siah1* 5' UTR CLONING*

Primer	Sequence
Forward	5' CGCTGGGCTAAATCAGCAGAC3'
Reverse	5' ACTTACCTGTGGGCGGAGAG 3'
Forward (<u>KpnI</u>)	5' AAGGT <u>ACCAGCAACGGTAGC</u> 3'
Reverse (<u>HindIII</u>)	5' ATTAAGCTTTGTGGGCGGAGAG 3'

*PRIMER SEQUENCES USED FOR *siah2* PROMOTER CLONING*

Primer	Sequence
Forward	5' CCCAATGCTTCTCGTCCTGACTC3'
Reverse	5' GCTTCTGGAACAGCCGCTGAC 3'
Forward (<u>KpnI</u>)	5' AGAGGT <u>ACCGACTCCGAACACAG</u> 3'
Reverse (<u>HindIII</u>)	5' TGTAAGCTTCTTCTGGAACAGCCG 3'

APPENDIX VII

REACTION CONDITION FOR PCR OF siah1 5' UTR

	Temperature (°C)	Time	No. of cycles
Initial Denaturation	95	10 min	1
Denaturation	95	30 sec	35
Annealing	54-63	30 Sec	
Extension	72	1 min	
Final extension	72	7 min	1

REACTION CONDITION FOR PCR OF siah2 PROMOTER

	Temperature (°C)	Time	No. of cycles
Initial Denaturation	95	10 min	1
Denaturation	95	30 sec	35
Annealing	47.8-64.2	30 Sec	
Extension	72	1 min	
Final extension	72	7 min	1

REACTION CONDITION FOR PCR ON PCR OF siah1 5' UTR

	Temperature (°C)	Time	No. of cycles
Initial Denaturation	95	10 min	1
Denaturation	95	30 sec	35
Annealing	54.85	30 Sec	
Extension	72	1 min	
Final extension	72	7 min	1

REACTION CONDITION FOR PCR ON PCR OF siah2 PROMOTER

	Temperature (°C)	Time	No. of cycles
Initial Denaturation	95	10 min	1
Denaturation	95	30 sec	35
Annealing	58.45	30 Sec	
Extension	72	1 min	
Final extension	72	7 min	1

APPENDIX VIII

*PRIMER USED FOR *siah1* 5' UTR EBS MUTATION*

Mutagenesis Primer	Sequence
EBS [#]	5' GTCGGTCTCGGCGCC <i>ATT</i> AAGAGGCGGTGGCGC 3'

WT EBS=GGAA; [#] Mutations are shown in boldface and in italics

*PRIMER USED FOR *siah2* PROMOTER EBS AND TBS MUTATION*

Mutagenesis Primer	Sequence
EBS [#]	5' CCCGCAGCCCGAGCA <i>TTA</i> AGCGCCGGCGCTAGG 3'
TBS [#]	5' GCCCCCTGCGCTGC <i>TTGCTA</i> AGAGCCGGGCGGAGC 3'

WT EBS=GGAA; WT TBS=CANNTG; [#] Mutations are boldfaced and in italics.

PCR REACTION CONDITION FOR SITE-DIRECTED MUTAGENESIS

	Temperature (°C)	Time (min)	No. of cycles
Initial Denaturation	95	1	1
Denaturation	95	1	30
Annealing	55	1	
Extension	65	10 [#]	
Final extension	65	10	1

[#]2min/kb of plasmid length

APPENDIX IX

REACTION CONDITION FOR REAL-TIME RT-PCR

Stage	Temperature (°C)	Time (min)	No. of cycles
Hold	50	2	1
Hold	95	10	1
Cycles	95	0.15	40
Cycles	72	1	

APPENDIX X

BIOTINYLATED OLIGOS OF *siah1* 5' UTR EBS

5' Biotinylated Primer	Sequence
Forward ^{\$} WT	5' TCTCGGCGCC <u>GGAAGAGGCGGTGGCG</u> 3'
Reverse WT	5' CGCCACCGCCTCTTCCCGGCGCCGAGA 3'
Forward [#] Mutant	5' TCTCGGCGCC <u>ATT</u> AAGAGGCGGTGGCG3'
Reverse Mutant	5' CGCCACCGCCTCTTAATGGCGCCGAGA3'

^{\$}EBS is underlined, [#]Mutations are underlined and bold

BIOTINYLATED OLIGOS OF *siah2* PROMOTER EBS

5' Biotinylated Primer	Sequence
Forward ^{\$} WT	5' CAGCCCGAGCAGGAAGCGCCGGCGCTA 3'
Reverse WT	5' TAGCGCCGGCGCTTCCTGCTCGGGCTG 3'
Forward [#] Mutant	5' CAGCCCGAGCA <i>TTA</i> AGCGCCGGCGCTA 3'
Reverse Mutant	5' TAGCGCCGGCGCTTAATGCTCGGGCTG 3'

^{\$}EBS are underlined, [#]Mutations are bold faced italics

BIOTINYLATED OLIGOS OF *siah2* PROMOTER TBS

5' Biotinylated Primer	Sequence
Forward ^{\$} WT	5' CCCTGCGCTGCC <u>CAGCTGG</u> AGCCGGGCG 3'
Reverse WT	5' CGCCCGGCTCCAGCTGGCAGCGCAGGG 3'
Forward [#] Mutant	5' CCCTGCGCTGC <i>TTGCTA</i> AGAGCCGGGCG 3'
Reverse Mutant	5' CGCCCGGCTCTAGCAAGCAGCGCAGGG 3'

^{\$}TBS is underlined, [#]Mutations are boldfaced and in italics

APPENDIX XI

*PRIMER SEQUENCES USED FOR *siah1* 5' UTR CHIP ASSAY*

Primer	Sequence
Forward (Specific)	5' CGCAGTGTGTGGTATTTAGCG 3'
Reverse (Specific)	5' TCCTGGCACCAACGCG 3'
Forward (Non-Specific)	5' CACTAGCCACTACTTGAGGTTTA 3'
Reverse (Non-Specific)	5' GCTTTTGATGGTGGCTTTACT 3'

*PRIMER SEQUENCES USED FOR *siah2* PROMOTER CHIP ASSAY*

Primer	Sequence
Forward (Specific)	5' ACCCAGAAAAGACAACCCCGCG 3'
Reverse (Specific)	5' GACGTGACGCCTGGACACGT 3'
Forward (Non-Specific)	5' CTGGTAGACACTTTGAAAGAGA 3'
Reverse (Non-Specific)	5' TCCACTCTCTTCCACAAAAG 3'

REACTION CONDITION FOR PCR OF *siah1* CHIP ASSAY

	Temperature (°C)	Time	No. of cycles
Initial Denaturation	95	4 min	1
Denaturation	95	30 sec	35
Annealing	59.8	30 Sec	
Extension	68	30 sec	
Final extension	68	10 min	1

REACTION CONDITION FOR PCR OF *siah2* CHIP ASSAY

	Temperature (°C)	Time	No. of cycles
Initial Denaturation	95	4 min	1
Denaturation	95	30 sec	35
Annealing	59	30 Sec	
Extension	68	30 sec	
Final extension	68	5 min	1

PUBLICATIONS

ETS2 and Twist1 promote invasiveness of *Helicobacter pylori*-infected gastric cancer cells by inducing Siah2

Lopamudra Das*, Shrikant Babanrao Kokate*, Suvasmita Rath*, Niranjan Rout†, Shivaram Prasad Singh‡, Sheila Eileen Crowe§, Asish K. Mukhopadhyay|| and Asima Bhattacharyya*¹

*School of Biological Sciences, National Institute of Science Education and Research (NISER), P.O. Bhipur-Padanpur, Via Jatni, Dist. Khurda 752050, Odisha, India

†Department of Oncopathology, Acharya Harihar Regional Cancer Centre, Cuttack 753007, Odisha, India

‡Department of Gastroenterology, SCB Medical College, Cuttack 753007, Odisha, India

§School of Medicine, Division of Gastroenterology, UC San Diego, CA 92093, U.S.A.

||Division of Bacteriology, National Institute of Cholera and Enteric Diseases (NICED), Kolkata 700010, India

Helicobacter pylori infection is one of the most potent factors leading to gastric carcinogenesis. The seven in absentia homologue (Siah2) is an E3 ubiquitin ligase which has been implicated in various cancers but its role in *H. pylori*-mediated gastric carcinogenesis has not been established. We investigated the involvement of Siah2 in gastric cancer metastasis which was assessed by invasiveness and migration of *H. pylori*-infected gastric epithelial cancer cells. Cultured gastric cancer cells (GCCs) MKN45, AGS and Kato III showed significantly induced expression of Siah2, increased invasiveness and migration after being challenged with the pathogen. Siah2-expressing stable cells showed increased invasiveness and migration after *H. pylori* infection. Siah2 was transcriptionally activated by E26 transformation-specific sequence 2 (ETS2)- and Twist-related

protein 1 (Twist1) induced in *H. pylori*-infected gastric epithelial cells. These transcription factors dose-dependently enhanced the aggressiveness of infected GCCs. Our data suggested that *H. pylori*-infected GCCs gained cell motility and invasiveness through Siah2 induction. As gastric cancer biopsy samples also showed highly induced expression of ETS2, Twist1 and Siah2 compared with noncancerous gastric tissue, we surmise that ETS2- and Twist1-mediated Siah2 up-regulation has potential diagnostic and prognostic significance and could be targeted for therapeutic purpose.

Key words: ETS2, gastric cancer, *H. pylori*, metastasis, Siah2, Twist1.

INTRODUCTION

Gastric cancer is one of the most common malignant cancers. It is generally diagnosed at very late stages when the cancer has already metastasized to neighbouring lymph nodes or tissues. This occurs mostly due to the complex initiation and progression mechanisms of the disease as well as the lack of symptoms and detection markers at early stages. Therefore, in spite of a decline in gastric cancer cases in recent years, this disease still remains the second leading cause of cancer-related mortality in the world [1,2]. *Helicobacter pylori* infection is the prime factor responsible for gastric cancer. Up to 80% of people in certain parts of the world are infected with *H. pylori* [3]. Host responses towards infection and the possession of a ~40 kb stretch of genetic element by the pathogen called the cytotoxin-associated gene (*cag*) pathogenicity island (PAI) play a role in determining the outcome of infection. Like any other solid tumour of epithelial origin, development of the invasive gastric cancer phenotype employs epithelial–mesenchymal transition (EMT) wherein the epithelial cells lose their epithelial characteristics, gain mesenchymal features and show enhanced motility. Aberrant EMT has been closely associated with gastric carcinogenesis. *H. pylori* induce migration of the primary gastric epithelial cells [4], and enhance motility of the gastric epithelial cancer cell line AGS

as well as Madin–Darby canine kidney (MDCK) epithelial cells [5,6]. However, the precise molecular events that contribute in inducing motility and invasiveness of *H. pylori*-infected gastric cancer cells remain to be determined.

Crucial roles for E3 ubiquitin ligases have been recently identified in modulating cancer progression and metastasis for adenocarcinoma [7]. The really interesting new gene (RING) family E3 ubiquitin ligases regulate metastasis in several cancers [8] and have drawn attention as potential drug targets [9]. The seven in absentia homologue (Siah) proteins belong to the RING family of E3 ubiquitin ligases. Siah proteins impart specificity to proteasomal degradation of target proteins and are required for the ubiquitin-dependent proteolysis of their targets. Siah proteins interact with and regulate the stability of multiple factors involved in oncogenesis including prolyl hydroxylases, β -catenin, NUMB, tumour necrosis factor receptor 2-associated factor and Sprouty [10–14]. Increased Siah2 expression in various cancers signifies its oncogenic role [15–19]. Moreover, enhanced expression of Siah2 in breast, prostate and liver cancer cells is associated with malignancy and cancer invasiveness [15,16]. Wong *et al.* have shown that loss of Siah2 causes delayed tumour onset and increases the efficacy of chemotherapy in a transgenic model of aggressive breast cancer [20]. Elaborate studies have been performed to identify downstream targets of Siah2 proteins.

Abbreviations: *cag*, cytotoxin-associated gene; EBS, ETS2-binding site; EMT, epithelial–mesenchymal transition; ETS2, E26 transformation-specific sequence 2; GCCs, gastric cancer cells; HDAC1, histone-deacetylase 1; HIF1 α , hypoxia-inducible factor 1 α ; MOI, multiplicity of infection; PAI, pathogenicity island; real-time RT-PCR, real-time reverse transcription PCR; RING, really interesting new gene; Siah, the seven in absentia homologue; TBS, Twist1-binding site; Twist1, Twist-related protein 1.

¹ To whom correspondence should be addressed (email asima@niser.ac.in).

Recently Siah2 has been reported to regulate tight junction integrity and cell polarity in the hypoxic milieu through the regulation of apoptosis-stimulating proteins of p53 (ASPP) 2 stability [21]. Siah2 mediates ubiquitination and degradation of the CCAAT/enhancer-binding protein δ (C/EBP δ) during breast cancer progression, thus contributing to the transformation of breast tumour cells [22].

Siah2 up-regulation in breast cancer is caused by oestrogen which leads to the proteasomal degradation of the transcriptional co-regulator nuclear receptor corepressor (N-CoR) [23]. Although the exact mechanism is not known, Wnt5a has been found to induce Siah2 expression in colon cancer cells [24]. Hypoxia is another potent inducer of Siah2 [13] and it regulates Siah2 stability by modulating the p38 MAPK and Akt pathways [25,26]. Although independent studies have reported that Siah2 and *H. pylori* infection can induce stability and accumulation of the hypoxia-inducible factor 1 α (HIF1 α), a major oncogenic transcription factor induced during hypoxia [13,27], to date no study has identified the effect of *H. pylori* infection on gastric epithelial Siah2 expression.

Given the crucial role of Siah2 in driving cellular transformation and tumorigenesis in several human cancers, we examined the effect of *H. pylori* infection on Siah2 expression. We identified that proto-oncogenic transcription factors E26 transformation-specific sequence 2 (ETS2) and Twist-related protein 1 (Twist1) induce *siah2* in *H. pylori*-infected gastric cancer cells (GCCs) and also demonstrated that Siah2 regulates motility and invasiveness of infected GCCs. Our study thus established the role of Siah2 in regulating *H. pylori*-mediated gastric cancer progression. As human gastric cancer biopsy samples also showed highly-increased expression of Twist1 and ETS2 along with Siah2, these molecules could be tested as novel molecular targets to treat gastric cancer.

EXPERIMENTAL

Cell culture, *H. pylori* strains, infection and treatments

The human GCCs MKN45, Kato III, AGS along with *H. pylori* 26695 and 8-1, a *cag* PAI (+) strain (A.T.C.C.) and a *cag* PAI (-) strain, respectively, were cultured and maintained as reported previously [28,29]. Another *cag* PAI (-) strain D154 was received from the archived collection of *H. pylori* strains at National Institute of Cholera and enteric Diseases, Kolkata, India. Strain 8-1 is an isogenic derivative of the reference strain 26695 lacking the entire *cag* PAI [28] (DNA isolated from D154 does not produce any *cagA* or *cag* PAI amplicon). GCCs were infected with various multiplicity of infection (MOI) of *H. pylori* strain 26695 for specified periods. Strain 26695 was used for all studies except for comparison studies involving 26695, 8-1 and D154 strains. For inhibitor studies, cells were treated with the proteasome inhibitor MG132 (Sigma-Aldrich) at 50 μ M dose for 6 h prior to bacterial infection.

Human gastric mucosal biopsy specimen collection

Gastric biopsy samples from the antral gastric mucosa were collected from patients suffering from gastric cancer and undergoing diagnostic esophagogastroduodenoscopy following a National Institute of Science Education and Research (NISER) Review Board-approved protocol and research was carried out in accordance with the Declaration of Helsinki (2013) of the World Medical Association. Written informed consent was obtained from all patients prior to the study. Note that gastric

adenocarcinoma biopsy samples were obtained from patients lacking any previously established case-history. Because the gastric cancer samples were from patients that were urea breath test, rapid urease test as well as tissue-invasion negative, these adenocarcinoma cases could not be linked to *H. pylori* infection status.

Plasmids and mutagenesis

Twist1 overexpression construct was obtained as a kind gift from Dr Kimitoshi Kohno. ETS2 construct was purchased from Addgene (Addgene plasmid 28128). The Siah2 plasmid was purchased from Origene Technologies (Origene Technologies). The full length human *siah2* promoter (NM_005067) was cloned into the pGL3 basic vector (Promega) using restriction sites for KpnI and HindIII. *siah2* WT promoter construct was used as a template to generate individual mutations at the ETS2-binding site (EBS) and Twist1-binding site (TBS) using the QuikChange site-directed mutagenesis kit (Agilent Technologies) as per manufacturers' standard procedure. Sequencing was done to confirm mutations at the EBS and TBS. Primer sequences are shown in Supplementary Figure S1.

Transient transfection of plasmids or siRNAs and generation of stable cell lines

For transient expression of ETS2 and Twist1, 1×10^6 MKN45 cells were seeded in 6-well cell culture plates 24 h prior to transfection. Cells were transfected with 2 μ g of plasmid DNA and 10 μ l of Lipofectamine 2000 reagent (Invitrogen, CA, USA). Cells were infected after 36 h of transfection. To generate stable cell lines, MKN45 or AGS cells were seeded in 96-well plates 24 h before transfection and transfection was done as mentioned. Cells were cultured in the presence of 300 μ g/ml G418 (Sigma-Aldrich) for 4 weeks. Positive clones were picked using cloning discs (Sigma-Aldrich) and expanded to establish stable cell lines. To knockdown expression of ETS2 and Twist1, 0.2×10^6 MKN45 cells were seeded in 6-well cell culture plates 24 h prior to transfection. Cells were transfected with 50 nM of siRNA duplexes of ETS2 or Twist1 (Origene) along with 10 μ l of Lipofectamine 3000 reagent (Invitrogen). Control duplexes were also transfected. After 60 h of transfection, cells were infected with *H. pylori*.

In vitro binding assay

5' biotinylated double-stranded *siah2* EBS oligonucleotides [WT (wild-type) or Mut (mutant)] were captured by Streptavidin-coated superparamagnetic beads (Dynabeads M-280 Streptavidin, DYNAL, Invitrogen) and binding assays were performed using nuclear lysates as described previously [28]. Bound proteins were dissociated by boiling in $1 \times$ Laemmli sample buffer and analysed by Western blotting. Oligonucleotide sequences are shown in Supplementary Figure S1.

Luciferase assay

Activation of the *siah2* promoter after *H. pylori* infection was measured by dual luciferase assays. For this, cells were co-transfected with either the WT or ETS2 and Twist1-Mut *siah2* luciferase promoter constructs (cloned in pGL3 basic vector) along with the phRL-TK *Renilla* luciferase construct (Promega) at a ratio of 50:1 using Lipofectamine

2000 reagent (Invitrogen). For some experiments, cells were co-transfected with the WT *siah2* promoter construct along with the WT ETS2 or Twist1 overexpression plasmid and the phRL-TK *Renilla* luciferase construct at a ratio of 25:25:1 using Lipofectamine 2000 reagent (Invitrogen). At 36 h post-transfection, cells were either left uninfected or were infected with *H. pylori* for 2 h. Cells were thereafter lysed and luciferase activity was estimated using the Dual-Luciferase Reporter Assay System (Promega) as per manufacturers' instructions. Quantification of luminescence signal was done using *MicroBeta2 LumiJET™ Microplate Counter* (PerkinElmer).

MTT assay

pcDNA3.1⁺ and Siah2 overexpressing stable cells were seeded on 96-well microplates with a seeding density of 5×10^3 cells per well 24 h before transfection. Cell proliferation was assessed using an MTT cell proliferation kit according to the manufacturer's protocol (HiMedia). The absorbance was measured at 595 nm test and 650 nm reference wavelengths. Data were analysed by *t* test, and presented as mean \pm S.E.M., and confirmed by three independent experiments.

Transwell migration and invasion assays

Cell migration and invasion assays were performed using 8- μ m pore size Transwell Biocoat control inserts (migration assay) or matrigel-coated inserts, as per manufacture's instruction (Becton Dickinson). In brief, 5×10^4 AGS cells were seeded on a transwell plate. The chambers were incubated at 37°C, 5% CO₂. After incubating for 24 h, cells on the top surface of the transwell were scraped off. Cells were fixed for 30 min with 4% paraformaldehyde, and stained for 30 min with haematoxylin. We counted the number of cells (five high-power fields) that invaded inserts under an inverted microscope (Primo Vert, Carl Zeiss). Individual experiments were repeated thrice.

Soft agar assay

MKN45 cells stably expressing Siah2, ETS2 and Twist1 protein or empty vector were seeded in 24-well plates at a density of 0.1×10^6 cells per well. After 24 h cells were infected with *H. pylori* for 6 h followed by 2 h gentamicin treatment to kill extracellular bacteria. Cells were harvested and 1000 cells were mixed with 0.3% top agar and plated on to 0.6% bottom agar in 6 cm cell culture plates. These plates were fed twice weekly and maintained for 3 weeks in humidified incubators containing 5% CO₂. At the end of the incubation period, visible colonies on the top agar were directly counted and colony sizes were compared between various treatment groups.

Wound healing assay

We wanted to assess the effect of ETS2, Twist1 or Siah2 expression on wound-healing property of GCCs. As MKN45 cells are partly adherent and partly floating in nature [30], we did not consider these cells suitable for wound-healing assays. Rather, AGS cells being adherent cells were considered more appropriate for this purpose. Various stable cells were seeded in 6-well cell culture plates and were allowed to grow in monolayer till 90% confluency was obtained in complete media. Multiple uniform streaks were made on the monolayer culture with 100 μ l pipette tips. Streaked plates were immediately washed with

PBS to remove detached cells followed by infection with *H. pylori* in serum-free media. Cell migration was monitored up to 24 h, and pictures were taken at 0, 6, 12 and 24 h time points using a digital camera attached to an inverted microscope (Primo Vert, Carl Zeiss). Six to eight fields were analysed, and cells filling the wound mark were counted using ImageJ 1.45 software.

To study the effect of Siah2 suppression on wound healing property of GCCs, 0.5×10^6 AGS cells were seeded in 6-well cell culture plates 24 h prior to transfection of 50 nM of siRNA control or Siah2 duplex and 10 μ l of Lipofectamine 3000 reagent. Cells were infected and wound healing assay was performed after 48 h of transfection.

Statistical analysis

Statistical analysis of quantitative data was performed by Student's *t* tests. Values were given as mean \pm S.E.M. Statistical significance was determined at **P* < 0.05.

The online supplementary file contains additional EXPERIMENTAL methods that include immunoblotting, real-time RT (reverse transcription)-PCR, ChIP assay, immunofluorescence and confocal microscopy.

RESULTS

H. pylori induces Siah2 in cultured GCCs

To identify the effect of *H. pylori* infection on GCCs, MKN45 cells were infected with a *cag* PAI (+) *H. pylori* strain 26695 at a MOI of 100, 200 and 300 for 3 and 6 h. A representative Western blot result (*n* = 3) showed significant induction of Siah2 expression by *H. pylori* at 3 and 6 h post infection (p.i.) with MOI 200 and 300. Results further confirmed that at 6 h p.i., MOI 200 was equivalent to infection with MOI 300 for 6 h with respect to Siah2 induction (Figure 1A). Supplementary Figure S2(A) shows that MOI 200 at 6 h was optimum to induce Siah2 expression. Therefore, all future experiments were performed with MOI 200 with strain 26695 for 6 h to study Siah2 expression unless mentioned otherwise. Fluorescence microscopic images of uninfected cells and infected cells further confirmed *H. pylori* as a potent inducer of Siah2 (Supplementary Figure S2B). Confocal microscopy revealed that *H. pylori* substantially induced nuclear accumulation of Siah2 in the infected GCCs (Supplementary Figure S2C). Comparison of basal and p.i. expression of Siah2 at mRNA level (real-time RT-PCR) also showed significant increase in Siah2 expression after *H. pylori* infection (Figure 1B). As various GCCs could show difference in their protein expression pattern, we sought to determine whether MOI 200 was effective in inducing Siah2 in other GCCs. Western blot of the comparative study revealed that MOI 200 also induced Siah2 in Kato III and AGS cells (Figure 1C). There was an equivalent induction of Siah2 protein when MKN45 cells were infected with either 26695, 8-1 or D154 *H. pylori* strains indicating that Siah2 induction was not dependent on *cag* PAI status (Figure 1D).

ETS2 and Twist1 are induced in H. pylori-infected GCCs

In order to identify transcription factors regulating Siah2 expression, we performed promoter analysis for *siah2* using bioinformatics tools such as MatInspector (professional version 6.2.2). Although several transcription factor binding sites were implicated in the *siah2* promoter region, ETS2 and Twist1 showed very high probability of binding. The putative EBS

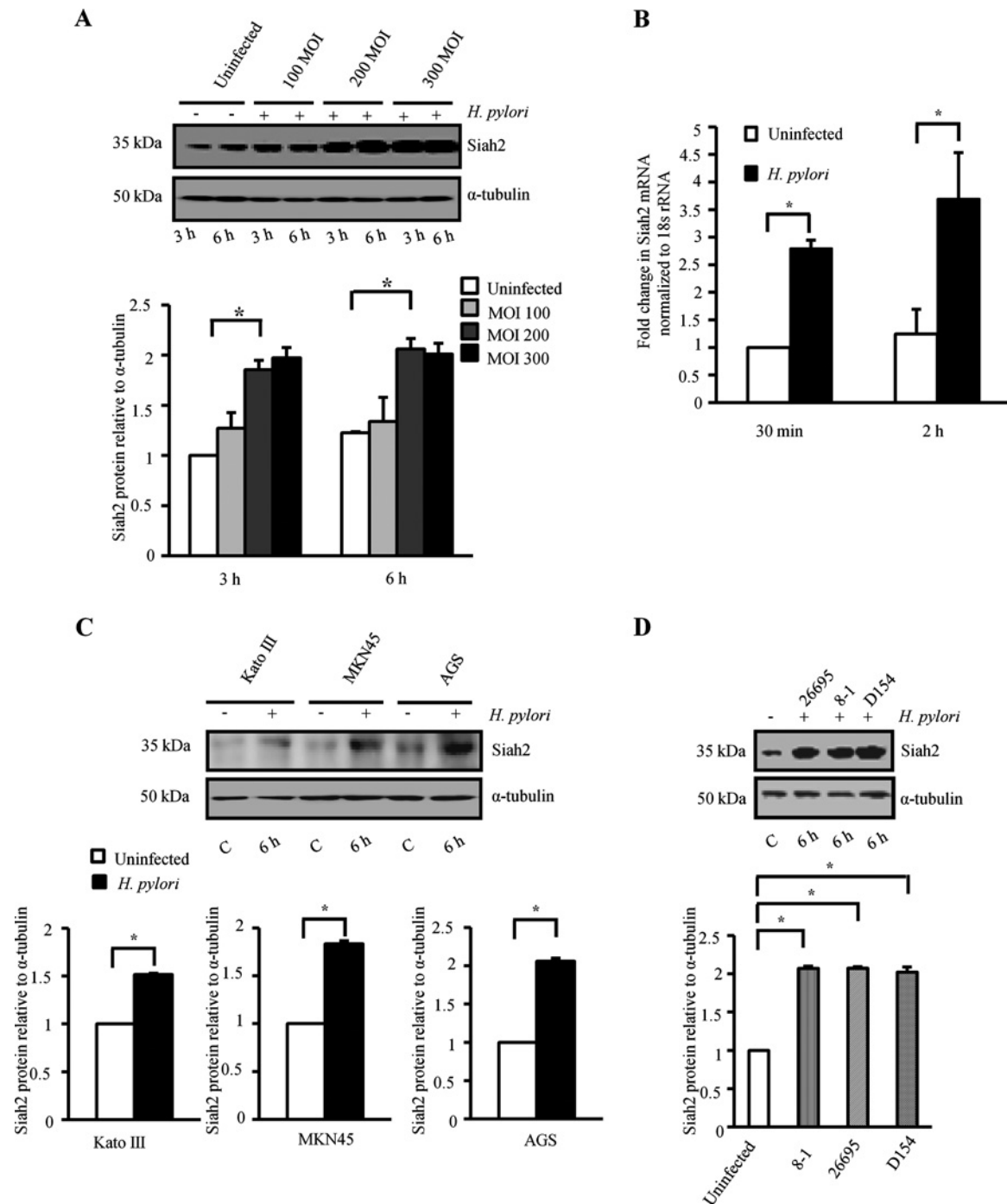


Figure 1 Siah2 is induced in *H. pylori*-infected GCCs

(A) A representative Western blot ($n=3$) of whole cell lysates prepared from uninfected and infected (3 and 6 h with MOI 100, 200 and 300) MKN45 cells shows Siah2 induction in infected GCCs. α -Tubulin was used as a loading control. A graphical representation of the data confirms that MOI 200 at 6 h is optimal in inducing Siah2. Bars depict normalized data (mean \pm S.E.M., $n=3$), $*P < 0.05$. (B) Siah2 expression in MKN45 cells at mRNA level as detected by real-time RT-PCR. Bars depict normalized data (mean \pm S.E.M., $n=3$), $*P < 0.05$. (C) A representative Western blot ($n=3$) shows Siah2 induction in Kato III, MKN45 and AGS cells after being infected with MOI 200 of *H. pylori* for 6 h. Bars shown below represent normalized data (mean \pm S.E.M., $n=3$), $*P < 0.05$. (D) Western blot results ($n=3$) showing expression of Siah2 in cell lysates prepared from uninfected or infected MKN45 cells. Strains of *H. pylori* used for the experiment were *cag* PAI (+) strain 26695, *cag* PAI (-) strains 8-1 and D154. Bars shown below represent normalized data (mean \pm S.E.M., $n=3$), $*P < 0.05$.

(GGAA/T) was between the -465 and -462 bp and TBS (CANNTG) was between the -431 and -426 bp upstream of the *siah2* transcription initiation site (Figure 2). We performed Western blot analysis to assess ETS2 expression at protein level in MKN45 cells infected with *H. pylori*. Although the optimal

time and dose for Siah2 expression were determined in Figure 1, we needed to identify the same for ETS2 and Twist1. A time-dependent study showed induced expression of ETS2 as early as 1 h p.i. and that was maintained at the same level even at 6 h p.i. whereas no ETS2 expression was noticed at any time point in

- 793 GCTTCGCCCT CTTCTCCTGC GTGCTGGTGA CTCAGCCCTG AGAAGAGAAA
 - 743 CCTCTCGGTT TTTTCCGACT AGTGACAGGG GCCTCCGCC CCGCCCTCGC
 - 693 CCGCCCGCGT CCGGTCCCAC CCACCGTCCA CGCTCCCGCC CCGCCTGAAG
 - 643 TTGCCTTTCT CGTTTGAGCT GAGGGACGCG TCAGCCAGGC ACCCCGGGGT
 - 593 GTGGCCAGAG GACTTCGGCG ACGCTTCCCC GAGAGTAGCC CCCCTCTCA
 - 543 ACCCAGAAAA GACAACCCCG CGGGGCTGCA GCGAGCCAGG CATGCTCACT
 - 493 GGCAGCAGCC CCGCCCGCAG CCCGAGCAEG AACGCCGGCC GCTAGGCGGC
 - 443 CCCCTGCGCT GCCAGCTGCA GCGGGCGGA GCCAGCGCCC CCGCGCAGGG
 - 393 TGGCTCTGCC AGTCCCGCG CGCCTGGGG GCGGCACACG TGTCAGGGC
 - 343 TCACGTCCGC GCGCGCCCC GGGGCTTGG TCAGCGGCTG TTCCAGAAGC
 - 293 GGGTGGGCCA GGGCTCTGCG CACCGCTGGG GTTCGGGGCC CGGGACGCCG
 - 243 CCGGGAGGAG GGCACCGCG GGGTCCGAC GCGGAGGCGT GCTCGGAACG
 - 193 CCGGGGGCTG CGGAGTGCAT CAGCGCGGTC CAGCCCTCCG CTGCCCCGGC
 - 143 GCCGAGCGTC TCCGCCGCC GACCTGGGC TGGCGCCGT GCGTTGCCCT
 - 93 CGGAGCTCGC TGCCCGCGGG GCGGCACCG CTTGACCCG GCGCGCCCCG
 - 43 CCGCAGGAG GCGCCCGCAG TTCCATGGTT GGTTCGGAGC GCGATG

Figure 2 Analysis of human *siah2* promoter. The EBS and TBS of the human *siah2* promoter are shown. The ATG start codon is underlined.

uninfected cells (Figure 3A). The same study also revealed that the expression of Twist1 was induced at 1 h p.i. and was maintained at the same level up to 3 h and decreased at 6 h. Dose-kinetics performed at 3 h and 6 h p.i. with MOI 100 and 200 clearly showed that 200 MOI was more effective in inducing ETS2 (Figure 3B) and Twist1 (Figure 3C) expression than MOI 100. We performed Western blotting on cell lysates prepared from other GCCs such as Kato III and AGS along with MKN45 cells at 3 h p.i. (MOI 200) to assess the expression of ETS2 and Twist1. Representative Western blots from independent experiments ($n = 3$) showed marked enhancement in ETS2 (Figure 3D) and Twist1 expression (Figure 3E) in all cell lines. We observed that strain 8-1 and strain D154 were equally effective in inducing ETS2 and Twist1 as strain 26695 (Figures 3F and 3G respectively). As we observed that although Twist1 was induced at 3 h of infection, the level of Twist1 at 6 h p.i. was equal to its basal expression level of either 3 or 6 h, we presumed that proteasomal degradation might have caused Twist1 degradation at 6 h of infection. Pretreatment of MKN45 cells with MG132 prior to *H. pylori* infection clearly rescued Twist1 protein from degradation indicating that ubiquitination-mediated proteasomal degradation of Twist1 was underway at 6 h p.i. (Figure 3H). Graphical representation of all data is shown in Supplementary Figure S3.

Antral biopsy samples obtained from consenting patients during gastric endoscopy were used to study expression of Twist1, ETS2 and Siah2 proteins in gastric adenocarcinoma. Fluorescence microscopic analysis of gastric biopsies from adenocarcinoma patients with samples from adjacent non-cancer gastric tissue samples revealed that Siah2 (Supplementary Figure S4A), ETS2 (Supplementary Figure S4B) and Twist1 (Supplementary Figure S4C) were highly increased in adenocarcinoma biopsy samples compared with non-cancer tissues.

ETS2 and Twist1 bind with *siah2* promoter in *H. pylori*-infected GCCs

Next we assessed ETS2 binding with the *siah2* EBS and TBS in uninfected and infected MKN45 cells. Nuclear extracts were prepared from 3 h *H. pylori*-infected (MOI 200) MKN45 cells. WT as well as EBS and TBS-Mut *siah2* promoter oligonucleotides (Supplementary Figure S1) were synthesized. Magnetic beads were coated with oligonucleotides just prior to incubation with nuclear lysates from infected and uninfected cells. Analysis of bead-bound proteins by Western blot determined binding of ETS2 with the *siah2* EBS (Figure 4A) and Twist1 with *siah2* TBS only after *H. pylori* infection (Figure 4B). Input nuclear lysates were also run to assess the expression of ETS2 (Figure 4A) and Twist1 (Figure 4B) in nuclear lysates and histone-deacetylase 1 (HDAC1) was used as a nuclear loading control. Results confirmed that both ETS2 and Twist1 were increased in the nuclear fraction by *H. pylori* infection. We did not detect any ETS2 expression in the uninfected cells whereas low level of Twist1 expression was observed in the nucleus of uninfected cells.

In order to detect binding of ETS2 and Twist1 to the *siah2* promoter *in vivo*, MKN45 cells were infected with MOI 200 of strain 26695 for 3 h and nuclear lysates were assessed by ChIP assay using ETS2 (Figure 4C) and Twist1 (Figure 4D) antibodies. The PCR products of DNA in these immunocomplexes corresponding to the *siah2* promoter flanking the EBS and TBS (S = specific PCR product), respectively, were not present in the PCR product corresponding to the 5' far upstream sequence (NS = non-specific PCR product).

ETS2 and Twist1 enhance Siah2 expression in *H. pylori*-infected GCCs

Dual luciferase assays were performed to assess the role of ETS2 and Twist1 in *H. pylori* infection-induced *siah2* transcription. MKN45 cells were first co-transfected with the *Renilla* luciferase construct phRLTK along with the WT or EBS or TBS-Mut *siah2*-reporter constructs followed by infection with *H. pylori* for 2 h. Significant enhancement of *siah2* transactivation was observed in the infected MKN45 cells expressing WT *siah2* luciferase constructs. The effect was significantly reduced in the EBS Mut (Figure 5A) or TBS Mut-expressing cells (Figure 5B) confirming that ETS2 and Twist1 mediate *siah2* transcription in the infected GCCs.

We next sought to determine the effect of ectopic expression of ETS2 and Twist1 on *siah2* transcription. For this, the empty vector or ETS2 overexpression plasmids were transfected along with the WT *siah2* promoter construct and the *Renilla* luciferase construct phRLTK followed by infection with *H. pylori* for 2 h (Figure 5C). Dual luciferase assay data confirmed that ETS2 significantly enhanced *H. pylori*-induced *siah2* transcription. Twist1 overexpression showed a similar inducing effect of Twist1 on *siah2* luciferase activity (Figure 5D). Western blot analysis further established that overexpression of ETS2 and Twist1 mediated induction of Siah2 protein expression in *H. pylori*-infected GCCs (Figures 5E and 5F respectively). We also noted that although Twist1 was highly induced in uninfected Twist1-expressing cells as compared with the infected pcDNA3.1⁺-expressing cells, Siah2 expression was lower in the first group which indicated the possibility of a post-translational modification of Twist1 only after infection with *H. pylori* that might be responsible for its activation.

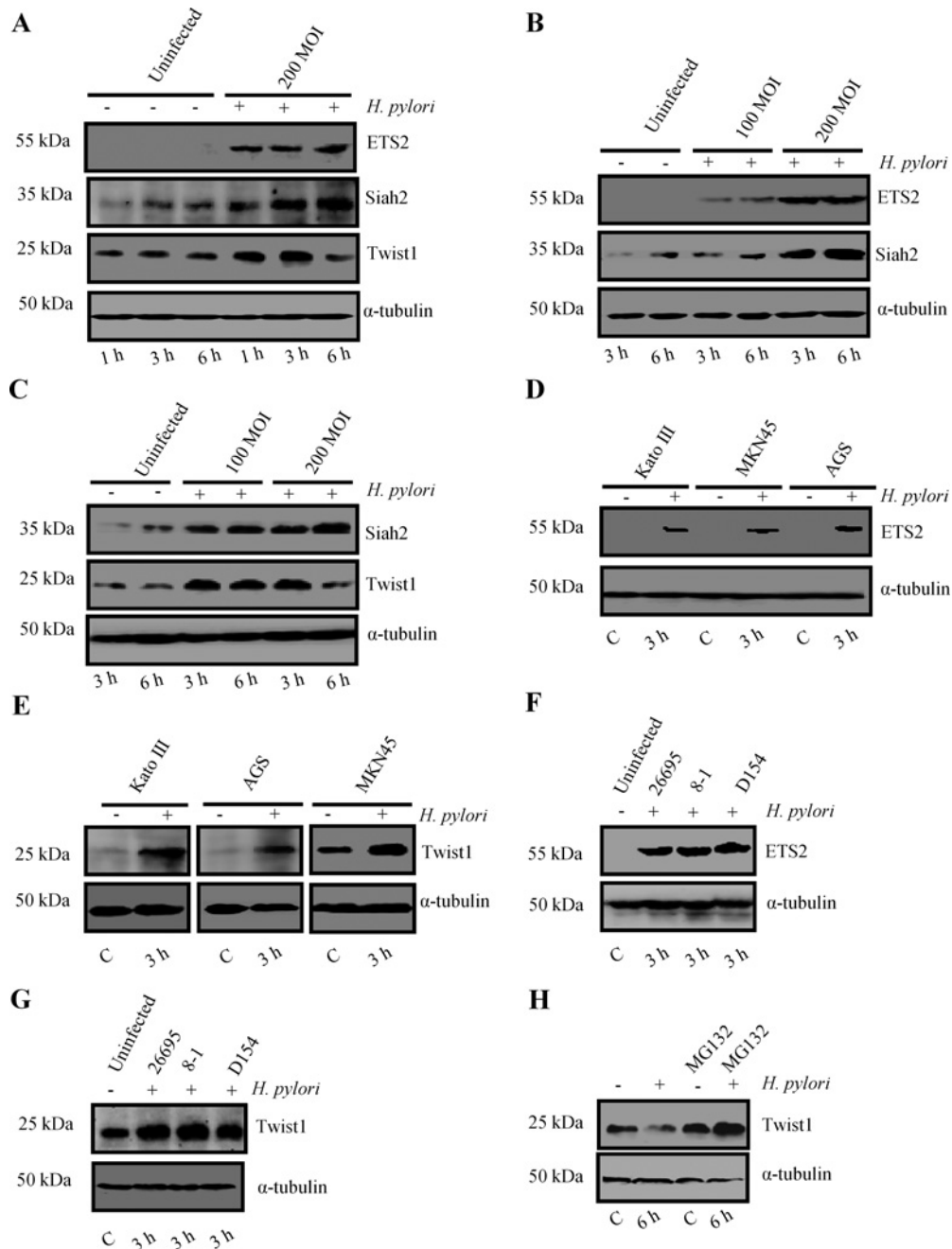


Figure 3 *H. pylori* infection induces ETS2, Twist1 and Siah2 expression in GCCs

(A) Time kinetics of ETS2, Twist1 and Siah2 expression in the infected MKN45 cells ($n=3$). (B) A representative Western blot shows that MOI 200 is more effective in inducing ETS2 and Siah2 than MOI 100 at both 3 h p.i. and 6 h p.i. ($n=3$). (C) Twist1 expression pattern at MOI 100 and 200 is compared at 100 and 200 MOI and at 3 and 6 h. (D) Assessment of ETS2 expression in Kato III, MKN45 and AGS cells by Western blot ($n=3$). (E) Twist1 expression pattern in Kato III, MKN45 and AGS cells ($n=3$). (F) Representative Western blots from independent experiments ($n=3$) shows that strain 8-1 and D154 were equally effective as strain 26695 in inducing ETS2 and (G) Twist1 ($n=3$). (H) Western blot ($n=4$) showing Twist1 expression in MKN45 cells treated with 50 μ M MG132 for 6 h prior to infection with MOI 200 of *H. pylori* for 6 h.

Siah2 induces migration and invasiveness of *H. pylori*-infected GCCs

H. pylori induce EMT in infected GCCs. In order to assess the effect of Siah2 overexpression on the migration ability of GCCs, we performed transwell migration and matrigel invasion assays. MKN45 cells are partially adherent and therefore, a more adherent gastric adenocarcinoma cell AGS was used to study the effect of

Siah2 expression on cell migration. The inhibitory effects of Siah2 siRNA on *H. pylori*-induced AGS cell migration and invasion were found to be significant over control siRNA-transfected cells (Figures 6A and 6B respectively). Exogenous overexpression of Siah2 in AGS cells significantly increased *H. pylori*-mediated cell migration and invasion (Figures 6C and 6D respectively). In addition, we performed wound-healing assays. pcDNA3.1⁺ or Siah2 stably-transfected AGS cells grown in monolayer were

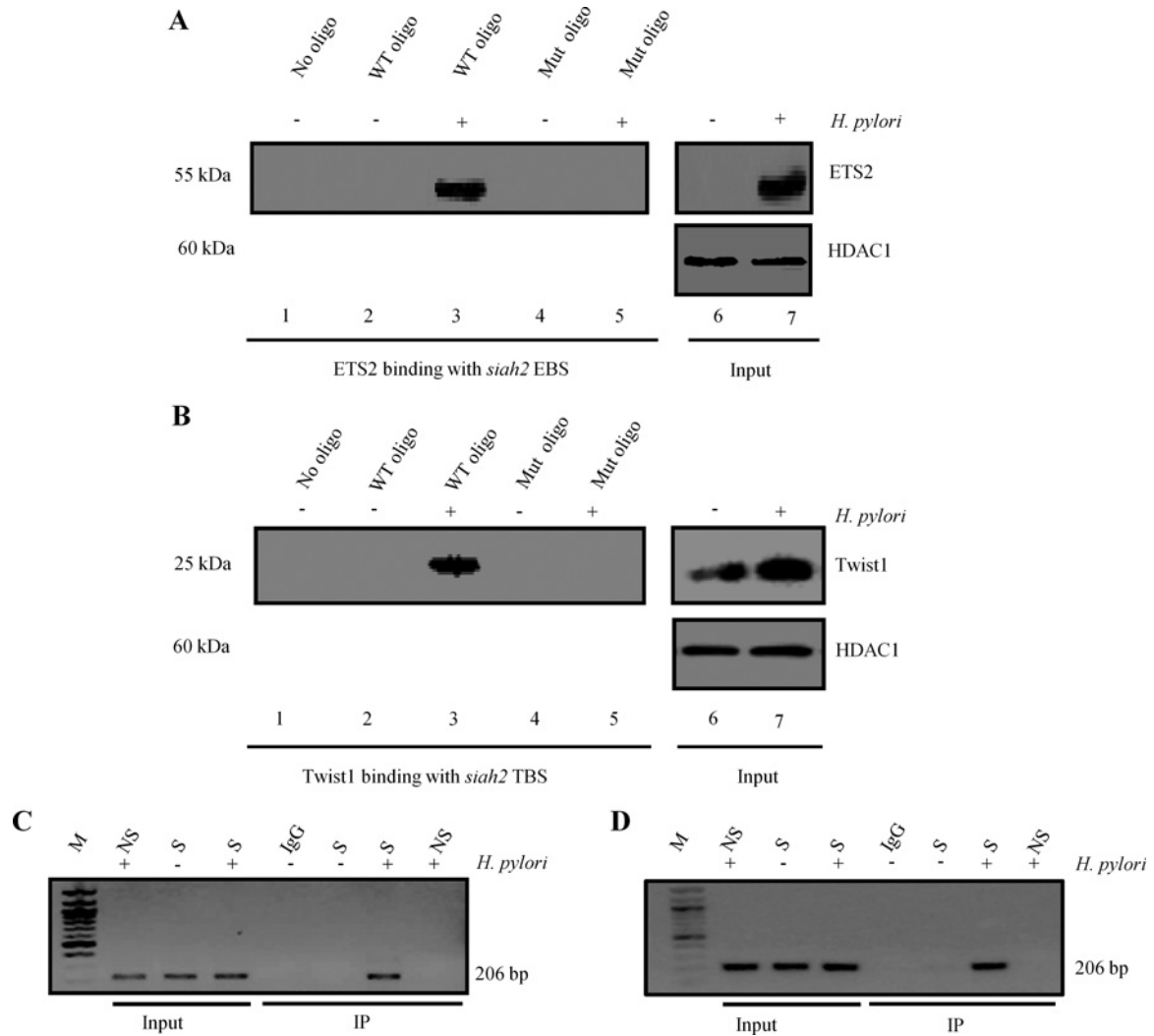


Figure 4 ETS2 and Twist1 bind to the *siah2* promoter in *H. pylori*-infected GCCs

(A) Western blot showing *H. pylori*-induced ETS2 binding with the *siah2* promoter ($n = 3$). ETS2 binds to the WT EBS only but not with the EBS-Mut oligo. Input lanes show expression of ETS2 in the nuclear lysates. HDAC1 is the loading control for nuclear lysates. (B) Western blot showing *H. pylori*-induced Twist1 binding with the *siah2* promoter ($n = 3$). Twist1 specifically binds to the WT TBS but not to the TBS-Mut oligo. Input lanes show expression of Twist1 in the nuclear lysates. (C) ChIP analysis of ETS2 immunocomplex for *siah2* EBS. (D) ChIP analysis of Twist1 immunocomplex for *siah2* TBS. IgG, immunoglobulin G; M, MW marker; NS, non-specific primer, S, specific primer.

used to prepare wound marks and cells were incubated in the presence or absence of *H. pylori*. Siah2-expressing *H. pylori*-infected AGS cells showed significantly higher migration than empty-vector-expressing infected cells (Supplementary Figures S5A and S5B) indicating that Siah2 induced cell migration ability of infected GCCs. The effect of Siah2 overexpression and *H. pylori* infection on AGS cell proliferation was tested by MTT assay. Siah2 overexpression significantly induced cell proliferation which was further induced by *H. pylori*, at 24 h of infection (Supplementary Figure S5C). Anchorage-independent growth, an additional indicator of more aggressive cancer cell behaviour, was evaluated by soft-agar colony formation assays. We found a substantial induction in colony formation by *H. pylori*-infected Siah2 stably-expressing MKN45 cells as compared with the uninfected empty-vector expressing cells (Supplementary Figure S5D). Siah2 protein expression status in the stable MKN45 cells used for the soft-agar assay is shown in the accompanying Western blot image (Supplementary Figure S5D).

ETS2- and Twist1-mediated induction of Siah2 migration and wound-healing properties of *H. pylori*-infected GCCs

Wound healing assay was performed to examine the involvement of ETS2 and Twist1 in *H. pylori*-mediated enhancement of GCC migration. For this, pcDNA3.1⁺, ETS2 or Twist1 stably-expressing AGS cells were used. Both ETS2- and Twist1-expressing cells showed significantly higher wound-healing properties following *H. pylori* infection compared with the pcDNA3.1⁺-expressing infected cells (Supplementary Figures S6A and S6B respectively). In order to assess the effect of ETS2 and Twist1 in *H. pylori*-mediated induction of cell invasion, we used stable-transfected cells. Our results confirmed that ETS2 and Twist1 dose-dependently induced colony formation ability of *H. pylori*-infected cells (Supplementary Figures S7A and S7B respectively). Accompanying Western blot images show ETS2 and Twist1 expression status in stable cells. To further ascertain the role of ETS2 and Twist1 in Siah2 expression we transfected MKN45 cells with ETS2 and Twist1 siRNAs along with control

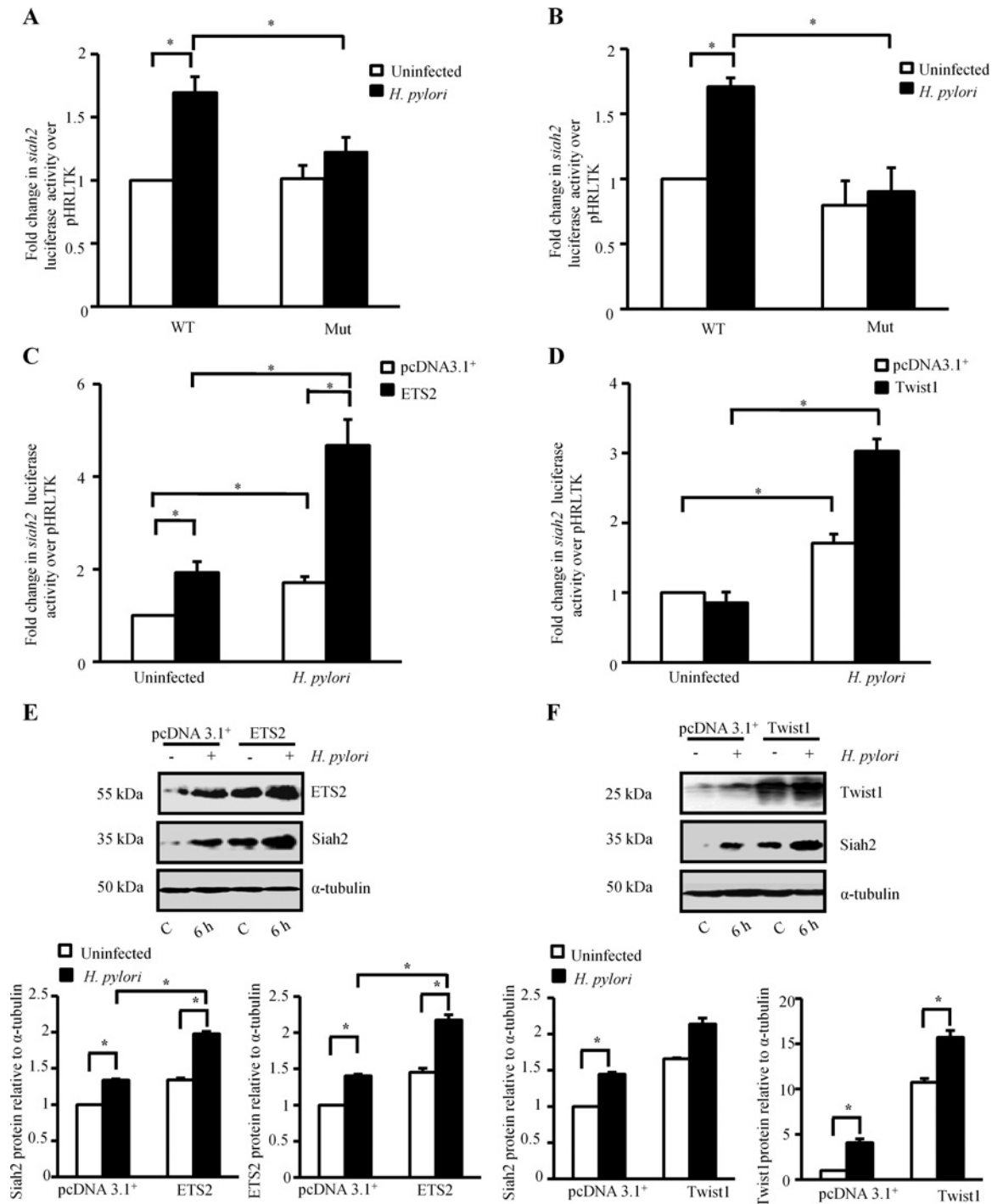


Figure 5 ETS2 and Twist1 enhance *siah2* transcription

(A) Bar graph of dual luciferase activities (mean \pm S.E.M., $n = 3$) driven by the WT and ETS2-Mut *siah2* promoters in MKN45 cells with or without *H. pylori* infection. $*P < 0.05$. (B) Bar graph of dual luciferase activities (mean \pm S.E.M., $n = 3$) to show the effect of Twist1 binding with the WT and Twist1-Mut *siah2* promoters in presence or absence of *H. pylori* infection in MKN45 cells. $*P < 0.05$. (C) Dual luciferase assay to show the effect of ectopically expressed ETS2 on the transcriptional activation of WT *siah2* promoter (mean \pm S.E.M., $n = 3$). $*P < 0.05$. (D) Dual luciferase assay showing the effect of ectopically expressed Twist1 on the WT *siah2* promoter luciferase activity (mean \pm S.E.M., $n = 3$). $*P < 0.05$. (E) Western blot analysis showing the effect of overexpression of ETS2 on Siah2 protein expression in *H. pylori*-infected GCCs. Bars below represent normalized data (mean \pm S.E.M., $n = 3$). $*P < 0.05$. (F) Western blotting shows the effect of Twist1 overexpression on Siah2 expression in *H. pylori*-infected GCCs. Bars depict normalized data (mean \pm S.E.M., $n = 3$). $*P < 0.05$.

duplex siRNA. Western blotting showed significant reduction in Siah2 expression in ETS2- and Twist1-suppressed and *H. pylori*-infected cells (Supplementary Figures S8A and S8B respectively). Next, we suppressed Siah2 in MKN45 cells to find out its role in *H. pylori*-mediated cell migration. Siah2-suppressed cells showed

significantly less wound-healing property following *H. pylori* infection compared with the control duplex-expressing infected cells (Supplementary Figure S8C). Accompanying Western blot results represent Siah2-suppression status in MKN45 cells used for the above experiment.

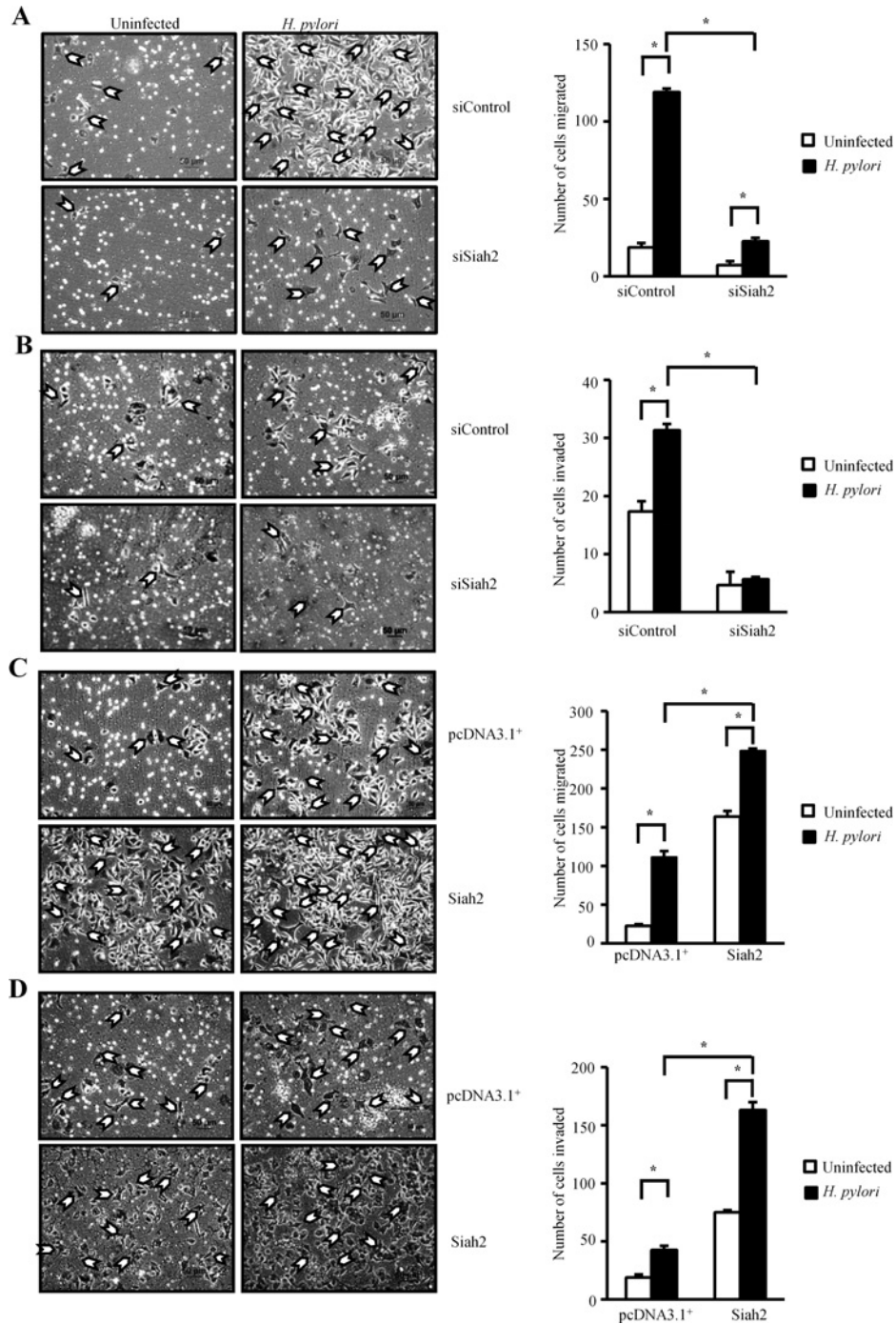


Figure 6 Siah2 increases migration and invasion property of *H. pylori*-infected GCCs

(A) Transwell migration assay using siControl and siSiah2-transfected AGS cells ($n = 3$). Cells were seeded in serum-free media on to the upper chamber of Transwell. After 24 h of infection (with or without *H. pylori*), migrated cells at the lower surface of the membrane were stained with haematoxylin and counted. Imaging was done using an inverted microscope. Scale shown = 50 μm . Bars represent number of cells migrated from three independent experiments (mean \pm S.E.M.). * $P < 0.05$. (B) Results of Transwell invasion assay on the Siah2 siRNA and siControl expressed AGS cells (infected with or without *H. pylori*). Cells were seeded on the upper chamber of the matrigel-precoated Transwell. Cells were allowed to invade through the membrane for 24 h. Invaded cells were counted from three independent experiments. Scale shown = 50 μm . Bar graph represents the average number of invaded cells (mean \pm S.E.M.). * $P < 0.05$. (C) Transwell migration was performed using empty vector and Siah2-overexpressing infected and uninfected AGS cells following procedures mentioned in Figure 6A. Scale shown = 50 μm . Bars represent (mean \pm S.E.M.). * $P < 0.05$. (D) Cell invasiveness was measured using empty vector and Siah2-overexpressing AGS cells with or without infection as explained in Figure 6B. Scale shown = 50 μm . Bar graph represents the average number of invaded cells (mean \pm S.E.M.). * $P < 0.05$.

Taken together, our results consistently proved that ETS2- and Twist1-regulated induction of Siah2 had a significant positive effect on *H. pylori*-mediated enhancement of GCC migration and invasiveness.

DISCUSSION

Gastric cancer is one of the prime causes of mortality in the developing as well as in the industrialized world. The major contributor in this disease-associated mortality is metastasis which presents either with peritoneal dissemination or haematogenous spread to the liver and lungs. Therefore, understanding the mechanisms regulating gastric cancer progression and metastasis is imperative for the development of effective treatment strategies. We observed Siah2 induction in *H. pylori*-infected GCCs and identified ETS2 and Twist1 as two novel inducers of Siah2. Further, Siah2 was established as an inducer of motility and invasiveness of infected GCCs. Consistent with our *in vitro* data, gastric cancer biopsy samples collected from metastatic gastric tumours (stage III) showed marked induction of ETS2, Twist1 and Siah2 expression. Although all tissue samples analysed (see Experimental section) were from urease-negative patients (suggesting absence of *H. pylori* when biopsies were obtained), it is intriguing to speculate that alterations in Siah2 expression due to initial *H. pylori* infection may contribute to the development of gastric cancer. Moreover, our observations indicate that Siah2 along with ETS2 and Twist1 may represent promising therapeutic targets for the treatment of gastric cancer.

The metastasis promoting role of Twist1 was reported in various cancers [20,31] including gastric carcinoma [32]. Although, enhancement of lymph node metastasis and distant metastasis were observed with Twist1 induction in GCCs [33], ETS2 had been associated with increased apoptosis or tumour suppression in GCCs [34] and suppression of lung cancer [35]. These results are quite surprising considering the fact that members of the ETS-family of transcription factors are effectors of the RAS/ERK proto-oncogenic pathway [36]. ETS2 was known to be associated with c-Myc induction [37] and angiogenesis in breast cancer cells [38]. Very high expression of ETS2 along with other ETS family proteins was found to be required for the neoplastic transformation of thyroid cancer cells [39], progression of prostate [40] and colon cancer [41]. Although Ras was known to be induced in *H. pylori*-infected gastric epithelial AGS cells [42], we do not know yet whether it is involved in *H. pylori*-induced ETS2 expression in GCCs.

The speed of cancer metastasis is accelerated if any or all of the processes that take place during EMT, for example, cell migration and invasion, alteration in cell adhesion, intravasation and extravasation occur with increased rate. The EMT is regulated by a diverse set of growth factors and transcription factors including the HIF1 α [43]. Recently Siah proteins were identified as important enhancers of breast cancer [19] and hepatocellular malignancy [15]. Increased metastasis of mouse melanoma [17], prostate cancer [16] and lung cancer [18] has also been associated with enhanced Siah2 expression. Moreover, Siah2 was found responsible for disruption of the tight junction integrity and cell polarity in hypoxic bone-osteosarcoma cells by degrading the tumour suppressor protein apoptosis-stimulating proteins of p53-2 (ASPP2) [21]. For some time now, *H. pylori* is known to increase cell motility [4,44]. However, Siah2-mediated enhancement of motility in *H. pylori*-infected GCCs is so far unknown. Our study suggests that Siah2 has a significant role in gastric cancer metastasis. Whether Siah2 is important or not in determining the stage and progression of the disease requires further research.

H. pylori-mediated changes in the GCC morphology and invasiveness, events that play crucial roles in enhancing gastric cancer metastasis, were found to be mediated by defects induced in the apical-junctional complexes; activation of β -catenin and its enhanced nuclear accumulation [45] as well as down-regulation of E-cadherin [46]. Bebb *et al.* [47] reported *H. pylori*-mediated disruption of the adherens junction. They found that acute *H. pylori* infection-mediated disruption of the β -catenin was not dependent on the *cag* PAI status. We also confirmed that *siah2* induction by ETS2 and Twist1 in infected GCCs was independent of the *cag* PAI. We presume that some *cag*-independent virulence factors induce ETS2 and Twist1. Other than *cag* PAI, the blood group antigen-binding adhesion *babA* and the vacuolating cytotoxin *vacA* are the two other genes highly associated with gastric cancer risk. Unlike 26695 and 8-1 (both *vacA* s1/m1 strains), D154 has *vacA* s2/m2 genotype. Effects of *babA* and *vacA* on the epithelial expression of ETS2, Twist1 and Siah2 need to be determined by using respective isogenic and non-isogenic mutants. Nuclear accumulation of Siah2 was recently associated with the majority of hepatic cell carcinomas (HCCs) and was correlated with induced hepatic cell proliferation, tumour progression and distant metastasis [15]. We found very high nuclear accumulation of Siah2 in *H. pylori*-infected GCCs, which we surmise, could be regulated by posttranslational modifications of Siah2 which are currently being investigated by our group.

GCC responses to *H. pylori* infection are presented with contradictory effects. For example, *H. pylori* induce both apoptosis and anti-apoptotic events [29,48]. We observed up-regulated GCC proliferation under the influence of *H. pylori* in the present study whereas induction of apoptosis was earlier noted [29]. Increased apoptosis induced by *H. pylori* has been strongly believed to act as a stimulus for continued cell proliferation resulting in neoplastic changes [49,50]. Unfortunately, the mechanism is still not clearly understood. At this point, we find this missing link as a very important area of research and would pursue more studies to understand how exactly *H. pylori*-mediated apoptosis helps in promoting gastric epithelial cell proliferation and promotes gastric carcinogenesis. Cells undergoing EMT may become less responsive to apoptosis. It is not yet known what role Siah2 plays in GCC apoptosis. It is also not known whether gastric cancer chemoresistance is controlled by Siah2 or not. However, as we identified that *H. pylori*-mediated Siah2 induction contributed to EMT properties in the infected GCCs, this mechanism could be explored further for therapeutic possibilities. Once thought as very effective anticancer agents, the proteasomal inhibitors showed severe cytotoxicity, inhibition of apoptosis and increased treatment resistance [51,52]. Since, Siah2 could be specifically targeted by RNA interference (RNAi) sparing other ubiquitin ligases including Siah1, untoward side effects during treatment could possibly be avoided.

Collectively, our data represent a novel model of Siah2-mediated induction of cell invasion and motility in *H. pylori*-infected gastric epithelial cancer cells providing a major conceptual advancement in our understanding of the mechanism of Siah2 induction in *H. pylori*-infected GCCs. Since Siah2 induces metastasis associated with *H. pylori* infection, it could be targeted for therapy. The present study also indicates that Siah2, ETS2 and Twist1 might have prognostic significance in *H. pylori*-mediated gastric cancer.

AUTHOR CONTRIBUTION

Lopamudra Das performed experiments and analysed data; Shrikant Babanrao Kokate performed wound-healing and soft agar assays; Suvasmita Rath did confocal microscopy; Niranjan Rout and Shivaram Prasad Singh helped with gastric cancer biopsy collection

and analysis; Asish Mukhopadhyay provided a crucial reagent; Sheila Crowe gave expert comments; Asima Bhattacharyya conceived the work, designed experiments, analysed the data, supervised the work and wrote the paper.

FUNDING

This work was supported by the Department of Biotechnology, Govt. of India [grant number BT/PR15092/GBD/27/311/2011 (to A.B.)]; the Science and Engineering Research Board, Government of India [grant number SB/SO/BB-0015/2014 (to A.B.)]; the Indian Council of Medical Research fellowship [grant number 3/1/3/JRF-2010/HRD-94 (Roll- 41439) (to S.R.)]; and NISER fellowship, Department of Atomic Energy, Government of India (to L.D. and S.B.K.).

REFERENCES

- Jemal, A., Siegel, R., Ward, E., Hao, Y., Xu, J., Murray, T. and Thun, M.J. (2008) Cancer statistics, 2008. *CA Cancer J. Clin.* **58**, 71–96 [CrossRef PubMed](#)
- Tsugane, S. and Sasazuki, S. (2007) Diet and the risk of gastric cancer: review of epidemiological evidence. *Gastric Cancer* **10**, 75–83 [CrossRef PubMed](#)
- Bessede, E., Staedel, C., Acuna Amador, L.A., Nguyen, P.H., Chambonnier, L., Hatakeyama, M., Belleanne, G., Megraud, F. and Varon, C. (2013) *Helicobacter pylori* generates cells with cancer stem cell properties via epithelial-mesenchymal transition-like changes. *Oncogene* **33**, 4123–4131 [CrossRef PubMed](#)
- Krueger, S., Hundertmark, T., Kuester, D., Kalinski, T., Peitz, U. and Roessner, A. (2007) *Helicobacter pylori* alters the distribution of ZO-1 and p120ctn in primary human gastric epithelial cells. *Pathol. Res. Pract.* **203**, 433–444 [CrossRef PubMed](#)
- Amieva, M.R., Vogelmann, R., Covacci, A., Tompkins, L.S., Nelson, W.J. and Falkow, S. (2003) Disruption of the epithelial apical-junctional complex by *Helicobacter pylori* CagA. *Science* **300**, 1430–1434 [CrossRef PubMed](#)
- Churin, Y., Al-Ghoul, L., Kepp, O., Meyer, T.F., Birchmeier, W. and Naumann, M. (2003) *Helicobacter pylori* CagA protein targets the c-Met receptor and enhances the mitogenic response. *J. Cell Biol.* **161**, 249–255 [CrossRef PubMed](#)
- Pavlidis, S.C., Huang, K.T., Reid, D.A., Wu, L., Blank, S.V., Mittal, K., Guo, L., Rothenberg, E., Rueda, B., Cardozo, T. and Gold, L.I. (2013) Inhibitors of SCF-Skp2/Cks1 E3 ligase block estrogen-induced growth stimulation and degradation of nuclear p27kip1: therapeutic potential for endometrial cancer. *Endocrinology* **154**, 4030–4045 [CrossRef PubMed](#)
- Lipkowitz, S. and Weissman, A.M. (2011) RINGs of good and evil: RING finger ubiquitin ligases at the crossroads of tumour suppression and oncogenesis. *Nat. Rev. Cancer* **11**, 629–643 [CrossRef PubMed](#)
- Shen, M., Schmitt, S., Buac, D. and Dou, Q.P. (2013) Targeting the ubiquitin-proteasome system for cancer therapy. *Expert Opin. Ther. Targets* **17**, 1091–1108 [CrossRef PubMed](#)
- Habelhah, H., Frew, I.J., Laine, A., Janes, P.W., Relaix, F., Sassoon, D., Bowtell, D.D. and Ronai, Z. (2002) Stress-induced decrease in TRAF2 stability is mediated by Siah2. *EMBO J.* **21**, 5765–5765 [CrossRef PubMed](#)
- Matsuzawa, S.I. and Reed, J.C. (2001) Siah-1, SIP, and Ebi collaborate in a novel pathway for beta-catenin degradation linked to p53 responses. *Mol. Cell* **7**, 915–926 [CrossRef PubMed](#)
- Nadeau, R.J., Toher, J.L., Yang, X., Kovalenko, D. and Friesel, R. (2007) Regulation of Sprouty2 stability by mammalian Seven-in-Absentia homolog 2. *J. Cell. Biochem.* **100**, 151–160 [CrossRef PubMed](#)
- Nakayama, K., Frew, I.J., Hagensen, M., Skals, M., Habelhah, H., Bhoumik, A., Kadoya, T., Erdjument-Bromage, H., Tempst, P., Frappell, P.B. et al. (2004) Siah2 regulates stability of prolyl-hydroxylases, controls HIF1alpha abundance, and modulates physiological responses to hypoxia. *Cell* **117**, 941–952 [CrossRef PubMed](#)
- Susini, L., Passer, B.J., Amzallag-Elbaz, N., Juven-Gershon, T., Prieur, S., Privat, N., Tuynder, M., Gendron, M.C., Israel, A., Amson, R. et al. (2001) Siah-1 binds and regulates the function of Numb. *Proc. Natl. Acad. Sci. U.S.A.* **98**, 15067–15072 [CrossRef PubMed](#)
- Malz, M., Aulmann, A., Samarini, J., Bissinger, M., Longerich, T., Schmitt, S., Schirmacher, P. and Breuhahn, K. (2012) Nuclear accumulation of seven in absentia homologue-2 supports motility and proliferation of liver cancer cells. *Int. J. Cancer* **131**, 2016–2026 [CrossRef PubMed](#)
- Qi, J., Nakayama, K., Cardiff, R.D., Borowsky, A.D., Kaul, K., Williams, R., Krajewski, S., Mercola, D., Carpenter, P.M., Bowtell, D. and Ronai, Z.A. (2010) Siah2-dependent concerted activity of HIF and FoxA2 regulates formation of neuroendocrine phenotype and neuroendocrine prostate tumors. *Cancer Cell* **18**, 23–38 [CrossRef PubMed](#)
- Qi, J., Nakayama, K., Gaitonde, S., Goydos, J.S., Krajewski, S., Eroshkin, A., Bar-Sagi, D., Bowtell, D. and Ronai, Z. (2008) The ubiquitin ligase Siah2 regulates tumorigenesis and metastasis by HIF-dependent and -independent pathways. *Proc. Natl. Acad. Sci. U.S.A.* **105**, 16713–16718 [CrossRef PubMed](#)
- Ahmed, A.U., Schmidt, R.L., Park, C.H., Reed, N.R., Hesse, S.E., Thomas, C.F., Molina, J.R., Deschamps, C., Yang, P., Aubry, M.C. and Tang, A.H. (2008) Effect of disrupting seven-in-absentia homolog 2 function on lung cancer cell growth. *J. Natl. Cancer Inst.* **100**, 1606–1629 [CrossRef PubMed](#)
- Chan, P., Moller, A., Liu, M.C., Sceneay, J.E., Wong, C.S., Waddell, N., Huang, K.T., Dobrovic, A., Millar, E. K., O'Toole, S.A. et al. (2011) The expression of the ubiquitin ligase SIAH2 (seven in absentia homolog 2) is mediated through gene copy number in breast cancer and is associated with a basal-like phenotype and p53 expression. *Breast Cancer Res.* **13**, R19 [CrossRef PubMed](#)
- Shiota, M., Zardan, A., Takeuchi, A., Kumano, M., Beraldi, E., Naito, S., Zoubeidi, A. and Gleave, M.E. (2012) Clusterin mediates TGF-beta-induced epithelial-mesenchymal transition and metastasis via Twist1 in prostate cancer cells. *Cancer Res.* **72**, 5261–5272 [CrossRef PubMed](#)
- Kim, H., Claps, G., Moller, A., Bowtell, D., Lu, X. and Ronai, Z.A. (2014) Siah2 regulates tight junction integrity and cell polarity through control of ASP2 stability. *Oncogene* **33**, 2004–2010 [CrossRef PubMed](#)
- Sarkar, T.R., Sharan, S., Wang, J., Pawar, S.A., Cantwell, C.A., Johnson, P.F., Morrison, D.K., Wang, J.M. and Sternecke, E. (2012) Identification of a Src tyrosine kinase/SIAH2 E3 ubiquitin ligase pathway that regulates C/EBPdelta expression and contributes to transformation of breast tumor cells. *Mol. Cell. Biol.* **32**, 320–332 [CrossRef PubMed](#)
- Frasor, J., Danes, J.M., Funk, C.C. and Katzenellenbogen, B.S. (2005) Estrogen down-regulation of the corepressor N-CoR: mechanism and implications for estrogen derepression of N-CoR-regulated genes. *Proc. Natl. Acad. Sci. U.S.A.* **102**, 13153–13157 [CrossRef PubMed](#)
- MacLeod, R.J., Hayes, M. and Pacheco, I. (2007) Wnt5a secretion stimulated by the extracellular calcium-sensing receptor inhibits defective Wnt signaling in colon cancer cells. *Am. J. Physiol. Gastrointest. Liver Physiol.* **293**, G403–G411 [CrossRef PubMed](#)
- Jing, Y., Liu, L.Z., Jiang, Y., Zhu, Y., Guo, N.L., Barnett, J., Rojanasakul, Y., Agani, F. and Jiang, B.H. (2012) Cadmium increases HIF-1 and VEGF expression through ROS, ERK, and AKT signaling pathways and induces malignant transformation of human bronchial epithelial cells. *Toxicol. Sci.* **125**, 10–19 [CrossRef PubMed](#)
- Mo, C., Dai, Y., Kang, N., Cui, L. and He, W. (2012) Ectopic expression of human MutS homologue 2 on renal carcinoma cells is induced by oxidative stress with interleukin-18 promotion via p38 mitogen-activated protein kinase (MAPK) and c-Jun N-terminal kinase (JNK) signaling pathways. *J. Biol. Chem.* **287**, 19242–19254 [CrossRef PubMed](#)
- Bhattacharyya, A., Chattopadhyay, R., Hall, E.H., Mebrahtu, S.T., Ernst, P.B. and Crowe, S.E. (2010) Mechanism of hypoxia-inducible factor 1 alpha-mediated Mcl1 regulation in *Helicobacter pylori*-infected human gastric epithelium. *Am. J. Physiol. Gastrointest. Liver Physiol.* **299**, G1177–G1186 [CrossRef PubMed](#)
- Bhattacharyya, A., Chattopadhyay, R., Burnette, B.R., Cross, J.V., Mitra, S., Ernst, P.B., Bhakal, K.K. and Crowe, S.E. (2009) Acetylation of apurinic/aprimidinic endonuclease-1 regulates *Helicobacter pylori*-mediated gastric epithelial cell apoptosis. *Gastroenterology* **136**, 2258–2269 [CrossRef PubMed](#)
- Rath, S., Das, L., Kokate, S.B., Pratheek, B.M., Chattopadhyay, S., Goswami, C., Chattopadhyay, R., Crowe, S.E. and Bhattacharyya, A. (2015) Regulation of Noxa-mediated apoptosis in *Helicobacter pylori*-infected gastric epithelial cells. *FASEB J.* **29**, 796–806 [CrossRef PubMed](#)
- Sekiguchi, M. and Suzuki, T. (1994) 11 – gastric tumor cell lines. In *Atlas of Human Tumor Cell Lines* (Hay, R.K.M., Park, J.-G.B. and Gazdar, A., eds), pp. 287–316, Academic Press, San Diego [CrossRef](#)
- Croset, M., Goehrig, D., Frackowiak, A., Bonnelye, E., Ansieau, S., Puisieux, A. and Clezardin, P. (2014) TWIST1 expression in breast cancer cells facilitates bone metastasis formation. *J. Bone Miner. Res.* **29**, 1886–1899 [CrossRef PubMed](#)
- Yang, Z., Zhang, X., Gang, H., Li, X., Li, Z., Wang, T., Han, J., Luo, T., Wen, F. and Wu, X. (2007) Up-regulation of gastric cancer cell invasion by Twist is accompanied by N-cadherin and fibronectin expression. *Biochem. Biophys. Res. Commun.* **358**, 925–930 [CrossRef PubMed](#)
- Ru, G.Q., Wang, H.J., Xu, W.J. and Zhao, Z.S. (2011) Upregulation of Twist in gastric carcinoma associated with tumor invasion and poor prognosis. *Pathol. Oncol. Res.* **17**, 341–347 [CrossRef PubMed](#)
- Liao, Y.L., Hu, L.Y., Tsai, K.W., Wu, C.W., Chan, W.C., Li, S.C., Lai, C.H., Ho, M.R., Fang, W.L., Huang, K.H. and Lin, W.C. (2012) Transcriptional regulation of miR-196b by ETS2 in gastric cancer cells. *Carcinogenesis* **33**, 760–769 [CrossRef PubMed](#)
- Kabbout, M., Garcia, M.M., Fujimoto, J., Liu, D.D., Woods, D., Chow, C.W., Mendoza, G., Momin, A.A., James, B.P., Solis, L. et al. (2013) ETS2 mediated tumor suppressive function and MET oncogene inhibition in human non-small cell lung cancer. *Clin. Cancer Res.* **19**, 3383–3395 [CrossRef PubMed](#)
- Kabbout, M., Dakhallah, D., Sharma, S., Bronisz, A., Srinivasan, R., Piper, M., Marsh, C.B. and Ostrowski, M.C. (2014) MicroRNA 17–92 cluster mediates ETS1 and ETS2-dependent RAS-oncogenic transformation. *PLoS One* **9**, e100693 [CrossRef PubMed](#)

- 37 Al-azawi, D., Ilroy, M.M., Kelly, G., Redmond, A.M., Bane, F.T., Cocchiglia, S., Hill, A.D. and Young, L.S. (2008) Ets-2 and p160 proteins collaborate to regulate c-Myc in endocrine resistant breast cancer. *Oncogene* **27**, 3021–3031 [CrossRef PubMed](#)
- 38 Zabuawala, T., Taffany, D.A., Sharma, S.M., Merchant, A., Adair, B., Srinivasan, R., Rosol, T.J., Fernandez, S., Huang, K., Leone, G. and Ostrowski, M.C. (2010) An ets2-driven transcriptional program in tumor-associated macrophages promotes tumor metastasis. *Cancer Res.* **70**, 1323–1333 [CrossRef PubMed](#)
- 39 de Nigris, F., Mega, T., Berger, N., Barone, M.V., Santoro, M., Viglietto, G., Verde, P. and Fusco, A. (2001) Induction of ETS-1 and ETS-2 transcription factors is required for thyroid cell transformation. *Cancer Res.* **61**, 2267–2275 [PubMed](#)
- 40 Carbone, G.M., Napoli, S., Valentini, A., Cavalli, F., Watson, D.K. and Catapano, C.V. (2004) Triplex DNA-mediated downregulation of Ets2 expression results in growth inhibition and apoptosis in human prostate cancer cells. *Nucleic Acids Res.* **32**, 4358–4367 [CrossRef PubMed](#)
- 41 Flavin, P., Redmond, A., McBryan, J., Cocchiglia, S., Tibbitts, P., Fahy-Browne, P., Kay, E., Treumann, A., Perrem, K., McLlroy, M. et al. (2011) RuvB12 cooperates with Ets2 to transcriptionally regulate hTERT in colon cancer. *FEBS Lett* **585**, 2537–2544 [CrossRef PubMed](#)
- 42 Cho, S.O., Lim, J.W., Kim, K.H. and Kim, H. (2010) Involvement of Ras and AP-1 in *Helicobacter pylori*-induced expression of COX-2 and iNOS in gastric epithelial AGS cells. *Dig. Dis. Sci.* **55**, 988–996 [CrossRef PubMed](#)
- 43 Hanahan, D. and Weinberg, R.A. (2011) Hallmarks of cancer: the next generation. *Cell* **144**, 646–674 [CrossRef PubMed](#)
- 44 Moese, S., Selbach, M., Kwok, T., Brinkmann, V., Konig, W., Meyer, T.F. and Backert, S. (2004) *Helicobacter pylori* induces AGS cell motility and elongation via independent signaling pathways. *Infect. Immun.* **72**, 3646–3649 [CrossRef PubMed](#)
- 45 Vogelmann, R., Amieva, M.R., Falkow, S. and Nelson, W.J. (2004) Breaking into the epithelial apical-junctional complex—news from pathogen hackers. *Curr. Opin. Cell Biol.* **16**, 86–93 [CrossRef PubMed](#)
- 46 Terres, A.M., Pajares, J.M., O'Toole, D., Ahern, S. and Kelleher, D. (1998) *H. pylori* infection is associated with downregulation of E-cadherin, a molecule involved in epithelial cell adhesion and proliferation control. *J. Clin. Pathol.* **51**, 410–412 [CrossRef PubMed](#)
- 47 Bebb, J.R., Leach, L., Zaitoun, A., Hand, N., Letley, D.P., Thomas, R. and Atherton, J. C. (2006) Effects of *Helicobacter pylori* on the cadherin-catenin complex. *J. Clin. Pathol.* **59**, 1261–1266 [CrossRef PubMed](#)
- 48 Yanai, A., Hirata, Y., Mitsuno, Y., Maeda, S., Shibata, W., Akanuma, M., Yoshida, H., Kawabe, T. and Omata, M. (2003) *Helicobacter pylori* induces antiapoptosis through nuclear factor-kappaB activation. *J. Infect. Dis.* **188**, 1741–1751 [CrossRef PubMed](#)
- 49 Xia, H.H. and Talley, N.J. (2001) Apoptosis in gastric epithelium induced by *Helicobacter pylori* infection: implications in gastric carcinogenesis. *Am. J. Gastroenterol.* **96**, 16–26 [CrossRef PubMed](#)
- 50 Jang, T.J. and Kim, J.R. (2000) Proliferation and apoptosis in gastric antral epithelial cells of patients infected with *Helicobacter pylori*. *J. Gastroenterol.* **35**, 265–271 [CrossRef PubMed](#)
- 51 Kane, R.C., Farrell, A.T., Sridhara, R. and Pazdur, R. (2006) United States Food and Drug Administration approval summary: bortezomib for the treatment of progressive multiple myeloma after one prior therapy. *Clin. Cancer Res.* **12**, 2955–2960 [CrossRef PubMed](#)
- 52 Sloss, C.M., Wang, F., Liu, R., Xia, L., Houston, M., Ljungman, D., Palladino, M.A. and Cusack, Jr, J.C. (2008) Proteasome inhibition activates epidermal growth factor receptor (EGFR) and EGFR-independent mitogenic kinase signaling pathways in pancreatic cancer cells. *Clin. Cancer Res.* **14**, 5116–5123 [CrossRef PubMed](#)

Received 10 August 2015/30 March 2016; accepted 5 April 2016
Accepted Manuscript online 5 April 2016, doi:10.1042/BCJ20160187

ETS2 and Twist1 promote invasiveness of *Helicobacter pylori*-infected gastric cancer cells by inducing Siah2

Das L *et al.*

SUPPLEMENTARY EXPERIMENTAL

Immunoblotting

Whole-cell extracts were prepared from GCCs after infection with *H. pylori*. Proteins were separated by SDS-PAGE and electrotransferred onto PVDF membranes (Millipore, MA, USA). Blots were probed with primary antibodies to Siah2, ETS2 (1:1000) (Santa Cruz Biotechnology, CA, USA) and Twist1 (1:5000) (Abcam, MA, USA). α -tubulin (1:5000) (Abcam) and histone deacetylase 1 (HDAC1) (1:1000) (Cell Signalling Technology, MA, USA) antibodies were used for normalization of protein loading. Immunoreactivity was detected using Super Signal West Femto kit (Thermo Scientific, MI, USA). Immunoblot images were taken with Chemidoc XRS (Bio-Rad) which was equipped with Quantity One-4.6.9 software.

Real-time reverse transcription PCR (Real-time RT-PCR)

MKN45 cells were seeded in 6-well plates 24 h prior to infection with 200 MOI of *H. pylori*. Total RNA was extracted after 30 minutes and 2 h of infection with an RNeasy kit (Qiagen, CA, USA). cDNA was synthesized from RNA using SuperScript First Strand synthesis system (Invitrogen). Human Siah2 TaqMan Gene Expression Assay (Applied Biosystems, CA, USA) was used to perform real-time RT-PCR using the 7500 Real-time PCR system (Applied Biosystems).

Chromatin immunoprecipitation (ChIP) assay

ChIP assay was performed using the QuickChIP chromatin immunoprecipitation kit (Imgenex, CA, USA). Cells were infected as indicated; chromatin was sonicated into 0.5–3 kb long fragments followed by centrifugation at 12,000 \times g for 10 min. Supernatants were diluted in dilution buffer and immunoprecipitation was performed using ETS2 antibody (Santa Cruz Biotechnology) or Twist1 antibody (Abcam). DNA-protein cross-links of the immunocomplexes were reversed and *in vivo* binding of ETS2 to the *siah2* EBS and Twist1 to the *siah2* TBS was analyzed by performing PCR. Primers for the ChIP assay are shown in Supplementary Figure 1.

Immunofluorescence and confocal microscopy

MKN45 cells were grown on coverslips. Cells were either left uninfected or were infected with MOI 200 of *H. pylori* for 6 h followed by fixation with 4% paraformaldehyde, permeabilization with 0.1% Triton-X-100, and blocking with 3% bovine serum albumin. The cells were then treated with Siah2 primary antibody (Santa Cruz Biotechnology) for overnight and further incubated with fluorescently conjugated secondary antibody for 1 h followed by DAPI (4', 6-Diamidino-2-Phenylindole, Dilactate) (Invitrogen) treatment for 20 min. This experiment was repeated three times and cells were viewed with either a fluorescent microscope (Olympus BX51, Japan) or under a laser scanning confocal microscope (LSM 780 Systems, Carl Zeiss).

All gastric biopsy specimens for immunofluorescence examination were collected and fixed with 4% paraformaldehyde. 10 μ m tissue sections were prepared by cryomicrotomy, permeabilized, and blocked as mentioned before. The sections were then treated with primary antibodies against Siah2 or ETS2 (Santa Cruz Biotechnology) or Twist1 (Abcam) for overnight and further incubated with fluorescently conjugated secondary antibodies for 1 h and DAPI (Invitrogen) treatment for 20 min. Digital images were captured using a fluorescence microscope (Model BX51, Olympus Co., Japan).

***siah2* promoter primers**

WT forward: 5' AGAGGTACCGACTCCGAACACAG 3'

WT reverse: 5' TGTAAGCTTCTTCTGGAACAGCCG 3'

EBS mutant: 5' CCCGCAGCCCGAGCA***TTA***AGCGCCGGCGCTAGG 3'

TBS mutant: 5' GCCCCCTGCGCTGC***TTGCTA***AGAGCCGGGCGGAGC 3'

***siah2* promoter EBS oligos for *in vitro* binding assay**

5' Biotinylated WT forward: 5' CAGCCCAGCAGGAAGCGCCGGCGCTA 3'

5' Biotinylated WT reverse: 5' TAGCGCCGGCGCTTCTGCTCGGGCTG 3'

5' Biotinylated mutant forward: 5' CAGCCCAGCAGCA***TTA***AGCGCCGGCGCTA 3'

5' Biotinylated mutant reverse: 5' TAGCGCCGGCGCTTAATGCTCGGGCTG 3'

***siah2* promoter TBS oligos for *in vitro* binding assay**

5' Biotinylated WT forward: 5' CCCTGCGCTGCCAGCTGGAGCCGGGCG 3'

5' Biotinylated WT reverse: 5' CGCCCGGCTCCAGCTGGCAGCGCAGGG 3'

5' Biotinylated mutant forward: 5' CCCTGCGCTGC***TTGCTA***AGAGCCGGGCG 3'

5' Biotinylated mutant reverse: 5' CGCCCGGCTCTAGCAAGCAGCGCAGGG 3'

Primers for ChIP assay

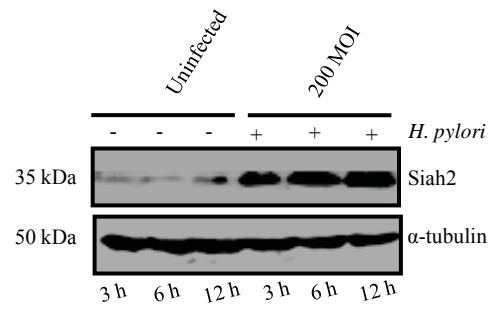
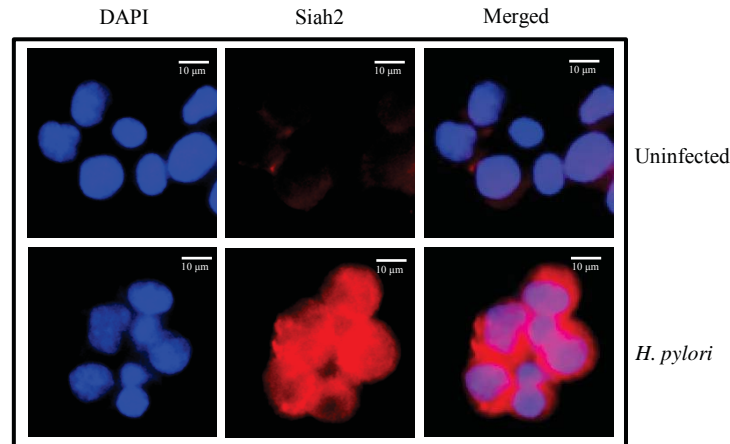
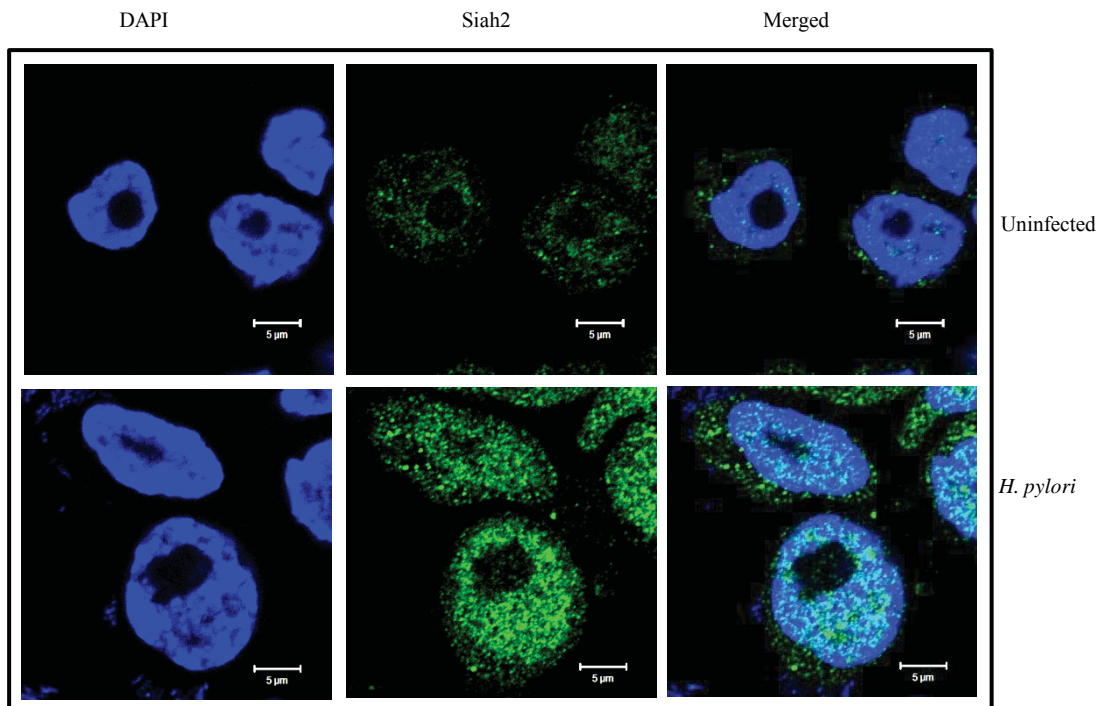
Forward (Specific): 5' ACCCAGAAAAGACAACCCCGCG 3'

Reverse (Specific): 5' GACGTGACGCCTGGACACGT 3'

Forward (Non Specific): 5' CTGGTAGACACTTTGAAAGAGA 3'

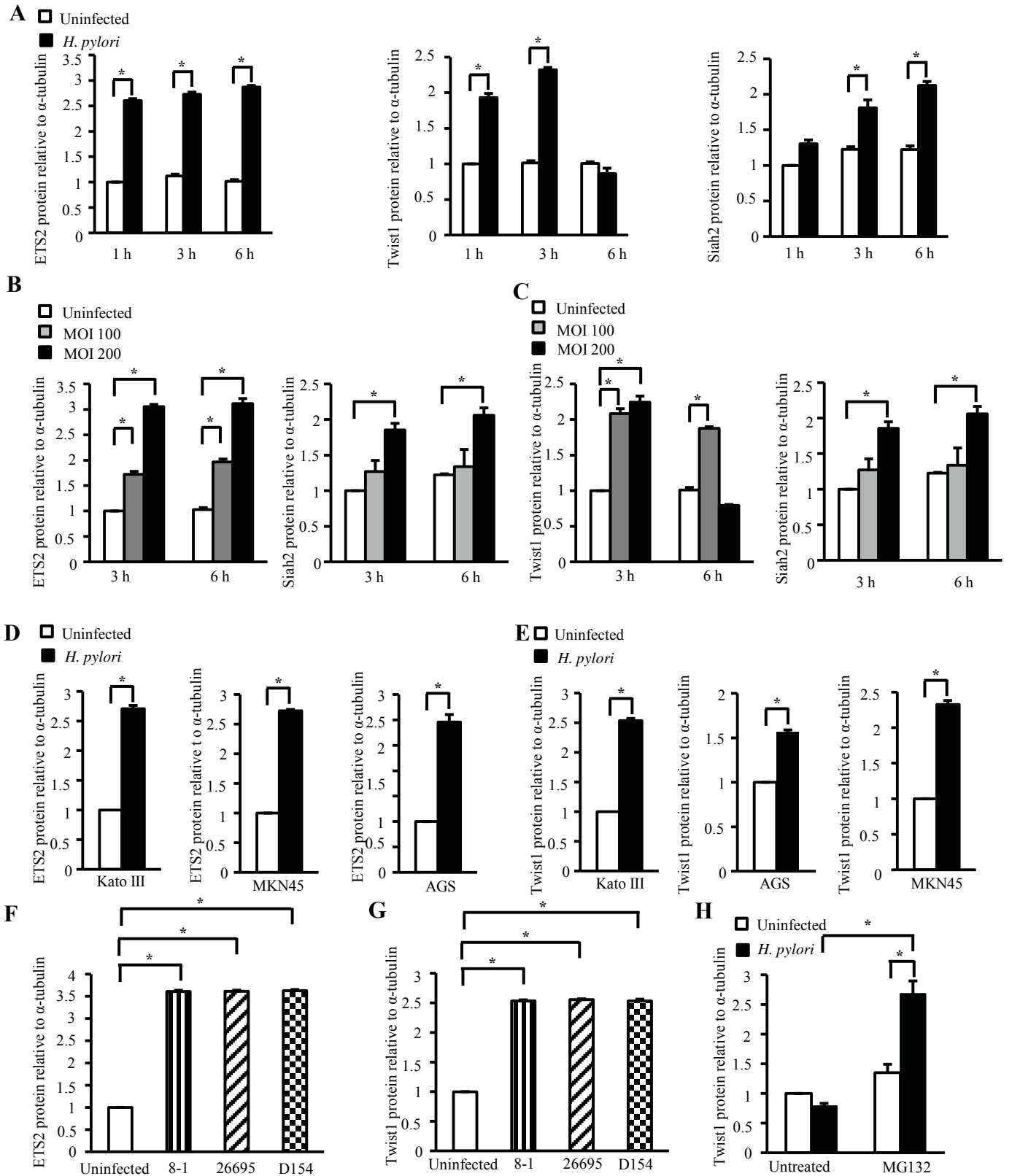
Reverse (Non Specific): 5' TCCACTCTCTCCACAAAAG 3'

Supplementary Figure 1 List of primers and oligonucleotides used in the study. Underlined are EBS and TBS. Mutations are shown in boldfaced italics.

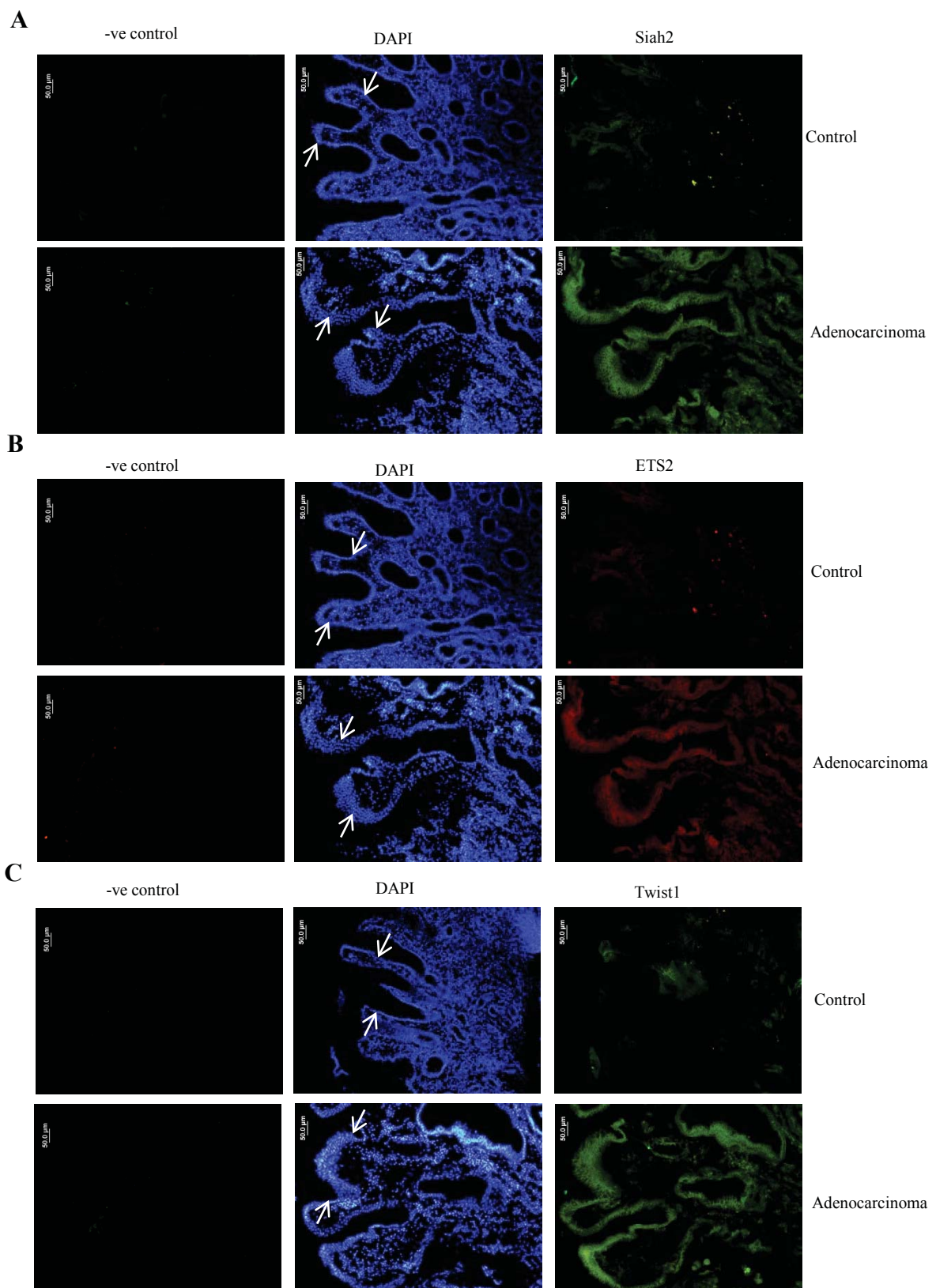
A**B****C**

Supplementary Figure 2 Siah2 induction by *H. pylori* in the infected GCCs

(A) A representative time-course study on *H. pylori*-infected MKN45 cells (n=3). *H. pylori* optimally induce Siah2 at 6 h of infection. (B) A representative fluorescence microscopic analysis showing Siah2 induction in *H. pylori*-infected MKN45 cells. (C) A representative confocal microscopic study showing very high nuclear accumulation of Siah2 in *H. pylori*-infected MKN45 cells.

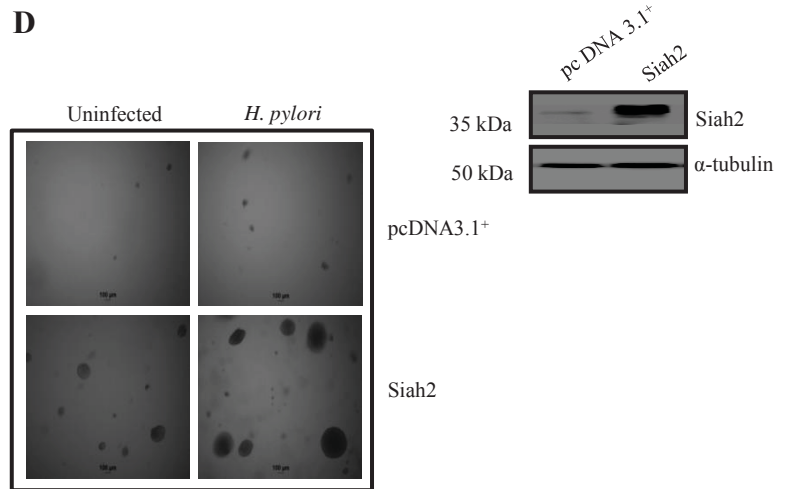
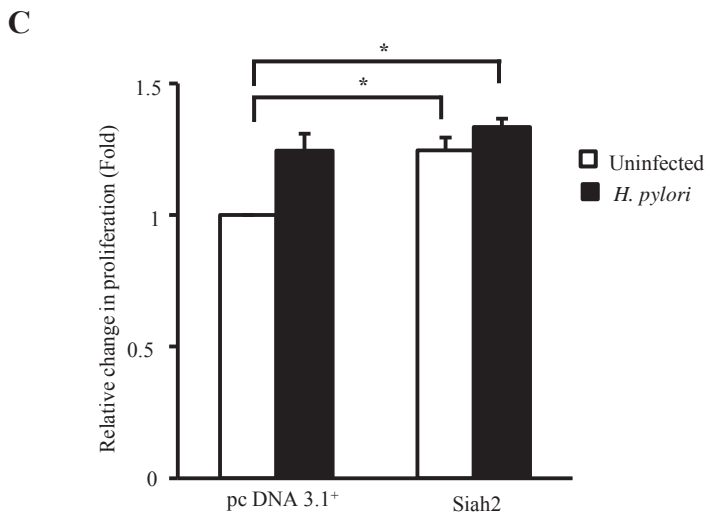
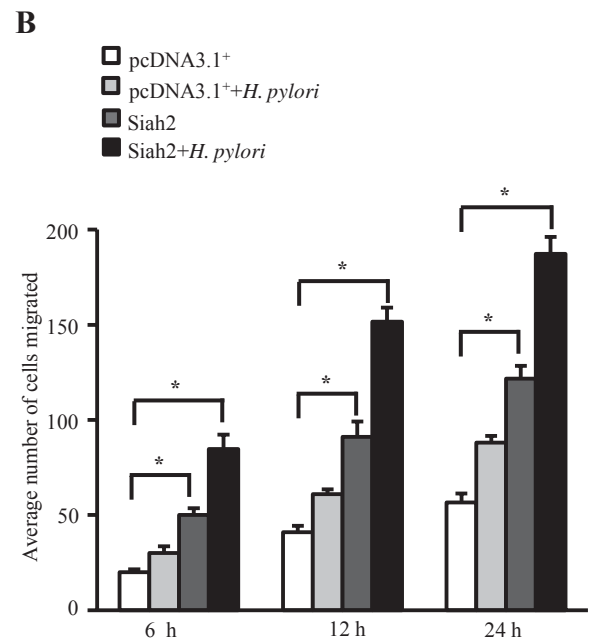
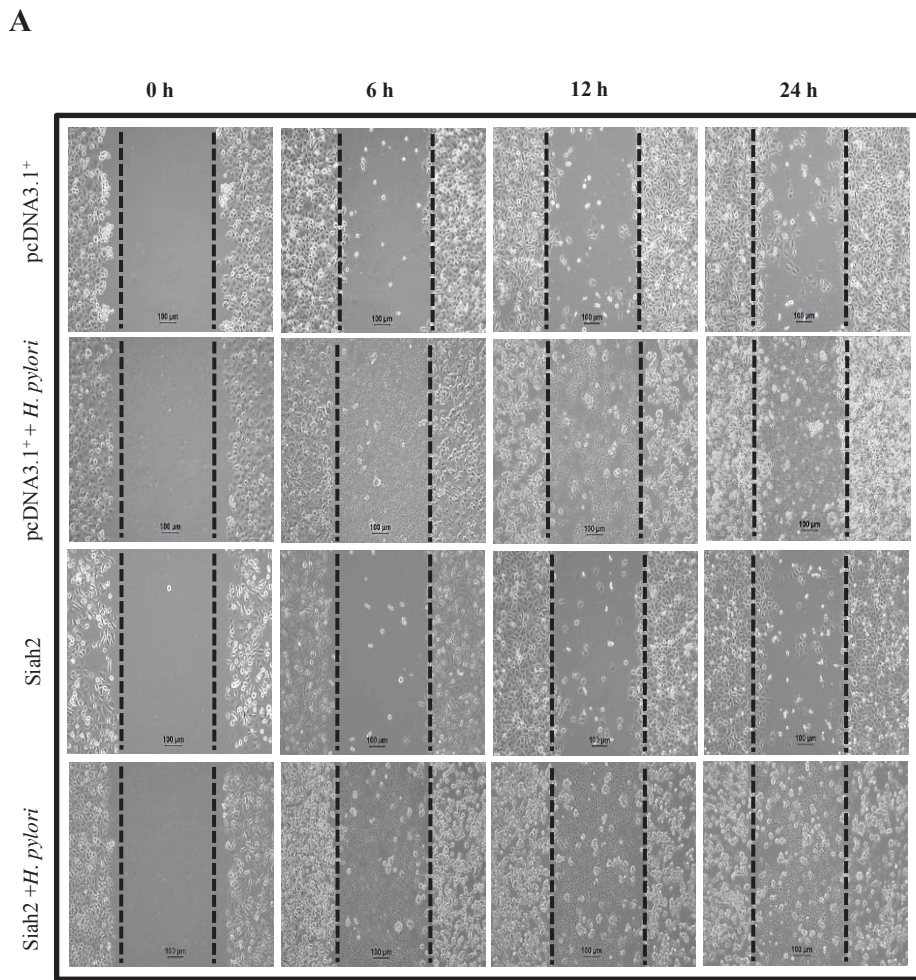


Supplementary Figure 3 *H. pylori* infection induces ETS2, Twist1 and Siah2 expression in GCCs
 Graphical representation of Figure 3A, 3B, 3C, 3D, 3E, 3F, 3G from three independent experiments (mean±SEM), * $P < 0.05$ (A-G); Bar graph of Figure 3H from four independent experiments (mean±SEM), * $P < 0.05$ (H).



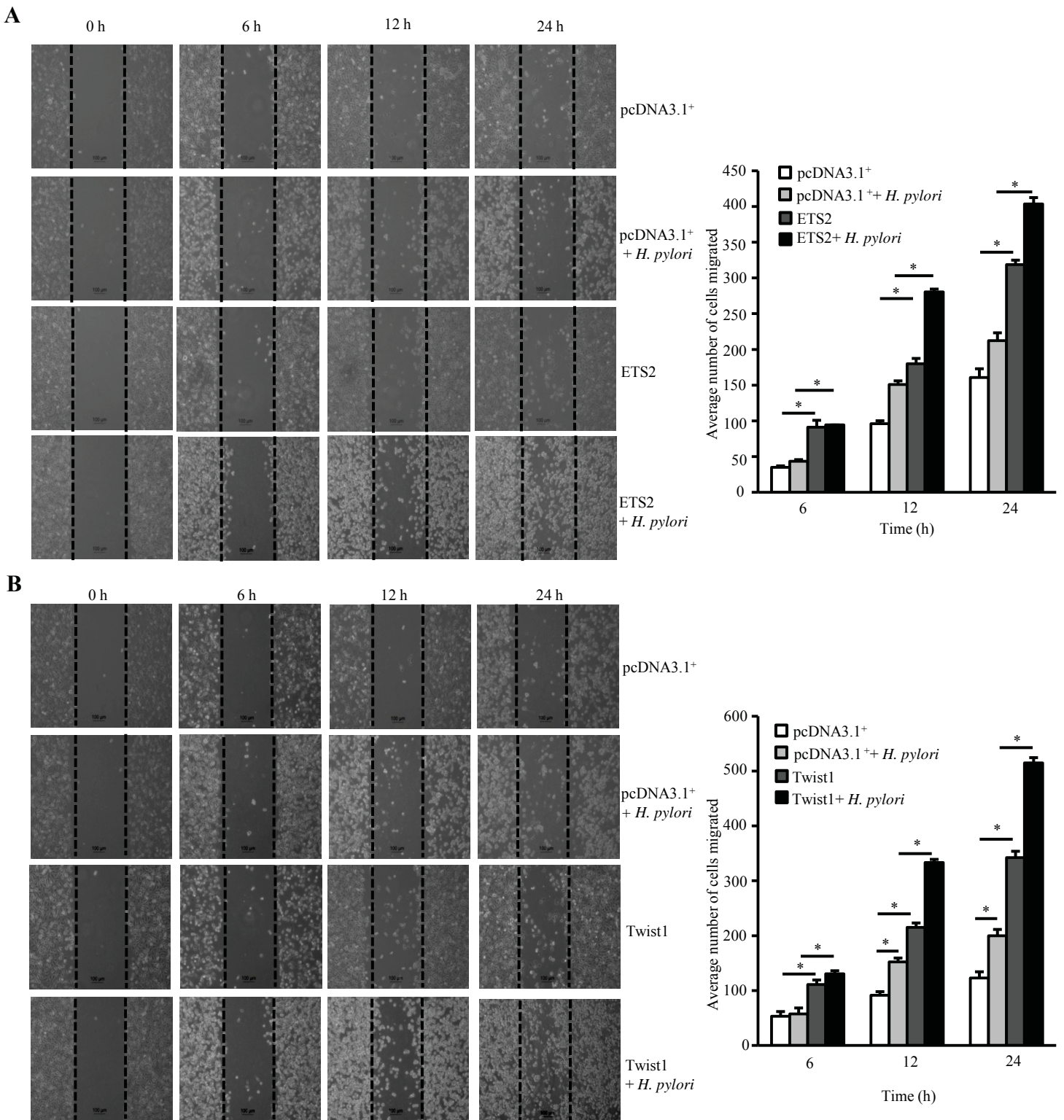
Supplementary Figure 4 Fluorescence microscopic analysis of gastric biopsies from adenocarcinoma patients

Comparison of adenocarcinoma biopsy samples with adjacent non-cancer gastric tissue samples (n=4 for each group) shows that (A) Siah2, (B) ETS2 and (C) Twist1 are highly induced in cancer samples compared to non-cancer tissues. Arrow indicates epithelial lining of the gastric mucosa. Negative (-ve) control contains no primary antibody.



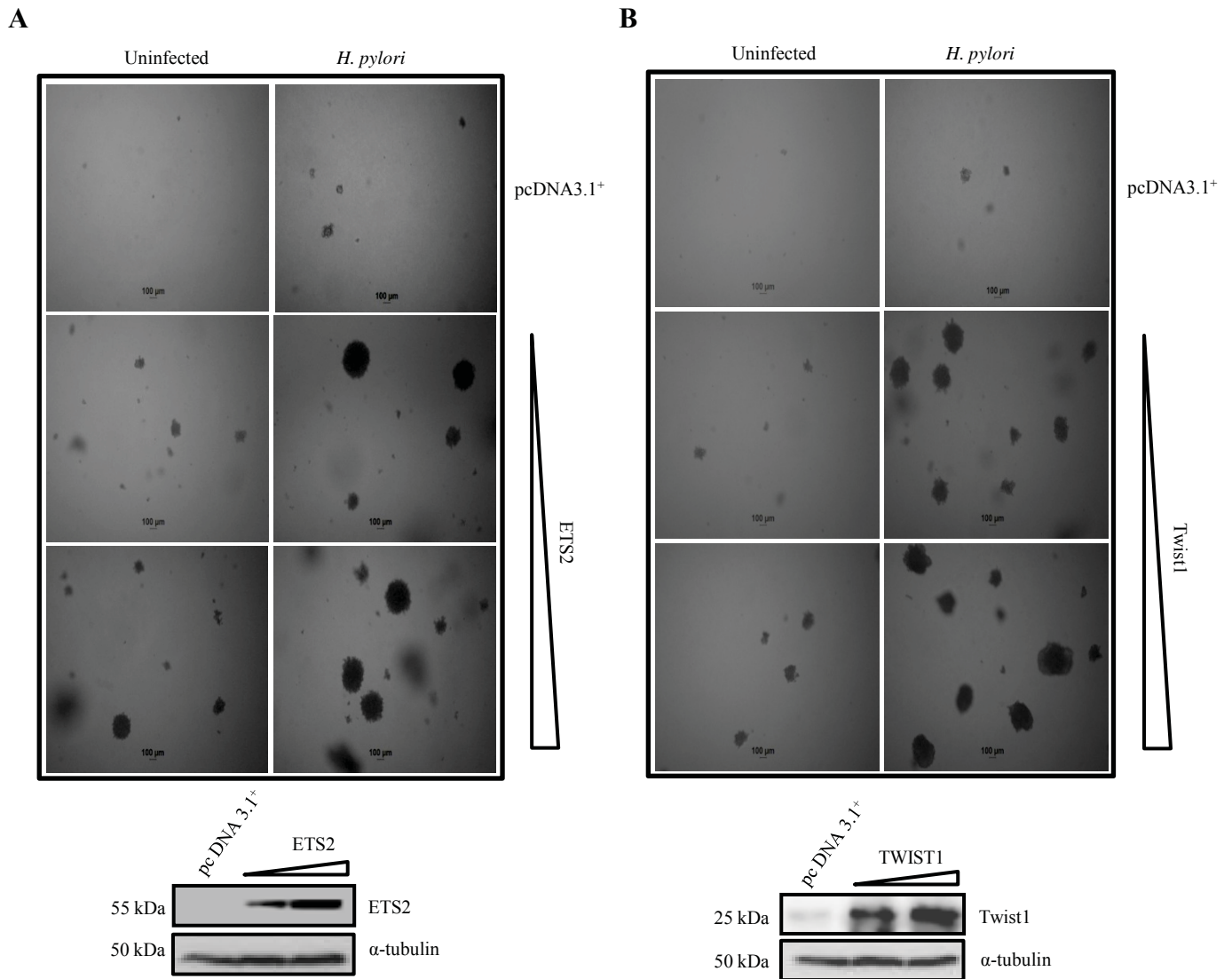
Supplementary Figure 5 Siah2 increases motility, wound-healing property and proliferation of *H. pylori*-infected GCCs

(A) Scratch assay using pcDNA3.1+ and Siah2 stably-expressing AGS cells (n=3). Migration of cells within the scratch area was tracked up to 24 h and results showed that Siah2 overexpression induced migration of the *H. pylori*-infected cells. Scale shown = 100 μ m. (B) Bar graph represents the average number of migrated cells in the wound area from three independent experiments (mean \pm SEM), * P < 0.05. (C) As measured by MTT assay, overexpression of Siah2 significantly induced AGS cell proliferation which was further potentiated by *H. pylori* infection. Bars depict relative proliferation. (mean \pm SEM, n=3), * P < 0.05. (D) Cell invasiveness in three dimensions was evaluated by soft-agar colony formation assays. A substantial increase in colony formation was noticed in Siah2-expressing MKN45 cells as compared to pcDNA3.1+-expressing infected cells. Siah2 protein level in stable cells is shown in the accompanying western blot result.



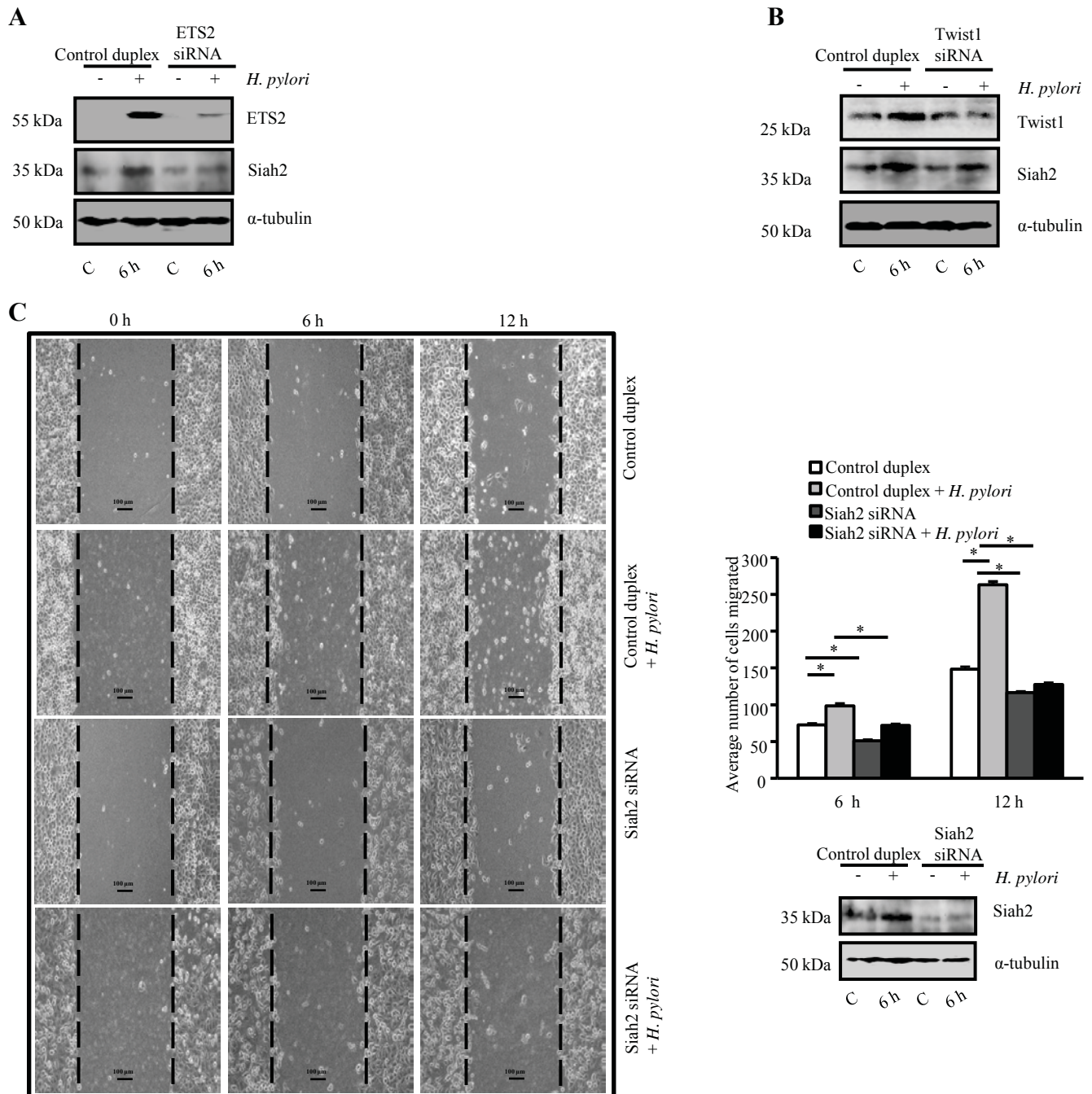
Supplementary Figure 6 ETS2 and Twist1 induce wound-healing ability of *H. pylori*-infected GCCs

(A) Scratch assay (n=3) using pcDNA3.1⁺ and ETS2 stably-expressing AGS cells. Wound healing property or the migration of cells within the scratch area is tracked up to 24 h. Scale shown = 100 μ m. Accompanying bar graph represents the average number of migrated cells in the wound from three independent experiments (mean \pm SEM). **P* < 0.05. (B) A representative wound-healing study similar to that shown in Supplementary Fig. 4, is performed using Twist1-stable cells. Its accompanying bar diagram is also shown (mean \pm SEM, n=3). **P* < 0.05.



Supplementary Figure 7 ETS2 and Twist1 dose-dependently induce invasiveness of *H. pylori*-infected GCCs

(A) Effect of ETS2 overexpression on invasiveness of MKN45 cells is evaluated by soft-agar colony formation assay (n=3). A substantial enhancement in colony formation ability of *H. pylori*-infected ETS2 stably-expressing MKN45 cells is noticed as compared to infected empty-vector expressing cells. (B) Twist1 enhances invasiveness of MKN45 cells is evaluated by soft-agar colony formation assay (n=3). Twist1 stably-expressing infected MKN45 cells show increased invasiveness as compared to infected empty-vector expressing cells.



Supplementary Figure 8 ETS2 and Twist1-mediated Siah2 induction enhances wound-healing ability in *H. pylori*-infected GCCs

(A) Effect of ETS2 suppression by siRNA on *H. pylori*-induced Siah2 expression in MKN45 cells (n=3). (B) Twist1 suppression in MKN45 cells markedly decreases *H. pylori*-mediated Siah2 expression (n=3). (C) Siah2 siRNA significantly decreases wound-healing property of *H. pylori*-infected MKN45 cells. Accompanying bar diagram is also shown (mean \pm SEM, n=3). * $P < 0.05$. Western blot data indicates Siah2 protein expression in cells used for the experiment.